



**The Abdus Salam
International Centre for Theoretical Physics**



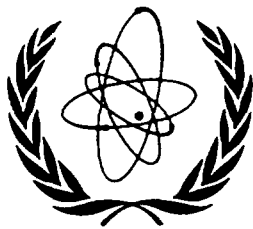
1944-2

**Joint ICTP-IAEA Workshop on Nuclear Reaction Data for Advanced
Reactor Technologies**

19 - 30 May 2008

Uncertainties in physics calculations for gas cooled reactor cores.

J.M. Kendall
Global Virtual LLC
Prescott
USA



International Atomic Energy Agency

INTERNATIONAL WORKING GROUP ON GAS COOLED REACTORS

UNCERTAINTIES IN PHYSICS CALCULATIONS FOR GAS COOLED REACTOR CORES

PROCEEDINGS OF A SPECIALISTS MEETING
ORGANIZED BY THE
INTERNATIONAL ATOMIC ENERGY AGENCY
AND HELD IN VILLIGEN, SWITZERLAND, 9-11 MAY 1990

INTERNATIONAL ATOMIC ENERGY AGENCY, VIENNA, 1991

**UNCERTAINTIES IN PHYSICS CALCULATIONS
FOR GAS COOLED REACTOR CORES**

PROCEEDINGS OF A SPECIALISTS MEETING
ORGANIZED BY THE
INTERNATIONAL ATOMIC ENERGY AGENCY
AND HELD IN VILLIGEN, SWITZERLAND, 9-11 MAY 1990

INTERNATIONAL ATOMIC ENERGY AGENCY, VIENNA, 1991

UNCERTAINTIES IN PHYSICS CALCULATIONS
FOR GAS COOLED REACTOR CORES
IAEA, VIENNA, 1991
IWGGCR/24

Printed by the IAEA in Austria
April 1991

FOREWORD

The Specialists Meeting on Uncertainties in Physics Calculations for Gas-Cooled Reactor Cores was held at the Paul Scherrer Institute (PSI), Villigen, Switzerland, 9-11 May 1990. The meeting was convened by the International Atomic Energy Agency on the recommendation of the International Working Group on Gas Cooled Reactors. It was attended by 29 participants from Austria, China, France, Germany, Japan, Switzerland, the Union of Soviet Socialist Republics and the United States of America. The meeting was chaired by Dr. Rudi Brogli, PSI, and subdivided into four technical sessions:

- 1) Analytical Methods, Comparison of Predictions with Results from Existing HTGRs, Uncertainty Evaluations
- 2) Analytical Methods, Predictions of Performance of Future HTGRs, Uncertainty Evaluations-Part 1
- 3) Analytical Methods, Predictions of Performance of Future HTGRs, Uncertainty Evaluations-Part 2
- 4) Critical Experiments - Planning and Results, Uncertainty Evaluations

The participants presented 19 papers on behalf of their countries or organizations. Each presentation was followed by an open discussion in the general area covered by the paper.

At the end of the meeting an open discussion was held regarding Directions for Future Core Physics Efforts and International Co-operation.

EDITORIAL NOTE

In preparing this material for the press, staff of the International Atomic Energy Agency have mounted and paginated the original manuscripts as submitted by the authors and given some attention to the presentation.

The views expressed in the papers, the statements made and the general style adopted are the responsibility of the named authors. The views do not necessarily reflect those of the governments of the Member States or organizations under whose auspices the manuscripts were produced.

The use in this book of particular designations of countries or territories does not imply any judgement by the publisher, the IAEA, as to the legal status of such countries or territories, of their authorities and institutions or of the delimitation of their boundaries.

The mention of specific companies or of their products or brand names does not imply any endorsement or recommendation on the part of the IAEA.

Authors are themselves responsible for obtaining the necessary permission to reproduce copyright material from other sources.

This text was compiled before the unification of Germany in October 1990. Therefore the names German Democratic Republic and Federal Republic of Germany have been retained.

CONTENTS

Summary of Sessions	7
Directions for future core physics efforts and international co-operation: Summary of an open discussion	15
<i>J. Cleveland</i>	
ANALYTICAL METHODS, COMPARISON OF PREDICTIONS WITH RESULTS FROM EXISTING HTGRs, UNCERTAINTY EVALUATIONS (Session I)	
Experimental and theoretical analysis of spent AVR fuels	19
<i>H. Werner, F. Thomas, F. Woloch, G. Reitsamer, G. Falta, A. Strigl</i>	
French experience in thermohydraulics calculations of gas cooled reactors	31
<i>F. Boutard, G. Carvallo, G. Chevalier</i>	
Progress and problems in modelling HTR core dynamics: the TINTE code tested at AVR power transients	36
<i>W. Scherer, H. Gerwin</i>	
ANALYTICAL METHODS, PREDICTIONS OF PERFORMANCE OF FUTURE HTGRs, UNCERTAINTY EVALUATIONS — PART 1 (Session II)	
Determination of the temperature coefficients and the kinetic parameters for the HTTR safety analysis	45
<i>K. Tokuhara, T. Nakata, I. Murata, K. Yamashita, R. Shindo</i>	
Calculational methods of power distribution in the HTTR and verifications	53
<i>T. Nakata, K. Tokuhara, I. Murata, K. Yamashita, R. Shindo</i>	
The plant dynamics analysis code ASURA for the high temperature engineering test reactor (HTTR)	59
<i>Y. Shimakawa, M. Tanji, S. Nakagawa, N. Fujimoto</i>	
Physical status of the 10 MW test module	66
<i>Jingyu Luo</i>	
Effects of the fuel elements pebble bed structural non-uniformity on the HTGR physical and thermophysical characteristics	72
<i>V.I. Yevsejev, A.I. Kiryushin, N.G. Kuzavkov, V.M. Mordvintsev, Yu.P. Sukharev</i>	
ANALYTICAL METHODS, PREDICTIONS OF PERFORMANCE OF FUTURE HTGRs, UNCERTAINTY EVALUATIONS — PART 2 (Session III)	
Uncertainties in calculations of nuclear design code system for the high temperature engineering test reactor (HTTR)	81
<i>R. Shindo, K. Yamashita, I. Murata</i>	
Automated differentiation of computer models for sensitivity analysis	86
<i>B.A. Worley</i>	
Impact of different libraries on the performance calculation of a MODUL-type pebble bed HTR	92
<i>U. Ohlig, H. Brockmann, K.A. Haas, E. Teuchert</i>	

Nuclear data related to HTRs	98
<i>S. Pelloni, W. Giesser</i>	
A review of reactor physics uncertainties and validation requirements for the modular high-temperature gas-cooled reactor	104
<i>A.M. Baxter, R.K. Lane, E. Hettergott, W. Lefler</i>	
Uncertainties in the analysis of water ingress accident for the HTGR cores	112
<i>V.S. Gorbunov, V.F. Golovko, E.S. Glushkov, A.I. Kiryushin, N.G. Kuzavkov, Yu.P. Sukharev</i>	
 CRITICAL EXPERIMENTS — PLANNING AND RESULTS, UNCERTAINTY EVALUATIONS (Session IV)	
Measurements of temperature coefficient of reactivity of the VHTRC-1 core by the criticality method	119
<i>H. Yasuda, F. Akino, T. Yamane, Y. Kaneko</i>	
Present status of the PROTEUS HTR experiments	124
<i>Paul Scherrer Institute</i>	
Present HTR physics calculational methods at the Paul Scherrer Institute	130
<i>S. Pelloni</i>	
Uncertainties in HTGR neutron-physical characteristics due to computational errors and technological tolerances	136
<i>E.S. Glushkov, V.N. Grebennik, V.D. Davidenko, V.G. Kosovskij, O.N. Smirnov, V.F. Tsibul'skij, Yu.P. Sukharev</i>	
Summary of discussion of the future HTGR PROTEUS experiments and other planned experiments	145
<i>W. Scherer</i>	
List of Participants	148

SUMMARY OF SESSIONS

SESSION I

ANALYTICAL METHODS, COMPARISON OF PREDICTIONS WITH RESULTS FROM EXISTING HTGRs, UNCERTAINTY EVALUATIONS

H. Yasuda
Chairman

The results of experimental and theoretical analysis of spent AVR fuels were presented by Dr. Woloch of OEFZS - Seibersdorf. Burn-up was measured at Jülich and Seibersdorf by gamma spectrometric and mass spectroscopic methods where contents of heavy metals including Cs and Nd were measured. Theoretical analyses were made for these fuel pebbles to give heavy metal inventories by using the new HTR-2000 program system including TOMKU and HTRROGEN with the libraries MUPO and WIMS-D. The system can solve the equations for 1156 nuclides taking into accounts the flow path of pebbles in the core during many refueling period by using 25 spectral zones and 139 regions in the core. An equivalence principle was introduced to take account the resonance absorption of heavy metals. Comparisons of heavy metal inventories between calculation and experiments were shown for HEU and LEU pebbles at various burn-up stages up to 10.5 % FIMA.

A French experience in thermohydraulics calculations of gas-cooled reactors were presented by Ms. Boutard of CEA. The LOTE code has been developed in CEA to be applied to the analysis of transient behaviour in accidental conditions up to several months. The code consists of independent modules, modelling the primary flow circuit and main heat exchangers, shut down heat exchanger, blowers and the different materials making up the core. Details of the code, i.e., assumptions, geometrical modelling, and basic equations were explained. Comparisons of core exit temperature and flow rate between calculation by LOTE code and readings of Chinon-3 power plant showed very good agreement in the medium (-1h) and long (-4h) terms. The results suggested the special importance of (1) axial and radial zoning of reactor, (2) Heat exchanger transient modelling and (3) Blower characteristics at low speed.

Extensive work on time dependent neutronics and temperature code (TINTE) was presented by Dr. Scherer of KFA. The code is able to model the primary circuit of HTR plant using modern numerical techniques and relevant physical variables. The HTR core is treated in 2-D R-Z geometry, 2 energy group diffusion theory and 14 decay heat groups model. Gamma ray heating effect can be considered in the calculation by using local and nonlocal heat sources. Validation of TINTE was conducted using the various transient tests, such as rod drop, rod withdrawal, blower speed change and shut-down Xe effect, data obtained at AVR. The results showed good accordance between experiment and calculation. Further validation work is also planned for natural convection and core heat up experiments. The effects of water ingress on reactivity, fuel element corrosion and cooling properties are now being incorporated into the code.

SESSION II

ANALYTICAL METHODS, PREDICTIONS OF PERFORMANCE OF FUTURE HTGRs, UNCERTAINTY EVALUATIONS - PART 1

W. Scherer
Chairman

The session was made up by 5 papers from 3 countries, namely Japan, China and USSR. Three papers were dedicated to the Japanese HTTR project.

The first paper was presented by K. Tokuhara (Fuji Electric Co. Ltd.). The doppler- and moderator-temperature coefficients were calculated using a whole core model by uniform changing of the temperatures. Control rods were assumed to be withdrawn. It was shown that the doppler coefficient lies in the range of $-5.0 \cdot 10^{-5}$ to $-1.5 \cdot 10^{-5} \text{ C}^{-1}$. The moderator coefficient covers the area between $-17 \cdot 10^{-5}$ up to $+1 \cdot 10^{-5} \text{ C}^{-1}$. Despite of this positive value the power coefficient stays negative in all situations. The kinetic parameters effective delayed neutron fraction and prompt neutron lifetime were shown to be $\beta_{\text{eff}} = 0.0047$ to 0.0065 and $\lambda_{\text{prompt}} = 0.00067$ to 0.00078 sec. respectively. These data are necessary for kinetic calculations using point kinetics techniques.

The second paper was presented by T. Nakata (Kawasaki Heavy Ind. Ltd.). The design procedure and the results of the power distribution evaluation for the HTTR were given. One of the main design goals was to minimize the maximum fuel temperature. Therefore a careful fuel zoning and loading of burnable poisons was performed. By combining the results of different core models using the diffusion code CITATION the local power peaking factor was obtained to be about 7% slightly decreasing in time. The effect of local power spikes due to the block end graphite was found to be in the order of 4% at the point of maximum fuel temperature. The accuracy of the calculational methods was tested using Cu reaction rate measurements in the critical facility VHTRC with good results. It was stressed that the methods would meet all the design requirements.

The third paper was presented by Y. Shimakawa (Mitsubishi Atomic Power Ind. Inc.). The ASURA code was developed to design the HTTR plant control systems. It models the main components and systems of the HTTR and simulates the transient behaviour of the whole plant. The verification of this code was performed by evaluation of Fort St. Vrain dynamics experiments and comparison with the validated dynamics code THYDE-HTGR. Results were shown to be adequate and applicable for the HTTR control system design.

The fourth paper was dedicated to the 10 MW Test Module reactor project in China. The general design of this reactor was discussed and special design problems were pointed out. To keep the reactivity effect of water ingress accidents small the heavy metal loading was reduced to 5 g HWM/fuel ball. A reduction of the core diameter to 180 cm was found necessary to keep the shut down reactivity margin in an adequate bandwidth during operation. The reduction of control rod worth by water ingress was considered to be of major importance and additional detailed investigations in this field were announced.

The fifth paper of the session came from USSR and was presented by Yu. P. Sukharev. The effects of variations in the pebble flow velocity and the pebble bed porosity on reactivity, power distribution and temperatures were analyzed for the USSR HTGR projects VG-400 and VGM. It was shown that assumptions on the porosity variations near the core/reflector boundary and above the fuel discharge tubes based on previous theoretical analyses could lead to substantial modifications of the temperature distribution in the core. The maximum fuel element temperature may thus increase by some 200°C. In earthquake situations pebble bed compaction could lead to reactivity effects of about 0.4% as was explained using data from related experiments. The necessity of studies in this field at critical assemblies was emphasized.

In total the session gave an overview of status and problems in today's HTTR projects. It was felt that the Japanese HTTR licensing requirements are fulfilled by the methods available and the analyses yet performed. For the Chinese Test Module fields for future detailed analysis were defined and concerning the USSR projects additional experiments were asked for.

SESSION III

ANALYTICAL METHODS, PREDICTIONS OF PERFORMANCE OF FUTURE HTGRs, UNCERTAINTY EVALUATIONS - PART 2

S. Pelloni
Chairman

Session III included six papers from the different participating countries.

The first paper is from Japan, and was presented by R. Shindo. Neutronics calculations of the Very High Temperature Reactor Critical Assembly (VHTRC) based on the DELIGHT/TWOTRAN/CITATION codes were performed in connection with ENDF/B-IV based data libraries. The characteristics of the VHTRC are similar to those of the High Temperature Engineering Test Reactor (HTTR) of 30 MW thermal power. The core of the VHTRC consists of 280 fuel rods of UO_2 with 4% enriched uranium coated particles. The agreement with experimental values of the calculated eigenvalue k_{eff} , power distribution and of the calculated poison rod worths is good within 1%, 2.9%, and 1% respectively. Thus, the licensing requirements for the HTTR are met.

The second paper is from the USA, and was presented by B. Worley. First, the sensitivity and uncertainty analysis capabilities of the reactor physics models used at ORNL were summarized. Second, a new, generalized formalism for performing sensitivities studies by implementing direct and adjoint techniques into existing FORTRAN computer codes was described. This methodology is used in the code GRESS (Gradient Enhanced Software System). GRESS has been tested mostly for non nuclear applications. The code and the related documentation can be requested without any restriction from RSIC.

The third paper is from Germany, and was presented by U. Ohlig. Extensive physics calculations with the VSOP code system of a pebble bed HTR with LEU fuel characterized by 4% enriched uranium coated particles show that there are large discrepancies (up to 2.5%) between the eigenvalue k_{eff} of the initial core estimated using an old ENDF/B-II based library and a newer library based on ENDF/B-IV, ENDF/B-V, and JEF-1. The discrepancy between the eigenvalues almost vanishes for the equilibrium cycle, due to compensating effects arising from the build up of plutonium and fission products. Safety related properties of the reactor are only weakly affected by the turn to the new library.

The fourth paper is a common paper from Switzerland and from Germany, and was presented by S. Pelloni. A series of two-dimensional discrete-ordinates transport theory k_{eff} calculations with an (r,z) geometric model have been performed for a simple, typical LEU HTR configuration characterized by LEU AVR non irradiated fuel containing 6 grams of 16.7% enriched uranium per pebble, using different methods and data. For a 13 neutron group calculation in the well tested structure from HRB the eigenvalue ranges from 0.9896 for P_0 modified cross sections coming from MICROX-2 to 1.0083 for P_0 modified JEF-1 cross sections from WIMS-D obtained using a new method developed by Segev. Either the use of P_1 modified cross sections, or that of P_0 cross sections (suitably modified) in connection with a finer group structure, reduces the discrepancies between eigenvalues of small HTR cores.

The fifth paper is from the USA, and was presented by A.M. Baxter. The paper gives a very detailed review of the important, safety related, physics parameters for the low-enriched Modular High-Temperature Gas-Cooled Reactor (MHTGR), and estimates are presented of the uncertainties in the calculated values of these variables. The MHTGR core contains 20% enriched fissile uranium oxycarbide and fertile thorium oxide fuel. It is pointed out that the core physics experimental data base is adequate to ensure that the temperature coefficient obtained using a broad class of methods and data libraries available in the USA can be calculated with an uncertainty of less than 20%. The present uncertainties of the control rod bank reactivity worth, of the local power distributions, of the core reactivity, of water ingress effects, and of the production of decay heat are of less than 10%, 13%, 1.5%, 10%, and 10% respectively.

The sixth paper is from the USSR and was presented by Yu. P. Sukharev. Uncertainties from calculations of low enriched HTR cores characterized by water ingress accidents were described. The reactor analysis was made with the code system NEKTA/VIANKA/GAVROSH in connection with WIMS-D cross sections. Results of the analysis show that the water inventory in the core as a result of an accident varies from between 10 Kg and 80 Kg to 400 Kg. Corresponding changes of the positive reactivity are between 0.05% and 2%. The discrepancy of water ingress effects predicted by different codes and libraries is about 30%. Since the assessed uncertainties are different in various papers, it was recommended to define a simple LEU HTR Benchmark to be calculated in the frame of the cooperative work.

SESSION IV

CRITICAL EXPERIMENTS - PLANNING AND RESULTS, UNCERTAINTY EVALUATIONS

R. Chawla
Chairman

There were five presentations in this session - four being contributed papers and the fifth being a summary report by W. Scherer, acted as the Chairman of the 2-day Research Co-ordination Meeting held at PSI earlier in the week.

In the first paper, presented by H. Yasuda, an account of the experimental procedures employed at the VHTRC critical facility in Japan for determination of the temperature coefficient over several different temperature steps between 8 and 200°C is given. The importance of correcting for various effects in the measurements was stressed. Lower values of the temperature coefficient were found in the lower part of the temperature range investigated. The agreement with calculations based on the SRAC code was within -2%.

In the second paper presented by D. Mathews, the current status of work in the HTR-PROTEUS program is described. The safety report for the planned experiments is being reviewed by the Swiss authorities, and measurements are scheduled to begin in Summer 1991. During the currently planned phase (-3 years of experimentation), first-of-its-kind integral data should be made available for (a) criticality of LEU pebble-bed configurations with different moderator/fuel pebble ratios and lattice geometries, (b) neutron balance changes upon water ingress and (c) control absorber effects.

An overview of the HTR-relevant calculational methods and data available at PSI was provided by S. Pelloni in the third paper. The cell codes employed are MICROX-2, WIMS-D (with a specially developed double-heterogeneity treatment) and TRAMIX. The data libraries most commonly used are based on the JEF-1 file. Whole-reactor calculations are usually carried out with the 2-D transport code TWODANT.

The fourth contributed paper was presented by E.S. Glushkov and described how uncertainties for LEU pebble-bed systems have been assessed in the USSR. For K_{eff} predictions an uncertainty of -2% has been estimated, this being based on (a) comparisons of calculated and experimental results from the ASTRA and GROG critical facilities and (b) an explicit consideration of tolerances on various technical specifications in these experiments. Uncertainty estimates were also presented for temperature coefficient, water ingress, Xe-poisoning, control rod worths and power distributions - the various values being broadly consistent with those given by other speakers at the Meeting.

The fifth paper was presented by W. Scherer who summarized findings from the 1st IAEA CRP Meeting on "Validation of Safety Related Physics Calculations for Low-Enriched HTGRs", held at PSI on May 7-8, 1990. The CRP agreement has been signed by China, Japan, Switzerland, the USSR and the Federal Republic of Germany, and the USA is expected to join soon. Viewpoints and needs are somewhat different in the individual countries,

but there was unanimous expression of the need for the planned HTR-PROTEUS program which will form the focal point for activities within the CRP. Experimental results from past and on-going LEU/HTR experiments (VHTRC in Japan and ASTRA/GROG in the USSR) will also be made available, and these should form an additional basis for intercomparisons of methods/data. As a first step, a calculational benchmark exercise will be carried out by the CRP members on the basis of a specified HTR-PROTEUS configuration. Priorities on the types of measurements to be carried out in PROTEUS (paper entitled "Present Status of the PROTEUS HTR Experiments") were discussed and found to be somewhat constrained by the amount of fuel available. The prospect of a second phase of experiments was raised with the suggestion that the USSR might later provide a larger number of LEU (21% enriched) fuel pebbles. Finally, the delegation of scientific staff to PSI for direct participation in the HTR-PROTEUS program was recognized by all as being an important feature of the CRP agreement.

**DIRECTIONS FOR FUTURE CORE PHYSICS EFFORTS
AND INTERNATIONAL CO-OPERATION**

Summary of an open discussion

J. Cleveland

Division of Nuclear Power,
International Atomic Energy Agency,
Vienna

The purpose of this open discussion was to obtain suggestions from participants in the Specialists' Meeting for worthwhile future core physics efforts and international co-operation. The open exchange of experience which occurred in the papers and associated discussions during the four sessions of the Specialists' Meeting provided a good basis for this discussion.

In general it was noted that the HTGR core physics community has the challenge to extract the maximum amount of information from limited experimental data. In that context, the specialists were encouraged to make optimal use of existing data from power reactors including the Thorium High Temperature Reactor (THTR), the Arbeitsgemeinschaft Versuchs Reaktor (AVR), Fort St. Vrain, British and French GGRs and report results of comparisons with analytical predictions at the next IAEA Specialists' Meeting.

In the future, core physics data from the Japanese HTTR will be of considerable international interest. The international project underway at the PROTEUS criticals facility at Paul Scherrer Institute will provide needed validation data. Also data from existing critical experiments, for example VHTRC (in Japan), ASTRA, GROG (in the USSR) and the LEU experiments at the CNPS (in USA) would be very useful to the international community for methods validation. The IAEA Co-ordinated Research Programme on Validation of Safety Related Reactor Physics Calculations for Low-Enriched HTGR's provides a forum for detailed information exchange from such experiments.

It was noted that HTGR core physics experts should be closely involved in the various working groups which establish basic nuclear cross section data files to assure high quality data appropriate to HTGR conditions. Some problem areas, including important U^{235} cross section data, in new nuclear data files were discussed.

It was also noted that the accuracy of decay heat predictions is important to assessments of safety margins especially in new HTGRs which rely on passive systems for decay heat removal. The accuracy of decay heat formulations relative to experimental information, and the sensitivity of the reactor behaviour to uncertainties in decay heat generation was identified as a topic which could be addressed in papers presented at the next Specialists' Meeting.

The value of comparisons of international benchmark calculations was also discussed. Comparing analytical predictions for a well defined problem is a method of examining important aspects of different analytical approaches such as the method of preparation of cross section sets, geometric representation of reactor components and theoretical techniques. The consensus was that establishment of two well defined

benchmark problems (one for a prismatic MHTGR and one for a pebble bed modular system) should be recommended to the International Working Group on Gas Cooled Reactors (IWGGCR) at their next meeting. The benchmark problems should be provided to the international HTGR core physics community for analysis and results should be reported to the next Specialists' Meeting.

The importance of close co-ordination in the area of HTGR core physics between IAEA and the OECD NEA Reactor Physics Committee was also stressed.

Finally, to answer questions related to safety, it is important to confirm predictions of reactor behaviour at accident conditions. Where large margins exist, the predictions need not be extremely accurate; rather the important phenomena must be clearly understood. In this context new experiments examining important phenomena at accident conditions should be pursued. The specialists had the consensus that the IWGGCR should consider what could be done to establish international co-operation in new experiments at new conditions which would confirm predictions of reactor behaviour under accident conditions.

ANALYTICAL METHODS,
COMPARISON OF PREDICTIONS WITH RESULTS FROM EXISTING HTGRs,
UNCERTAINTY EVALUATIONS

(Session I)

Chairman

H. YASUDA
Japan

EXPERIMENTAL AND THEORETICAL ANALYSIS OF SPENT AVR FUELS

H. WERNER, F. THOMAS
Forschungszentrum Jülich GmbH,
Jülich, Federal Republic of Germany

F. WOLOCH, G. REITSAMER,
G. FALTA, A. STRIGL
Österreichisches Forschungszentrum Seibersdorf,
Seibersdorf, Austria

Abstract

The KFA-Juelich and the OEFZ-Seibersdorf are cooperating in a programme of experimental and theoretical analysis of spent AVR-fuel elements. These elements are of the HEU and LEU type with different Uranium enrichment and Thorium content. The burn up of the HEU and LEU pebbles selected have been measured in Juelich before shipment for detailed analysis in OEFZ and show FIMA values ranging up to 20% and 18% respectively.

The detailed experimental analysis in the OEFZ started with pebbles of 17% enriched (GLE-4) and of 93% enriched (GO) fuel showing FIMA values of about 3.5, 7.5 and 10.5% respectively. The isotopic composition of coated particles from different positions within the pebbles were measured by both gamma spectrometric and mass spectroscopic methods. To gain FIMA values from both methods Cs and Nd isotopes were included. Further work is in progress.

Drawing on the experience of OEFZ personnel gained in Winfrith during its participation in the OECD Dragon Project a general method of calculating the resonance equivalence parameters is put forward in a programme called TOMKU.

Theoretical calculations use the new HTR-2000 programme system of KFA to perform the in-core-following of the pebbles as they move through the core. The reactor model contains 25 spectral zones and 139 regions in three dimensions in the core, fit to represent the movements of the pebbles including recycling between the inner and outer core regions.

For the GLE-4 fuel spectrum calculations have been done twice: one time with the MUPO-library and another time with the WIMS-D-library. To model the HTR-fuel as intimately mixed with graphite the 25 homogeneous spectrum calculations suffice. However for the resonance cross sections an equivalence principle containing the multicell idea for up to nine different fuel types and up to 10 burn up steps in each spectral zone is employed including the double heterogeneity of the HTR-fuel (TOMKU).

After buckling and temperature iterations for 7 reload stages (WB305 to 311) the burn up of the GLE-4 fuel element can be followed up again using a double strategy: once with a one-group picture and the other time with a four group picture of the neutron microscopic cross sections allowing for smoother spectrum effects (HTROGEN).

Results for GLE-4 and GO fuel types are compared with the measured heavy metal contents. The double strategy of the calculations hopefully will isolate ambiguities in the use of libraries or group representations from uncertainties due to the actual path and time taken by fuel elements of high burn up after many refuelling periods through the pebble bed reactor core.

INTRODUCTION

Whilst in the past the AVR reactor operation had been followed up with two dimensional diffusion, simpler spectrum and burn up calculations the new developed code systems, HTR-2000 and HTROGEN are now in use in the KFA. These new systems use a data basis starting from October 1982 in reevaluating reactor physical and operational data. It uses a three dimensional diffusion code to generate neutron fluxes and is supported in its spectrum part DITO by a new programme TOMKU. It produces all the data needed for the equivalence principle to determine the resonance absorption of Th 232 and U 238 for both purposes

- 1) to calculate the average spectra in 25 core zones
- 2) to evaluate individual fuel element cross sections

for burn up calculations in HTROGEN.

HTR-2000 and HTROGEN together are therefore useful tools to predict heavy metal inventories of spent AVR fuel elements.

In this paper the heavy metal inventories of depleted GLE-4 and GO fuel elements of the AVR reactor as measured in the Institute for Chemistry in the Austrian Research Center at Seibersdorf (OEFZS) are compared with results from HTR-2000 and HTROGEN calculations. The nuclear data library used in DITO was the MUPO library 5 updated with ORIGEN data. As an alternative to these data the WIMS-D-Library 1981 will also be used in the comparison for the GLE-4 fuel.

THE AVR-REACTOR

The AVR Reactor is a high temperature gas cooled and graphite moderated reactor. The thermal power is 46 MW_{t,h} with an electrical gross output of 15 MW_{e,1}. The reactor core is cooled by a helium

flow rate of 13 kg/sec at a pressure of 10.9 bar. The core inlet helium temperature is 270°C and the outlet temperature is 950°C. The steam generator works under a steam pressure of 72 bar and a temperature of 505°C.

Fig. 1 to 3 shown at the meeting as foils contain details of the AVR reactor design.

In Fig. 4 an overview of the nine fuel types mentioned are shown. All fresh elements contain 1 g U235 per fuel element. The types abbreviated with GFB mark the high enriched feed breed elements with two types of coated particles, one with feed (high enriched uranium 235) and one with breed fuel (Thorium 232). The high enriched fuel types GO and GK* contain a single coated particle type with uranium and Thorium together. From the low enriched fuel types marked with GLE, only GLE-1 had also two separate coated particles, one with 15% enriched fuel and one with natural uranium. Whilst the high enriched fuel types No. 1 to 4 contain 5g Thorium per fuel element, the high enriched types 6 and 7 contain 10 g Thorium. The coated particles show a kernel diameter of a few hundred microns and are mostly threefold coated. One extra coating can be made of silicon carbide providing a hold-back barrier against fission product diffusion.

There are about tens of thousands coated particles per fuel element.

THE CODE SYSTEMS HTR-2000 AND HTR0GEN

To meet the increasing demands on the simulation of the reactor operation the system of codes HTR-2000 [1] was developed, taking care of all experiences of earlier programs like AVR-70 and AVR-80. Another of these new developments is the TOMKU code, introducing the concept to represent individual element parameters as well as their averaged ones [2]. Since it is impossible to represent all phenomena occurring in a nuclear reactor in detail a series of models were developed describing in an adequate way the reactor itself as well as the nuclear events taking place (nuclear reactions are calculated in module DITO, flow of fuel elements in FLIMO, temperature changes in TERRAK).

A full 3 dimensional geometry is used for neutron diffusion calculations. This was needed, since near the graphite noses housing the shut down rods higher thermal fluxes and higher temperatures occur and do not allow simple cylindrical approximations for detailed power distributions and temperature distributions. A total of 164000 mesh points are used for the reactor model. For the burnup 50 classes are provided into which all elements can be classified, following the capacity of the burnup measurement unit. The time is discretized in reloading steps of about 14 to 29 days.

*GO: statically pressed oxidic fuel.
GK: statically pressed carbidic fuel.

Measured quantities:

Constructional details:

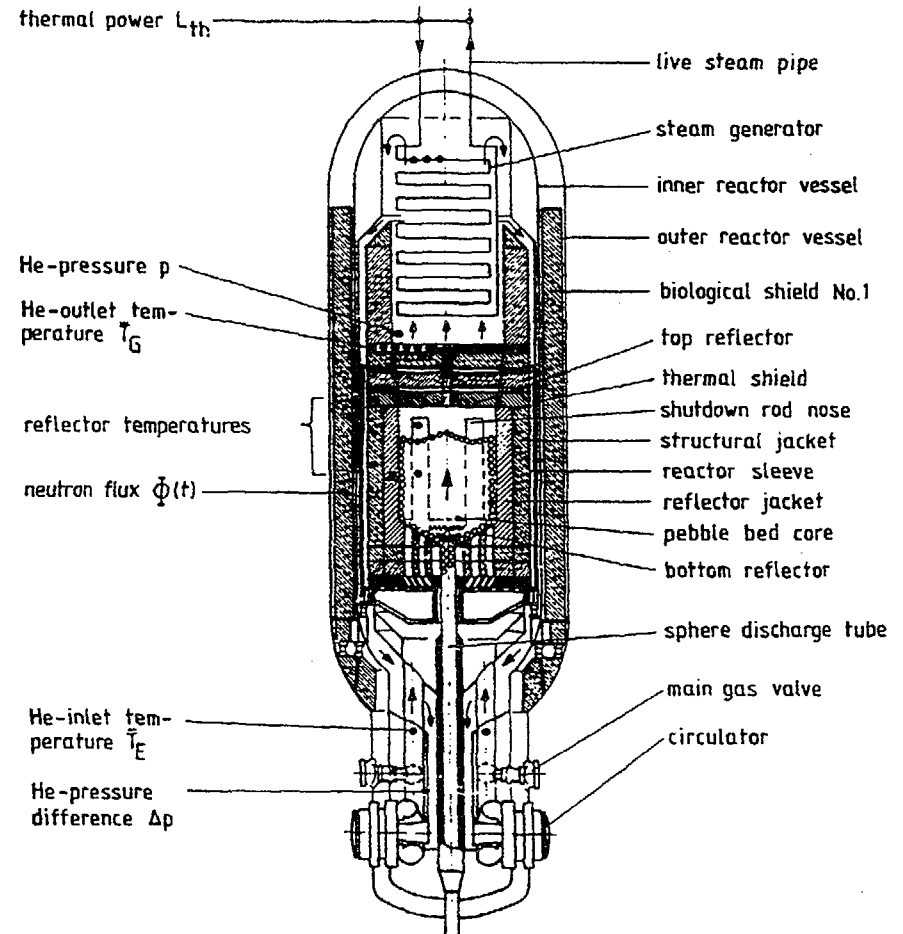


FIG. 1.

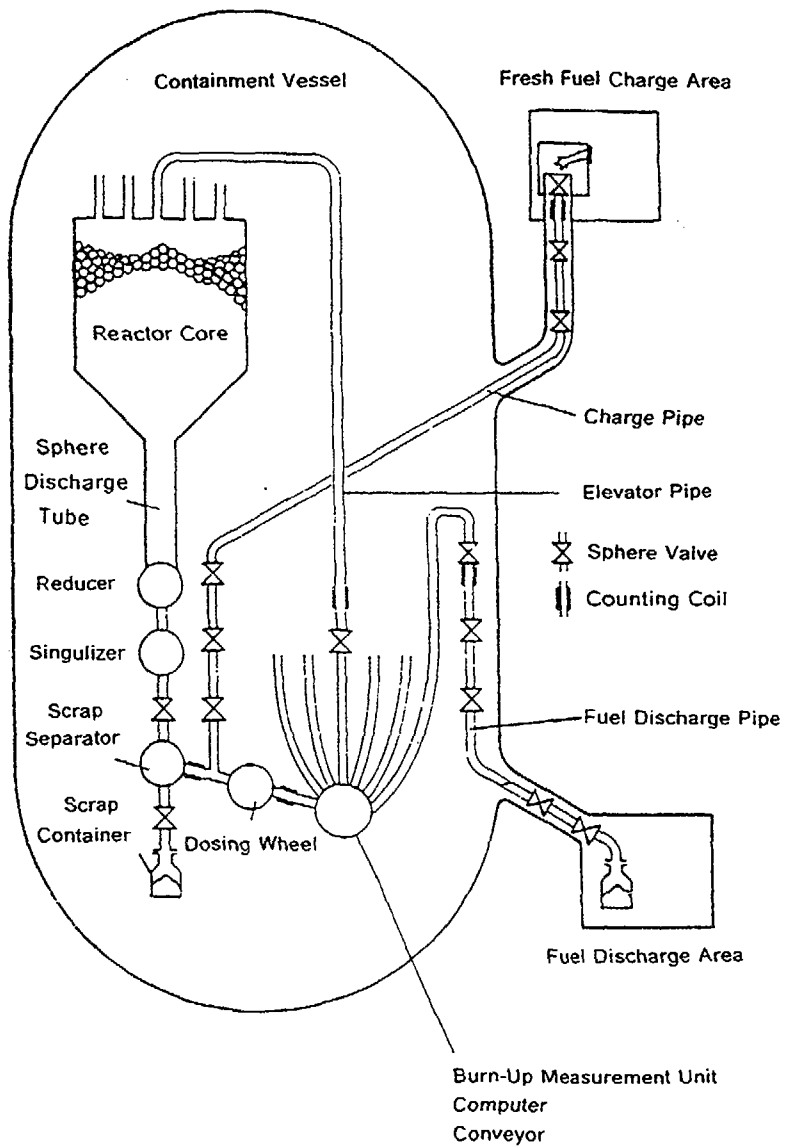


FIG. 2.

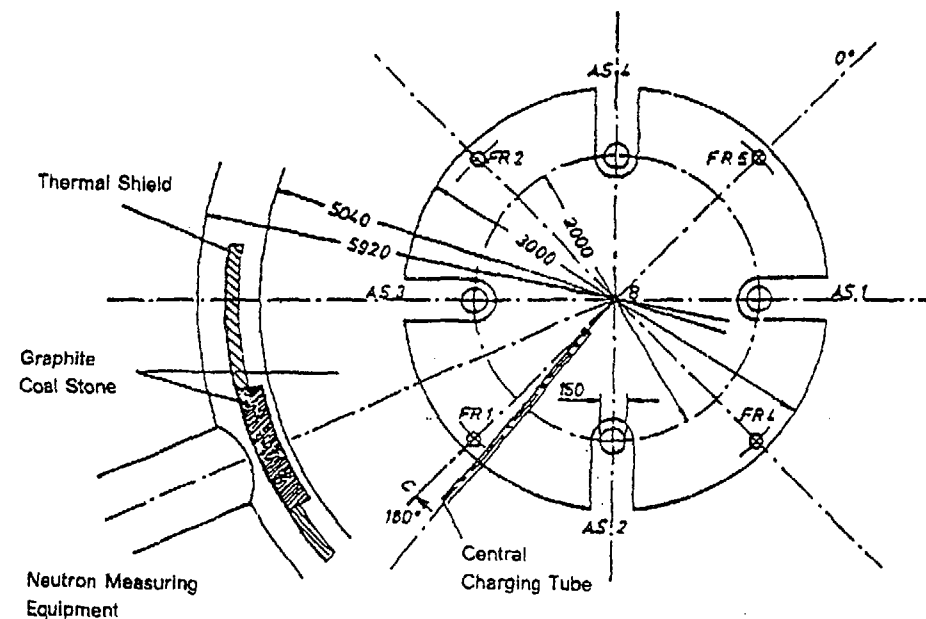


FIG. 3.

ID-Nr. in RTR-2000	1	2	2	3	4	5	6	6	7	8	9					
FE-Type	GFB-3	GFB-4	GFB-5	GK	GO	GLE-1	GFB-1	GFB-2	THTR	GLE-3	GLE-4					
PA-Class	2	2	2	2	2	1	3	3	3	1	1					
Mass U235(g)	1	-	1	-	1	1	1.32	0.08	1	-	1	-	0.96	1	1	
Mass Uges(g)	1.08	-	1.08	-	1.08	1.08	20	20	1.08	-	1.08	-	1.03	10	6	
Mass Th232(g)	-	5	-	5	-	5	5	-	-	10	-	10	10	-	-	
Number of CP-Types	2	2	2	1	1	2	2	2	2	1	1	1	1	1	1	
Fuel	UC2	-	UC2	-	UC0	-	UC2	U02	U02	U02	U02	-	U02	-	U02	U02
Breedmaterial	-	Th02	-	Th02	-	Th02	ThC2	Th02	-	-	-	Th02	-	Th02	Th02	-
Enrichment (%)	90	-	90	-	92	-	93	93	15	07	93	-	3	-	93	10
																16.7

FIG. 4. Summary of AVR fuel element types.

As nuclear data library the 43 group MUPO-Library 5 [3] has been used in DITO [4] with updates from ORIGEN [5] arriving now at a total of 77 isotopes. As an alternative it is planned to integrate the WIMS-D Library [6] into the system. First calculations indicate that predictions with MUPO and WIMS-Libraries show a different sensitivity to spectrum and leakage effects during buckling iterations.

One important point in the HTR model describes the movement of the fuel elements in nine channels of near cylindrical shell shape (Fig. 5). This mesh net is generated in FLIMO and transformed in MAGI to r - z - ϕ geometry. It contains 139 burnup regions where the fuel reshuffling and recycling has to take place. The burn up module has to be fed with one group fluxes obtained from the four group flux solution from the CITATION code [7]. CITATION solves the 3 dimensional model diffusion equation. Fig. 6 and 7 show axial neutron fluxes and radial temperatures for two different reloading stages. A schematic diagram of the two main blocks of HTR-2000 are shown in Fig. 8 with the buckling iteration between spectrum and diffusion calculation.

To follow selected fuel elements within the reactor during its burn up and movement in the core as realistically as possible a further development beyond the 77 isotopes of HTR-2000 has been undertaken starting from the Isotope Generation and Depletion Code ORIGEN [5]. This code has been named HTROGEN. It can solve the burn up equations for 1156 nuclides including such transmutations as

(n, α) -, (n, γ) -, (n, p) -, $(n, 2n)$ - and $(n, 3n)$ -processes.

The code works with three groups of neutron energies and has to be fitted to give the same reaction rates as the four group picture in HTR-2000 (Fig. 9).

For licensing purposes the KFA is obliged to use HTROGEN under safeguard aspects to calculate all fuel inventories and other radioactive materials.

In an earlier test HTR-2000 and HTROGEN were used successfully to follow the reactor operation since September 1982 up to the shutdown in 1988 [8]. It provides results for gamma-activities, shut down heat and the build-up of heavy metal isotopes beyond plutonium.

TOMKU

For the determination of the effective potential scatter cross sections in HTRs with spherical fuel elements of different types the program TOMKU was written. According to the reactor model of the AVR 9 different fuel types in 10 burn up groups are catered for covering 25 spectral zones. Separate calculations are performed for the Thorium 232 and Uranium 238 resonances.

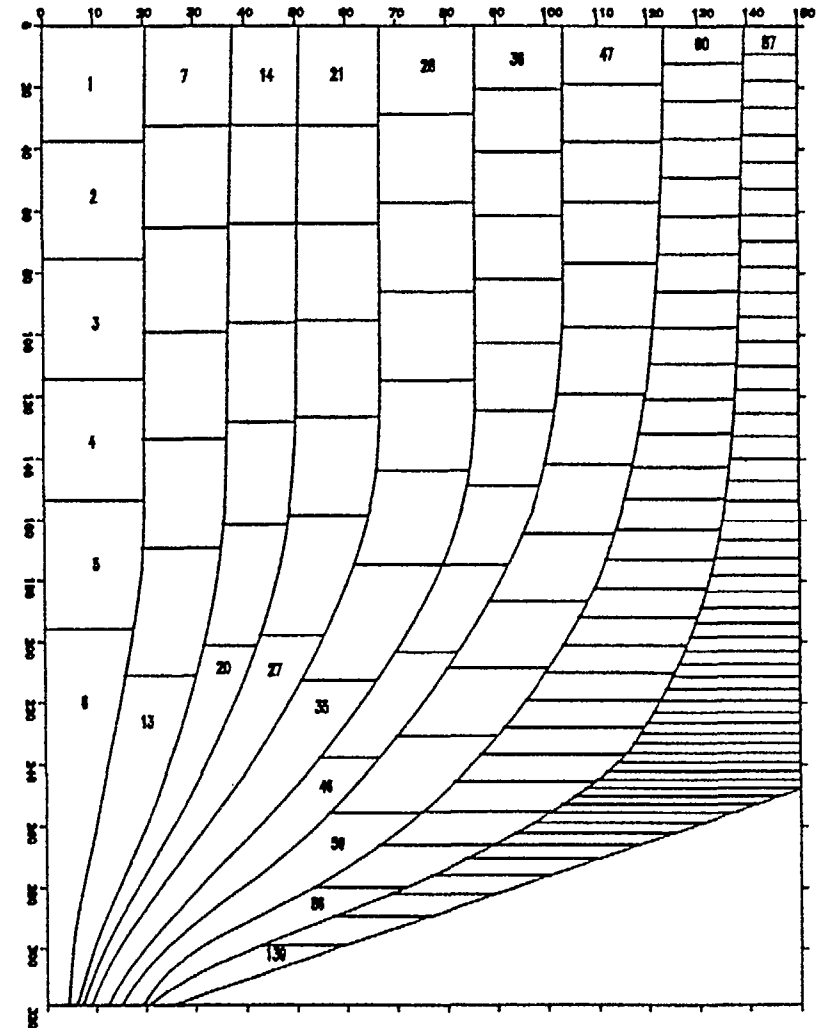


FIG. 5.

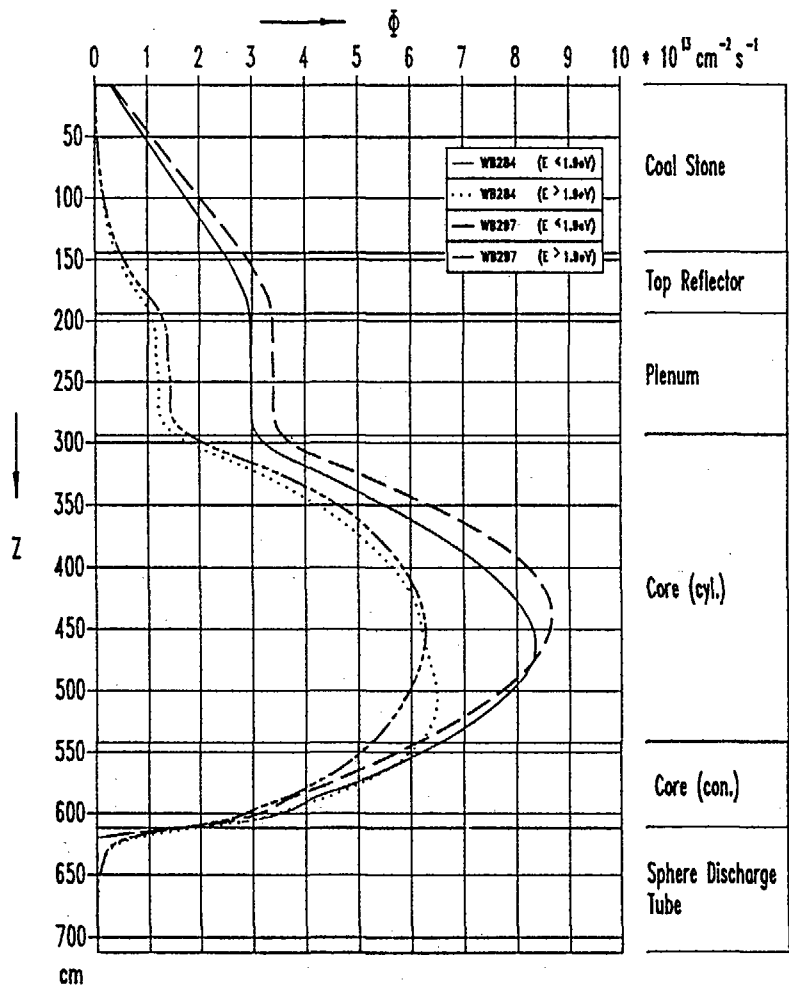


FIG. 6.

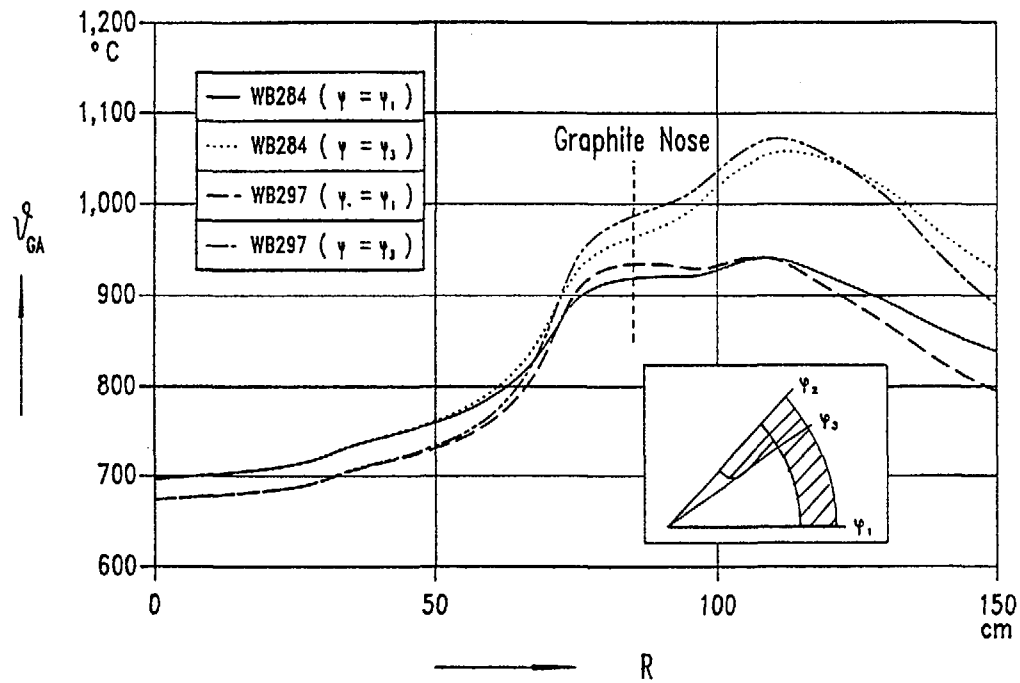


FIG. 7.

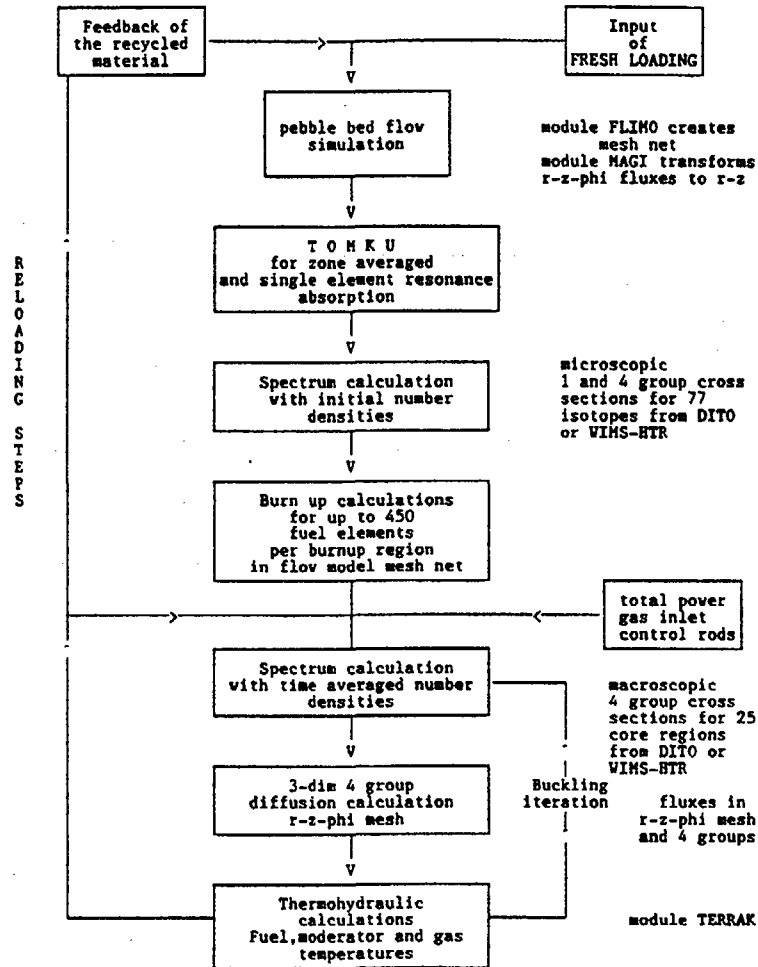


FIG. 8. Flow diagram for reactor physics in HTR-2000.

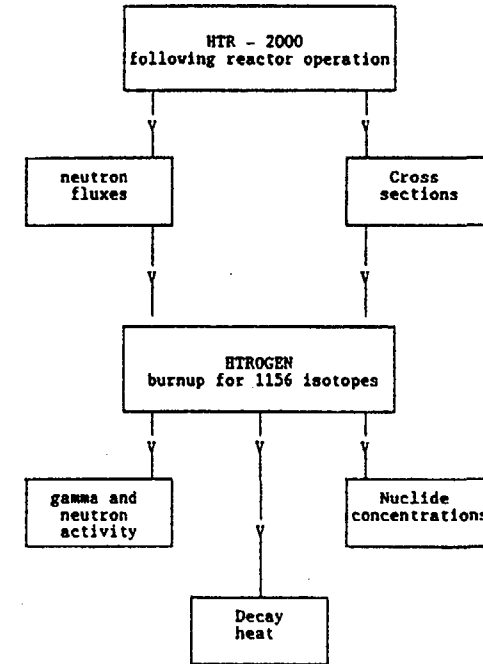


FIG. 9. Tasks for HTROGEN and connections with HTR-2000.

To understand the principle followed by the method one has to realise that the problem of a representative cell calculation has to be solved facing the multitude of different fuel types in a spectral zone. Due to the intimate mixing of graphite with the fuel material in the fuel elements only a weak thermal disadvantage effect occurs, which can be neglected where no absorber elements are dealt with. In the resonance energy range however no such homogenisation can be used in the model. However an equivalent homogeneous system can be constructed from the results of detailed calculations for the resonance energies of Thorium 232 and of Uranium 238 separately.

The basic idea of the method originates from the PROCOL-Method of the UKAEA as also applied at the OECD-DRAGON-Project. This method was applicable to single fuel types of cylindrical fuel cells.

The extensions of the method had to be performed for spherical fuel and to cover a number of up to a few thousand fuel elements per spectrum zone of different type and burnup. The number of unknown flux depressions to be determined can thus be restricted to 360. This is achieved by allowing 10 burn up groups of the 9 fuel element types, each one being represented by the depressions in the kernels, the coatings, the matrix and the outer spherical fuel shell. To account for transmissions these regions are smeared using an equivalent particle cross section Σ_0 .

The most important step of extending the PROCOL-Method is however to define such an average flux depression for the representative spectrum calculation that reproduces the same resonance absorption for Thorium 232 and Uranium 238 as the sum total of the individual fuel elements amounts to. All flux depressions can be expressed as effective potential scatter cross sections for the equivalence principle of resonance absorption. This step is particularly important for mixtures of high and low enriched fuel elements occurring in experimental reactors.

The model flux equations for a single group covering a resonance absorption equivalent to the total resonance integral is written:

$$\Sigma_{T_k} \phi_k V_k = \sum_{i=1}^N [\lambda_i \Sigma_{s,i} \phi_0 + (1-\lambda_i) \Sigma_{s,i} \phi_i] V_i P_{ik} \quad (1)$$

with the following notation:

ϕ_0 asymptotic flux level above the single resonance group
 ϕ_k flux in region k
 Σ_{T_k} total neutron cross section in region k
 V_k volume of region k
 N total number of regions (maximum number = 360)
 λ_i averaged scatter efficiency
 $\Sigma_{s,i}$ scatter cross section of region i
 P_{ik} synthetic collision probability for neutrons arising in region i and colliding in region k

To solve this system of equations an iterative process is needed starting from a vector of guessed ϕ_i -values.

The formula according to which the effective potential scatter cross section is determined in every region i is written as

$$\Sigma_{p_{i,i}} = \Sigma_{T_i} \phi_i / (\phi_0 - \phi_i) \quad (2)$$

A typical P_{ik} -term has the following synthetic structure:

Neutrons in a spectral zone originating in a kernel of type m can collide in the same kernel or in a neighbouring kernel of type m in the same or a neighbouring fuel element and have the following collision probability.

$$P_{mm}^* = P_{mm} + \frac{P_{mB} P_{Bm} (P_{FF} - P_{GG})}{(1 - P_{BB})(1 - P_{GG})} \quad (3)$$

The symbols signify

P_{mm} collision probability of neutrons originating in a kernel of type m having its first collision in the same kernel of type m
 P_{mB} probability of neutrons originating in a kernel of type m to pass to the boundary of the matrix region adjacent to the kernel
 P_{Bm} probability of neutrons originating from the boundary of a matrix region to collide within an equivalent smeared particle
 P_{BB} transmission probability of equivalent smeared particle having a smeared cross section Σ_0
 P_{GG} collision probability of equivalent smeared particle having a smeared cross section Σ_0
 P_{FF} collision probability for the neutrons originating from a smear of kernel and matrix regions within the spherical shell of a fuel element to collide within the same or a neighbouring fuel smear. This term is again synthetic as shown below.

Amongst others this term includes the Dancoff-Factors and equals unity for an unlimited system of coated particles. Then it is written

$$P_{mm} = P_{mm} + P_{mB} P_{Bm} / (1 - P_{BB}) \quad (4)$$

$$P_{FF}(A) = Q_{FF}(A) + \frac{Q_{FS}(A) Q_{SF}(A) N(A)}{N_{TOT} - Q_{SS}(A) N(A) - Q_{SS}(B) N(B) - \dots} \quad (5)$$

It contains the statistical boundary condition that the probability to meet as a neighbouring fuel element one of the M fuel elements contained in the spectrum zone under consideration is 1/M. In this term the multicell point of view is assumed allowing different fuel types and burnup stages.

Here $Q_{FF}(A)$ stands for the collision probability of neutrons originating in a kernel of a single fuel element of type A to collide in the same fuelled region contained in the spherical shell of the same fuel element.

$Q_{FS}(A)$ stands for the transmission probability for neutrons originating in the fuelled region of a fuel element of type A to reach the outer boundary of the outer spherical graphite shell of the same fuel element

$Q_{sr}(A)$ stands for collision probability for neutrons originating from such an outer boundary to collide within the fuelled region of type A fuel elements

$Q_{ss}(A)$ stands for the transmission probability for neutrons crossing whole fuel elements of type A

$N(B)$ is the number of fuel elements of neighbours of type B in the same spectrum zone

N_{TOT} is the sum total of all fuel elements of all fuel types (and burnup groups) present in the spectrum zone

To obtain the formula for the effective potential scatter cross section representing the resonance absorption of all fuel types present in a spectrum zone a proper averaging has to be performed.

$$\int_k N_k \cdot V_k \cdot RI(\Sigma_{pk}) = RI(\Sigma_{p,v}) \int_k N_k V_k \quad (6)$$

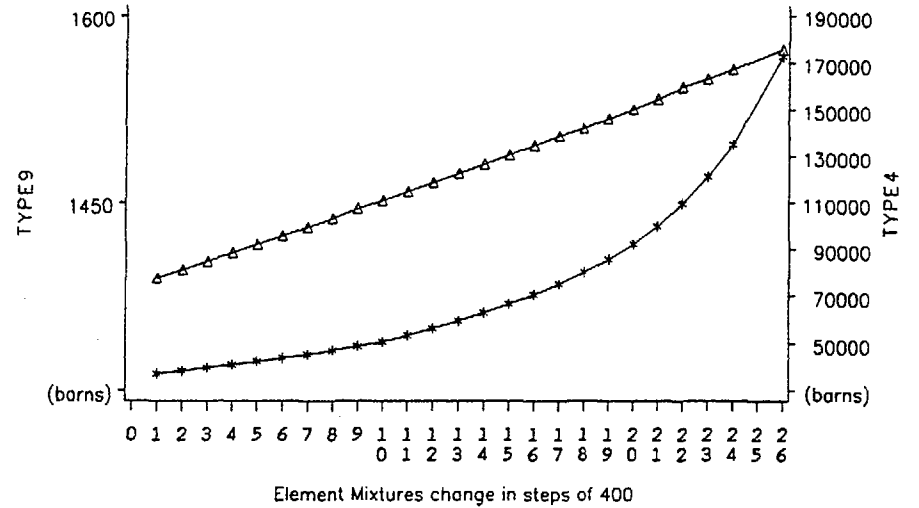
The sum goes over all fuel element types including their burn up groups. Here RI stands for the total resonance integral at the potential scatter cross section Σ_p . With this formula it is ascertained that using $\Sigma_{p,v}$ as the effective potential scatter cross section for a representative spectrum calculation the resonance absorption of all resonance material present in the spectrum zone is preserved.

Fig. 10 and 11 are shown at the meeting as demonstration of TOMKU results.

COMPARISON OF GLE-4 AND GO FUEL EXPERIMENTS WITH CALCULATIONS

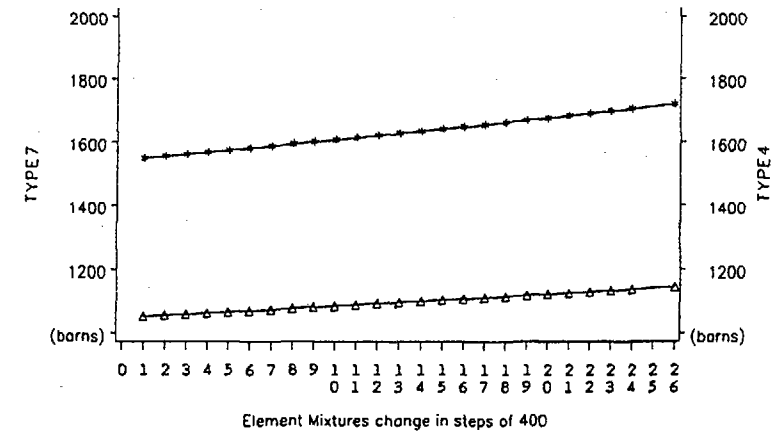
In table 1 an overview of the heavy metal inventories of GLE-4 and GO fuel experiments are shown as measured in the Austrian Research Center at Seibersdorf. The GLE-4 elements had been added through the central fuelling tube, whilst the GO elements have been added through the outer tubes and were recycled a number of times.

As a consequence for the GLE-4 experiment which was added to the core during the reloading step 305 averaged values over the four central channels are compared with the measurements. First results in table 2 show the Pu-Isotopes as calculated with HTR-2000 following the reloading steps in detail, that is to say, a new flux distribution is calculated in successive time intervals of about fourteen days using one group cross sections only, once calculated with DITO and once with WIMS-HTR.



The number of LEU Elements is decreasing from left to right in steps of 400 from 10000 to 1

Fig.10 Sign Values of U238 for Mixtures of 10000 Elements
LEU(Type9)=Triangle HEU(Type4)=Star obtained with TOMKU



The number of THTR Elements is decreasing from left to right in steps of 400 from 10000 to 1

Fig.11 Sign Values of Th232 for Mixtures of 10000 Elements
THTR(Type7)=Triangle AVR(Type4)=Star obtained with TOMKU

TABLE 1. EXPERIMENTAL INVENTORY OF HEAVY METALS FOR AVR FUEL EXPERIMENTS Measured in OEFZS (given here in rounded figures)

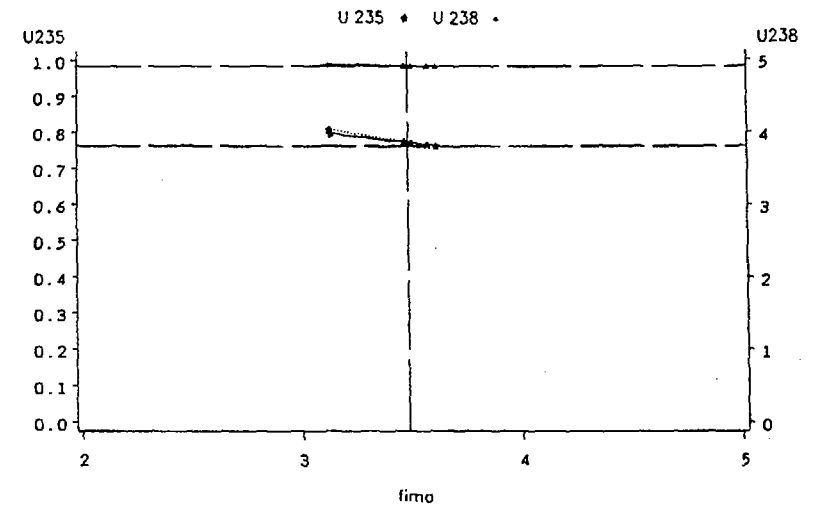
Fuel Type	FIMA (%)	Pu238 mg	Pu239 mg	Pu240 mg	Pu241 mg	Pu242 mg
GLE4	3.48	0.018	18.47	4.038	0.732	0.056
GO 1	10.5	0.674	0.661	0.448	0.206	0.099
GO 2	7.51	0.129	0.651	0.253	0.073	0.015

Fuel Type	FIMA (%)	U233 mg	U234 mg	U235 g	U236 g	U238 g
GLE4	3.48	--	--	0.761	--	4.912
GO 1	10.5	69.7	10.3	0.303	0.11	0.063
GO 2	7.51	46.3	7.64	0.482	0.08	0.068

As a second model HTROGEN was used to predict the burn up of the heavy metals. Starting with the same core situation (the reloading stage 305) the fuel elements were allowed to pass through a central channel but this time not with 1 group of neutron energies but 4 groups were used giving smoother spectrum transitions.

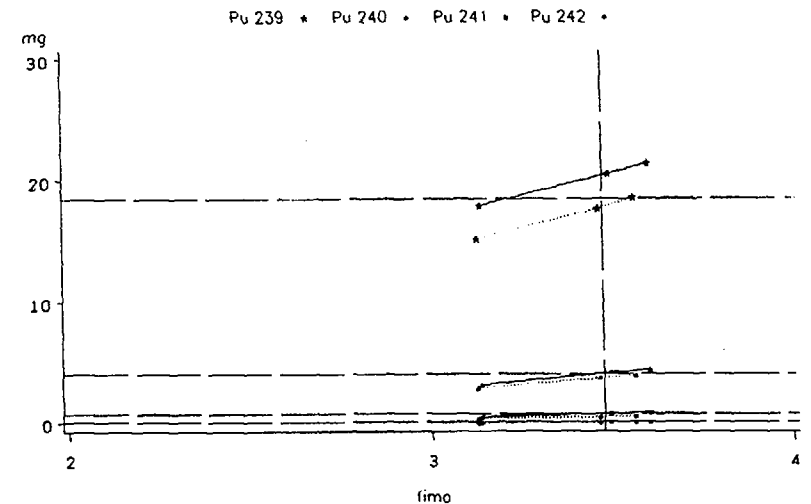
In both cases the FIMA value measured was used instead of a time scale as the basis of the comparison (Fig. 12 and 13). For the prediction of the heavy metal inventory of the GO fuel experiments the core situation at the start of the reloading stage 280 has been kept fixed (Fig. 14 to 21). No alternative cross section set could be produced with WIMS-HTR before the meeting. Results are presented from HTROGEN calculations using DITO to produce the neutron cross sections.

For the higher burn ups of fuel elements to be analysed in the future a disadvantage factor effect should arise. Use of WIMS-HTR would allow for such an option in the future. The reason for the late appearance of this effect is apart from the homogeneity of the fuel to thermal neutrons due to the compensation by the power normalisation of the reactor. Whilst the first purpose of calculations with HTR-2000 are to follow the reactor operation and to serve as a flux distribution supplier to HTROGEN the overprediction of important Pu-isotopes is often welcome for gaining upper limits in safety calculations, the demands and requirements of which have been growing steadily lately (Inclusion of Pu238 in the prediction that was not available in HTR-2000).



horizontal and vertical lines show experimental values

Fig.12 URANIUM-ISOTOPES (g) for GLE-4 vs. FIMA (%) from HTROGEN (DITO in full and WIMS-HTR in broken lines)



horizontal and vertical lines show experimental values

Fig.13 PLUTONIUM-ISOTOPES (mg) for GLE-4 vs. FIMA (%) from HTROGEN (DITO in full and WIMS-HTR in dotted lines)

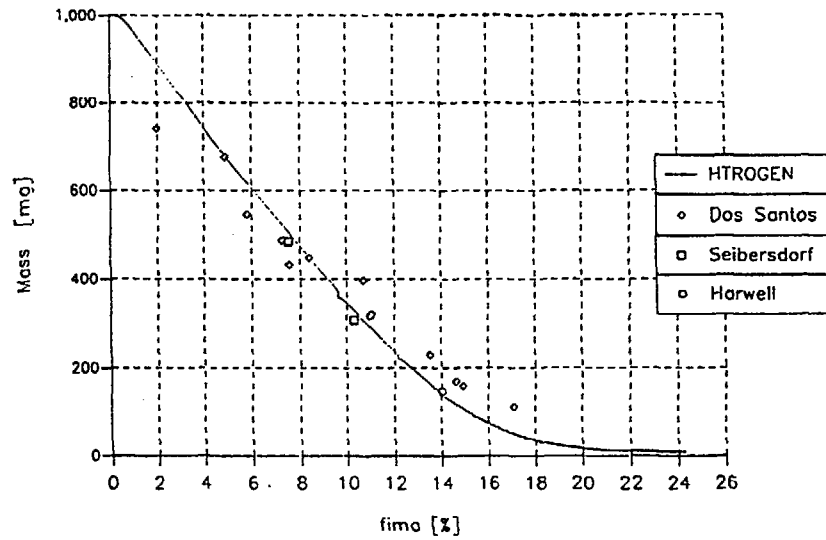


FIG. 14. Type of fuel element: GO U-235

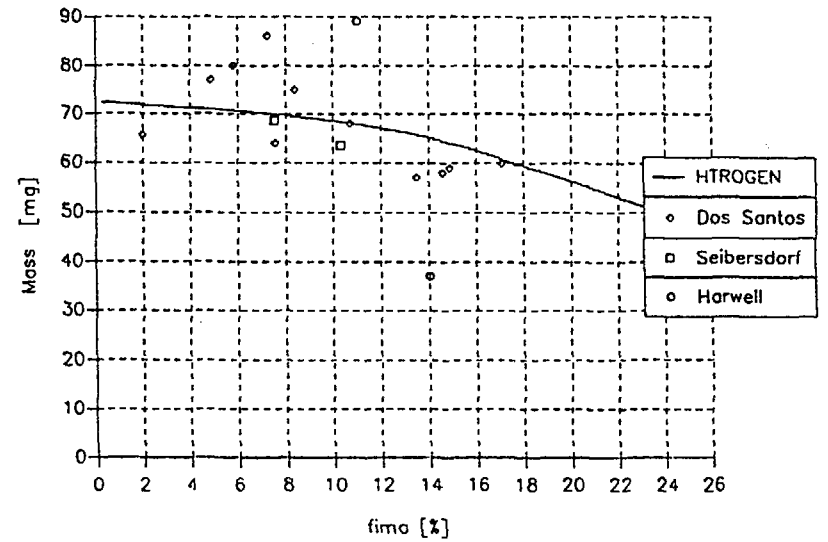


FIG. 16. Type of fuel element: GO U-238

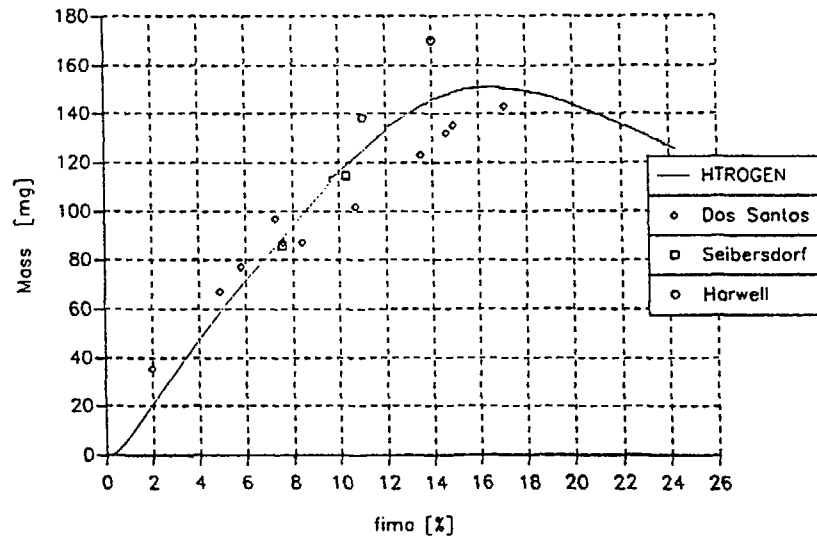


FIG. 15. Type of fuel element: GO U-236

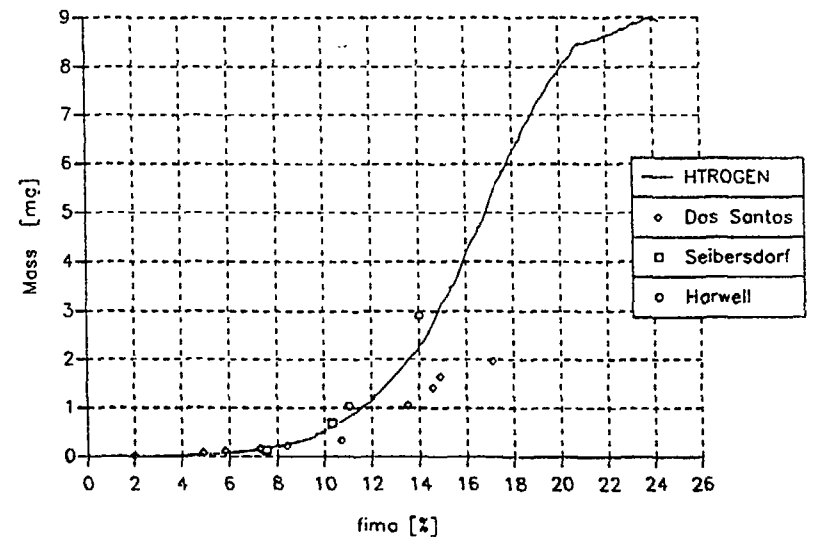


FIG. 17. Type of fuel element: GO Pu-238

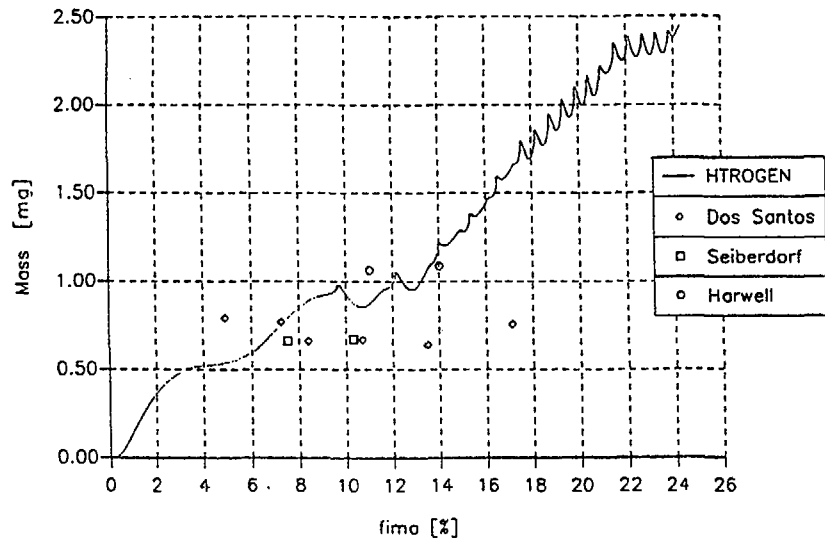


FIG. 18. Type of fuel element: GO
Pu-239

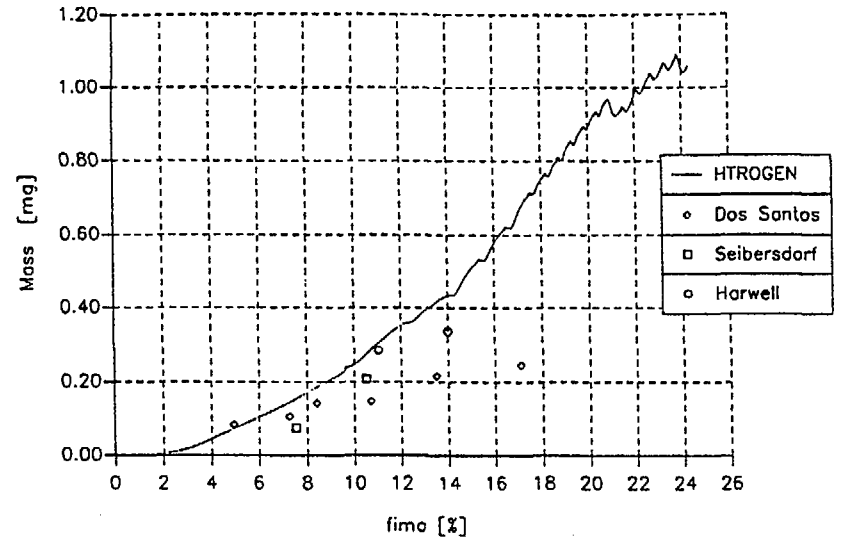


FIG. 20. Type of fuel element: GO
Pu-241

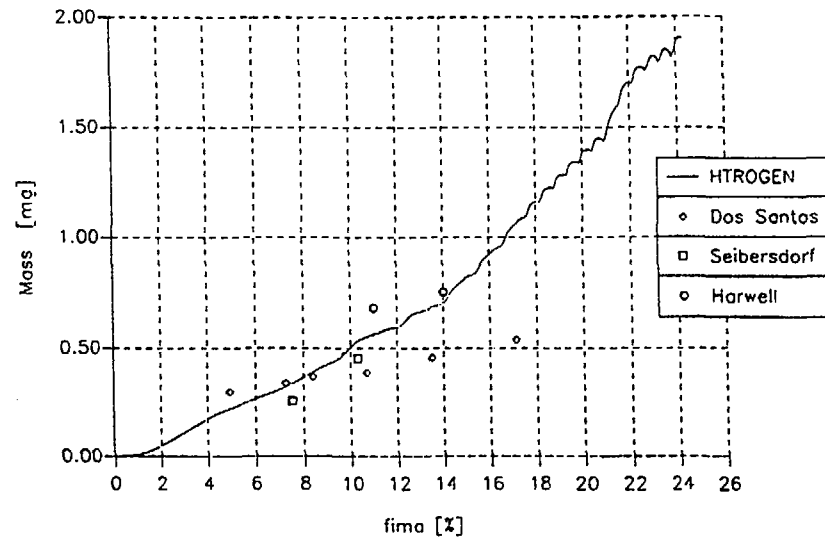


FIG. 19. Type of fuel element: GO
Pu-240

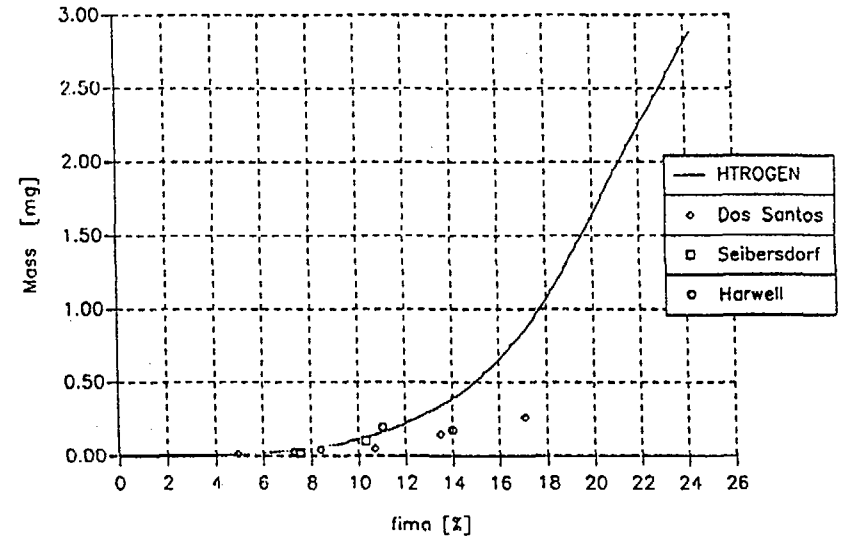


FIG. 21. Type of fuel element: GO
Pu-242

Table 2: Comparison for GLE-4 fuel experiment with HTR-2000

Isotope	Averaged Pu-weights over 4 central channels				
	Cross sections from			Cross sections from	
	Experiment (mg)	DITO (mg)	difference (%)	WIMS-HTR (mg)	difference (%)
Pu 239	18.48	19.9	+ 7.6	16.7	-10.6
Pu 240	4.04	3.82	- 5.8	3.35	- 8.3
Pu 241	0.73	0.66	- 9.4	0.54	- 7.4
Pu 242	0.56	0.049	- 8.8	0.047	- 8.3

EXPERIMENTAL WORK

Within the framework of a collaborative program between KFA and OEFZS a total of further 24 spent AVR fuel elements are to be analysed. The following table shows a summary of element types and ranges of FIMA values as measured by KFA before shipment to Austria.

Table 3: Further AVR fuel elements to be analysed

Element type	FIMA (%)	Number of elements
GO	8 - 21	9
THTR	12.5	3
GLE3	7 - 10	8
GLE4	9.1 - 17.4	4

The analysis will consist of heavy metal inventory and burnup determination.

REFERENCES

- [1] H. Werner, F. Thomas:
HTR-2000: Programmzyklus zur nuklearen und thermodynamischen Berechnung von Kugelhaufenreaktoren - eingesetzt zur rechnerischen Betreuung der AVR-Leistungsfahrt
Vortrag: Jahrestagung Kerntechnik Mai 1989

F. Thomas:
HTR-2000: Programmcode zur rechnerischen Betriebsbegleitung von HTR's
Jül.-Report: Jül-2261, Jan. 1989

- [2] F. Woloch:
Ertüchtigung theoretischer Methoden für die Coreauslegung des HTR
OEFZS-A-1260, EA-322/88
- [3] W. Gießler, et al.:
Die neue MUPO-Datenbibliothek (Library 5)
Arbeitsbericht E1-69/3
BBC/KRUPP
Mannheim 1969
- [4] H. Werner, F. Thomas, F. Woloch:
Bericht in Vorbereitung
- [5] Bell:
ORIGEN - the ORNL Isotope Generation and Depletion Code
ORNL-4628-73
- [6] M.J. Halsall, C.J. Taubmann:
The "1989" WIMS NUCLEAR DATA LIBRARY
AEEW-R 1442, Sept. 1983
- [7] T. Fowler et al.
Nuclear Reactor Core Analysis Code: CITATION
ORNL-TM-2496, Rev. 2, Oak-Ridge 1971
- [8] H. Werner, F. Thomas, G. Falta, G. Reitsamer, A. Strigl, F. Woloch, A. Baxter:
Aufbau der Plutonium-Isotope in LEU-Brennelementen - eingesetzt im AVR-Reaktor - Vergleich zwischen Vorausrechnung und chemischer Analyse
Vortrag: Jahrestagung Kerntechnik Mai 1989
- [9] J.R. Askew et al.
A general description of the lattice code WIMS
Journal of the British Nuclear Energy Society
Vol.5, No.4, p.564 (1966)

FRENCH EXPERIENCE IN THERMOHYDRAULICS CALCULATIONS OF GAS COOLED REACTORS

F. BOUTARD, G. CARVALLO, G. CHEVALIER

CEA, Département des études mécaniques
et thermiques,
Centre d'études nucléaires de Saclay,
Gif-sur-Yvette, France

Abstract

For the different kinds of gas-cooled reactor built in France, the CEA has developed several versions of a thermohydraulics computer code which simulates the long-term behavior of these gas-cooled reactors.

The code, called LOTE, computes the thermohydraulic processes occurring in the primary flow circuit of these reactors, whether integrated in concrete vessels or built with outer loops.

The fact that the reactor is modeled by a succession of independent boxes permits the computation of transient behavior and the study of scenarios lasting several days.

These models include the entire primary flow circuit and the main heat exchangers, shutdown heat exchangers, blowers and the different materials making up the core.

The calculation simulates the temperature variations in the materials with convection and conduction processes to remove the thermal power during shutdown transients.

The code has been a decisive asset for recent studies concerning reactor safety, operation and maintenance.

1 INTRODUCTION

France has developed two types of gas-cooled reactor, the outer loop model (Chinon power plant) and the so-called integrated model (Saint Laurent and Bugey power plants).

These two types of reactor have common technological features :

- a prestressed concrete vessel with a steel liner, the vessel being cooled by water tubes,

- four high-power blowers driven by steam or electricity,
- steam generators: in the integrated models, these generators are placed in the vessel, below the core.

In the earlier reactors of the series, the cooling gas flow in the core was upflow, and subsequently downflow in the later reactors.

The fuel rods are of three types :

- tubular or tubular with graphite core (Saint Laurent and Chinon): the graphite core rods display better mechanical strength,
- annular (Bugey): this type of rod has a larger heat exchange surface with CO₂, and the uranium is cooler.

The shutdown of Chinon 3, planned for June 1990, has raised questions concerning the operation of the reactor, especially in its shutdown phase. These problems will be analyzed with the LOTE code, a thermohydraulics code developed for studies related to the safety, operation and maintenance of gas-cooled reactors.

2 THE LOTE CODE

The LOTE code was developed by the CEA to calculate the cooling of the primary flow circuit of GCR reactors over long periods (up to several months) in accidental conditions (e.g. depressurization or blower shutdown).

Over these long periods, the object is more to check the heat balance of the reactor than to perform an exact quantitative simulation of reactor operation. This allows for greater latitude in the choice of simplifying assumptions.

2.1 Assumptions

The following assumptions are made :

- The system, which includes the entire primary cooling circuit and the heat exchangers, is treated unidimensionally. The blowers and the core have parallel streams.
- The CO₂ pressure and overall flow rate in the circuit are assumed to be uniform at every point of the reactor, at any given time. The properties of the CO₂ are calculated in accordance with these values.
- The CO₂ equations are processed in steady-state conditions at each time step.
- The main heat exchangers are represented by two models, at the choice of the user :
 - a model with water side phase change,

- a model in which the water side is ignored, but the CO₂ outlet temperature of the exchangers is imposed.

The assumptions selected also include those concerning heat exchanges taken into account in the code :

- Removal of heat across the outer wall by conduction in the heat insulation.
- In the core, subdivided into families of channels (see figure 5) of the same radial power, heat exchanges concern exchanges between materials or CO₂/materials exchanges :
 - Between the CO₂ and materials in contact (clad, jacket), exchanges take place by convection.
 - Axial conduction takes place in the graphite bricks and jackets of the different channels. Radial conduction occurs between the bricks of the adjacent channels. In channel, radiation takes place between the brick and the jacket, and pure conduction in the CO₂ gap between them. Radiation between the jacket and the clad is also taken into account.
- In the heat exchangers, and if the water side is analyzed, exchange takes place by convection between the water, or steam, and the tubes. Similarly, heat exchange takes place by convection between the CO₂ and the tubes.

2.2 Modeling

The geometric model selected consists of successive 'boxes' representing the different parts of the reactor. These 'boxes' are covered in closed circuit by the cooling gas, which is either CO₂, or air in the case of injection. Figure 4 shows the model adopted for the Chinon A3 reactor.

2.3 General calculation principle

The general calculation principle is based on the cooling of the materials making up the reactor, taking place by convection through the gas flowing in the circuit.

In each 'box' described above, where the mass of the materials exchanges energy with CO₂, the thermal inertia of each material is initially calculated:

$$X = M C_p T_m$$

where:

- M mass of the material (kg),
- C_p specific heat (J/kg per °C),
- T_m material mean temperature (K).

The heat flux exchanged with the CO₂ is :

$$\Phi = HS \left(T_m - \frac{T_e + T_s}{2} \right)$$

where:

- H convection heat transfer coefficient (W/m² per °C),
- S surface in contact with CO₂ (m²),
- T_e and T_s CO₂ inlet and outlet temperature (K).

By writing that the energy in the materials is reduced by:

$$\frac{dX}{dt} = -\Phi$$

a first-order differential equations system is obtained. The solution of this system serves to determine the changes in thermal inertia and the temperatures of the materials at each time step.

The CO₂ side balance is written:

$$\Phi = Q C_p (T_s - T_e)$$

where:

- Q CO₂ flow rate (kg/s),
- C_p specific heat (J/kg per °C).

Thus, if the average temperature of the material is known, the CO₂ outlet temperature T_s can be calculated. Hence, at each time step, it suffices to know an inlet temperature in a 'box' to determine all the CO₂ temperatures in succession. The state of the CO₂ at each time step is calculated in steady-state conditions. The convergence of these conditions is achieved by successive iterations between the flow rates and pressures on the one hand, and the temperatures on the other.

The momentum equation can be written in steady-state conditions for each 'box':

$$\Delta P = P_e - P_s = A'(I) Q + B(I)$$

by setting:

- A'(I) = A(I) Q by linearization of the pressure drop equation at time t,
- A'(I) is a function of friction and velocity,
- B(I) is the gravitational acceleration term,
- P_e and P_s are the inlet and outlet pressures of the 'box' considered.

Once the circuit is scanned, we can write:

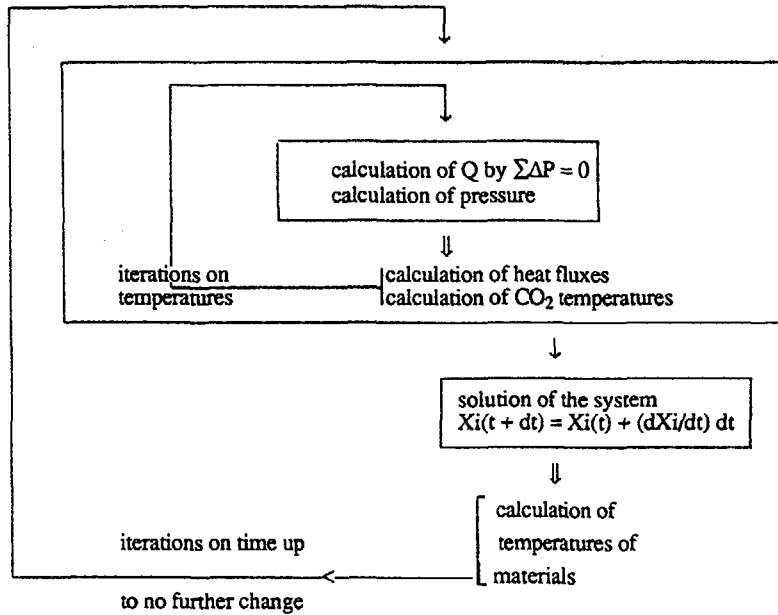
$$\Sigma[A'(I) Q + B(I)] = 0$$

and a CO₂ flow rate is determined.

Iteration is carried out on the flow rate until the relative difference between two successive flow rates is smaller than the required accuracy. The gas pressure is calculated at each time step as a function of the masses of CO₂ in the circuit.

2.4 Operation of the code

The operation of the code is illustrated in the flow chart below.



SOLUTION OF THE SYSTEM

The N equations $X_i(t + dt) = X_i(t) + dX_i/dt$ form a non-linear system of first-order differential equations with respect to time. The initial values of the unknowns $X_i(t)$ (thermal inertia of the reactor material i) are given. The overall system is solved by a method which is a modified form of the Adams Pece formulas [1]. The time step is adjusted automatically to check the local error.

A local extrapolation method is used to improve stability and accuracy. A round-off error check is performed, and execution is stopped if the desired accuracy is not achieved. The local error check is carried out as follows. For the calculation on a time step to be acceptable, it is necessary that :

$$\left[\begin{array}{c} N_{eq} \text{ local error} \\ \sum_{L=1} \left(\frac{\quad}{WT(L)} \right)^2 \end{array} \right]^{1/2} \leq \epsilon$$

where:

- N_{eq} number of equations,
- $WT(L)$ weight of unknown L in the error calculation,
- ϵ desired tolerance (set at 10^{-4}).

In the LOTE code, the value of the weights is taken as the absolute value of the unknowns, i.e. the tolerance set is in fact a relative accuracy. This is true unless the unknowns are zero, in which case the weights are taken as 1, and the tolerance represents an absolute accuracy.

3 EXAMPLES

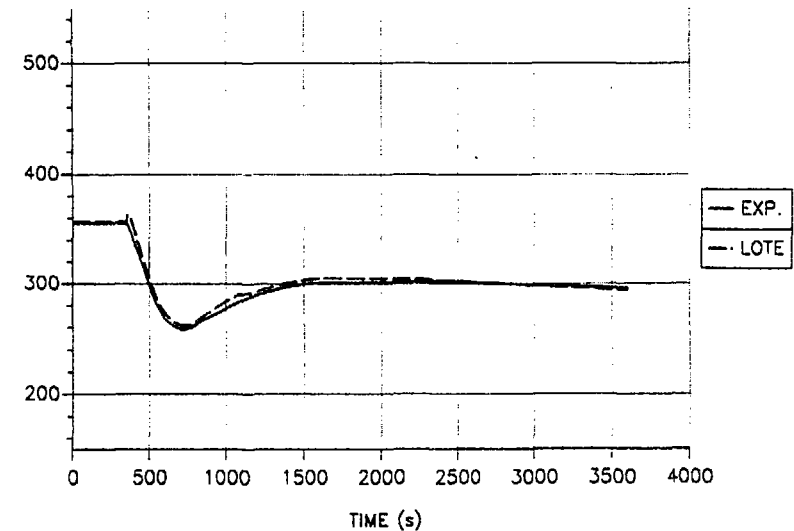
We provide examples of two cases of transient calculations for the Chinon A3 reactor.

3.1 Shutdown case

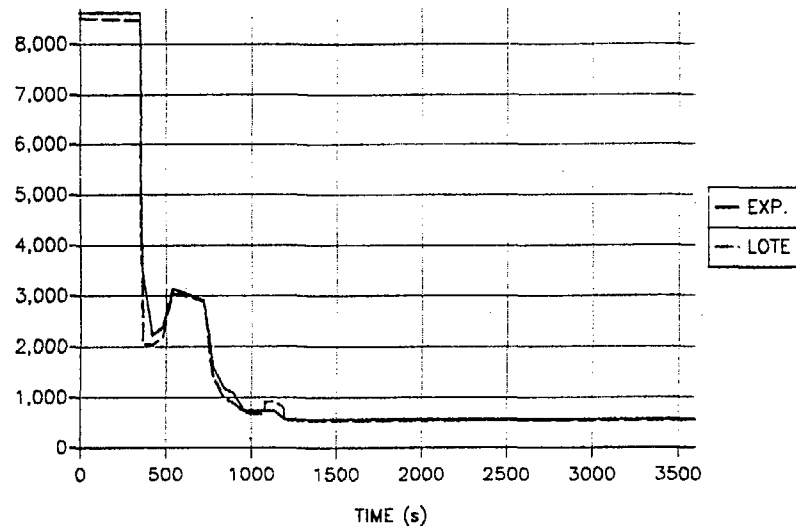
The shutdown occurs on the reactor operating at 1200 MWt. The rod drop lasts 350 s. One of the four blowers is shut down.

Figure 1 shows the comparison curve between the calculation and the readings of the power plant for the core outlet temperature. Figure 2 shows the comparative curves for the CO_2 flow rate. These curves, plotted over one hour of operation of the reactor, show good agreement between the changes in the CO_2 outlet temperature and the flow rate, resulting from the calculation, with the readings made at the Chinon power plant.

EXIT CORE TEMPERATURE (DEG C)



- Fig. 1 -
COMPARISON BETWEEN LOTE AND MEASUREMENTS

CO₂ FLOW (kg/s)

- Fig. 2 -
COMPARISON BETWEEN LOTE AND MEASUREMENTS

3.2 'Thermosiphon' case

The test occurs during stable operation at 1100 MWt. A rod drop occurs, with shutdown of the four blowers and operation in thermosiphon mode. Figure 3 shows the comparative curves of the core outlet temperature between the calculation with the LOTE code and the power plant readings. This comparison is made over 4 h. The difference between the two curves, which remains constant, can be explained by the uncertainty on the hydraulic resistance of the blowers at shutdown.

We find that the calculations for the LOTE code show very good agreement with reality, in view of the foregoing comparisons, both in the medium term and the long term.

4 CONCLUSIONS

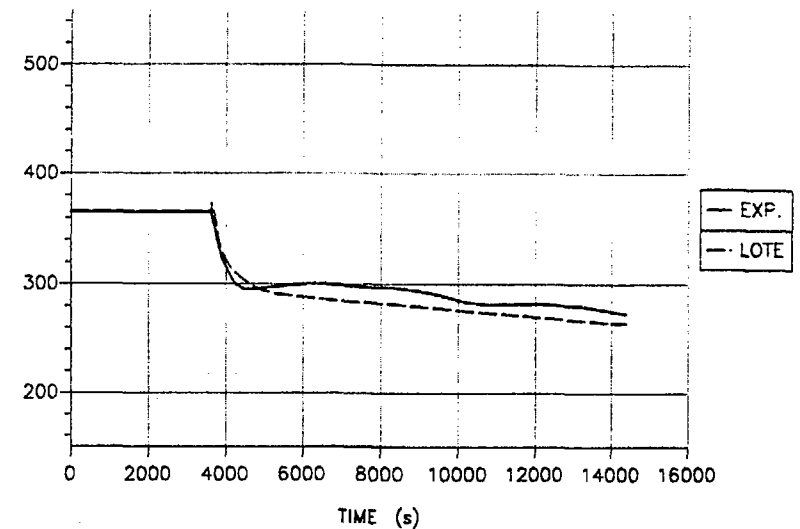
The LOTE code has been developed and used for the past five years. The modeling and solution flow chart it applies have been progressively refined in order to:

- approach more closely the power plant readings,
- predict the long-term changes, while complying with the physics of the accident processes.

The following factors have been identified as especially important :

- radial and axial zoning of the reactor,
- fine modeling of the heat exchanger during the disturbed phases (drying of the water side, for example),
- the accurate knowledge of the blower characteristics at low speed.

EXIT CORE TEMPERATURE (DEG C)



- Fig. 3 -
COMPARISON BETWEEN LOTE AND MEASUREMENTS
Thermosiphon

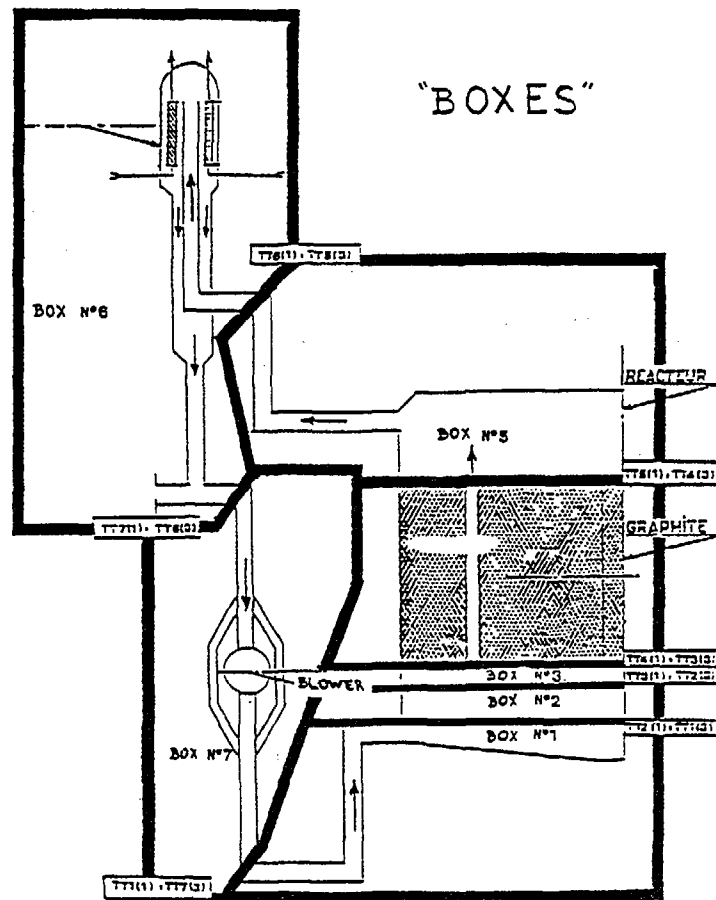


FIG. 4.

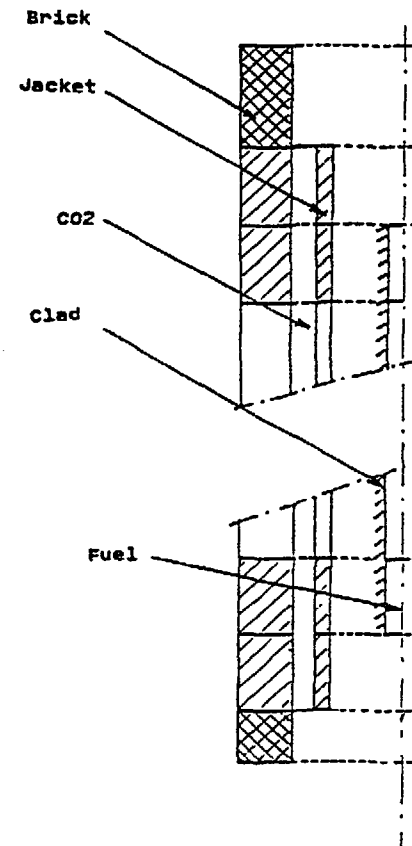


FIG. 5.

REFERENCE

- [1] Computer solution of ordinary differential equations, The initial value problem
L.F. Shampine and M.K. Gordon, Sandia Laboratories and University of New Mexico, W.H. Freeman and Company, San Francisco.

PROGRESS AND PROBLEMS IN MODELLING HTR CORE DYNAMICS

The TINTE code tested at AVR power transients

W. SCHERER, H. GERWIN

Institut für Sicherheitsforschung und Reaktortechnik,
Forschungszentrum Jülich GmbH,
Jülich, Federal Republic of Germany

Abstract

In recent years greater effort has been made to establish theoretical models for HTR core dynamics. At KFA Jülich the TINTE (Time dependent Neutronics and TEmperatures) code system has been developed, which is able to model the primary circuit of an HTR plant using modern numerical techniques and taking into account the mutual interference of the relevant physical variables. The HTR core is treated in 2-D R-Z geometry for both nucleonics and thermo-fluid-dynamics. 2-energy-group diffusion theory is used in the nuclear part including 6 groups of delayed neutron precursors and 14 groups of decay heat producers. Local and non-local heat sources are incorporated, thus simulating gamma ray transport. The thermo-fluid-dynamics module accounts for heterogeneity effects due to the pebble bed structure. Pipes and other components of the primary loop are modelled in 1-D geometry. Forced convection may be treated as well as natural convection in case of blower breakdown accidents.

Validation of TINTE has started using the results of a comprehensive experimental program that has been performed at the Arbeitsgemeinschaft Versuchsreaktor GmbH (AVR) high temperature pebble bed reactor at Jülich. In the frame of this program power transients were initiated by varying the helium blower rotational speed or by moving the control rods. In most cases a good accordance between experiment and calculation was found.

Problems in modelling the special AVR reactor geometry in two dimensions are described and suggestions for overcoming the uncertainties of experimentally determined control rod reactivities are given. The influence of different polynomial expansions of xenon cross sections to long term transients is discussed together with effects of burnup during that time.

Up to now the TINTE code has proven its general applicability to operational core transients of HTR. The effects of water ingress on reactivity, fuel element corrosion and cooling gas properties is now being incorporated into the code.

1. Introduction

The core dynamics of pebble bed high temperature reactors is characterized by the inherent properties of this reactor type, namely

- low power density
- large heat capacity
- negative temperature/reactivity feedback in all situations.

These lead to a generally very smoothly reaction of the system to changes in the operational parameters. Concerning mathematical and computational modelling of the dynamic behaviour, the relative strong coupling between nuclear and thermofluidal physical parameters plays an important role. Independent treatment of these two blocks has been shown to produce inadequate results. This holds true especially in accident situations when after some delay time a subcritical system may regain criticality. Such situations are mostly related to the ingress of a large amount of steam or water from the secondary loop into the primary system in case of steamgenerator failures.

The probability of accident scenarios in this domain was found to be very small but nevertheless at least the public opinion claims for demonstration of avoiding catastrophic consequences in these cases, too.

Therefore in recent years greater effort has been made to establish theoretical models for HTR core dynamics. At KFA Jülich the TINTE code system has been developed, which is able to model the primary circuit of an HTR plant using modern numerical techniques and taking into account the mutual interference of the relevant physical variables. The final goal is to prepare a tool for demonstration of the inherent passive selfstabilizing features of the pebble bed high temperature reactor. Within this scope a code like TINTE has to be able to describe not only neutronics and thermofluid-dynamics but also the effects of severe water and air ingress accidents with respect to corrosion, combustion and nuclear reactivity.

Validation of such a code system is a major task and because of the broad field of phenomena to be modelled asks for detailed experimental data in several areas. As a starting point the dynamics experiments at the Arbeitsgemeinschaft Versuchsreaktor GmbH (AVR) pebble bed reactor in Jülich (FRG) were used to validate the TINTE nucleonics and fluid-dynamics moduls.

2. The TINTE Code System

The TINTE (Time dependent Neutronics and TEmperatures) code system is being developed at the KFA Forschungszentrum Jülich Institute for safety research and reactor technique (ISR) /1,2/. It is planned to model the primary loop of pebble bed high temperature reactors including operational and safety related transients up to the description of severe hypothetical accident scenarios. The actual version provides moduls for neutron dynamics, thermodynamics and thermo-fluid-dynamics. Further development concentrates on nuclear, fluid-dynamic and chemical effects induced by ingress of large amounts of water, steam or air into the primary circuit in case of hypothetical accidents.

The model of the mutual feedback effects is based on the following considerations:

- The nuclear power production is coupled with changes in spectrum averaged cross sections due to temperature and other feedback effects, e.g. buckling, Xe- and steam-concentration.

- The temperature is governed by nuclear heat production, heat transport in the cooling gas, heat conductivity in fuel and graphite, and radiation.

- The large heat capacity of the graphite causes overall temperature changes to be very slow. Even small temperature deviations however, especially in the inner part of the fuel elements result in a sensitive feedback to the nuclear behaviour. The heat produced in the coated particles is transferred very rapidly to the graphite matrix (in about 1 ms). The transport of the heat to the fuel element surface takes about 30 s from where it is removed by the coolant, by global heat conduction and radiation. Because of these reasons a heterogeneous treatment of temperature is necessary.

- The modelling of the reflector nuclear and temperature feedback demands at least two spacial dimensions.

- The description of most of the out-of-core parts in the primary loop requests an additional network for gas flow handling.

Following these considerations the HTR core is treated in 2-D R-Z geometry for both nucleonics and thermo-fluid-dynamics. 2-energy-group diffusion theory is used in the nuclear part. Six groups of delayed neutrons are accounted for and in addition 14 groups of decay heat producers are explicitly followed in time. The problem of very small time steps induced by the short living delayed neutrons is overcome by an analytical integration assuming linear variation of neutron flux and condensed cross sections in time. So timesteps up to minutes can be tolerated.

The heat production is divided into a "local" part located in the fuel pellet itself and a "nonlocal" part to account for moderation of neutrons and absorption of gamma rays. The spatial shape of the latter part is assumed to correspond to the 2-group fast neutron removal rate.

The thermo-fluid-dynamics module accounts for heterogeneity effects due to the pebble bed structure. Pipes and other components of the primary loop are modelled in 1-D geometry. Forced convection may be treated as well as natural convection in case of blower breakdown accidents.

The equations describing the different physical properties of the reactor are very dissimilar and do not allow a simultaneous solution. Thus, a modular code system was developed. In Fig. 1 a block diagram of the actual TINTE system is shown.

The solution of most of the two-dimensional partial differential equations is found by the "leakage iterative method" as described by Naito et al. /3/ for neutron diffusion. The 2-D system is divided into axial and radial layers for which 1-D calculations are performed. The coupling between the layers is given by leakage terms obtained from the transversal calculations. In an iterative process a convergent solution from both transversal calculations is found.

Nuclear cross sections are provided in form of polynomial approximations with respect to various parameters, such as fuel- and moderator temperature, leakage, Xe-concentration and water or steam mass. The corresponding spectral calculations are performed prior to the TINTE run using convenient fast spectral codes. Time-dependent mixing of cross section sets is possible for simulation of control rod movements.

Starting from the steady state power and temperatures and some boundary conditions for temperatures and coolant flow the temperature distribution is calculated in independent program modules for the coolant, the graphite structures and the fuel pebbles. Because of the low heat capacity of the coolant gas compared to the graphite steady state approximations are used for the gas.

The heat flow from the solid parts to the gas is described as an effect of volume. The coupling of reflectors to the gas therefore is simulated by introducing a thin reflector layer allowing gas flow through it.

Especially in severe accidental situations a loss of coolant flow or even a loss of coolant may occur. In these cases effects of natural convection play an important role in heat transport. The TINTE algorithms are intended to operate under these conditions and up to now have proven their stability in such situations.

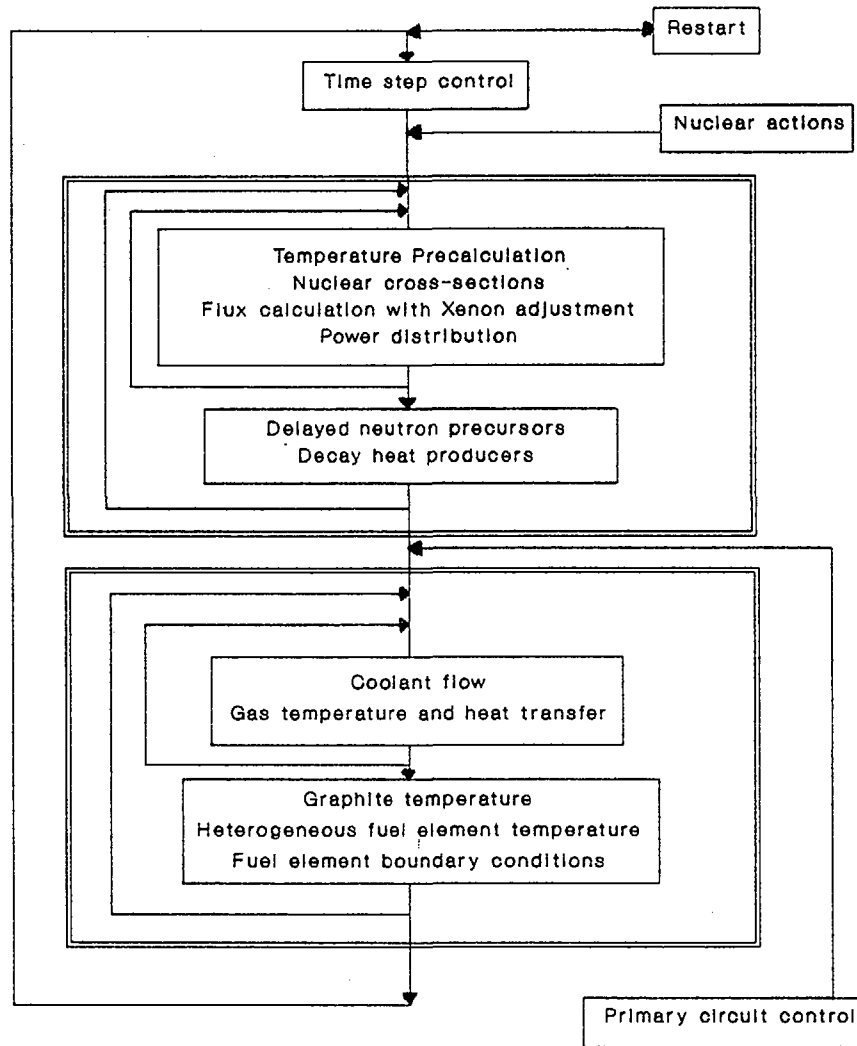


FIG. 1. TINTE block diagram.

3. Modelling the AVR Primary Loop

The Arbeitsgemeinschaft Versuchsreaktor GmbH (AVR) reactor is a 46 MW (thermal) pebble bed high temperature reactor located at Jülich (FRG). After 20 years of successful operation it was shut down at the end of 1988 and is now being decommissioned. A rough sketch of the primary system is given in Fig. 2. Detailed information may be found elsewhere /4/. Modelling the primary loop in two dimensions has to overcome the special problem of the reflector "noses". There are four of them containing the guide holes for the control rods as

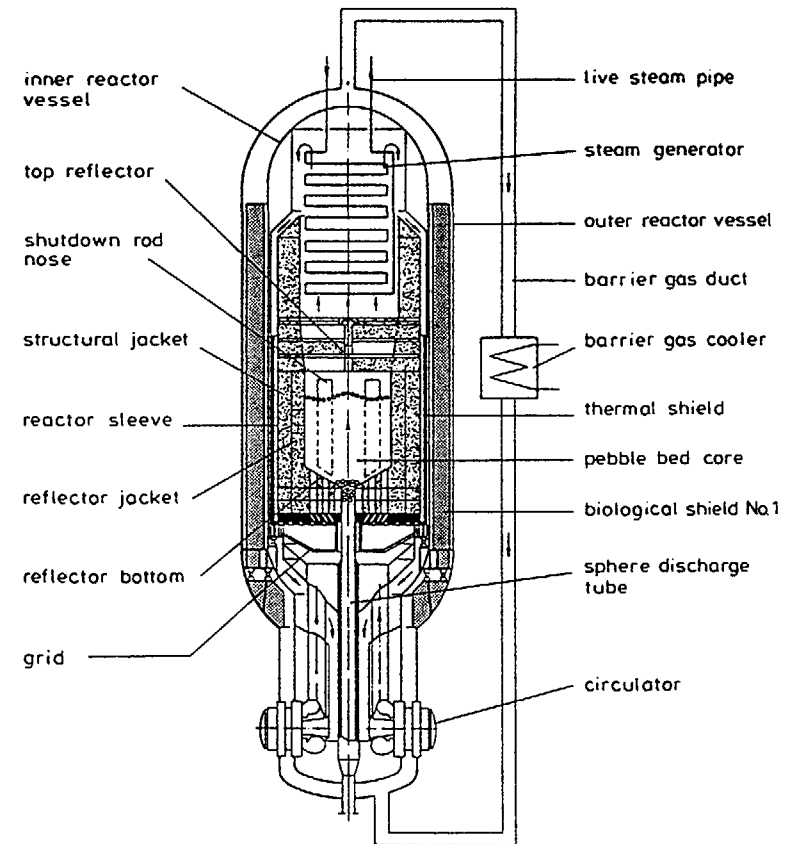


FIG. 2. The AVR reactor.

shown in fig. 3. After some tests the equivalent geometrical arrangement as given in fig. 3 was used. The mass of the graphite noses is conserved. However, the graphite ring has been made "transparent" for the helium gas in radial direction. A slit of 1 cm thickness was introduced to simulate the control rod guide holes. At the boundaries between bulk graphite and pebble bed special small regions allowing for gas flow were introduced to account for the heat coupling between graphite and cooling gas. The same technique was used at the radial reflector inner surface. Because of the smaller thickness of the ring (11 cm) in relation to the noses (30 cm) the radial heat conductivity was reduced in an appropriate way.

Another problem occurred in modelling the mass flow as a function of time. The experiments gave the blower rotational speed only and there was no possibility to measure the helium mass flow directly. Only a single blower characteristics was available, so additional

assumptions had to be made. Using a simple law of similitude a relationship between blower speed and mass flow was derived. Comparisons to the assumption of a proportionality showed certain minor differences in the power transients which finally were regarded to be tolerable.

Concerning the polynomial approximation for the nuclear cross sections some effort was necessary to get the right degree of expansion. Especially the dependence from xenon concentrations had to be described by fourth order polynomials which will be seen in the results given later.

Besides these special problems the modelling of the AVR core within the TINTE code system was strait forward. No difficulties were encountered during execution of the calculations which in general run five times faster than simulation time on an IBM 3081 host computer.

4. The AVR Dynamics experiments

Starting in 1982 a comprehensive experimental program has been undertaken at the AVR reactor /5/. This program was intended to follow the switch-over of the fuel cycle from high enriched uranium/thorium (HEU) fuel to low enriched uranium (LEU) fuel. One of the interesting questions dealt with the dynamic response of the reactor to reactivity perturbations. Screening calculations had shown, that the total temperature feedback should increase with increasing LEU fuel content mainly caused by the absolute increase of the moderator coefficient due to changes in the loading strategy. Despite the higher resonance absorption in the U-238 compared to TH-232 the fuel temperature coefficient should remain nearly constant because of the lower heavy metal loading per fuel sphere. So the relative importance of fuel temperature variations should decrease.

Based on these informations two types of dynamic experiments were planned:

- reactivity changes induced by control rod movement, keeping the cooling at normal values.
- reducing the helium blower speed, keeping the control rods at their normal positions.

In the first case neutron multiplication and therewith power generation is affected directly. Temperature changes should affect the fuel coated particles at first, thus starting feedback effects governed by the fuel reactivity coefficient. Later on temperature changes should involve the moderator, too. In the second case the cooling force is reduced at first, resulting in

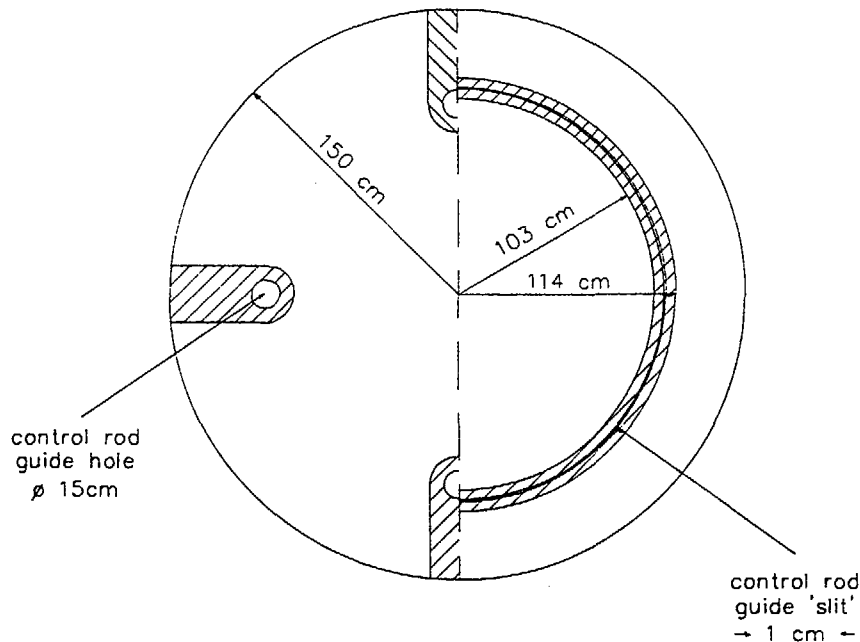


FIG. 3. The TINTE AVR model.

increasing moderator temperatures and starting feedback effects due to the moderator reactivity coefficient. Later on because of decreasing power the fuel reactivity feedback should come into play.

After the first experiments had been carried out it was recognized, that the above "philosophy" didn't work. The time constant for the heat transfer from the fuel particle kernels to the surrounding inner graphite matrix is in the order of 1 ms. The corresponding value for the transfer to the fuel element surface is about 30 s. Because of technical boundary conditions the transient inducing events (rod movement, blower speed reduction) could only be initiated within about 1/2 minute. Therefore a decoupling of the fuel and moderator feedback effects could not be made visible and in fact the reactor always reacted with his total feedback coefficient.

The dynamics experiments of the first kind started with a control rod insertion of about 50 mNile within about 20 sec. Then the rods were stopped and the free transient of the system was recorded up to about 15 minutes. The inverse process of withdrawing the rods was performed too with the modification that this procedure could be initiated at reduced power and with very slow rod velocity only, because of the neutron flux "overshooting" effect. Otherwise the reactor safety system would have initiated a scram.

The experiments of the second kind were initiated by reducing the helium blower rotational speed to about 50% of the rated values within 1 min. In addition after some minutes the feedwater mass flow of the steamgenerator was adjusted to keep the steamgenerator temperatures relatively constant. Again the reactor transient behaviour was recorded for about 15 min. Here again the inverse operation was performed at reduced power.

A third kind of transient was followed starting in the same way as the second with a blower speed reduction to about 80%. Then the xenon governed long term transient was observed for about 48 hours. The theoretical modelling of this transient is not easy, because even small effects like changes in the reactor gas inlet temperature or the non compensated burnup of the core during that time - the pebble transport was stopped during the experiment - had an important impact to the transient.

In the Fig. 4 to 9 a summary of TINTE results for the experiments described are given together with the experimental values.

The typical AVR response to the initial perturbations is a change in the power following the perturbation. After the initialization has ended feedback effects become dominant and establish a driving force in the opposite direction. Finally after very few oscillations a quasi-stabilization of the power is observed. This holds true for both types of transients and quantitative values were influenced by the fuel type on a large time scale only.

As can be seen on fig. 8 the above mentioned polynomial expansion had a significant influence on the long term xenon transient. The burnup of two days, which was not compensated by fuel shuffling reduces the core reactivity and has to be taken into account as shown in that figure, too.

Finally, fig. 9 shows the effect of control rod worth on the dynamic response. The "experimental" reactivities were derived from measurements at the initial HEU core. Probably the control-rod S-curve has changed during switching over to LEU. Using the same reactivity information gave significantly worse TINTE results for later core configurations. The assumption of having inserted about 60 mNile of reactivity in the 1985 campaign instead of 49 mNile as given by the experimentalists would improve the calculation significantly as is shown in fig. 9. There are other indications for the correctness of this idea /6/.

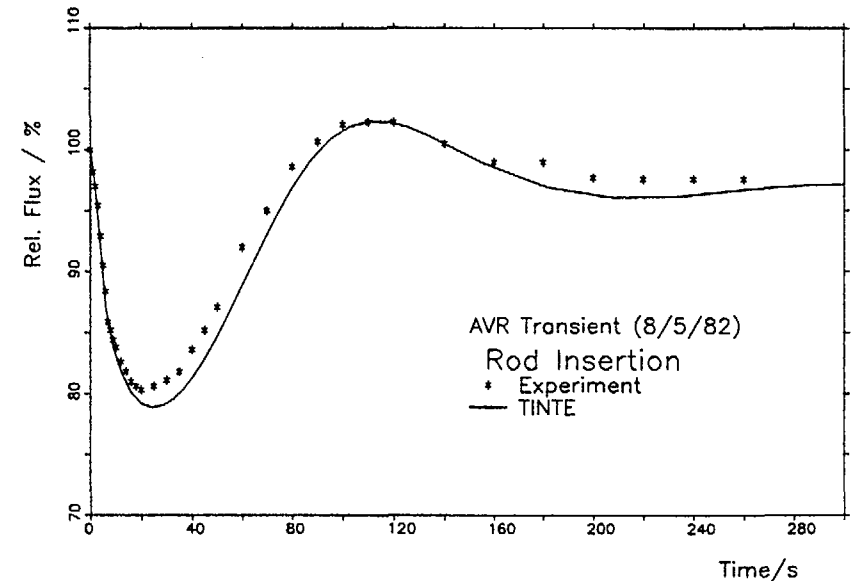


FIG. 4. AVR rod insertion transient.

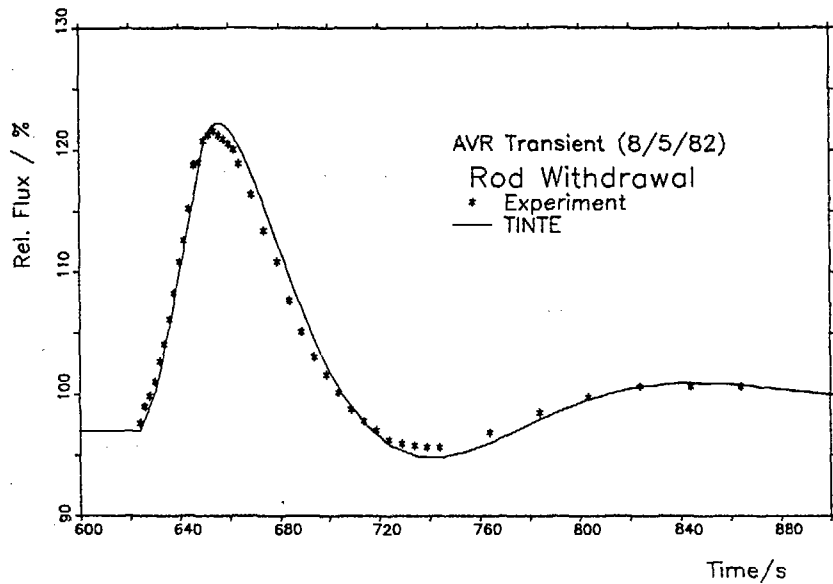


FIG. 5. AVR rod withdrawal transient.

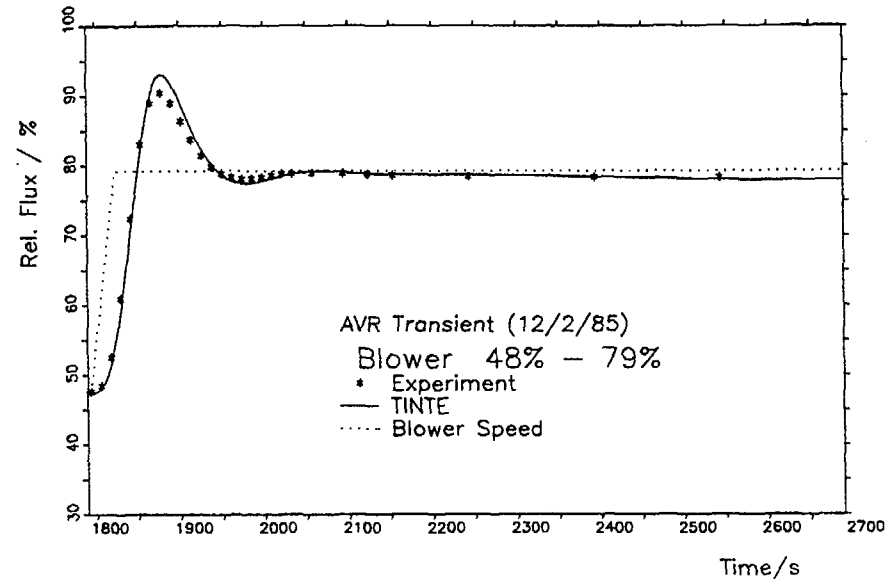


FIG. 7. AVR blower speed increasing transient.

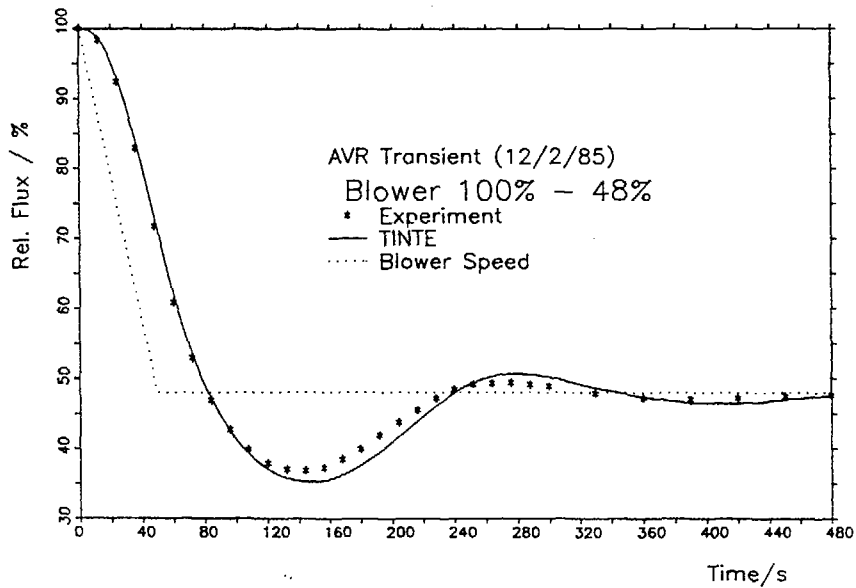


FIG. 6. AVR blower speed reduction transient.

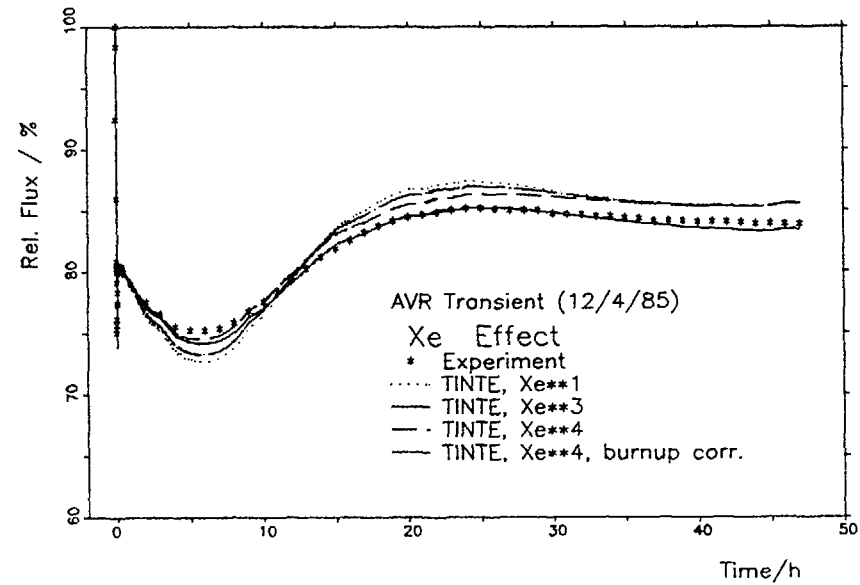


FIG. 8. AVR xenon transient.

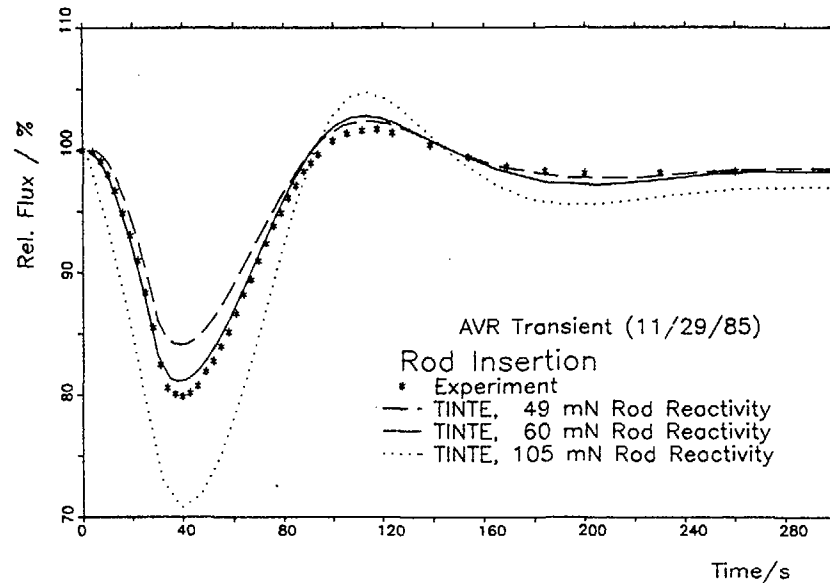


FIG. 9. AVR LEU rod insertion transient.

5. Conclusions

The TINTE code system is developed to describe the dynamics of the primary loop in a pebble bed high temperature reactor in operational, accidental and hypothetical accidental situations. Up to now calculation moduls for core neutronics, thermodynamics and thermo-fluid-dynamics are available. Models describing the effects of water/steam and air ingress with respect to reactivity, corrosion and combustion are in preparation.

The AVR dynamics experiments gave the opportunity to start a validation program for the code system. Despite the lack of detailed experimental values the TINTE system has shown its general applicability to such questions and the accordance with the experiments is very encouraging.

Further validation work will cover situations of natural convection and simulation of core heat-up accidents as they were simulated in later AVR experiments /7/.

Experiments usable for validation of the planned moduls concerning chemical and nuclear effects of water ingress are heavily asked for.

References

- /1/ H. Gerwin
Das zweidimensionale Reaktordynamikprogramm TINTE
Teil 1: Grundlagen und Lösungsverfahren
JÜL-2167 (Nov. 1987)
Teil 2: Anwendungsbeispiele
JÜL-2266 (Febr. 1989)
Teil 3: (to be published)
- /2/ H. Gerwin, W. Scherer, E. Teuchert
Nucl. Sci. Eng. 103, 302 (1989)
- /3/ Y. Naito, M. Maekawa, K. Shibuya
Nucl. Sci. Eng. 58, 182 (1975)
- /4/ R. Schulten, W. Cautius et al.
Atomwirtschaft, 11, 218 (1966)
- /5/ M. Wimmers, P. Pohl
Nucl. Sci. Eng. 97, 53 (1987)
- /6/ F. Thomas
HTR-2000. Programmcode zur rechnerischen Betriebsbegleitung
von HTRs
JÜL-2261 (Jan. 1989)
- /7/ K. Krüger
Simulation des Kühlmittelverluststörfalles mit dem AVR
VDI-Meeting "AVR-20 Jahre Betrieb", Aachen, 17/18 May 1989

ANALYTICAL METHODS,
PREDICTIONS OF PERFORMANCE OF FUTURE HTGRs,
UNCERTAINTY EVALUATIONS
PART 1

(Session II)

Chairman

W. SCHERER
Germany

DETERMINATION OF THE TEMPERATURE COEFFICIENTS AND THE KINETIC PARAMETERS FOR THE HTTR SAFETY ANALYSIS

K. TOKUHARA
Fuji Electric Company Limited,
Tokyo

T. NAKATA
Kawasi Heavy Industries Limited,
Tokyo

I. MURATA, K. YAMASHITA, R. SHINDO
Japan Atomic Energy Research Institute,
Oarai-machi, Higashi-Ibaraki-gun, Ibaraki-ken
Japan

Abstract

This report describes the calculational methods which were employed to determine the temperature coefficients and the kinetic parameters for the safety analysis in the HTTR (High Temperature Engineering Test Reactor).

The temperature coefficients (Doppler, moderator temperature) and the kinetic parameters (prompt neutron life time ℓ , effective delayed neutron fraction β_{eff}) are important for the point model core dynamic analysis and should be evaluated properly.

The temperature coefficients were calculated by the whole core model. Doppler coefficient was evaluated under the conditions of all control rods withdrawn and the uniform change of fuel temperature. The minimum and the maximum value of the evaluated Doppler coefficients in a burnup cycle are -4.6×10^{-5} and $-1.5 \times 10^{-5} \Delta K/K/^\circ C$ respectively. The moderator temperature coefficient was evaluated under the conditions of all control rods withdrawn and the uniform change of moderator temperature. The minimum and the maximum value of the evaluated moderator temperature coefficients in a burnup cycle are -17.1×10^{-5} and $0.99 \times 10^{-5} \Delta K/K/^\circ C$ respectively. In spite of positive moderator temperature coefficient, the power coefficient is always negative. Therefore the HTTR possesses inherent power-suppressing feedback characteristic in all operating

condition. We surveyed the effects of the Xe existence, the control rods existence, the fuel temperature and the region in which the temperature was changed on the moderator temperature coefficients.

The kinetic parameters were calculated by the perturbation method with the whole core model. The minimum and the maximum value of the evaluated effective delayed neutron fraction (β_{eff}) are 0.0047 and 0.0065 respectively. These of the evaluated prompt neutron life time (ℓ) are 0.67 and 0.78 ms respectively. We have surveyed the effects of the fuel depletion and the core power level on these parameters, and considered these effects on the kinetic parameters.

From above evaluation, we determined the temperature coefficients and the kinetic parameters.

1. Introduction

Japan Atomic Energy Research Institute (JAERI) has extensively carried out the research and development to construct the High Temperature Engineering Test Reactor (HTTR) of 30MW(th)¹⁾. The main objectives of the HTTR are to establish basic technologies for advanced HTGRs in future and to be served as an irradiation test reactor in order to conduct researches in innovative high-temperature technologies.

The temperature coefficients and the kinetic parameters are important for the point model core dynamic analysis and should be evaluated properly.

This report describes the evaluation methods and the evaluation results of the temperature coefficient (Doppler coefficient, moderator temperature coefficient) and the kinetic parameters (the effective delayed neutron fraction, the prompt neutron life time), which are needed for the point model core dynamic analysis in the safety evaluation in the HTTR.

2. The nuclear design code system for the HTTR

The temperature coefficients and the kinetic parameters were calculated with the nuclear design code system shown in Fig.1

2-1 The lattice calculation of the fuel and the burnable poison

The neutron spectrum was calculated with multi group constants edited from the ENDF/B-IV and the lattice calculation of the fuel and the burnable poison (BP) were carried out in reduced neutron groups of 40. DELIGHT²⁾ is used for the

lattice calculation of fuel and burnable poison, which is developed to analyse the fuel lattice characteristics of high temperature gas cooled reactor. The few group constants which were used for the core characteristics calculation were produced through condensing these reduced group constants. The calculational model of the fuel lattice is cylindrical and the model consists of the fuel rod and the helium coolant, which are surrounded by the graphite block. The calculational model of the BP lattice is cylindrical and the model consists of the BP rod which is surrounded by the homogenized fuel.

2-2 The lattice calculation of the control rod

The lattice calculation of the control rod was carried out to produce the averaged group constants in the control rod guide block under the conditions that the control rods were inserted and the region around the control rod column was the homogenized fuel. The flux in the control rod guide block was used as the weight for this space averaging. For this calculation, we used the two dimensional neutron transport code TWOTRAN-2³⁾.

2-3 The core calculation

For the calculation of the temperature coefficients and the kinetic parameters, we used the diffusion code CITATION-1000VP⁴⁾ which was vectorized and extended core dimension version of CITATION. The three dimensional triangular prism mesh are employed in the calculation. The group constants of the fuel, the reflector and the control rod were produced through the above mentioned lattice calculations.

3. The temperature coefficients (Doppler coefficient, Moderator temperature coefficient)

We have carried out the parametric study to determine the proper evaluation model and evaluated the doppler coefficient and the moderator temperature coefficient, which were important for the point model core dynamic analysis in the safety evaluation.

3-1 Parametric study

i) The effect of the moderator temperature on the doppler coefficient

In order to survey the effect of the moderator temperature on the evaluated doppler coefficient we have calculated the doppler coefficient for different moderator temperature with the fuel lattice calculation model. The change of the

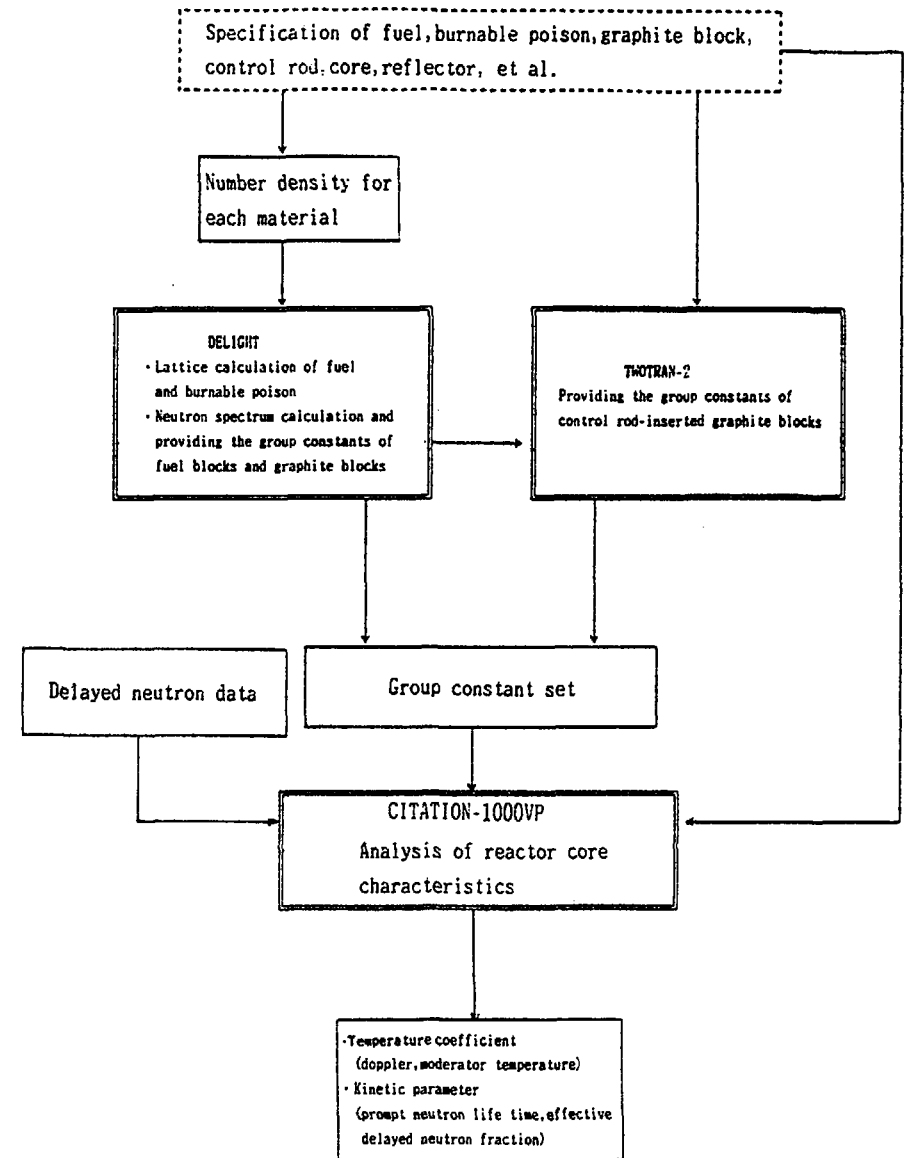


FIG. 1. Calculation flow of the nuclear design.

doppler coefficient for different moderator temperature was shown in Fig.2. The moderator temperature was set to 200 °C, 747 °C and 1200 °C. It is clear from this figure that the characteristic of the doppler coefficient is not so affected by the moderator temperature.

ii) The effect of the evaluation model on the moderator temperature coefficient

We investigated the effect of the evaluation model (shown below) on the moderator temperature coefficient.

- ① The region in which the graphite temperature is changed
- ② The temperature of the permanent reflector
- ③ The Xe existence
- ④ The control rod existence
- ⑤ The fuel temperature

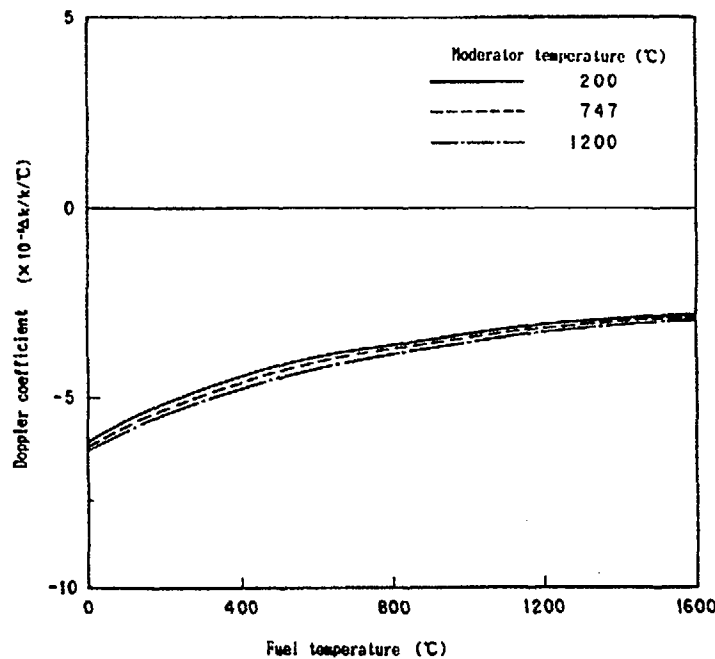


FIG. 2. Effect of the moderator temperature on the Doppler coefficient (lattice calculation).

These effects were evaluated as follows.

① The region in which the graphite temperature is changed

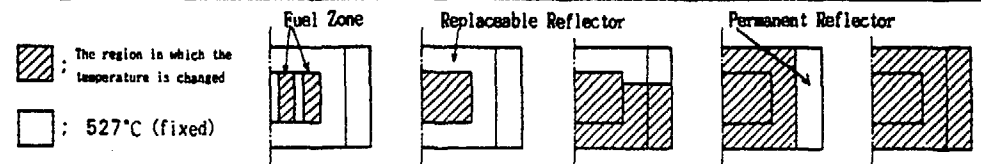
The moderator region in which the temperature is changed affects the moderator temperature coefficient, this effect is shown in Table 1. The dashed parts are the region in which the graphite temperature is changed. As this dashed part gets larger, the moderator temperature coefficient increases. A rapid increase of the local core power level causes only increase of the temperature of the fuel zone of the model 1, and doesn't cause the rapid increase of the temperature of the replaceable reflector. In order to evaluate the conservative moderator temperature coefficient for the safety analysis, we used the model 4 where the graphite temperature in the replaceable reflector is changed simultaneously for the evaluation of the moderator temperature coefficient.

② The temperature of the permanent reflector

The effect of the permanent reflector temperature on the moderator temperature coefficient can be obtained through comparison between the model 4 and the model 4-1 of Table 2. The temperature of the permanent reflector is 27°C

TABLE 1. RELATION BETWEEN THE EXTENSION OF THE REGION IN WHICH THE TEMPERATURE IS CHANGED AND THE MODERATOR TEMPERATURE COEFFICIENT

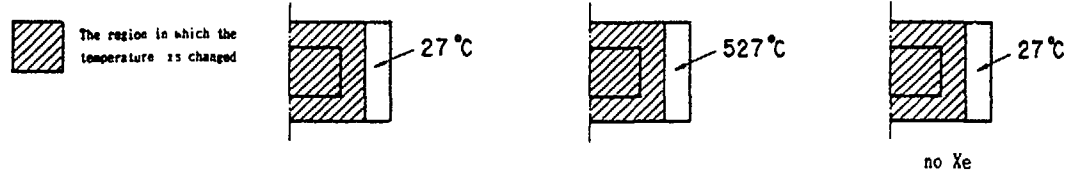
Moderator temperature T_m (°C)	Fuel temperature T_f (°C)	Effective multiplication factor and moderator temperature coefficient for each model				
		Model 1 fuel	Model 2 core	Model 3 core and lower replaceable reflector	Model 4 core and replaceable reflector	Model 5 core replaceable reflector and permanent reflector
27	27	1.0459	1.0439	1.0386	1.0338	1.0290
127	27	1.0406	1.0388	1.0348	1.0314	1.0276
Moderator temperature coefficient $\Delta k/k/°C$		-4.87×10^{-5}	-4.66×10^{-5}	-3.57×10^{-5}	-2.33×10^{-5}	-1.27×10^{-5}



note : Effective multiplication factor was calculated on burnup 660 day under the conditions of all control rods withdrawn

TABLE 2. EFFECT OF THE PERMANENT REFLECTOR TEMPERATURE (T_m^{fix}) ON THE MODERATOR TEMPERATURE COEFFICIENT

Moderator temperature T_m (°C)	Fuel temperature T_f (°C)	Model 4 $T_m^{fix} = 27^\circ\text{C}$		Model 4-1 $T_m^{fix} = 527^\circ\text{C}$		Model 4-2 $T_m^{fix} = 27^\circ\text{C}$	
		K	Mod. temp. coeff. ($\Delta K/K/^\circ\text{C}$)	K	Mod. temp. coeff. ($\Delta K/K/^\circ\text{C}$)	K	Mod. temp. coeff. ($\Delta K/K/^\circ\text{C}$)
227 $\bar{T}_m = 277$	227	1.0175	$+0.11 \times 10^{-5}$	1.0221	-0.07×10^{-5}	1.0562	-2.27×10^{-5}
327	227	1.0176		1.0221		1.0537	
727 $\bar{T}_m = 777$	727	1.0041	-3.28×10^{-5}	1.0090	-3.87×10^{-5}	1.0304	-5.71×10^{-5}
827	727	1.0002		1.0051		1.0244	



(room temperature) for the model 4 and 527°C for the model 4-1. The moderator temperature coefficient of the model 4 is larger than that of the model 4-1 by $(0.2\sim 0.6) \times 10^{-5} \Delta K/K/^\circ\text{C}$ in case of $T_m = 277^\circ\text{C}$ and $T_m = 777^\circ\text{C}$. Then the temperature of the permanent reflector was set equal to the room temperature so as to avoid underestimation of the moderator temperature coefficient.

③ The Xe existence

The effect of the Xe existence on the moderator temperature coefficient can be obtained through comparison between the model 4 and the model 4-2 in Table 2. In the model 4, Xe exists in the core and in the model 4-2 Xe does not exist in the core. The temperature of the permanent reflector was set to 27°C . The moderator temperature coefficient of the model 4 is larger than that of the model 4-2 in case of $T_m = 277^\circ\text{C}$ and $T_m = 777^\circ\text{C}$. Then, the moderator temperature coefficient was evaluated larger by $2.4 \times 10^{-5} \Delta K/K/^\circ\text{C}$ in case of Xe existence than in case of no Xe. We evaluated the moderator temperature coefficient with Xe.

④ The control rod existence

The effect of the control rod existence on the moderator temperature coefficient is shown in Fig.3. The Model 5 in Table 1 is used for this survey. The solid line in Fig.5 shows the temperature coefficient change under the conditions of the all control rods withdrawn. The dashed line shows the temperature coefficient change under the conditions of the all control rods inserted. This shows that the moderator temperature coefficient is evaluated larger under the former conditions than the latter conditions. Therefore the conditions in which the control rods were withdrawn is chosen for the evaluation of the moderator temperature coefficient.

⑤ The fuel temperature

We investigated the effect of the fuel temperature on the moderator temperature coefficient. The change of the moderator temperature coefficient is shown in Fig.4. The fuel temperature is varied to 200°C , 897°C and 1400°C in

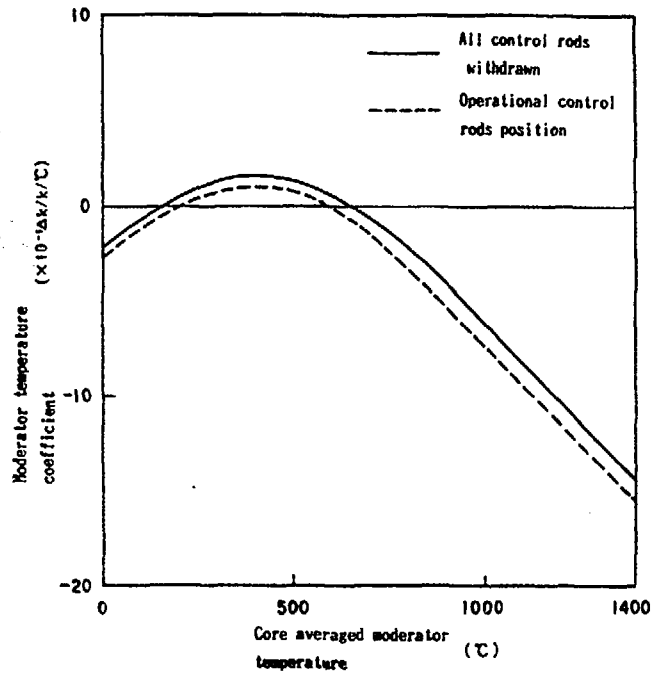


FIG. 3. Effect of the control rod on the moderator temperature coefficient (model 5).

this investigation. This figure shows that the values of the moderator temperature coefficient are almost the same for these different fuel temperatures.

3-2 Evaluation model

i) Doppler coefficient

Although the fuel temperature has the distribution in the core, we have evaluated the doppler coefficient by using the core averaged fuel temperature. The adequacy of using core average temperature for the temperature coefficient is mentioned by Massimo⁶⁾. As the doppler coefficient has the weak dependence on the moderator temperature, the moderator temperature is set to constant. All control rods were completely withdrawn.

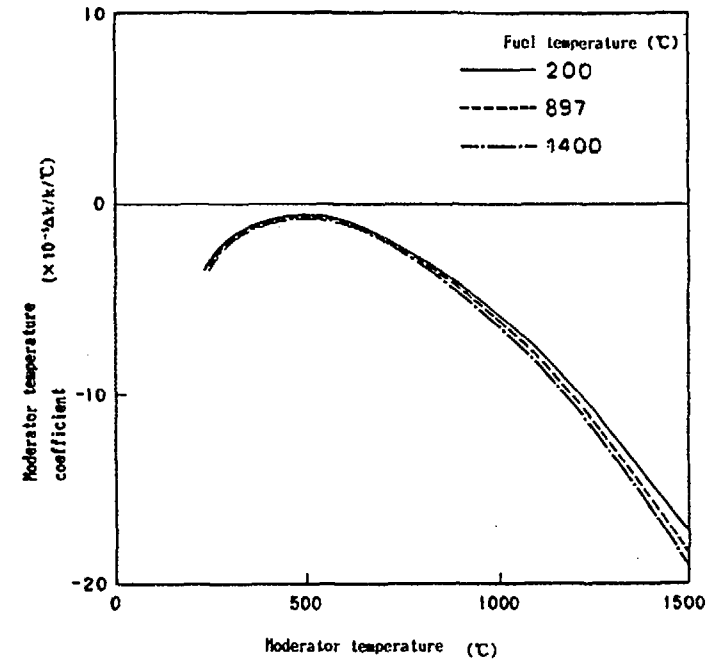


FIG. 4. Effect of the fuel temperature on the moderator temperature coefficient (lattice calculation, EOC).

ii) Moderator temperature coefficient

The fuel temperature was set equal to the averaged moderator temperature $(T_{M1} + T_{M2})/2$. The regions whose moderator temperatures were changed were replaceable reflector and the fuel region containing the control rod guide column. The temperatures of these regions were changed uniformly. The temperature of the permanent reflector was set equal to the room temperature, for the moderator temperature coefficient became small according to the temperature increase of the permanent reflector. In the evaluation of the moderator temperature coefficient at the end of cycle (EOC; full power 660 days), we considered the Xe existence in the core, for the Xe existence has a positive effect on the moderator temperature coefficient. At the beginning of cycle (BOC) we evaluated

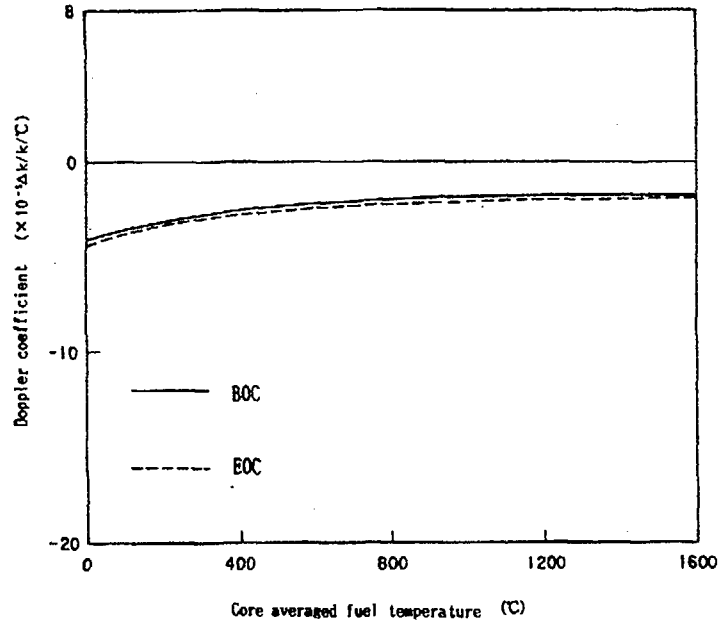


FIG. 5. Doppler coefficient.

it with the conditions of no Xe existence. The control rods were all withdrawn, for the control rods had negative effect on the moderator temperature coefficient.

3-3 Evaluated results

i) Doppler coefficient

The evaluated values of the doppler coefficient on full power 0 day (BOC) and 660 days (EOC) are shown in Fig.5. The temperatures of the fuel and the moderator were the same in the calculation of the base effective multiplication factor. We changed the fuel temperature to calculate the doppler coefficient and averaged these to produce the doppler coefficient. These results show that the minimum and the maximum value of the evaluated doppler coefficients in a burnup cycle are -4.6×10^{-5} and $-1.5 \times 10^{-5} \Delta k/k/^\circ C$ respectively and they are negative in all fuel temperature range. Then this reactor has the negative feedback characteristic.

ii) Moderator temperature coefficient

The evaluated values of the moderator temperature coefficient on full power 0 day (BOC) and 660 days (EOC) are shown in Fig.6. The temperatures of the fuel and the moderator were the same in the calculation of the base effective multiplication factor. We changed the moderator temperature to calculate the moderator temperature coefficient and averaged these to produce the moderator temperature coefficient. These results show that the minimum and the maximum value of the evaluated moderator temperature coefficients in a burnup cycle are -17.1×10^{-5} and $0.99 \times 10^{-5} \Delta k/k/^\circ C$ respectively. The maximum value appears near 430 °C on full power 660 days. The moderator temperature coefficient increases compared to the standard case as the fission cross section increases or the absorption cross section decreases. As the moderator temperature increases, the thermal neutron spectrum moves to higher energy region and the absorption by Xe-135 decreases and the fission by Pu-239 is increases. This

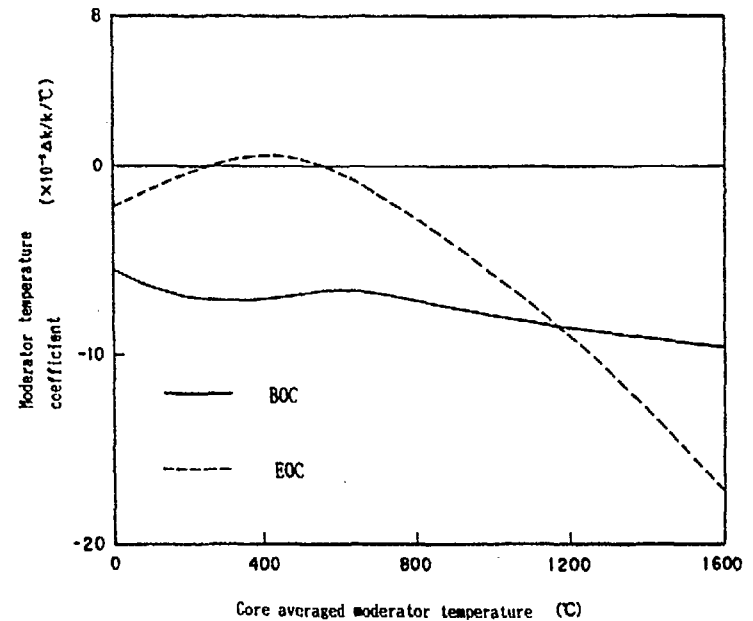


FIG. 6. Moderator temperature coefficient (model 4).

leads the moderator temperature coefficient to larger side. At higher moderator temperature, that is, when the distribution of the thermal neutron spectrum moves to higher energy region, the absorption by Pu-240 increases and the moderator temperature coefficient moves to lower side. The increase of the moderator temperature coefficient is caused mainly by Xe-135 and Pu-239 in the moderator temperature range from the room temperature to about 430 °C, and the decrease of that is caused mainly by the absorption of Pu-240 in higher moderator temperature region than about 430 °C.

4. The kinetic parameters (effective delayed neutron fraction : β_{eff} , prompt neutron life time : ℓ)

We evaluated the delayed neutron fraction and prompt neutron life time, which are important for the point model core dynamic analysis in the safety evaluation.

4-1 Evaluation model

The effective delayed neutron fraction and the prompt neutron life time were calculated by the perturbation method⁵⁾ with the whole core model. For β_i (i : the number of the delayed neutron group), we used the value evaluated by G.R.Keepin etc.^{7), 8)} For these calculations, the effect of the fuel depletion and the core power level were taken into account.

4-2 Evaluation results

i) Effective delayed neutron fraction β_{eff}

The calculated β_{eff} is shown in Fig.7 in relation with the fuel burnup. β_{eff} becomes smaller as burnup increases. The reason of this is that the fission in the lower burnup is caused almost by U-235 which has large delayed neutron fraction and the fission in the higher burnup is caused not only by U-235 but also by Pu-239 and Pu-241 which have small delayed neutron fraction. On burnup 660 days, the fission fraction caused by Pu-239 is about 34%. The change of β_{eff} by the core power level for burnup 0, 330 and 660 days is shown in Fig.8. For burnup 330 and 660 days, β_{eff} becomes smaller with the increase of the core power level. The reason of this is that the neutron spectrum is hardened by the increase of the core averaged temperature and the fission rate of Pu-239 is increased. On burnup 0 day, most of the fission reaction in the core is caused

by U-235 and then β_{eff} is not varied by the core power level. From these results, the minimum and the maximum value of the evaluated β_{eff} are 0.0047 and 0.0065 respectively.

ii) Prompt neutron life time ℓ

The change of ℓ with the fuel burnup is shown in Fig.9. This figure shows that ℓ decreases rapidly according to Xe production and ℓ becomes minimum at the middle of cycle (full power 110 days). After this date, ℓ increases gradually. The maximum value and the minimum value of ℓ are 0.78 ms and 0.67 ms respectively. The neutron velocity and the macroscopic absorption cross section of fuel have the maximum value at the middle of cycle and this is the reason that ℓ is minimum at the middle of cycle. The calculated ℓ is shown in Fig.10 in relation with the core power level on full power 0, 330 and 660 days. This figure shows that ℓ decreases with increase of power level. The core temperature increases and the neutron spectrum is hardened with the increase of

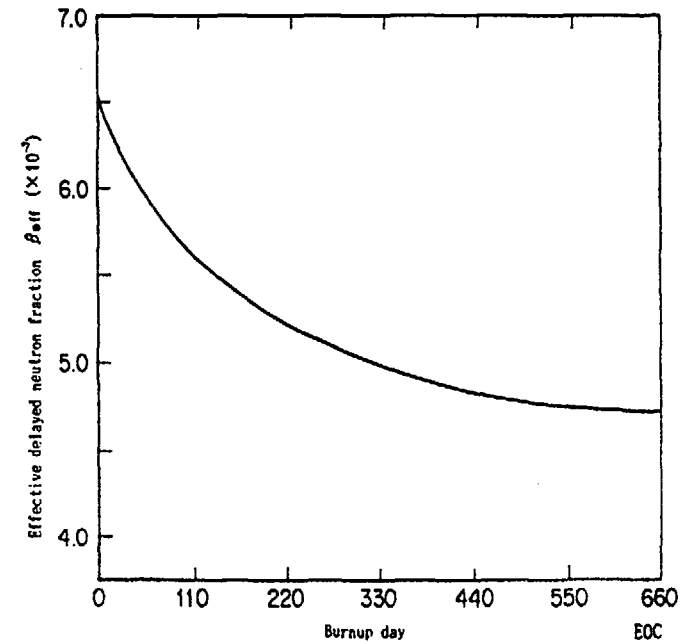


FIG. 7. Relation between the effective delayed neutron fraction and the burnup day.

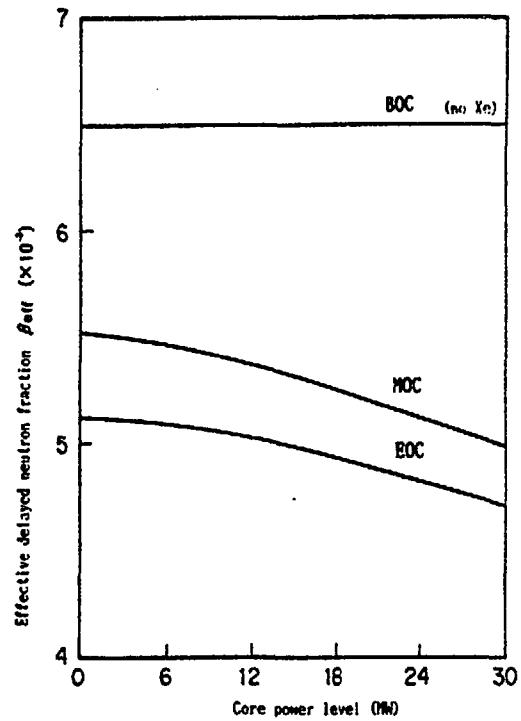


FIG. 8. Relation between the effective delayed neutron fraction and the core power level.

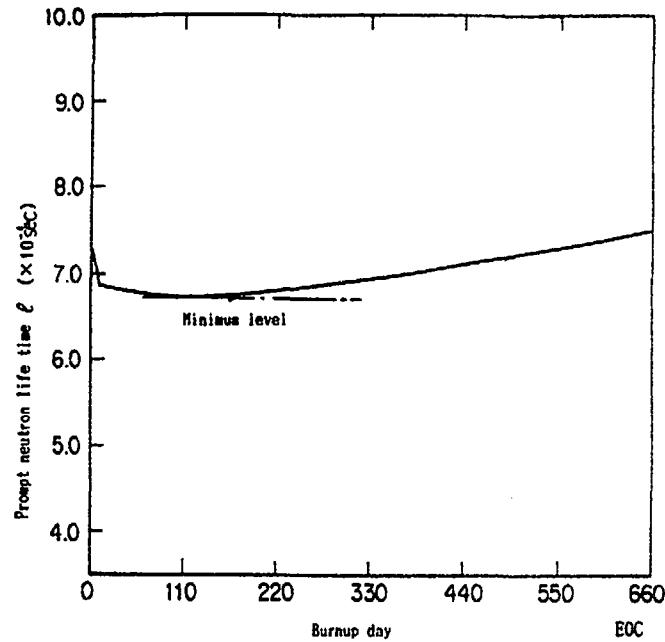


FIG. 9. Relation between the prompt neutron lifetime and the burnup day.

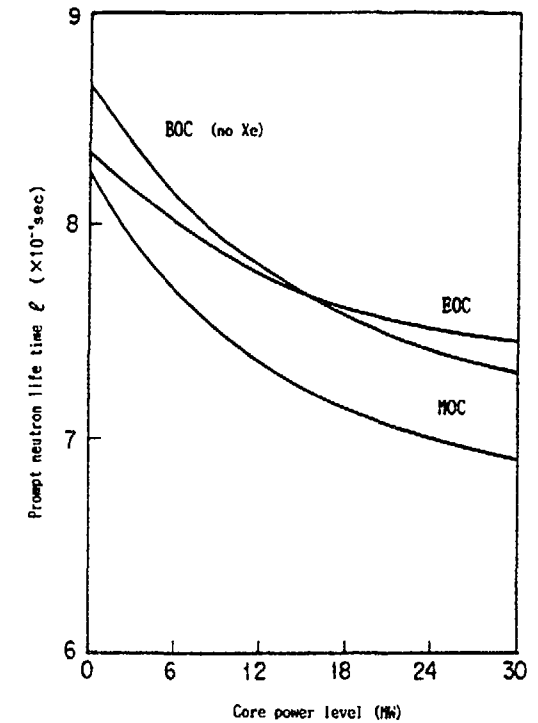


FIG. 10. Relation between the prompt neutron lifetime and the core power level.

the core power level. They resulted in the increase of the neutron velocity and the absorption cross section of U-238. From these results, the minimum and the maximum value of the evaluated λ are 0.67 and 0.78 ms respectively.

5. Summary

The temperature coefficients were calculated by the whole core model and the kinetic parameters were calculated by the perturbation method on this model. For the temperature coefficients, we determined the proper model for them by the parametric study. For the kinetic parameters, we considered the effects of the fuel depletion and the core power level on them. From these evaluation, it is

resulted in that the minimum and the maximum value of the evaluated doppler coefficients are -4.6×10^{-5} and $-1.5 \times 10^{-5} \Delta K/K/^\circ C$, these of the moderator temperature coefficients are -17.1×10^{-5} and $0.99 \times 10^{-5} \Delta K/K/^\circ C$, these of the delayed neutron fraction are 0.0047 and 0.0065 and these of the prompt neutron life time are 0.67 and 0.78 ms respectively.

ACKNOWLEDGEMENTS

Authors are deeply indebted to Messrs. S.Saito, T.Tanaka and Y.Sudo for useful comments and supports for this work.

REFERENCES

- 1) JAERI: "Present status of HTGR Research and Development", (1989)
- 2) Shindo R., Yamashita K. and Murata I.: "DELIGHT-7; One Dimensional Fuel Cell Burnup Analysis Code for High Temperature Gas-Cooled Reactor (HTGR)", JAERI-M 90-048 (1990) (in Japanese)
- 3) Lathrop, K.D. and Brinkley F.W.: "TWOTRAN- II; An Interfaced Exportable Version of the TWOTRAN code for Two-Dimensional Transport", LA-4848MS (1973)
- 4) Harada H., Yamashita K.: "The Reactor Core Analysis Code CITATION-1000VP for High Temperature Engineering Test Reactor", JAERI-M-89-135 (1989)
- 5) Fowler, T.B. and Vondy, D.R.: "Nuclear Reactor Core Analysis Code, CITATION", ORNL-TM-2496 (1969)
- 6) L. Massimo: "Physics of High Temperature Reactors", Pergamon Press.
- 7) G.R. Keepin, T.F. Wilmott, and R.K. Zeiger: "Delayed Neutrons from Fissionable Isotopes of Uranium, Plutonium, and Thorium", Physical Review, Vol. (107), No. 4 (1957)
- 8) G.R. Keepin and T.F. WILMETT; "Reactor Kinetic Functions; A New Evaluation" , Nucleonics (1958)

CALCULATIONAL METHODS OF POWER DISTRIBUTION IN THE HTTR AND VERIFICATIONS

T. NAKATA

Kawasaki Heavy Industries Limited,
Tokyo

K. TOKUHARA

Fuji Electric Company Limited,
Tokyo

I. MURATA, K. YAMASHITA, R. SHINDO

Japan Atomic Energy Research Institute,
Oarai-machi, Higashi-Ibaraki-gun, Ibaraki-ken

Japan

Abstract

This report describes the calculational methods of the power distribution in the High Temperature Engineering Test Reactor (HTTR; 30MW in thermal output and 950°C in reactor outlet coolant temperature) which was designed by Japan Atomic Energy Research Institute (JAERI), and the verifications of these methods.

In the HTTR, an accurate determination of power distribution is one of the important design requirements. We have designed the power distribution by zoning the fuels and burnable poisons (BP) in order to keep the maximum fuel temperature as low as possible. Additionally we precisely evaluated the power distribution in a fuel block by considering the spatial fine structures.

Radially these fine power distributions were calculated on the representative planes by using the 120-degree rotational model of CITATION, which could consider the spatial heterogeneity caused by the fuel rods and BP rods in a fuel block. Then we could obtain the local power peaking factor which was defined by the ratio between finely and coarsely determined power distribution. The maximum value of the local power peaking factor is about 7% and it gradually decreases with depletion.

We evaluated axially the effect of local power spikes due to the block end graphite, and we have considered 4% as these spikes for the fuel temperature calculation.

On the other hand, we have verified these methods by the analysis of copper reaction rate measurements in the Very High Temperature Reactor Critical Assembly (VHTRC) experiments. The agreement between calculation and experiment was good.

From these results, it was confirmed that the power distribution in the HTTR could be predicted with sufficient accuracy by our calculational method, and could meet the design requirements.

1. Introduction

Japan Atomic Energy Research Institute(JAERI) has been developing the High Temperature Engineering Test Reactor (HTTR). The HTTR, which employs pin-in-block type fuel, is a helium cooled and graphite moderated reactor with thermal power of 30MW and outlet coolant temperature of 950°C.

In this report, we describe the calculational methods of power distribution in the HTTR, and the verifications by analyzing the VHTRC experiment.

2. Main Features of HTTR Core Design

The major specification of the HTTR is listed in Table 1. The active core consists of 30 fuel columns and 7 control rod guide columns. Each column is composed of 5 hexagonal fuel blocks. A standard fuel block, 36cm across flats and 58cm in height, is made up of fuel rods and a hexagonal graphite block. A fuel rod consists of fuel compacts contained by graphite sleeve. Furthermore a fuel compact consists of TRISO coated particles of low enriched uranium dioxide whose average enrichment is about 6wt%. These fuel block structures are shown in Fig.1.

From the safety viewpoint, the HTTR core is so designed that the maximum fuel temperature may not exceed 1600°C under the normal operation and any anticipated operational transients. In order to meet this requirement, to achieve the high outlet coolant temperature of 950°C and to increase the design margins, it is necessary to keep the maximum fuel temperature as low as possible. Therefore we have designed the power distributions by zoning fuels and burnable poisons(BP) so as to achieve following characteristics through a burnup cycle.

- (1) An uniform radial power distribution
- (2) A flat axial fuel temperature distribution

Table 1 Major specification of the HTTR

Thermal power	30 MW
Outlet coolant temperature	850°C/950°C
Inlet coolant temperature	395°C
Fuel	Low enriched UO ₂
Fuel element type	Prismatic block
Direction of coolant flow	Downward-flow
Pressure vessel	Steel
Number of main cooling loop	1
Heat removal	IHX and PWC (parallel loaded)
Primary coolant pressure	4 MPa
Containment type	Steel containment
Plant lifetime	20 years

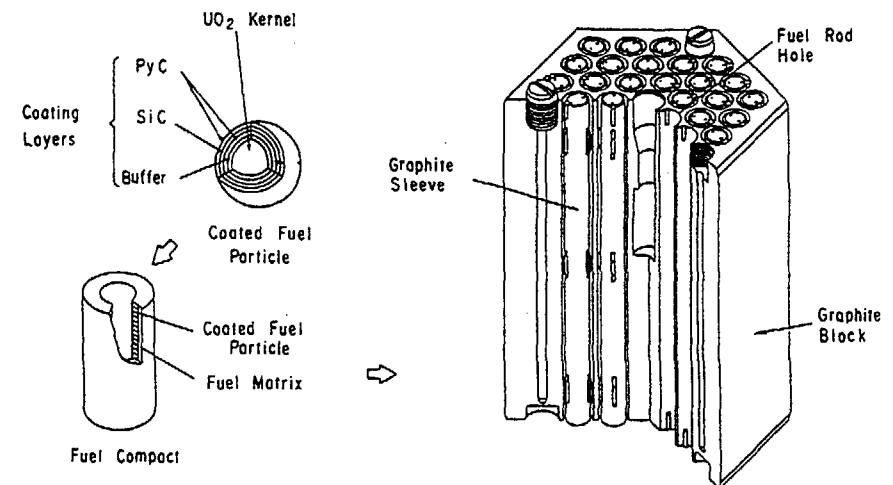


Fig.1 HTTR fuel block

3. Evaluation of Power Distribution in the HTTR

Fuel temperatures are calculated using the power distribution which is obtained by the verified calculational method.

This power distribution is evaluated by following three types of calculational methods. The first method calculate the coarse power distribution, and other methods calculate the fine power distribution in radial and axial direction. Figure 2 shows the fuel rods arrangement in the HTTR, and the coarse and fine mesh models which are employed for these calculations. We calculate the coarse power distribution for each burnup step as described in section 3.1. Then we evaluate the local power peaking factor due to the spatial heterogeneity caused by the fuel rods and BP rods in a fuel block which is determined from the fine mesh calculation on horizontal planes as described in section 3.2. In addition, we describe the calculational method of the local power spikes due to the fuel block end graphite as an example of axial fine distributions in section 3.3.

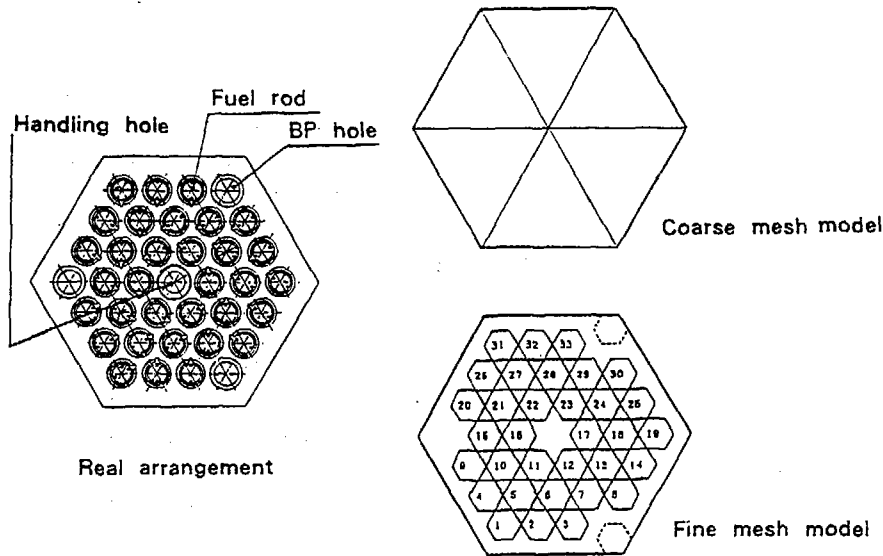


Fig.2 Fuel rod arrangement and models

3.1 Coarsely determined Power Distribution

(1) Calculational method and model

As these calculational methods of the power distribution are a part of nuclear design code system, the production procedure of group constants is the same as calculating other characteristics. The group constants for fuel regions are prepared to each burnup step by the DELIGHT⁽¹⁾ code which could deal with the double heterogeneity of fuel rod and grain, and the existence of burnable poison rod. This cell calculation is performed by 40 energy groups (20 in fast, 20 in thermal), and they are condensed to 6 energy groups (3 in fast, 3 in thermal) in each region. The effective group constants for control rods and reserve shut down elements are produced by composing the cross sections from the DELIGHT code and the shielding factors which are calculated by the TWOTRAN-2 code.

The coarse power distributions are calculated to each burnup step by the CITATION-1000VP⁽²⁾ using these constants and the three dimensional full core model shown in Fig.3. Each block is divided into 24 triangular prism meshes, 6 on horizontal plane, and 4 in axial direction. The fuel rods and BP rods are mixed with block graphite homogeneously in this model.

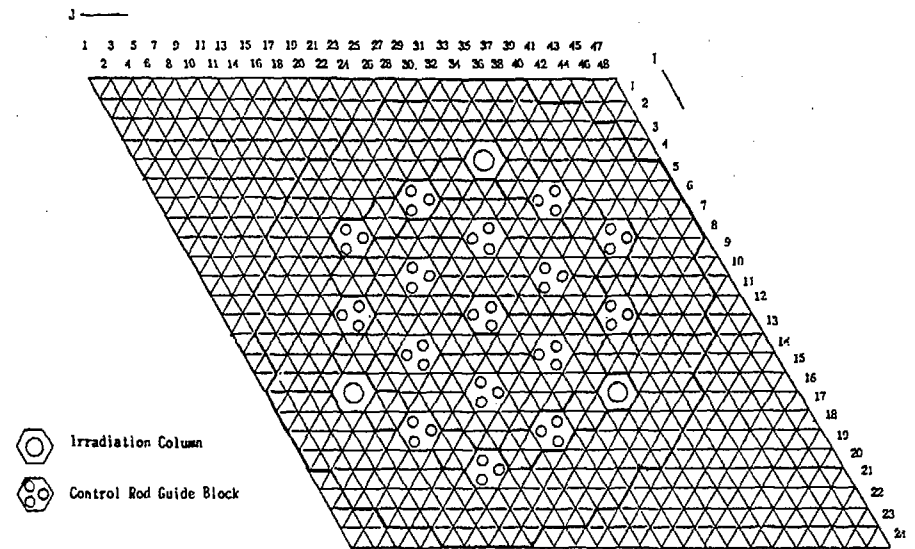


Fig.3 Coarse mesh model (3D Tri.-Z full core)

(2) Results

One example of these results compared with the axial fine power distribution is shown in Fig.6.

3.2 Finely Determined Power Distribution in Radial Direction

As the calculational method of power distribution with coarse mesh could not consider the heterogeneity caused by the fuel rods and BP rods in a fuel block, we took it into account with the fine mesh calculation.

(1) Calculational method and model

Figure 4 shows this calculation procedure. The group constants are prepared by the same procedure shown in section 3.1. We execute the two types of burnup calculations for the 6 horizontal planes which have different fuel loading, control rod conditions and temperatures. One is the same homogeneous coarse mesh model shown in section 3.1. Another is the heterogeneous fine mesh model which could deal with the fuel rod and BP rod by small hexagonal 6 meshes. Figure 5 shows this heterogeneous fine mesh model.

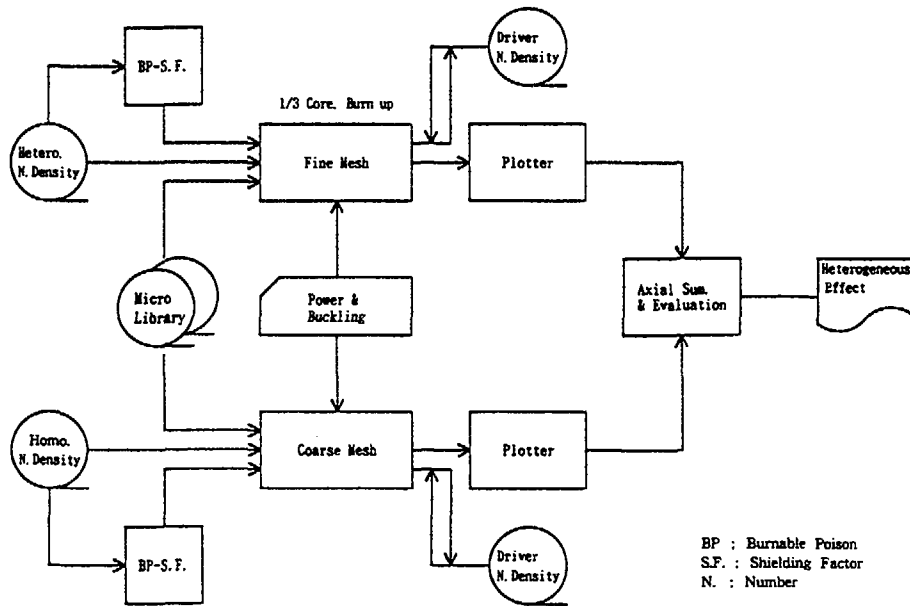


Fig.4 Fuel Heterogeneity Analysis Code System

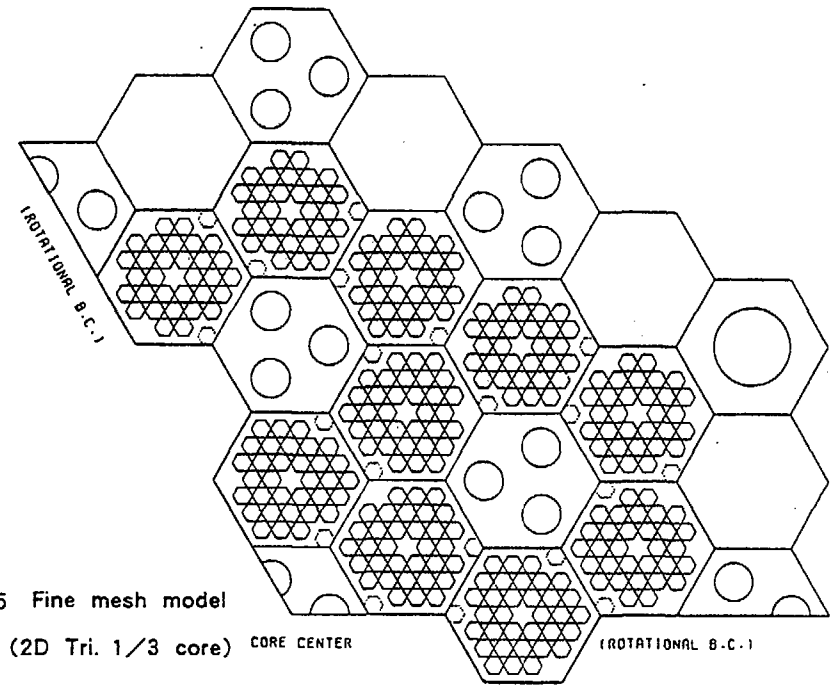


Fig.5 Fine mesh model

(2D Tri. 1/3 core) CORE CENTER

(ROTATIONAL S.C.)

The spatial heterogeneity in radial direction caused by the fuel rods and BP rods is expressed by the local power peaking factor (F_i). This value is obtained from the comparison between the peak channel power ratios calculated by above two methods at the same burnup state as follows.

$$F_i = \frac{\sum_j \{ (P_{ij}^* / \bar{P}_{ij}^*) \cdot W_j \}}{\sum_j \{ (P_{ij} / \bar{P}_{ij}) \cdot W_j \}}$$

P_{ij}^* ; Peak channel power(Hetero.)
 \bar{P}_{ij}^* ; Region average (Hetero.)
 P_{ij} ; Peak mesh power (Homo.)
 \bar{P}_{ij} ; Region average (Homo.)
 W_j ; Averaging weight
 i ; Column index (1-10)
 j ; Axial index (1-6)

The weights(W_j) are evaluated from the regionwise axial power distribution. Core calculations are performed by the CITATION-2 code which was improved in order to treat a 120 degree rotational symmetry model and 500 zones in this version.

(2) Results

The local power peaking factor due to the spatial heterogeneity caused by the fuel rods and BP rods is evaluated as the maximum 7% from those results, and it is confirmed that this value gradually decreases with burnup. The cause of this tendency is considered that the fuel with higher power at the peripheral site of block depletes faster than at the inner region, and the influence of BP rods becomes weak with its burnup.

3.3 Finely Determined Power Distribution in Axial direction

As the calculational method of power distribution with coarse mesh could not consider the effect of local power spike due to the fuel block end graphite, we performed to evaluate this effect by using the axial heterogeneous fine mesh model.

(1) Calculational Method and Model

This model and procedure are the same as ones described in the section 3.1 except the axial divisions and material heterogeneities. The block is axially divided by 10 meshes whose width are not equal each other, and whose both ends are composed of graphite regions. The calculated condition is the initial hot clean core in which the control rods level is deepest, and the largest spike is caused during a burnup cycle.

The hot spot factor for this power spike is evaluated from the ratio of axial fine to coarse power distributions at the lower end of 3rd block where the maximum fuel temperature usually arises.

(2) Results

Figure 6 shows the comparison of axial power distributions obtained from the fine mesh and coarse mesh model calculation.

The hot spot factor of 4% is evaluated from those results for the local power spike effect due to the fuel block end graphite.

4. Verification by VHTRC experiments

For the verification of accuracy, it is indispensable to compare the calculation with the experiment performed on a graphite moderated critical assembly whose characteristics are similar to HTTR's. Therefore, the Very High Temperature Reactor Critical Assembly (VHTRC)^{(3),(4)} at JAERI is very convenient to investigate the accuracy of the nuclear design code system. Among the various experiments conducted at VHTRC, we describe here the reaction rate measurements and its analysis.

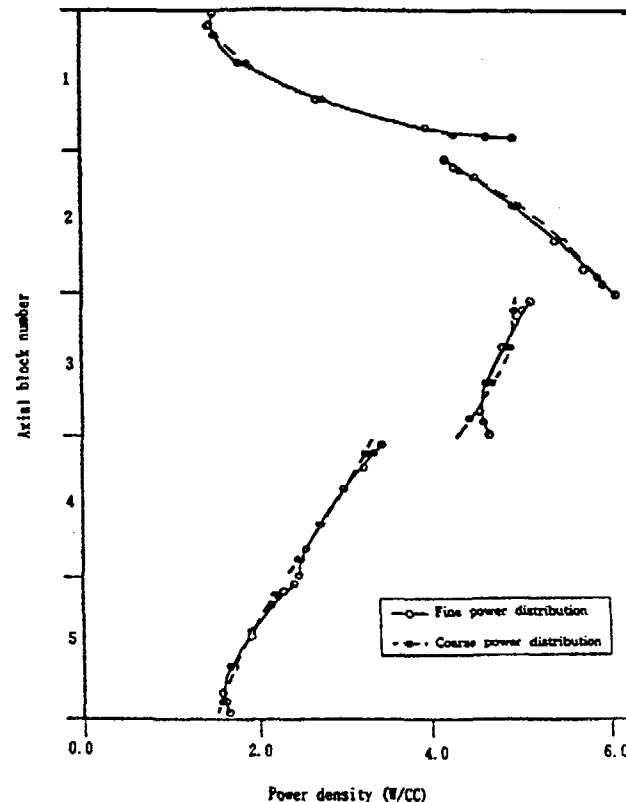


Fig.6 Comparison of axial power distribution

(1) Outline of VHTRC

The VHTRC is a split table type critical assembly which consists of two halves ones. The VHTRC is shaped in a hexagonal prism, whose side and axial length are 175cm and 240cm respectively. Core configuration could be flexibly changed by loading the fuel and graphite rods. The fuel rods are made up of graphite sleeve and fuel compacts. Each fuel compact consists of the graphite matrix and the coated fuel particles.

The reaction rate distribution of copper was measured in the radial and axial direction on the VHTRC-1 core which was composed by 280 fuel rods. The cross sectional view of VHTRC-1 core is shown in fig.7.

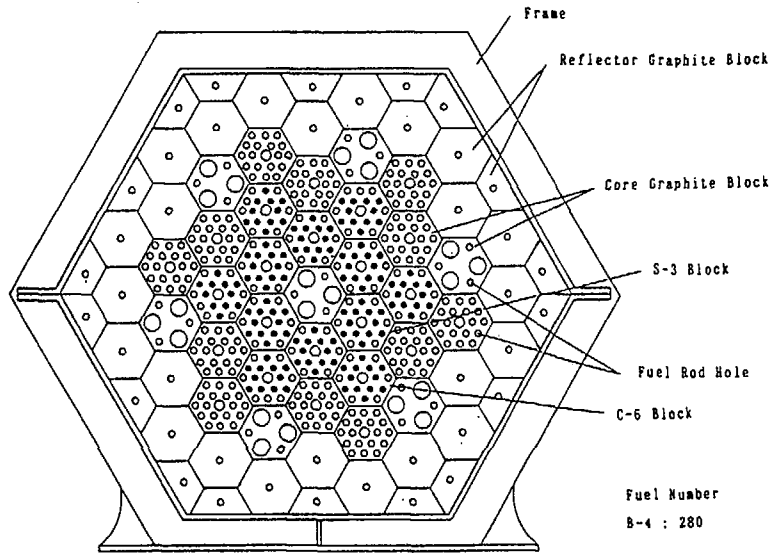


Fig.7 Cross section of VHTRC

(2) Analysis method and code

The analysis method is the same as the nuclear design code system in the HTR except some special treatments derived from the specific characteristic of VHTRC.

We used the DELIGHT code for the calculation of group constants. Core calculations were performed by the CITATION-1000VP code employing the three dimensional triangular mesh model.

(3) Results

The reaction rate distributions are analyzed as the product of neutron flux and the activation cross section of ^{63}Cu in a radial and axial direction. (5)

Figure 8 shows the typical distribution in the axial direction of the VHTRC-1 and figure 9 shows the deviations from the measurements at the radial position of fuel rods.

The agreement between calculation and experiment was good, and the discrepancy was within 3% in the fuel region at both directions.

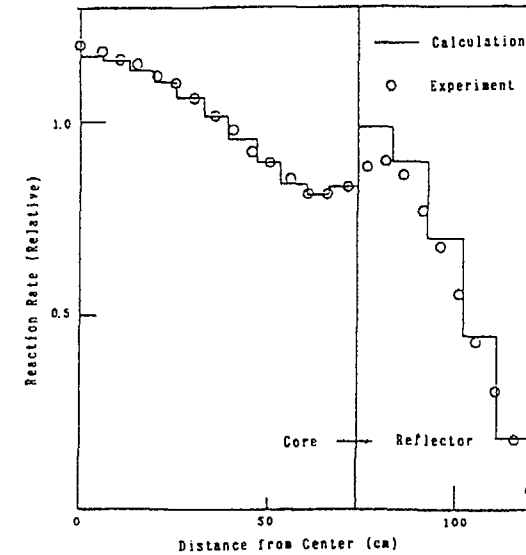


Fig.8 Axial Reaction Rate Distribution (VHTRC-1, Room temperature)

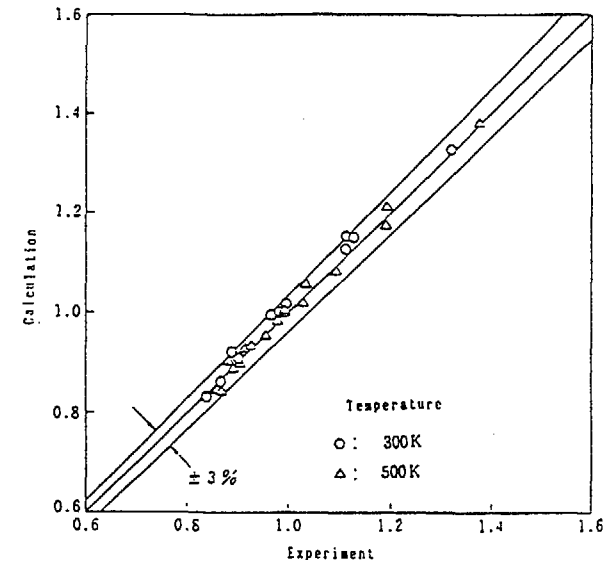


Fig.9 Comparison of Radial Reaction Rate Between Calculation and Experiment

5. Summary

We described the calculational methods of power distribution in the HTTR and the verifications by the VHTRC experiment.

We calculated the local power peaking factor due to the spatial heterogeneity caused by the fuel rods and BP rods in a fuel block, the local power spike due to the fuel block end graphite, and evaluated the design values of 7% and 4% respectively. For these power distribution calculations, we have verified the design code system by analyzing the VHTRC experiment.

From those results, it was confirmed that the power distribution in the HTTR could be predicted with sufficient accuracy, and could meet the design requirements.

ACKNOWLEDGEMENTS

Authors are deeply indebted to Messrs. S.Saito, T.Tanaka, Y.Sudo, H.Yasuda, F.Akino, T.Yamane for useful comments and supports for this work.

REFERENCES

- (1) Shindo, R., Yamashita, K., and Murata, I.: "DELIGHT-7 ; One Dimensional Fuel Cell Burnup Analysis Code for High Temperature Gas-cooled Reactors (HTGR)", JAERI-M 90-048 (1990), (in Japanese).
- (2) Harada, H. and Yamashita, K.: "The Reactor Core Analysis Code CITATION-1000VP for High Temperature Engineering Test Reactor", JAERI-M 89-135 (1989).
- (3) Yasuda, H., et al.: "Construction of VHTRC (Very High Temperature Reactor Critical Assembly)", JAERI 1305
- (4) Akino, F., et al.: "Critical Experiment on Initial Loading Core of Very High Temperature Reactor Critical Assembly (VHTRC)", J. Atomic Energy Society, 31 p.p. 682-690 (1989), (in Japanese)
- (5) Yamashita, K., Murata, I., Shindo, R., Watanabe, T.: "Accuracy Investigation of nuclear Design Method for HTTR Based on VHTRC Experimental Data", JAERI-M 88-245 (1988), (in Japanese)

THE PLANT DYNAMICS ANALYSIS CODE ASURA FOR THE HIGH TEMPERATURE ENGINEERING TEST REACTOR (HTTR)

Y. SHIMAKAWA, M. TANJI
Advanced Reactor Division,
Mitsubishi Atomic Power Industries, Inc.,
Tokyo

S. NAKAGAWA, N. FUJIMOTO
HTTR Development Division,
Japan Atomic Energy Research Institute,
Oarai-machi, Higashi-Ibaraki-gun, Ibaraki-ken
Japan

Abstract

This report summarizes the analytical models and the verification results of the plant dynamics analysis code, ASURA, which has been developed for designing the reactor control system of HTTR (High Temperature Engineering Test Reactor). ASURA consists of models of major components and systems of HTTR, such as the reactor, heat exchangers and the reactor control system, to simulate whole-plant transients.

ASURA has been verified by (1) a comparison with Fort St. Vrain (FSV) test data and (2) a comparison with another verified dynamics analysis code, THYDE-HTGR.

INTRODUCTION

Japan Atomic Energy Research Institute (JAERI) is proceeding with the construction of HTTR to establish the HTGR technology basis and to conduct innovative basic researches on high temperature technology.

HTTR shown in Fig.1 is a test reactor with thermal output of 30 MW and reactor inlet/outlet coolant temperature of 395 °C/950 °C, using pin-in-block type fuel. The heat generated in the core is transferred to pressurized water through the intermediate heat exchanger (IHx) and the primary/secondary pressurized water coolers (PWCs) of the main cooling system, and finally removed to atmosphere at the air cooler (A/C). In addition, the auxiliary cooling system (ACS) and the two vessel cooling systems (VCSs) are provided for decay heat removal and emergency reactor cooling, respectively. The reactor control system shown in Fig.2 is designed to accomplish a stable operation with the rated condition of reactor power and reactor outlet temperature.

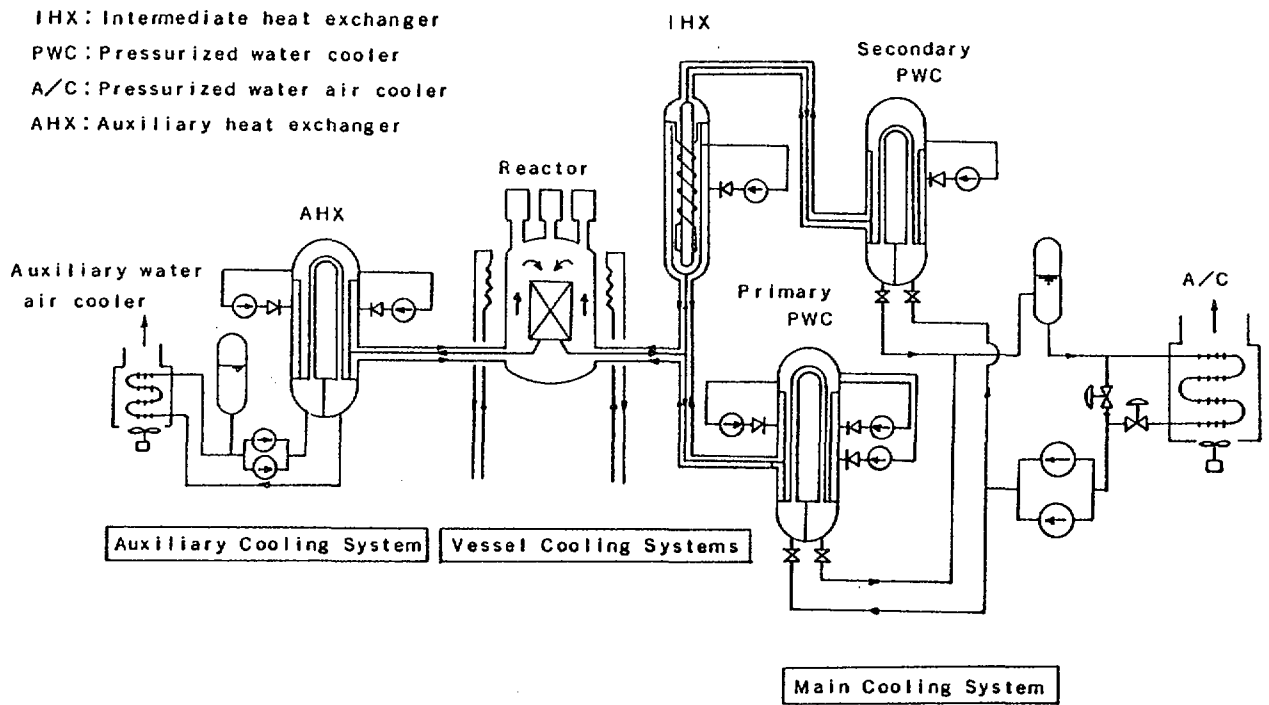


Fig.1 System Scheme of HTTR

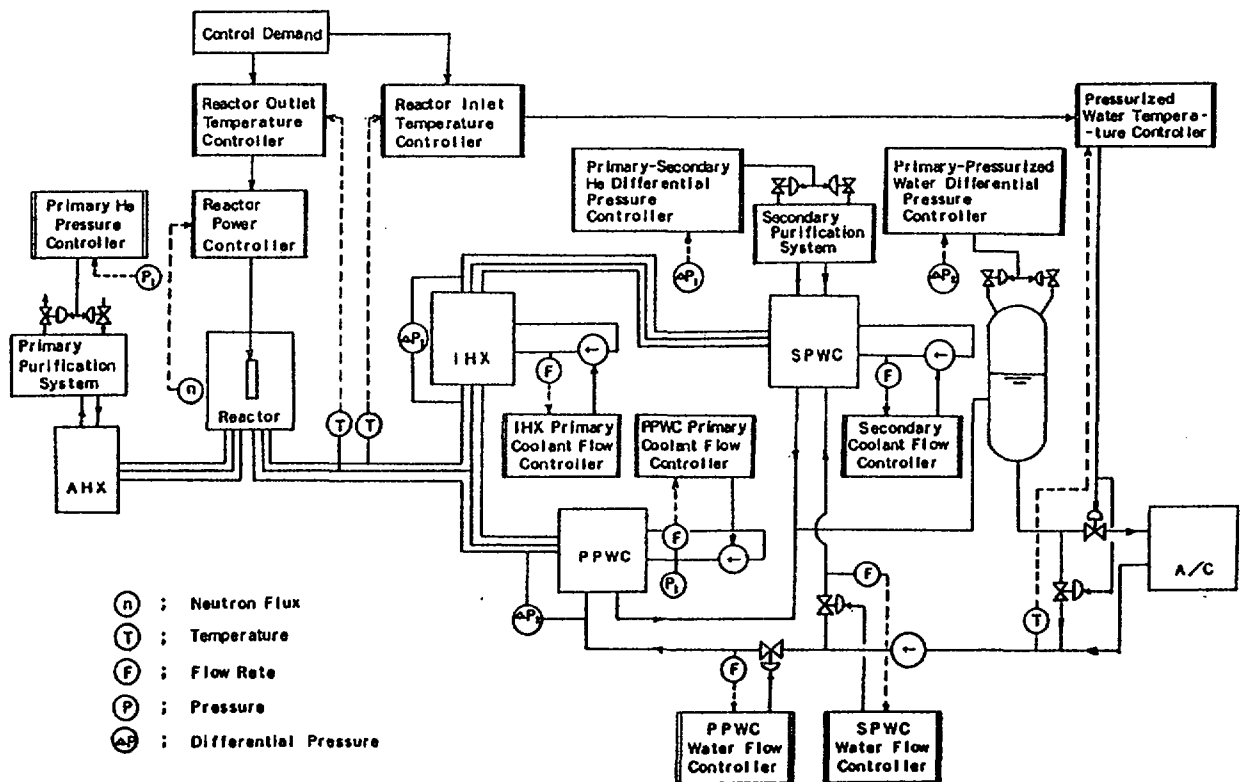


Fig.2 HTTR Reactor Control System

A plant dynamics analysis code, ASURA, has been developed mainly for design and evaluation work of the HTTR reactor control system. ASURA consists of models of major components and systems of HTTR to simulate whole-plant transients. This report describes the analytical models of ASURA and verification results.

OUTLINE OF ASURA

Code Structure

The ASURA code has been designed based on a modular structure. The various physical phenomena in the HTTR plant are categorized into the following five groups from a view point of the basic equations and the boundary conditions, as shown in Fig.3;

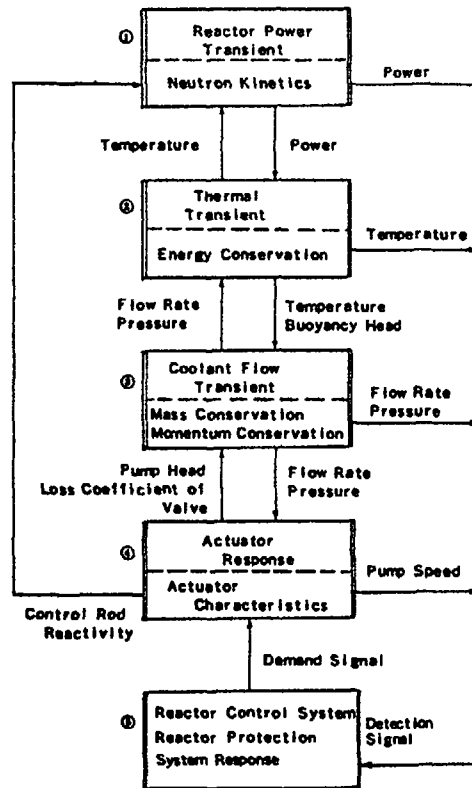


Fig. 3 Transient Analysis Scheme of ASURA

(1) reactor power transient, (2) thermal transient of the reactor and cooling systems, (3) coolant flow transient, (4) actuator response, and (5) response of the reactor control system and the reactor protection system. These five groups are subdivided into thirteen modules as shown in Table 1, corresponding to the HTTR components. ASURA is a complex of these thirteen modular programs, and each modular program works as a stand-alone small code.

Selecting some modular programs and connecting the interfaces by input data, an analytical system appropriate to a purpose can be constructed flexibly. In addition, the modular structure makes ASURA easy to modify and maintain.

Reactor Power Generation

The neutron flux level is calculated by solving the point kinetics equations with six delayed neutron groups, applying the prompt jump approximation. The reactor power is determined from

Table 1 List of Modular Programs

Phenomenon	Objective
① Reactor Power Transient	Neutron Kinetics
② Thermal Transient	Reactor Core
	IHX: Intermediate heat exchanger
	PWC: Pressurized Water Cooler
	A/C: Air Cooler
	Piping of Primary and Secondary Cooling System
	Piping of Pressurized Water Cooling System
③ Coolant Flow Transient	Primary, Secondary, and Pressurized Water Cooling System
	Mixing Element
④ Actuator Response	Gas Circulator, Pressurized Water Pump
	Control Valve
⑤ Control and Protection System Response	Reactor Control System
	Reactor Protection System

the neutron flux level and the decay heat, assuming that the spatial distribution of the reactor power generation is independent of time. The reactivity is changed by the position of the control rods and the temperature of the fuel and the moderator.

Thermal Calculation on Reactor and Cooling System

The thermal model of the reactor is shown schematically in Fig.4. The core is modeled as a single channel of a representative fuel pin. The spatial temperature distribution of the fuel and the moderator is calculated by solving a two-dimensional cylindrical thermal conduction equation. The reactor internal structures (such as the reflector, the shield and the reactor vessel) are modeled as several lumped heat capacity terms considering their shapes.

The heat exchangers are modeled as a single channel of a representative heat transfer tube. The thermal models of the IHX and the primary PWC are shown schematically in Fig.5 and Fig.6, respectively. Internal structures (such as the liner, the thermal insulator and the shell) are modeled as heat capacity terms in the same way. The temperature of coolants and structures is calculated by solving one-dimensional energy conservation equations in the direction of the flow.

The co-axial double wall helium pipes are modeled as heat capacity terms and the pressurized water piping is modeled as a transport lag. Energy gain of helium from compression works of the gas circulators is calculated by an adiabatic compression model of an ideal gas. A static approximation neglecting time-dependence is applied in energy conservation equations of the helium and the air.

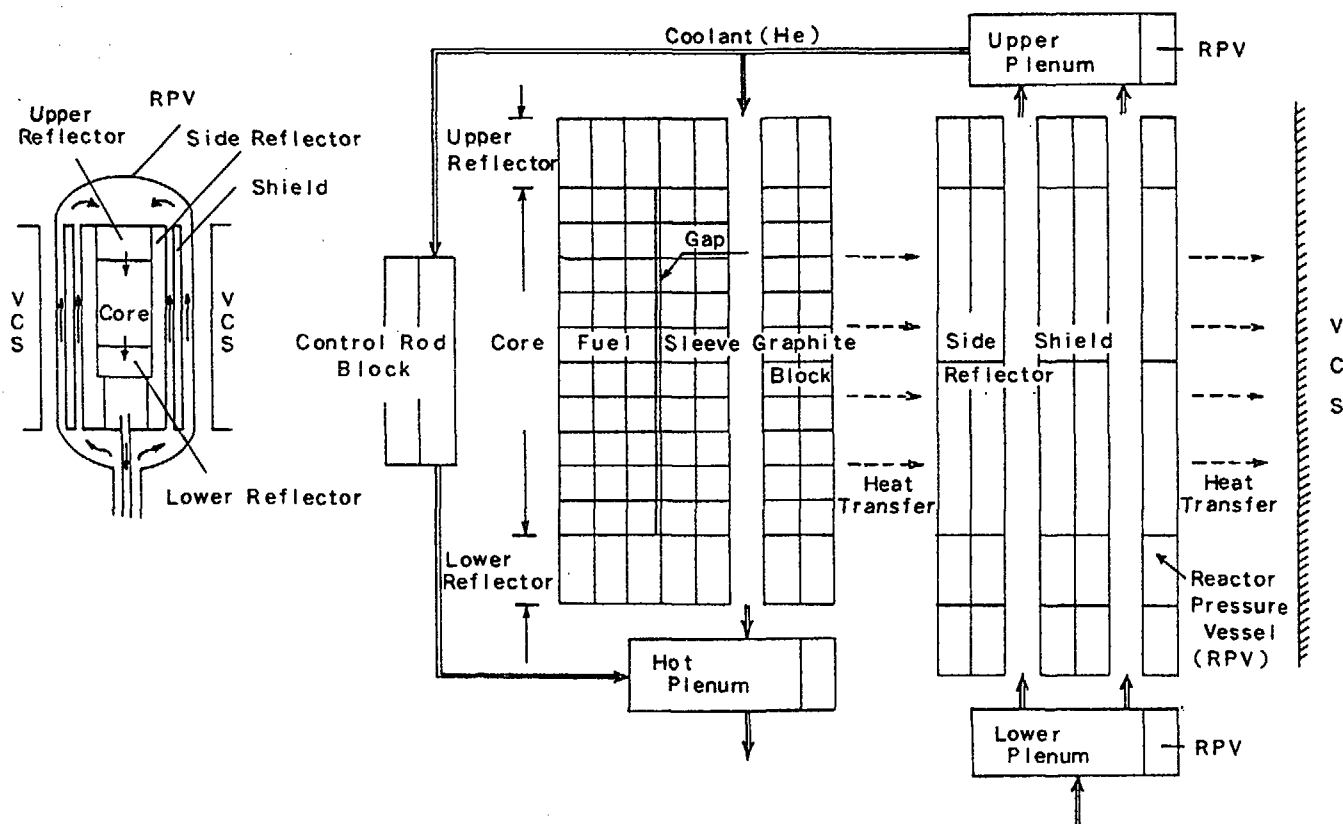


Fig.4 Reactor Thermal Model

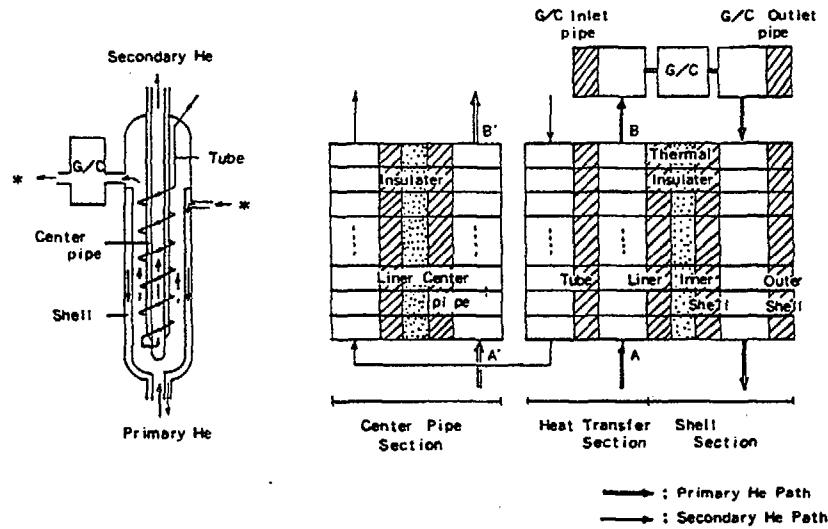


Fig. 5 IHX Thermal Model

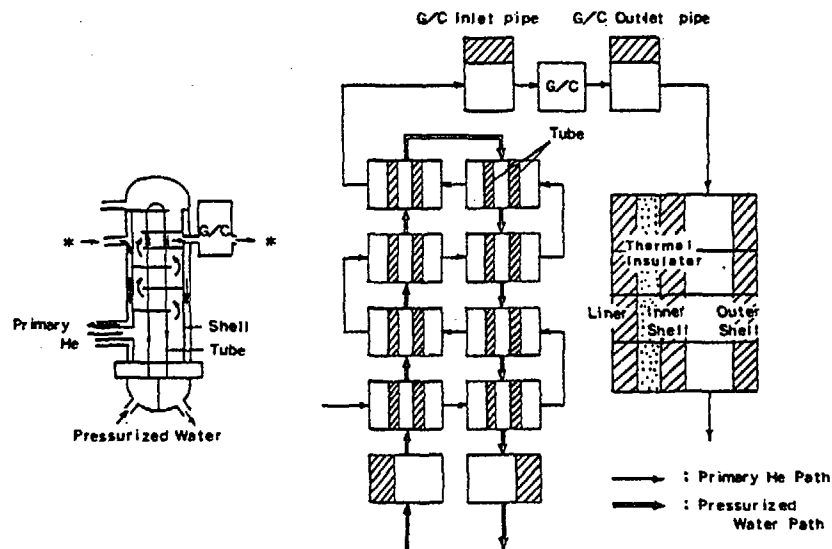


Fig. 6 Primary PWC Thermal Model

Coolant Flow Calculation

The flow rate of the helium and the pressurized water is calculated by a flow-network model, which describes the cooling system by some representative pressure nodes and flow paths. Fig. 7 shows the flow-networks of the primary and the pressurized water cooling systems. The distribution of flow rate and pressure is calculated by solving mass conservation equations on pressure nodes and momentum conservation equations on flow paths simultaneously. The model composes arbitrary flow-networks by input data, and it is possible to place pumps (the gas circulators or the pressurized water pumps) and valves on any paths of the flow-networks. The pump speed is calculated by the torque balance equation and the pump head is calculated by the Q-H characteristics.

COMPARISON WITH FSV TEST DATA

Using experimental data of control rod withdrawal/insertion tests performed in the United States' FSV (Fort St. Vrain) reactor, verification of ASURA has been carried out. Though the type of the core and the cooling system of FSV is different from those of HTTR, the FSV test data are available for verification of the neutron kinetics and the thermal calculation model of the reactor core by modifying the analytical models of ASURA for a multi-hole type fuel. The following two cases have been calculated.

- (1) control rod withdrawal test --- add the reactivity of +9.54¢ in 6 seconds.
- (2) control rod insertion test --- add the reactivity of -6.54¢ in 21 seconds.

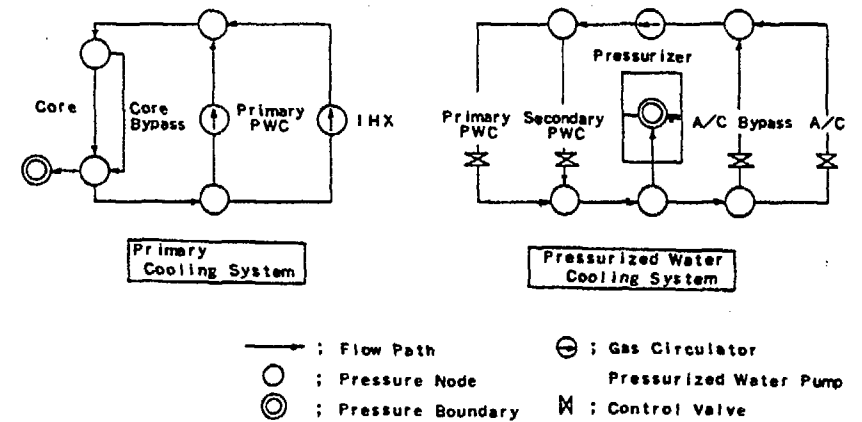


Fig. 7 Flow-Networks

The calculation results are compared with the experimental data in Fig.8. Though only the reactor power transient is compared, excellent agreements are obtained in both cases, and the neutron kinetics and the reactor thermal calculation model of ASURA has been verified.

COMPARISON WITH THYDE-HTGR

The analytical results of ASURA are compared with the results of another verified whole-plant dynamics analysis code, THYDE-HTGR, developed by JAERI, and used for the HTTR licensing safety analysis. The following two cases are compared.

- (1) A/C bypass valve accidental closure, and
- (2) Loss of off-site electric power.

A/C Bypass Valve Accidental Closure

Upon a A/C bypass valve accidental closure, heat removal in the secondary cooling system increases by increase of the pressurized water flow rate in the A/C. In this event, the main cooling system continues the heat removal without reactor trip. Transients of the IHX and the primary PWC has been compared in Fig.9. Coolant temperature transients at the outlet of these components showed excellent agreement.

Loss of Off-Site Electric Power

Upon a loss of the off-site electric power, all gas circulators and pressurized water pumps coast down, and the reactor is tripped by the reactor protection system. With some time delay, emergency electric power is generated, and the ACS starts

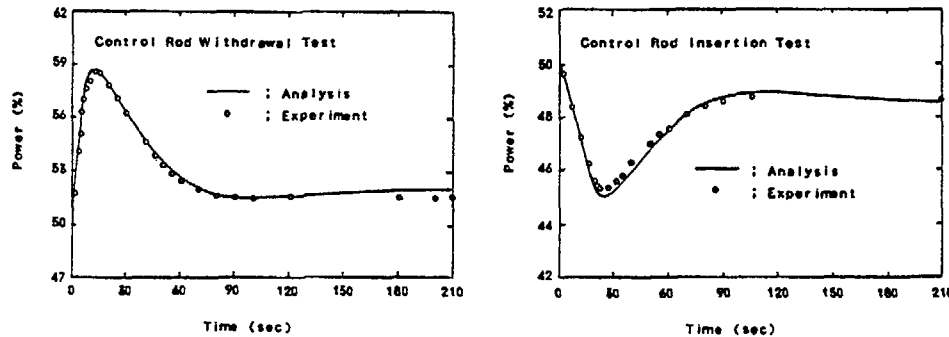


Fig 8 Comparison with FSV Test Data

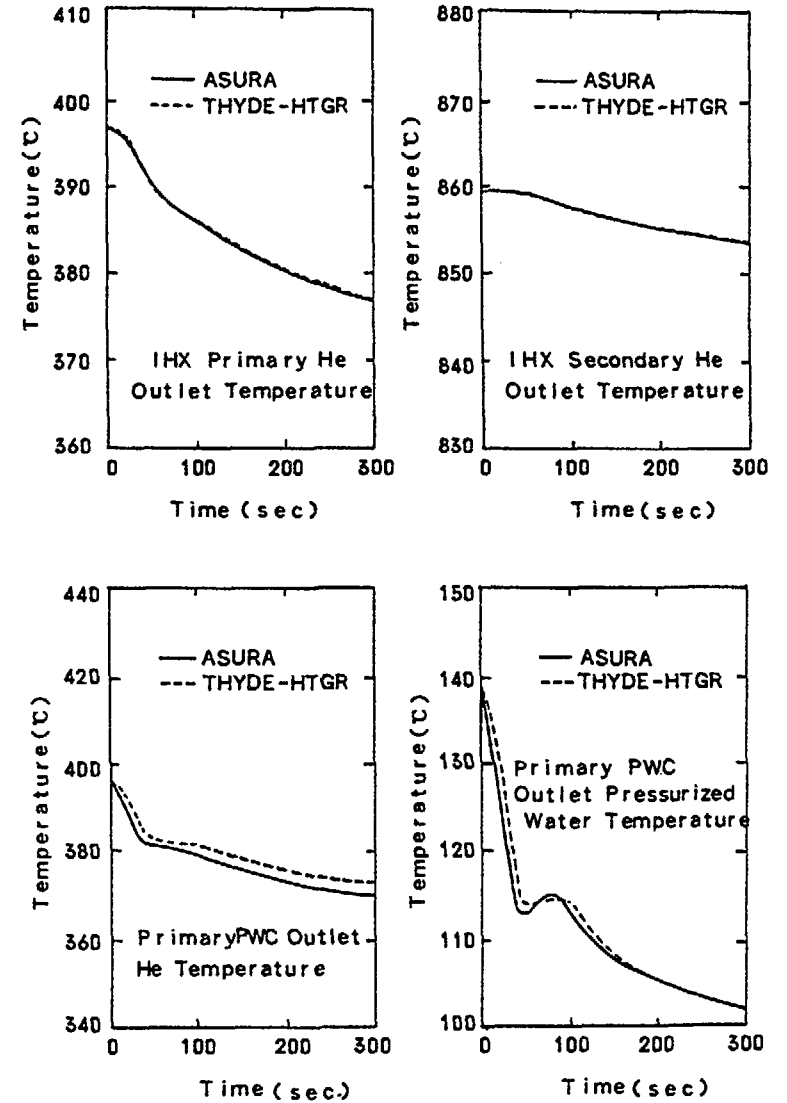


Fig.9 Comparison with THYDE-HTGR (A/C Bypass Valve Accidental Closure)

to cool the core. In this event, as the main cooling system stops its operation, the core is cooled only by the ACS. Therefore, the comparison is performed for transients on the reactor and the ACS.

Fig.10 shows the comparison of calculation results between ASURA and THYDE-HTGR. Good agreements are obtained on transients of the reactor power and the helium flow rate. However, there is a difference of the AHX inlet temperature transient for a time period of low helium flow rate until the start-up of the ACS. This difference is caused by the application of the static approximation to the energy conservation equations of helium coolant. As the objective plant condition of the code is limited

to a normal operation condition with high flow rate of helium coolant, this difference is not important for ASURA.

CONCLUSION

The plant dynamics analysis code ASURA for design and evaluation work of the HTR reactor control system has been developed. Performing verification studies (comparison with the PSV test data and comparison with calculation results of THYDE-HTGR), it has been confirmed that the analytical models of ASURA are adequate for the purpose.

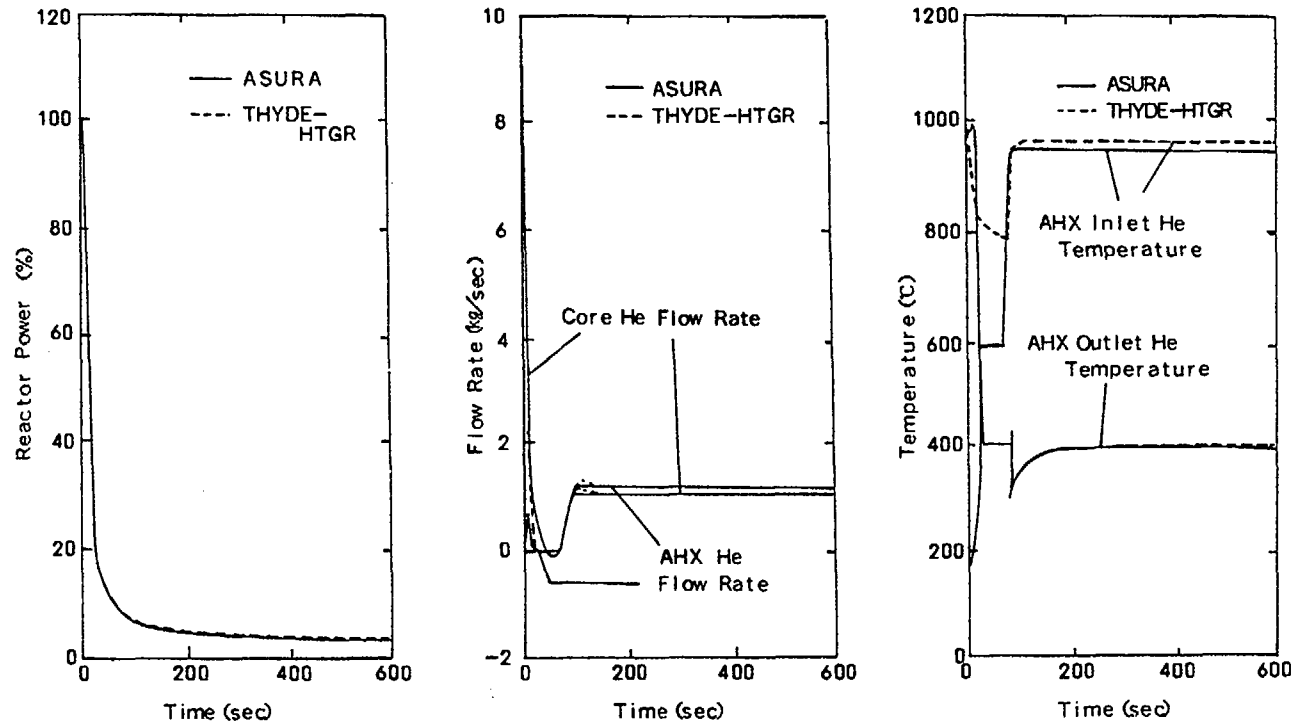


Fig. 10 Comparison with THYDE-HTGR
(Loss of Off-Site Electric Power)

ACKNOWLEDGEMENTS

The authors wish to thank Messrs. S. Saito, T. Tanaka and Y. Sudo for useful comments and supports.

REFERENCES

1. JAERI; "Present Status of HTGR Research & Development, (1988)"
2. S. S. Clark, et al. ; "AEC RESEARCH AND DEVELOPMENT REPORT TAC2D A GENERAL PURPOSE TWO-DIMENSIONAL HEAT TRANSFER COMPUTER CODE MATHEMATICAL FORMULATIONS AND PROGRAMMER'S GUIDE", GA-9262
3. GA-A 15159 UC-99 "Fort St. Vrain surveillance program, Transient Analysis Program (TAP) Verification"
4. Asahi, Y. et al. ; "THYDE-P2: RCS (Reactor-Coolant-System) Analysis Code", JAERI 1300 (1986)
5. Public Service of Colorado, ; "Fort St. Vrain Reactor Final Safety Report", Docket No. 50-267

PHYSICAL STATUS OF THE 10 MW TEST MODULE

Jingyu LUO
Institute of Nuclear Energy Technology (INET),
Tsinghua University,
Beijing, China

Abstract

Like most graphite moderated HTR systems, the 10 MW Test-Module reactor is undermoderated. This means if the water ingress is into the pebble bed that this system will gain reactivity as moderator is added to the core. The reactivity increase caused by water ingress strongly depends on the geometry of the core, the temperature, the burnup status and especially the moderator to fuel ratio (the metal content per fuel element). For the equilibrium core 5 gram of heavy metal per fuel element is chosen in order to limit the effect of water ingress.

Another important effect of water ingress is to reduce the worth of control rods which are usually located in the reflector. The distance between core and control rods in the reflector are carefully calculated. In the 10 MW Test-Module reactor the core shutdown capability of 12 control rods are selected such that any accident reactivity can be counterbalanced and only half of the rods have to be available to render the reactor down from normal operation to the cold, permanent subcritical condition.

1 INTRODUCTION

In order to introduce and develop the module HTR technique in practice a joint project on construction of 10 MW HTR Test Module which collaborated among the Institute of Nuclear Energy and Technology (INET) of Tsinghua University PRC, Siemens-Interatom GmbH and Nuclear Research Center Julich FRG is started.

The 10 MW Test Module will be constructed at the site of INET in the north west of Beijing.

The main object of the Test Module is to provide a nuclear test facility with which relevant and unique features of the HTR Module can be demonstrated. Therefore, the Test Module plant shall be designed in such a way:

*for a large wide of possible application, e.g. electricity, power generation, process heat generation, provide of district heat and so on,

*with a limits of what is physically possible, the Test Module shall as similar as possible to that of the HTR-Module. So that relevant components can be tested and proved at nominal conditions,

*shall be demonstrating the unique inherent safety features of the HTR-Module,

*shall be to verify computer codes, which are to be used to predict the physical behaviours (such as power response of the core due to water ingress, temperature coefficient and the worth of control rods) and temperature behaviours (the behaviour of the core during core-heating-up accidents),

*shall be capable of being able to withstand extremely high core temperature, so that fuel element mass-testing could be carried out for nominal reactor at temperature up to 1,600 C.

The overriding aims for the Test-Module may be as follows:

1. Product application

2. Components testing

— graphitic core structures

— steam generator

— helium blower

— fuel handling

3. Verification of HTR-Module inherent features

— negative temperature coefficient of reactivity

— temperature limitation due to passive decay heat removal

— control rod withdrawal

— limitation of power excursion due to water ingress

4. Fuel element mass test for temperatures up to 1,600 C.

2 BASIC DESIGN

As in the HTR-Module, the Test-Module is designed such that the heat source "reactor" is basically independent of its application. In the first operating phase the reactor is to be used for power generation or for the production of district heat only. For this reason all numerical data given in Table 1 are valid for this phase.

Fig.1 shows the design of the reactor. It should be understood that all given dimensions are subject to further detailed analyses.

The complete core structure is exclusively of ceramic material. For manufacturing reasons, a 15-segment design is selected for the graphite and carbon brick blocks. The graphitic cylinder which holds the pebble bed has a diameter of 1900 mm and height of approx. 2200 mm. This is adequate for the required volume of the active core which amounts to 5 cubic meters.

TABLE 1. MAIN DATA ON THE TEST MODULE

Maximum thermal power	20 MW
Average thermal power	10 MW
Primary helium pressure	30 bar
Secondary steam pressure	35 bar
Cold helium temperature	250 °C
Average hot helium temperature	700 °C
Steam temperature	435 °C
Core volume	5 m ³

New fuel elements can be injected into the core via five fuel element charging tubes where four tubes serve the outer core region and the central serves the inner region. Removal of the fuel elements is accomplished via a central fuel element discharge tube with an inner diameter of 500 mm. The large diameter guarantees that any bridging effect of fuel element which could cause a blockage of the discharge tube can be definitively excluded.

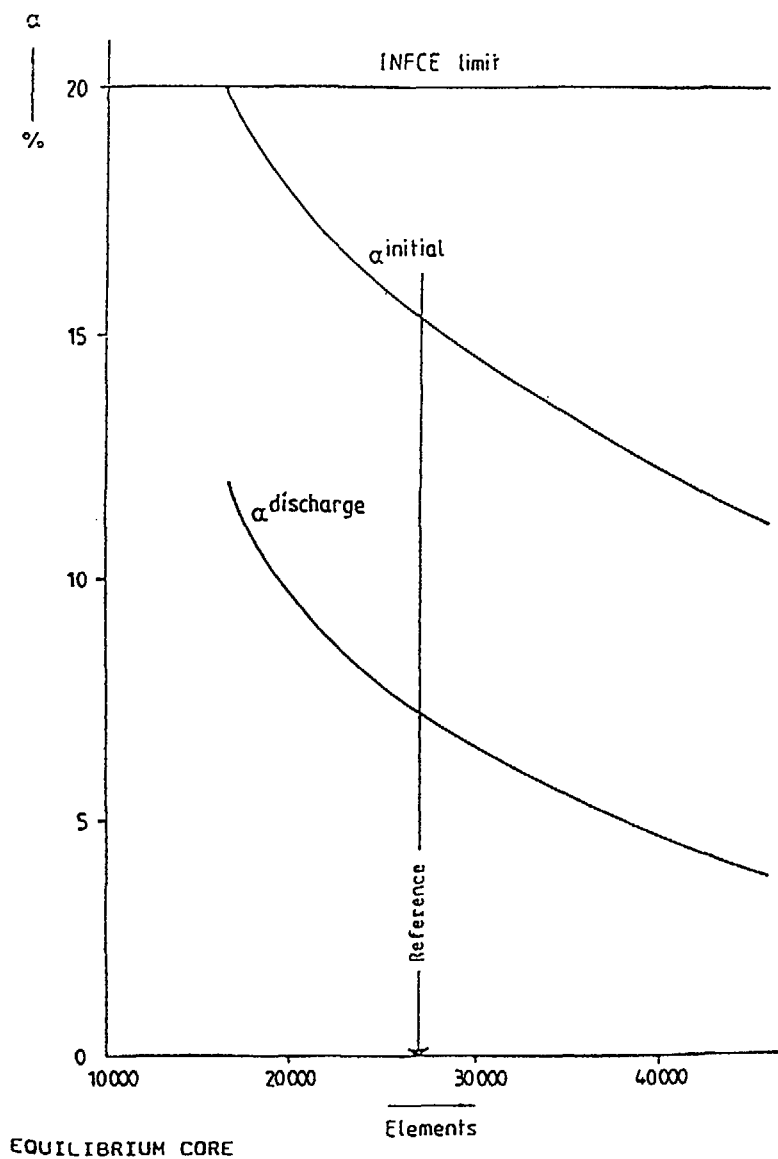
The fuel element migrates through the core only once (OTTO-loading scheme).

The reactor is provided with one shutdown system only. 12 reflector rods are necessary for the core shutdown. Due to the 15 segment design this leaves up to three reflector boring empty which could be used as irradiation channels or to add two extra control rods.

To obtain maximum rod worth the control rods are positioned as close as possible to the active core. Considering stability and strength of the graphitic side reflector the minimum distance between rods and core is set to be 6 cm.

3 CORE PHYSICS

In order to establish the basic core configuration the various interdependent effects of design burnup of the fuel element, uranium enrichment, pebble flow, core size, core shape and especially the moderation ratio (it directly related to water ingress reactivity effect) have been investigated.



EQUILIBRIUM CORE

FIG. 2. Fuel enrichment versus core volume (number of elements).

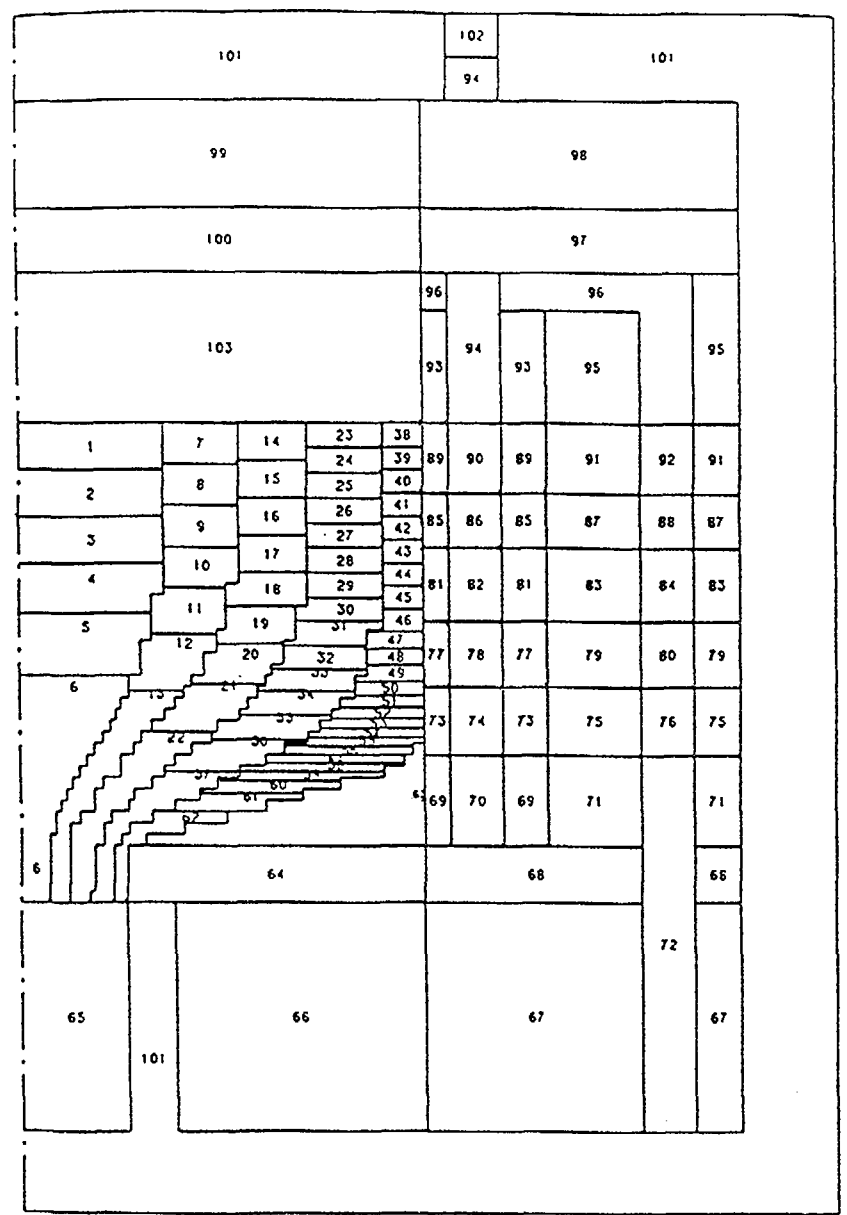


FIG. 3. Model of the numerical reactor simulation.

TABLE 2-1. DATA ON THE EQUILIBRIUM CORE

Thermal power (avg.)	10 MW
Power density (avg.)	2 MW/m ³
H/D - ratio	0.93
Core diameter	190 cm
Core height (avg.)	176 cm
Number of fuel elements	27000
Heavy-metal content	5 g/FE
Burn-up (avg.)	80.000 MWd/t
Fuel element incore time	1078 EFPD *
Number of fuel elements per day	25
Loading scheme	OTTO

* EFPD EQUAL FULL POWER DAYS

TABLE 2-2. DATA ON THE EQUILIBRIUM CORE

k_{eff}	1.0028
Enrichment (U ₂₃₅)	18 w%
U ₂₃₅ -content (BOC) *	0.9 g/FE
U ₂₃₅ -content	0.4 g/FE
Burn-up (avg.):	
• 1. flow path	51700 MWd/t
• 2. flow path	57000 MWd/t
• 3. flow path	70400 MWd/t
• 4. flow path	100700 MWd/t
• 5. flow path	131200 MWd/t
Conversion rate	0.24
Max. / avg. power density	1.46
Fissile inventory:	
• U ₂₃₅	14.9 kg
• PU ₂₃₉	0.6 kg
• PU ₂₄₁	0.1 kg
Neutron loss of core	29.6 %

* BOC BEGIN OF CYCLE

TABLE 2-3. DATA ON THE EQUILIBRIUM CORE

Temperature coefficient:	
• Doppler	- 2.5 mN/K
• Moderator	- 6.1 mN/K
• Reflector	+ 2.1 mN/K
Neutron flux in side reflector	
• thermal (E < 2.38 eV)	4.2 E+13 1/(cm ² s)
• fast (E > 0.1 MeV)	3.6 E+12 1/(cm ² s)

In Fig.4 results are shown as a function of steam inventory and various core geometries. It is obvious that the theoretical of reactivity increase due to the presence of steam are strongly dependent on the heavy metal content of the fuel elements i.e. the moderator to uranium ratio and could in principle reach extremely high values. So to choose it properly was a key point in the parametric study phase.

Fortunately in Test-Module, however the amount of steam that possibly could be placed into the pebble bed is physically limited to 7 kg per cubic meter. This value is obtained by assuming that the total primary circuit is filled with saturated steam, at the temperature of 250 C, taking as the maximum possible pressure the upper setpoint of the primary circuit safety value of 39 bar. Any other temperature will led to a small steam inventory.

As to the stated core geometry and size, 5 g. heavy metal per fuel element was chosen as a reference one. Than we can get from the graph that the maximum reactivity increase due to any water ingress into the reference core will be 0.04.

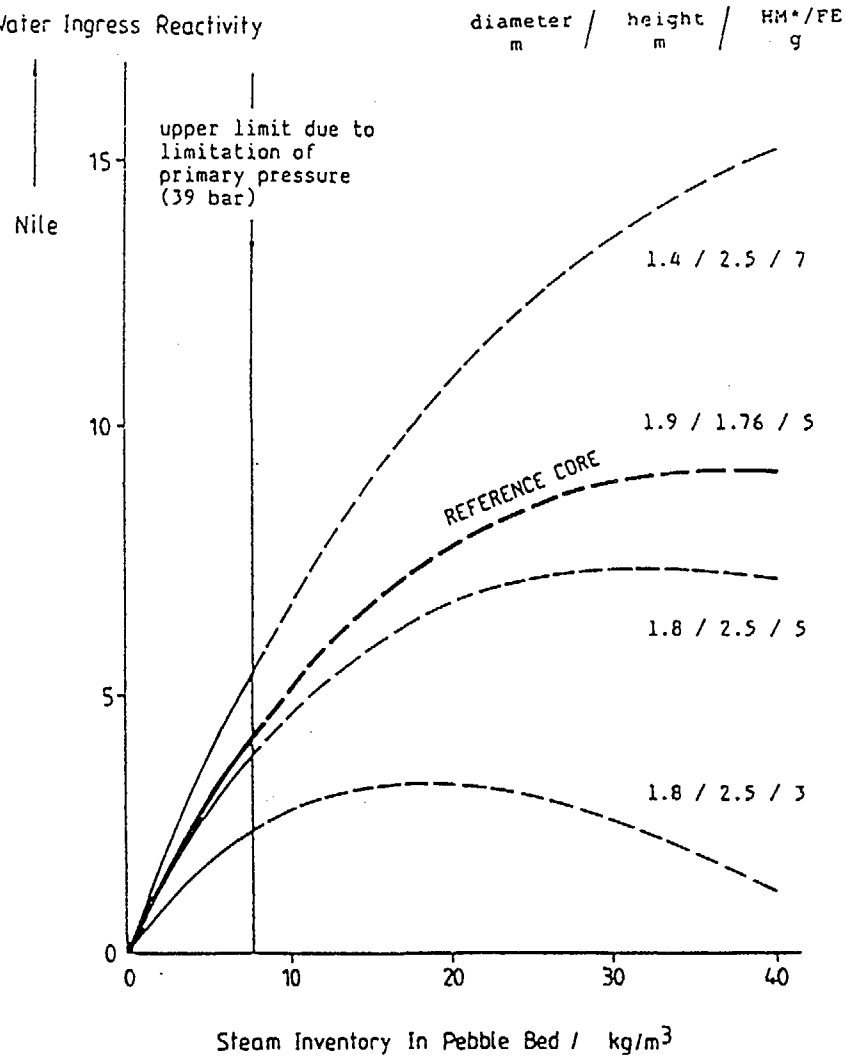
To safety shutdown the core even in this hypothetical event the control rod worth should be selected such that even this accident reactivity can be counterbalanced. Due to the uncertainties in the water ingress and related control rods worth calculation and to keep enough counterbalance ability, the arrangement of control rod were carried out once again.

Using the core diameter of 1.9 m the 12 control rods worth yields 0.154. If the diameter reduced by 10 cm, see Fig.5, then the 12 control rods worth will increase by 0.027 .

Due to the early design state it was decided to employ this large effect and reduce the core to 1.8 m. Hence, the capability of all 12 control rods worth increase to 0.181 and the results is given on Table 3.

It is apparent from the shown data that less than 0.08 of excess reactivity has to be compensated if the core should be rendered from normal operation to the cold subcritical state. This value includes xenon decay, temperature effect, excess reactivity for power control and subcriticality

Water Ingress Reactivity



* HM: Heavy Metal
EQUILIBRIUM CORE

FIG. 4. Reactivity increase due to an increase of steam inventory in the pebble bed.

but does include per definition the value for accident excess reactivity and the provision for experimental excess reactivity.

It is also important to note that only half of the control rods have to be available to render the core from normal operation to, the cold, permanent subcritical condition.

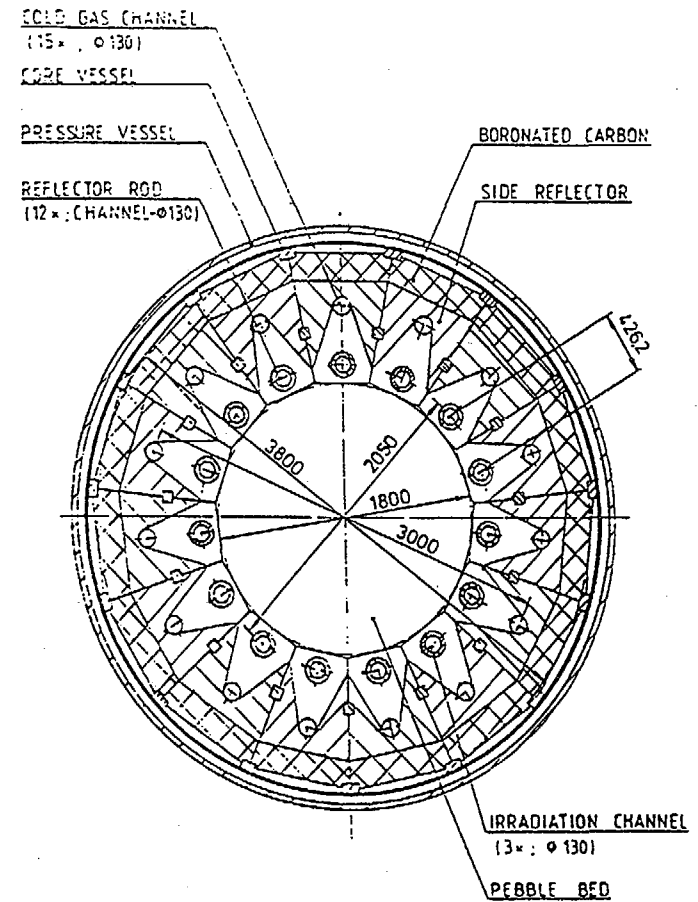


FIG. 5. Horizontal cross-section through the reactor pressure vessel (C-C).

TABLE 3. DATA ON CORE SHUTDOWN

Requirements (10 MW, 700 °C)	%
• Excess reactivity for power control	0.5
• Excess reactivity for experiments	1.0
• Temperature compensation 20 °C	3.6
• Xenon-decay	3.0
• Accident excess reactivity (steam)	4.0
• Subcriticality	0.3
• Total	12.4
• Rod capability	
• 12 rods	18.1
• Rod failure	-3.0
• Total	15.1

5 CONCLUSIONS

From the study presented in this paper it is clear that the the water ingress and the worth of control rods are two key points related to the safety of 10 MW Test-Module. More accuracy calculation methods and experiments for the low enrichment HTGR are necessary for our next design phase. Some other factors like temperature coefficient, reactivity decrease by nitrogen are also important for withstand accidents beyond usual basic design accidents.

EFFECTS OF THE FUEL ELEMENTS PEBBLE BED STRUCTURAL NON-UNIFORMITY ON THE HTGR PHYSICAL AND THERMOPHYSICAL CHARACTERISTICS

V.I. YEVSEVEV, A.I. KIRYUSHIN, N.G. KUZAVKOV,
V.M. MORDVINTSEV, Yu.P. SUKHAREV
Experimental Machine Building Design Bureau,
Gorki, Union of Soviet Socialist Republics

Abstract

The paper features results of the analysis of fuel elements velocities' field and porosity distribution effects in the pebble bed on the core power and temperature distribution in the VG-400 and VGM reactors designed in the USSR. Both normal operation of the plants and the accident with the pebble bed shrinkage under the seismic impact has been considered.

The analysis of power distribution has been made on the basis of experimental data dealt with porosity distribution obtained in the USSR during model experiments.

The need to take into account the detailed porosity distribution throughout the pebble bed in the reactor physics analysis has been emphasized.

It is shown, that the difference in the reactivity rise at the pebble bed shrinkage calculated using the average volumetric porosity changes from that calculated using the detailed porosity distribution can reach about 10%.

Increase of the fuel elements velocities' non-uniformity (i.e. changeover from the uniform field to the profile with the maximum non-uniformity) is followed by the radial power distribution non-uniformity increase from 1.15 to 1.3.

Porosity distribution changes substantially affect the power level in the area of disturbances (approximately in proportion with the changes of the fissiled nuclei concentration); in the rest of the core the energy release deformation is negligible.

Changes of the pebble bed porosity distribution may substantially affect the maximum values and pattern of the fuel temperature distribution. Thus, porosity reduction in the core periphery from 0.6 to 0.32 results in the maximum fuel temperature rise by approximately 200 C.

As far as the other physical characteristics changes are concerned, it has been pointed out, that variation of the velocities profile causes the fuel burn-up changes not higher than by 5%, and porosity variation not more than by 10%.

INTRODUCTION

In reactors with the pebble bed core apart from the uncertainties in the multiplication factor, power distribution, control and protection system (CPS) members efficiency etc. related to the physical calculations models there are specific uncertainties in the main functionals provided by the porosity changes throughout the pebble bed.

As a rule, statistical data on the average fuel elements velocities and porosity distributions throughout the pebble bed is used in reactor physical calculations. Nevertheless, local pebble bed porosity changes incurred by variation of its structure during reactor operation can be substantially different from those accepted in physical calculations and provide considerable disturbances of both power distribution and fuel temperature.

The importance of this analysis objective is augmented by the fact that during reactor operation it is impossible to obtain data on the porosity changes in the pebble bed by the ex-reactor control system (even if there is one) and all the more to identify the causes of these changes.

In the safety analysis of HTGR with the pebble bed deviations of the reactor key parameters caused by the pebble bed compaction should be also calculated.

The best way to reduce uncertainties of the reactor design process is to conduct experiments on critical assemblies simulating the actual reactor core structure both for verification of calculation methods and design parameters.

On the other hand, to obtain representative results of physical experiments the experimental substantiation of fuel elements velocity profile and porosity distribution throughout the pebble bed is required.

The paper aims to study dependence of the HTGR key physical characteristics on the fuel elements velocity profile and porosity distribution of the pebble bed, provided by random deviations or variations during the accidents, as well as to estimate errors in calculation of reactor characteristics provided by the calculation models (on the basis of reactors VE-400 and VGM).

1. SOME CHARACTERISTICS OF THE HTGR WITH PEBBLE BED

At present, in the USSR two HTGR of different power rating and reactor vessel design are being developed. Reactor VE-400 with thermal power of 1060 MW(t) is operated in the equilibrium mode on OTTD principle. Its core contains about 820000 fuel elements that are 60 mm in diameter with 6.5 % fuel enrichment on U-235, 6.15 g U loading per fuel element and has a diameter of 6.4 m and a height about 4.8 m. Withdrawal of fuel elements is effected through 3 discharge channels with inner diameter of 0.6 m. The reactor vessel is made of the prestressed concrete.

The absorber rods placed in side reflector are used as the CPS reactivity compensation members and inserted in the pebble bed ~2.5 m deep.

200 MW(t) VGM reactor is operated in equilibrium mode on the MEDUL principle. The core contains about 350000 fuel elements that are 60 mm in diameter, with 8% fuel enrichment and 7 g U loading per fuel element. The core diameter and height are 3 and ~9.4 m, respectively. Withdrawal of fuel elements is effected through one discharge channel with inner diameter of 0.6 m.

The reactor has a steel vessel and is designed provide residual heat removal through reactor vessel to the passive heat removal system. The absorber rods and KLAH channels placed in the side graphite reflector are used as the CPS reactivity compensation members.

2. MAJOR RESULTS OF PHYSICAL AND THERMOPHYSICAL CHARACTERISTICS CALCULATIONS

The average porosity in the moving pebble bed for the most likely irregular package of spherical fuel elements at a ratio of core diameter to fuel element diameter > 15 has a constant value of ~0.39.

At the same time, variations of porosity in the some regions pebble bed from its average value are possible. The experiments conducted on the fixed pebble bed^{1/} indicate that the greatest porosity changes occur at the side reflector boundary at a distance of

one fuel pebble diameter where it reaches ~ 0.6 . During the pebble bed movement fuel elements reshuffling occur near the side reflector boundary that may lead to substantial porosity reduction. As follows from [2], the porosity value may be ~ 0.32 at the side reflector boundary.

The following velocity profiles of fuel elements in the pebble bed have been considered to estimate the influence of porosity distribution on reactor's functionals:

1. uniform profile, obtained under assumption that all fuel elements are moved at the same velocity (fig.1a);
2. reference profile, accepted in calculations of VG-400 reactor core obtained during experiments, simulating reactor's dynamics (fig.1b);
3. profile with the maximum non-uniformity, obtained experimentally under the worst fuel elements friction against the side reflector surface (fig.1c).

The following porosity distribution in the pebble bed has been assumed (see fig.2):

- variant 1 - with lower density boundary layer, where porosity at a distance of 60 mm from the inner reflector surface was 0.6, while the average porosity was 0.39;
- variant 2 - with a dense boundary layer, where porosity is ~ 0.32 while in the adjacent layer ~ 140 mm thick it is ~ 0.26 at an average porosity of ~ 0.39 ;
- variant 3 - porosity over the discharge tubes is $\sim 10\%$ higher than that in variant 2 in the region with diameters between 3.8 and 4.2 m at an average porosity of ~ 0.39 .

Reactor physics calculations were performed using 2-dimensional (r, z) two-group diffusion computer code VIANKA [3]. The two-group macroscopic cross-sections of reactor physical zones were obtained using the NEKTAR [4] computer code applicable for the HTGR cell calculations. The core temperatures and hydraulics were calculated using computer code SFERA [5].

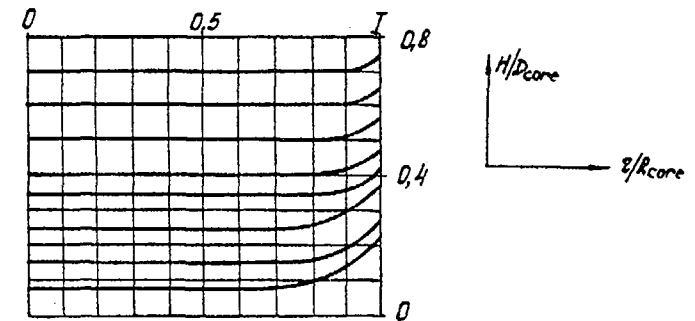


Fig.1a Fuel elements velocities distribution (uniform profile of pebble bed movement)

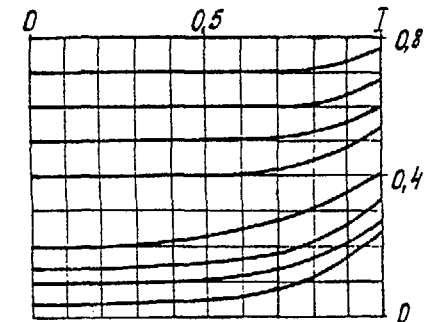


Fig.1b Fuel elements velocities distribution (reference profile of pebble bed movement)

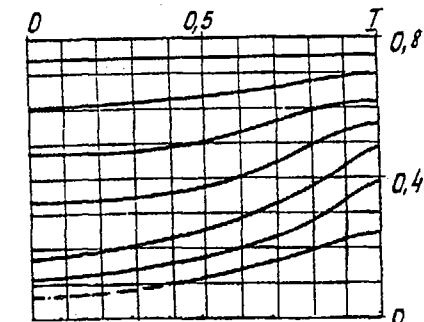


Fig.1c Fuel elements velocities distribution (profile with the maximum non-uniformity)

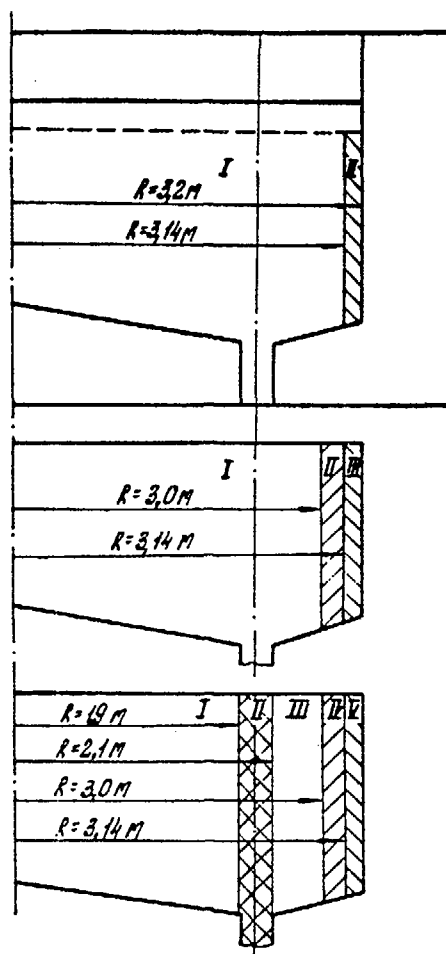


Fig. 2 Reactor calculation model

Variation 1
Porosity:
 $\epsilon_I = 0,382$
 $\epsilon_{II} = 0,6$
 $\epsilon_{III} = 0,39$

Variation 2
Porosity:
 $\epsilon_I = 0,405$
 $\epsilon_{II} = 0,26$
 $\epsilon_{III} = 0,325$

Variation 3
Porosity:
 $\epsilon_I = 0,399$
 $\epsilon_{II} = 0,468$
 $\epsilon_{III} = 0,399$
 $\epsilon_{IV} = 0,26$
 $\epsilon_V = 0,325$

The core temperature calculations results vs velocity profile and porosity distribution are summarized in the table:

Table

	maximum temperature, °C (without overheating factors)					
	uniform profile		reference profile		profile with maximum non-uniformity	
	variant 1	variant 2	variant 1	variant 2	variant 1	variant 2
At the central axis:						
helium temperature	1130	990	1220	1060	1310	1140
fuel temperature	1180	1120	1240	1120	1360	1210
At the boundary layer:						
helium temperature	690	1330	660	1200	650	1100
fuel temperature	710	1380	680	1240	660	1160

The maximum fuel temperature in variation 3 is close to that in variation 2.

The calculations revealed that:

1. increase of fuel elements velocities non-uniformity (change-over from uniform profile to profile with the maximum non-uniformity) resulted in the radial non-uniformity increase of power distribution. Coefficient of non-uniformity i.e. ratio of the maximum energy release to the average one throughout the core varied between 1.15 and 1.3:
2. variation of porosity distribution affected substantially the energy release in the area of perturbations (approximately in proportion to variation of fissile nuclei concentration), deformation in other core regions was negligible. Variation of

fuel elements velocity profiles caused changes in the burnup depth (less than 5%), porosity variations caused changes of the same functional by less than 10%;

3. variation of the pebble bed porosity distribution could substantially affect the maximum values and pattern of fuel elements temperature distribution. Thus, porosity reduction on the core periphery from 0.6 to 0.32 resulted in the fuel temperature rise up to 1320°C depending on the fuel elements velocity profile.

For VSM reactor with its limited potential of the reactivity compensation rods efficiency increase, estimation of the reactivity variation calculation error due to the pebble bed compaction is also important.

To estimate the maximum porosity changes the Experimental Machine Building Design Bureau performed comprehensive testing on the simplified hopper model registering spectra accelerogram of the real VSM structure response and modulation of conditions:

$\frac{a}{g} = idem, \frac{\omega^2 d}{g} = idem$, where. ω - frequency, a - acceleration, d - pebble diameter, with extended duration of seismic impact, as compared to the actual one. The pebble bed excitement was effected in the range of frequencies 5, 20 and 35 Hz and accelerations 0.75, 1.65 and 0.45g, respectively. Total duration of seismic impact was ~150 s.

As is evident from fig.3, the most intensive pebble bed compaction occurred at the maximum acceleration of 1.65g and at a frequency of 20 Hz, while at the change-over to another mode with 0.45 g and 35 Hz it virtually ceased. The total reduction of the average porosity was ~7.2%.

During the excitement local porosity redistribution was observed throughout the model volume (fig.4), as well as changing of free surface due to the upper pebbles layer reshuffling (the most intensive at 1.65 g and 20 Hz). The experimental relative error was ~2%.

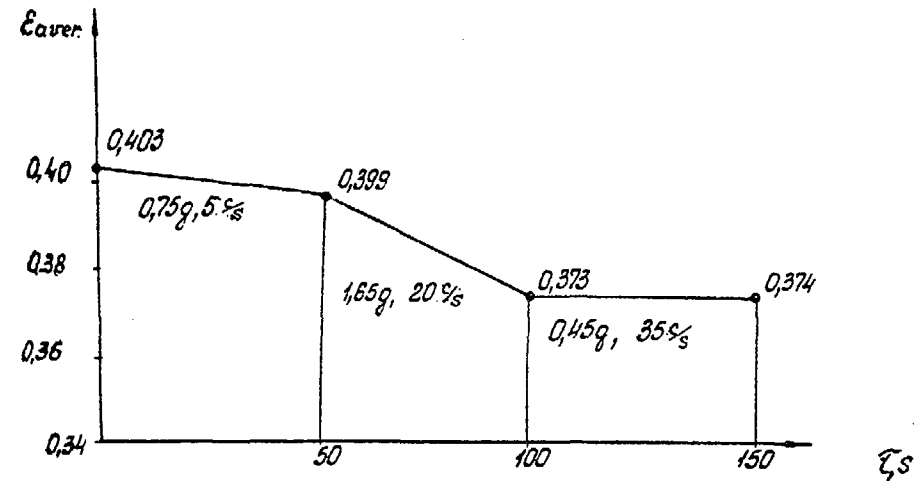


Fig.3 The pebble bed average porosity changes (ϵ_{aver}) depending on parameters and duration of dynamic impact

Reactor physics calculation to estimate porosity changes influence on the multiplication factor and power distribution has been performed on the basis of the foregoing computer code NEKTAR-VIANKA.

As is evident from fig.3, at the pebble bed compaction the average porosity changed from 0.403 to 0.374. Reactor physics calculation performed using the average porosity value revealed that the positive reactivity increase resulted from the pebble bed compaction amounted to ~0.55 % $\frac{\Delta k}{k}$, however, detailed treating of porosity distribution prior and after perturbation, as shown in fig.4, caused reduction of this functional by ~10-12%. Discrepancies of the local energy release provided by the porosity model did not exceed 7%.

The foregoing positive reactivity increase is evidently the upper limit estimate. For the most likely duration of seismic impact within the range of 10-20 s, the expected pebble bed compaction would not be more than 3%, and the positive reactivity increase - not more than 0.4% $\frac{\Delta k}{k}$.

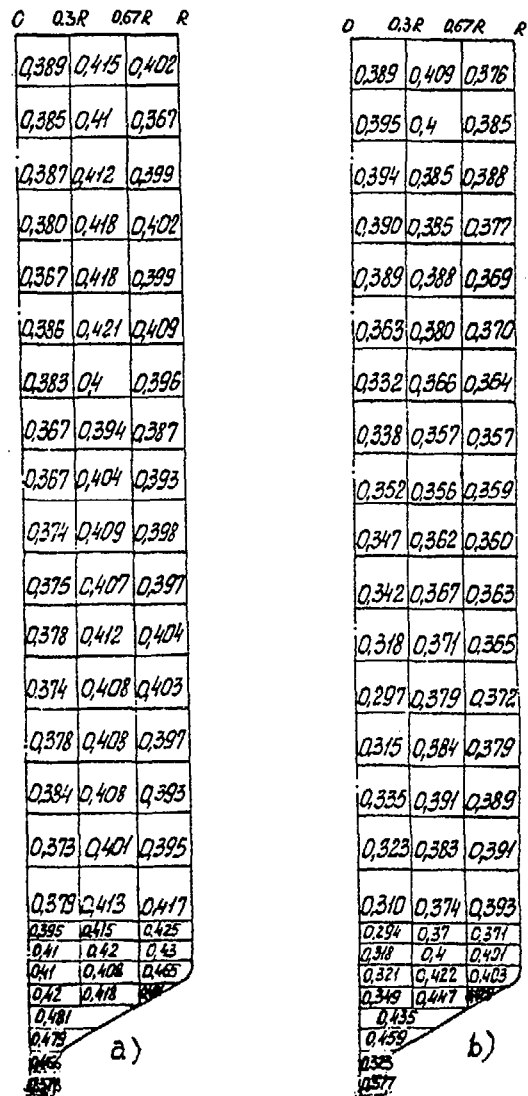


Fig. 4 The pebble bed porosity distribution in the hopper

a) after reloading of initial pebble bed ($E_{mv}=0.403$)
 b) after dynamic impact during 150 s. ($E_{mv}=0.374$)

CONCLUSION

The results of the foregoing studies indicate on the necessity of detailed treating of porosity distribution during the experiments on critical assemblies, simulating the reactor core with spherical fuel elements, to acquire the design parameters and verify calculation procedures.

REFERENCES

1. Костиков Л.Е., Лозовецкий В.Е., Перевазанцев В.В. "Теплообмен в активных зонах ядерных реакторов с шаровыми твэлами" Атомная техника за рубежом. 1978. № 6.
2. Богоявленский Р.Г. "Гидравлика и теплообмен в высокотемпературных реакторах с шаровыми твэлами" М. Атомиздат 1978.
3. Карпов В.А. "Использование конечно-разностных методов в многогрупповом диффузионном приближении для расчетного анализа топливных загрузок больших энергетических реакторов". Препринт ИАЭ-2639. М. 1976.
4. Гольцев А.С., Карпов В.А. "Нектар - программа расчета физических характеристик графитовых реакторов с учетом термализации и выгорания топлива". Препринт ИАЭ-2795. М. 1977.
5. Попов С.В. "Теплофизический расчет активной зоны ВТГР со свободно засыпанными шаровыми твэлами". Вопросы атомной науки и техники. Сер. Атомно-водородная энергетика и технология. 1980. вып.2 (7). с. 125

ANALYTICAL METHODS,
PREDICTIONS OF PERFORMANCE OF FUTURE HTGRs,
UNCERTAINTY EVALUATIONS
PART 2

(Session III)

Chairman

S. PELLONI
Switzerland

UNCERTAINTIES IN CALCULATIONS OF NUCLEAR DESIGN CODE SYSTEM FOR THE HIGH TEMPERATURE ENGINEERING TEST REACTOR (HTTR)

R. SHINDO, K. YAMASHITA, I. MURATA
Department of HTTR Project,
Japan Atomic Energy Research Institute,
Oarai-machi, Higashi-Ibaraki-gun, Ibaraki-ken,
Japan

Abstract

Japan Atomic Energy Research Institute(JAERI) has extensively done the research and development to construct the High Temperature Engineering Test Reactor(HTTR) of 30MW(t). The main objectives of the HTTR are to establish basic technologies for advanced HTGR in future and to be served as an irradiation test reactor in order to conduct researches in innovative high-temperature technologies. The HTTR is a graphite moderated and helium gas cooled reactor with prismatic fuel blocks. The inlet and outlet coolant temperatures are 395°C and 950°C, respectively. The reactor employs pin-in-block type fuel assemblies which contain low enriched UO₂.

The nuclear design code system for the HTTR consists of the computer codes DELIGHT, SRAC, TWOTRAN-2 and CITATION-1000VP. DELIGHT and SRAC are one dimensional cell burnup codes which have been developed in JAERI. TWOTRAN-2 is a transport code which is used to provide the average group constants of the graphite blocks where the control rods are inserted. CITATION-1000VP is a reactor core analysis code which has been improved from CITATION for the increase of memory and vectorization.

The nuclear characteristics of the HTTR such as shut down margin and power density distribution should satisfy safety related design criteria. In order to assure the sufficiency to the criteria, the uncertainty of the calculation was investigated.

For the uncertainty evaluation, the comparison of the calculations with the experiments was performed with a graphite

moderated critical assembly, Very High Temperature Reactor Critical Assembly(VHTRC), whose characteristics are similar to those of the HTTR. Among the various experiments performed at VHTRC, the following integral quantities were used to confirm the uncertainty; (1) effective multiplication factor, (2) neutron flux distribution, (3) control rod reactivity worth and (4) burnable poison rod reactivity worth. It was confirmed that the discrepancies between calculations and experiments were small enough to be allowable in the nuclear design of HTTR.

1 Introduction

Japan Atomic Energy Research Institute (JAERI) has extensively done the research and development to construct the High Temperature Engineering Test Reactor(HTTR) of 30MW(t)⁽¹⁾. The bird's-eye view of the HTTR is shown in Fig.1.

The main objectives of the HTTR are to establish basic technologies for advanced HTGRs in future and to be served as an irradiation test reactor in order to conduct researches in innovative high-temperature technologies.

The HTTR is a graphite moderated and helium gas cooled reactor with prismatic fuel blocks. The active core, 290cm in height and 230cm in effective diameter, consists of 30 fuel columns and 7 control rod guide columns(Fig.2). The inlet and highest outlet coolant temperatures are 395°C and 950°C, respectively. The reactor employs pin-in-block type fuel assemblies which contain low enriched UO₂. Also, burnable poison(BP) rods are distributed in the core.

The nuclear design code system for the HTTR consists of the computer codes DELIGHT⁽²⁾, SRAC⁽³⁾, TWOTRAN-2⁽⁴⁾ and CITATION-1000VP⁽⁵⁾. The program structure of nuclear design code system for HTTR is shown in Fig.3. DELIGHT is cell burnup code which has been developed in JAERI and is used to provide few-group constants of fuel blocks, graphite blocks and so forth for succeeding core calculation. TWOTRAN-2 is a transport code which is used to provide the average group constants of the graphite

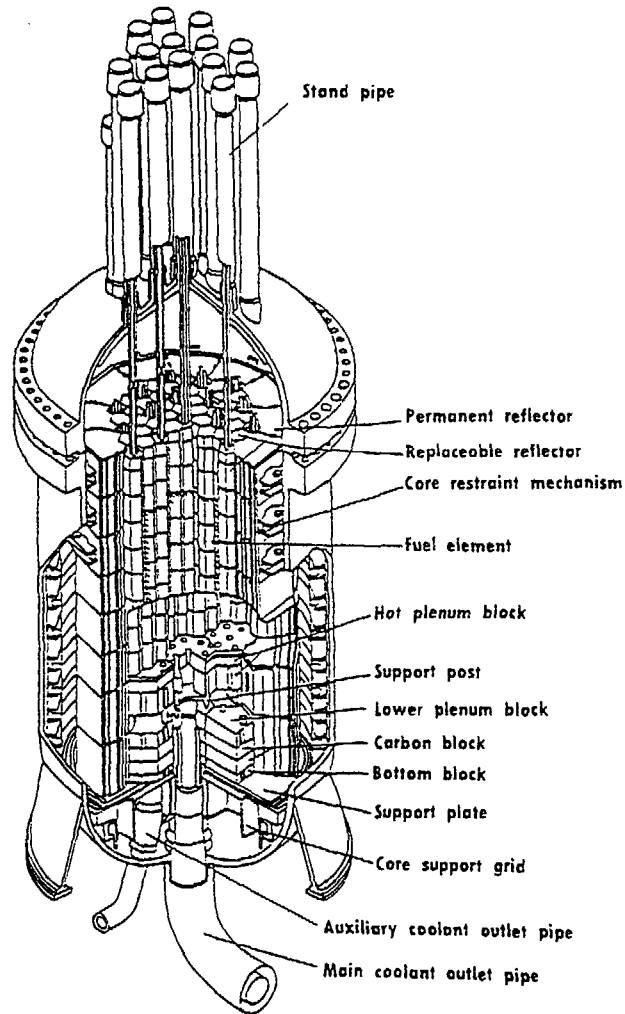


Fig.1 Bird's-eye view of the reactor vessel and core.

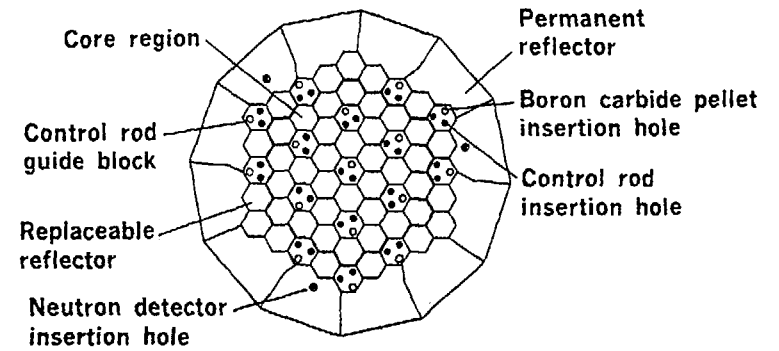


Fig.2 Cross sectional view of irradiation regions.

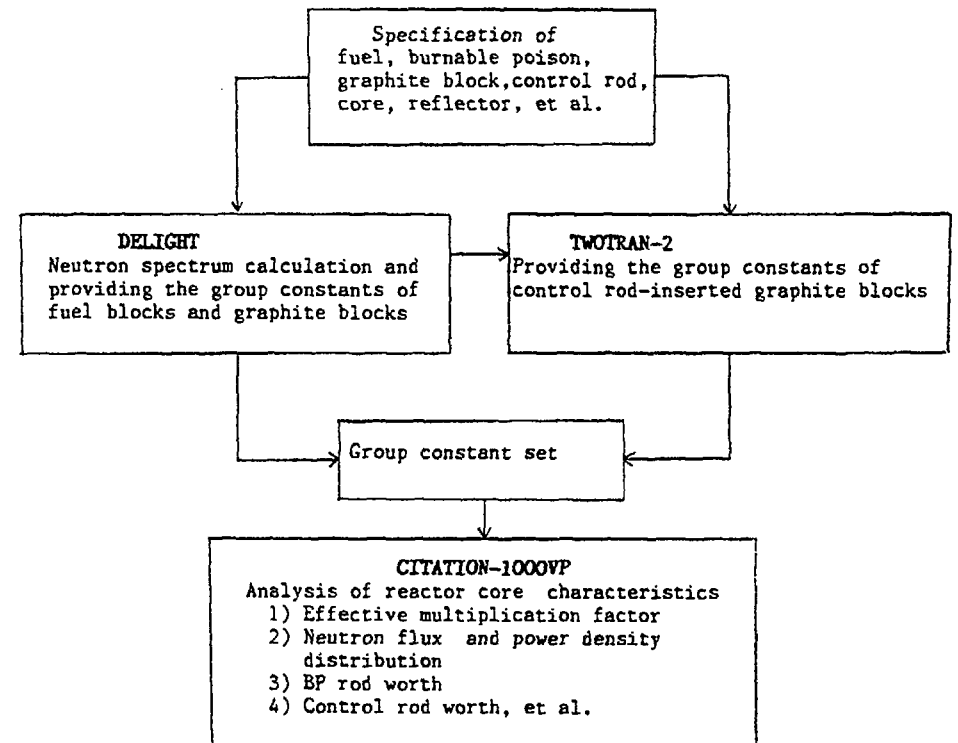


Fig.3 Program structure of nuclear design code system for HTTR.

blocks where the control rods are inserted. CITATION-1000VP is a reactor core analysis code which has been improved from CITATION⁽⁶⁾ to be able to analyze a full core of HTTR. The nuclear characteristics of the HTTR such as shutdown margin and power density distribution should satisfy safety related design criteria. In order to assure the sufficiency to the criteria, the uncertainties in calculations of nuclear design code system for HTTR were investigated.

For the uncertainty evaluation, the comparison of the calculations with the experiments was performed on a graphite moderated critical assembly, Very High Temperature Reactor Critical Assembly (VHTRC)^(7,8), whose characteristics are similar to those of the HTTR. Among the various experiments performed at VHTRC, the following integral quantities were used to confirm the uncertainty : (1) Effective multiplication factor, (2) Neutron flux distribution, (3) Control rod reactivity worth and (4) Burnable poison (BP) rod reactivity worth.

2 Accuracy requirements in safety design

The requirements for nuclear design in the safety related design are arisen from the confirmation of shutdown margin (effective multiplication factor, reactivity worths of control rod and burnable poison), the reduction of maximum fuel temperature (adjustment of power distribution), the preparation of the calculational conditions (addition rate of control rod reactivity worth and temperature coefficients) for safety analyses and so on.

3 Nuclear design code system

The nuclear design code system for the HTTR consists of DELIGHT, TWOTRAN-2 and CITATION-1000VP codes.

DELIGHT calculates the multi-group neutron spectrum of a fuel cell containing coated fuel particles and provides the group constants for core calculation. The calculations incorporated in this code are calculations of resonance, neutron spectrum, fuel cell, BP cell, criticality and burnup. The nuclear data is

based on the ENDF/B-4 mainly. In the resonance range, the code is able to consider the effect of double heterogeneity caused by coated fuel particles and assembled fuel rods. The neutron spectrum is obtained by cylindrical model using the collision probability method. The spectrum calculation is performed with 61 groups in the fast energy range from 2.38eV to 10MeV and with 50 groups in the thermal energy range from 0.0 to 2.38eV. The collision probability method is applied for the fuel and BP cell calculations.

TWOTRAN-2 is a two-dimensional neutron transport code which is employed to evaluate the shielding factors of control rods and to provide average group constants of a graphite block inserted a pair of control rods.

CITATION-1000VP is a reactor core analysis code which has been developed so as to enable the multi-neutron group calculation of the HTTR in the three dimensional full core model through extending number of zones and meshes of CITATION code and enhancing a calculation speed with the vectorization.

4 Very High Temperature Reactor Critical Assembly (VHTRC)

The VHTRC is a split table type critical assembly which consists of two halves-fixed and movable ones. The core of VHTRC is shaped in a hexagonal prism, whose side and axial length are 175cm and 240cm, respectively. Fuel blocks and reflector blocks are piled in a hexagonal iron frame to form the core and the reflector regions respectively. Core configuration could be flexibly changed by loading the fuel or graphite rods. Instead of the fuel and graphite rods, BP rods can be loaded into graphite block to measure a BP rod reactivity worth.

5 Analysis of experimental data of VHTRC

For the uncertainties of the nuclear design code system, the experimental data of the initial core (VHTRC-1) was analyzed. The VHTRC-1 core is made by loading about 280 fuel rods which contain fuel compacts of 4wt% enriched uranium coated particles. The cross section of VHTRC-1 core is shown in Fig.4.

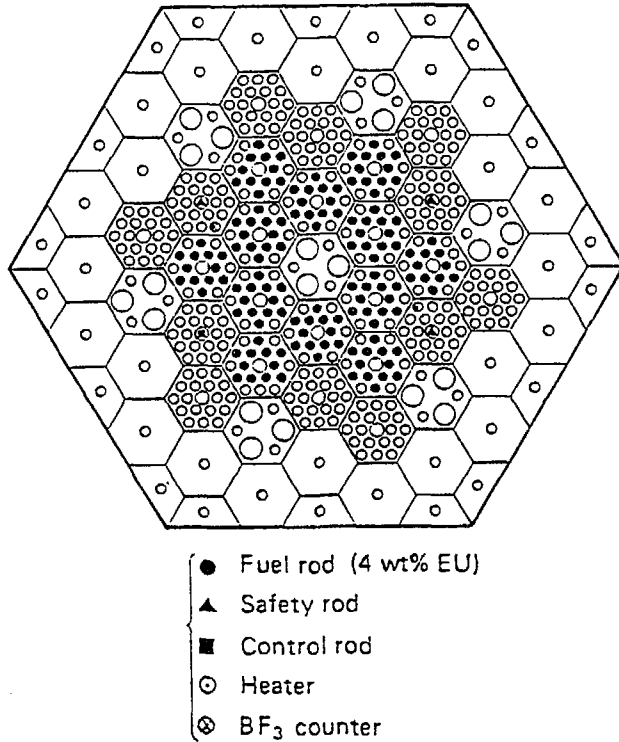


Fig.4 Cross section of VHTRC-1(7).

For the calculation of group constants of fuel with DELIGHT, one-dimensional cylindrical model is used. For the calculation of averaged group constants of a pair of control rods and a graphite block, TWOTRAN-2 with a two-dimensional X-Y model is used.

Core calculation performed by CITATION-1000VP employs the three-dimensional triangular-mesh model with triangular-mesh division in a fuel block.

(1) Effective multiplication factor (k_{eff})

The comparison between calculations and experiments was shown in Fig.5. The maximum discrepancy is about 1% Δk .

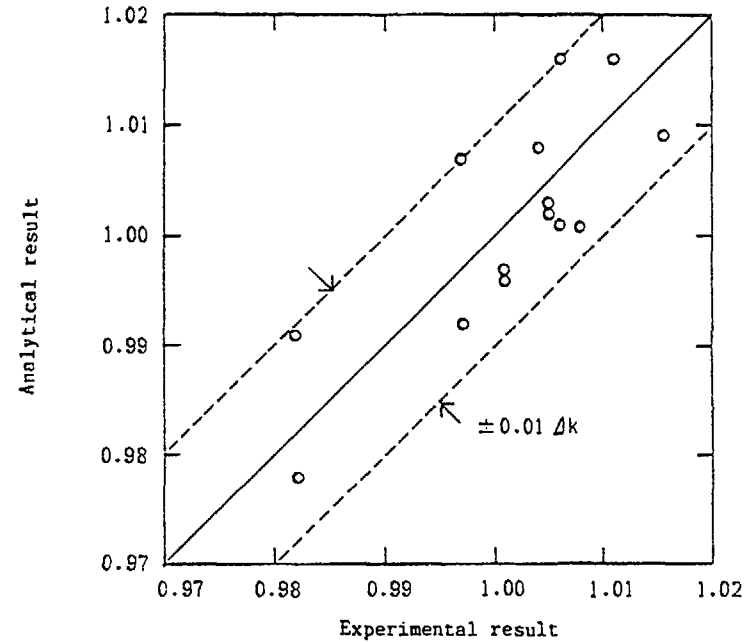


Fig.5 Comparison of the multiplication factors obtained by VHTRC experiment with the analytical results.

(2) Neutron flux distribution

The measurement of the neutron flux distribution is analyzed to grasp the uncertainty for calculation of power distribution in the HTTR. The analysis is performed for the VHTRC-1 with natural Cu foils and pins as irradiated material.

The comparison between the analytical and experimental radial reaction rate distributions is shown in Fig.6. A quite good agreement is obtained in the comparison. The maximum uncertainty between experimental and analytical values is about 2.9%.

(3) Burnable poison (BP) rod reactivity worth

The burnable poison rod reactivity worth is analyzed on the core configuration representing one poison rod inserted along core axis.

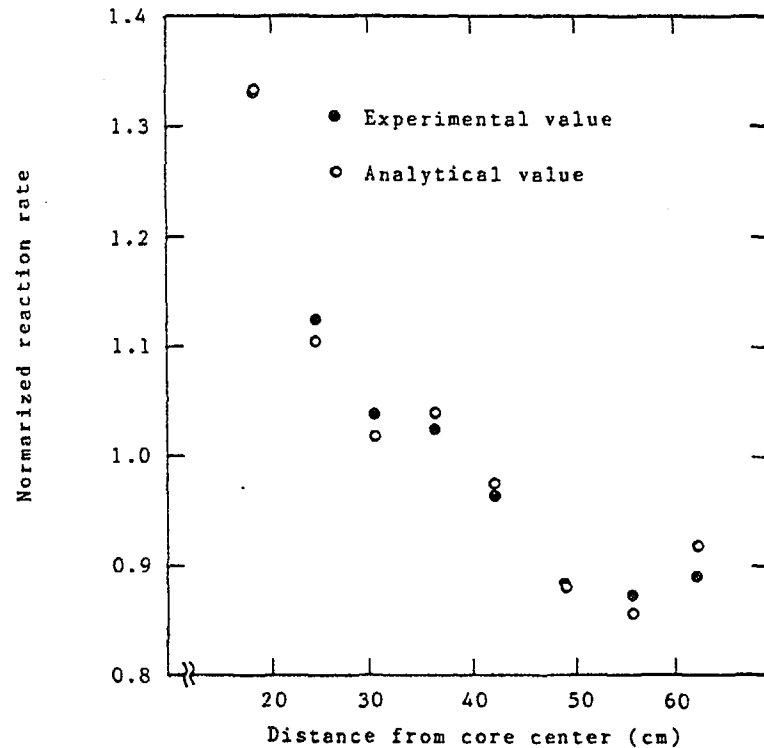


Fig.6 Comparison between the analytical and experimental radial reaction rate distributions.

The result of the analysis is compared with experimental data. A quite good agreement was obtained. The discrepancy is nearly 0%.

(4) Control rod reactivity worth

The measurement of control rod reactivity worth has been performed for the core with a pair of control rods inserted in core central axis.

The analytical result agrees with experimental result within about 2.6%.

6 Conclusion

The analyses have been performed for the experiments of VHTRC-1 core on effective multiplication factor, neutron flux distribution, BP rod reactivity worth and control rod reactivity worth.

The uncertainties between the experiments and calculations are 1% Δk , 2.9%, nearly 0% and 2.6%, respectively.

On the other hand, the targets for the uncertainties of the nuclear design items are as follows;

- 1) Effective multiplication factor (room temperature) $\leq 1\% \Delta k$
- 2) Reactivity worth of control rods $\leq 10\%$
- 3) Reactivity worth of burnable poisons $\leq 10\%$
- 4) Radial power distribution $\leq 3\%$
- 5) Temperature coefficient $\leq 20\%$

It was confirmed that the discrepancies for the nuclear design code system were small enough to be allowable in the nuclear design for HTTR.

ACKNOWLEDGEMENTS

The authors wish to thank Messrs. S. Saito, T. Tanaka, Y. Sudo, H. Yasuda, F. Akino and T. Yamane for useful comments and supports.

REFERENCES

- (1) JAERI: "Present Status of HTGR Research and Development" (1990).
- (2) Shindo, R., Yamashita, K., and Murata, I.: "DELIGHT-7; One Dimensional Fuel Cell Burnup Analysis Code for High Temperature Gas-cooled Reactors (HTGR)", JAERI-M 90-048 (1990), (in Japanese).
- (3) Tsuchihashi, K., et al.: Revised SRAC Code System, JAERI-1302 (1985).
- (4) Latherop, K. D. and Brinkley, F. W.: "TWOTRAN-2; An interfaced exportable version of the TWOTRAN code for two-dimensional transport", LA-4848-MS (1973).

- (5) Harada, H. and Yamashita, K.: The Reactor Core Analysis Code CITATION-1000VP for High Temperature Engineering Test Reactor, JAERI-M 89-135 (1989),(in Japanese).
- (6) Fowler, T. B., Vondy, D. R., Cunningham, G. W.: Nuclear reactor core analysis code; CITATION, ORNL-TM-2496 (1971).
- (7) Yasuda, H., et al.: Construction of VHTRC(Very High Temperature Reactor Critical assembly), JAERI-1305 (1986),(in Japanese).
- (8) Akino, F., et al.: Critical Experiment on Initial Loading Core of Very High Temperature Reactor Critical Assembly(VHTRC), J. Atomic Energy Society, 31 p.p.682-690 (1989),(in Japanese).

AUTOMATED DIFFERENTIATION OF COMPUTER MODELS FOR SENSITIVITY ANALYSIS

B.A. WORLEY

Oak Ridge National Laboratory,
Oak Ridge, Tennessee,
United States of America

Abstract

Sensitivity analysis of reactor physics computer models is an established discipline after more than twenty years of active development of generalized perturbations theory based on direct and adjoint methods. Many reactor physics models have been enhanced to solve for sensitivities of model results to model data. The calculated sensitivities are usually normalized first derivatives, although some codes are capable of solving for higher-order sensitivities. The purpose of this paper is to report on the development and application of the GRESS system for automating the implementation of the direct and adjoint techniques into existing FORTRAN computer codes. The GRESS system was developed at ORNL to eliminate the costly man-power intensive effort required to implement the direct and adjoint techniques into already-existing FORTRAN codes. GRESS has been successfully tested for a number of codes over a wide range of applications and presently operates on VAX machines under both VMS and UNIX operating systems.

I. INTRODUCTION

Sensitivity analysis is an important component of any computer code application for modeling physical systems. The role of sensitivity analysis is to provide a quantitative measure of the effect of computer code data and inputs upon key performance indices. Sensitivity analysis also helps limit the scope of the more complicated problem of quantifying uncertainties.

Sensitivity analysis of computer-generated results consists of determining the effect of model data upon the calculated results of interest. Because computer model equations can be differentiated analytically, sensitivities can be precisely defined and calculated in a deterministic fashion using both direct and adjoint methods.¹⁻⁸ The deterministic approach is particularly suited to large-scale problems for which direct perturbation of the model data becomes impractical from a cost standpoint. The main drawback to the deterministic approach has been the initial manpower investment to add the computational capability for calculating the necessary derivatives into existing computer models.

This paper presents the theory and application of the Gradient-Enhanced Software System, GRESS,⁹ and its role in calculating model derivatives and sensitivities without a prohibitive initial manpower investment. Storage and computational requirements are discussed.

II. DETERMINISTIC SENSITIVITY ANALYSIS

A brief description of general sensitivity theory is given here as an aid to understanding the problem of applying this theory to computer models. The example to be discussed will be that of a general set of nonlinear equations given by

$$y = F(y, c), \quad (1)$$

where y represents the dependent variables, c represents the user-specified model data or parameter set, and F defines the model equations. The particular form chosen in Eq. (1) is one that can be used to represent equations coded in the FORTRAN programming language. The left side of the equation can represent the stored value of the variable calculated from the functional formula on the right side.

Since the number of components of the vector y calculated in any typical large-scale modeling problem is large, it is useful to define a generic result for such a calculation that is of particular interest to the model user. Typically many results will be needed for analysis but in most cases they form a much smaller set than the elements of y . A typical result will be defined as

$$R = h(y), \quad (2)$$

where R is a single number that is a function of the solution to Eq. (1). For notational ease, the generic parameter α_i will be used to denote an individual element of c . The total number of parameters in the problem will be assumed to be M so that the index on α_i will run from 1 to M .

The basic problem in any sensitivity study is to find the rate of change in the result R arising from changes in any model parameters. For the generic parameter α_i , then, the quantity of interest is the numerical value of $dR/d\alpha_i$ given analytically by

$$\frac{dR}{d\alpha_i} = \frac{\partial h}{\partial y} \frac{dy}{d\alpha_i}. \quad (3)$$

Since the functional dependence of R on y through $h(y)$ is defined analytically by the model user, only $dy/d\alpha_i$ needs to be generated in order to evaluate Eq. (3). The procedure needed to get $dy/d\alpha_i$ is to differentiate Eq. (1) as follows:

$$\frac{dh}{d\alpha_i} = \frac{\partial F}{\partial y} \frac{dy}{d\alpha_i} + \frac{\partial F}{\partial c} \frac{dc}{d\alpha_i}. \quad (4)$$

Rearranging Eq. (4) yields the following set of coupled equations to solve for $dy/d\alpha_i$,

$$\left(I - \frac{\partial F}{\partial y} \right) \frac{dy}{d\alpha_i} = \frac{\partial F}{\partial c} \frac{dc}{d\alpha_i}, \quad (5)$$

or in more compact form,

$$Ay'_i = s_i, \quad i = 1, \dots, M, \quad (6)$$

where I is the identity matrix and A , y'_i , and s_i are given by

$$A = I - \frac{\partial F}{\partial y}, \quad (7)$$

$$y'_i = \frac{dy}{d\alpha_i}, \quad (8)$$

and

$$s_i = \frac{\partial F}{\partial c} \frac{dc}{d\alpha_i}. \quad (9)$$

If Eq. (6) were solved directly for y'_i , the result could be used in Eq. (3) to evaluate $dR/d\alpha_i$. This method of sensitivity analysis is called the "direct" approach and is a classical methodology that has received a great deal of attention in the literature.^{1,5} Since Eq. (6) must be solved each time a new α_i is defined, the direct approach is most suitable for problems with relatively few input parameters of interest, for problems in which the solution of Eq. (6) is very inexpensive compared to the solution of the model itself, or for analytical problems in which the inverse of A can be explicitly determined.

For large-scale models with a large database in which the ultimate objective is still the evaluation of $dR/d\alpha_i$ for many α_i , the intermediary step of solving for $dy/d\alpha_i$ and its inherent computational inefficiency can be avoided. For such problems, the "adjoint" approach is far more applicable. In this methodology, use is made of the fact that Eq. (6) is linear in y_i , and appropriate adjoint equations can therefore be developed specifically to evaluate Eq. (3).

Defining the matrix adjoint of A as A^* and using the usual definition of this adjoint give the identity,

$$u^{tr} Av = v^{tr} A^* u, \quad (10)$$

where u and v are arbitrary vectors and A^* is defined as

$$A^* = A^{tr}. \quad (11)$$

Here the tr superscript represents the transpose of the vector or matrix.

If specific vectors for the problem at hand are chosen for u and v , the problem-specific adjoint equation can be set up as follows:

$$A^* y^* = s^* , \quad (12)$$

where

$$A^* = A^{tr} = \left(I - \frac{\partial F}{\partial y} \right)^{tr} . \quad (13)$$

Choosing s^* as

$$s^* = (dh/dy)^{tr} , \quad (14)$$

Equation (3) can now be evaluated as follows:

$$\frac{dR}{d\alpha_i} = y^{*tr} \frac{\partial F}{\partial c} \frac{dc}{d\alpha_i} , i = 1, \dots, M , \quad (15)$$

where y^* is now the solution to

$$\left(I - \frac{\partial F}{\partial y} \right)^{tr} y^* = \left(\frac{dh}{dy} \right)^{tr} . \quad (16)$$

The simplicity of the adjoint approach lies in the fact that Eq. (16) needs to be solved only once to get any and all sensitivities in the problem. This is a result of Eq. (16) being independent of the definition of α_i . The particular choice of α_i is only reflected in the evaluation of Eq. (15), which involves simple vector products. In essence, the adjoint approach reduces the computational effort needed to evaluate $dR/d\alpha_i$ from solving many coupled linear equations to the evaluation of several vector products. For large-scale systems with many thousands or even millions of parameters, this represents orders of magnitude in computational efficiency.

It should be noted here that both the direct and adjoint equations [i.e., Eqs. (6) and (16)] are in any case far easier to solve than the original model [Eq. (1)]. Both Eqs. (6) and (16) are linear while Eq. (1) is nonlinear. The direct and adjoint approaches, however, require the results of the original model equations to be available in order to set up Eqs. (6) and (16), since the A matrix and the vectors s , and s^* depend on y .

In order to solve either the direct or adjoint sensitivity analysis, then, the model user must first generate the matrices $\partial F/\partial y$ and $\partial F/\partial c$ from the original nonlinear computer model. For large-scale problems, this generally requires a great deal of painstaking human effort. First, the model equations must be extracted from the computer coding. They must then be differentiated with respect to all parameters of interest, and finally direct or adjoint sets of equations must be set up for computational solution. Successful automation of this procedure greatly reduces the human effort involved, potentially by orders of magnitude.

The advantages of automation of sensitivity model development is, therefore, great indeed. The next two sections discuss the GRESS automated system that uses the rules of calculus to add capability to existing FORTRAN computer models for solving the direct or adjoint equations.

III. GRESS CHAIN OPTION (An Automated System for Solving the Direct Sensitivity Problem)

The basic principle of GRESS is to read the model source program and search for model equations. These are identified uniquely by the appearance in the FORTRAN source program of the "=" symbol. Since all FORTRAN "equations" so identified occur in the form of Eq. (1) (i.e., with a single dependent variable on the left side of such an expression), GRESS can search for and analyze each equation in terms of its functional dependence on y and c . The basic computer calculus operations of the GRESS CHAIN option is then used to compute the successive elements of $\partial F/\partial c$ and $\partial F/\partial y$ as each expression is encountered. The differentiation is carried out analytically using calculus software for all permissible FORTRAN functions and operators and the results are computed and stored numerically using the local (current) values of the independent and dependent variables. The CHAIN option takes advantage of the fact that in solving Eq. (5), the matrix $(I - \partial F/\partial y)$ is lower triangular and the y vector can be computed by forward substitution. The important point is that the components of y are solved successively as each equation is differentiated and that the $(I - \partial F/\partial y)$ matrix does not have to be stored. (The adjoint problem requires the storage of this matrix, as will be discussed in the next section.)

GRESS only recognizes real-variable store operations as valid equations (i.e., the left side variable in a FORTRAN equation must be real), since continuous derivatives are to be calculated. Also, the left-hand side of an equation is treated as a separate component of y each time it is executed (including each execution in a DO LOOP). The calculation of $\partial F/\partial y$ and $\partial F/\partial c$ in effect means that GRESS can be used to calculate the derivative of any real variable in the model with respect to any other real variable in the model. All derivatives are available for both internal and/or external use.

The application of GRESS to an existing FORTRAN model consists of an automated precompilation in which the automated code translation necessary to compute derivatives is performed using computer calculus. This step consists primarily of a rearrangement of the program data structure and a substitution of calls to GRESS interpretive software in place of all arithmetic lines of coding. All arithmetic operations of the original model are precompiled into a pseudomachine code (the GRESS P-code) for use during program execution. The two output files of this step are the enhanced model and the binary P-code file. These two files and a set of GRESS software subroutines supporting the enhanced model are compiled and run as a normal FORTRAN program to produce both the reference model results and gradient information. The gradients and reference results are used to calculate the sensitivities.

IV. GRESS ADGEN OPTION (An Automated System for Solving the Adjoint Sensitivity Problem)

The adjoint problem is defined by Eqs. (12-16). As previously mentioned, the calculation of the adjoint solution vector y^* from Eq. (16) is not a function of the selection of input parameter α_i and thus need only be performed once to determine the derivatives of a response of interest with respect to any parameter of interest. The matrix $\partial F/\partial c$ must also be determined, but it, too, is independent of the parameter of interest. The only parameter-dependent operation required to calculate the derivative $dR/d\alpha_i$ is the simple

matrix multiplication operation $(y^{*tr})(\partial F/\partial c)(dc/d\alpha_i)$ in which the vector $dc/d\alpha_i$ is a function of α_i . The option in GRESS to automate the calculation of derivatives based upon the solution of the adjoint equations is referred to as the ADGEN (ADjoint GENerator) option. Recall that GRESS solves Eq. (5), taking advantage of the fact that the matrix $(I - \partial F/\partial y)$ is lower triangular and the solution by forward substitution requires only that the vector $dy/d\alpha$ be stored. However, to solve the adjoint problem, all derivatives that constitute the $n \times n$ matrix $(I - \partial F/\partial y)^{tr}$ must be stored, where n = total number of equations, counting each time an equation is solved in a DO LOOP as a separate equation; the left-hand side of each equation in a DO LOOP is treated as a separate element of y . Although only the non-zero elements are saved, the storage of the matrix $(I - \partial F/\partial y)^{tr}$ may require a substantial amount of storage capability. The storage difficulties are counterbalanced by features of Eqs. (15) and (16) that make the ADGEN calculation of y^* both practical and cost efficient. Note that the matrix $(I - \partial F/\partial y)^{tr}$ is upper triangular and that the column vector $(dh/dy)^{tr}$ is a simple user-defined vector (for most cases a vector with a single non-zero entry of unity). Thus Eq. (16) is easily solved by back substitution and the values of y^* can be successively stored in the space allocated for the $(dh/dy)^{tr}$ vector. The calculation of $dR/d\alpha_i$ from Eq. (15) must be performed for each α_i , but this requires only trivial matrix multiplications and very little computer cost.

The ADGEN option calculates the normal model results as well as the derivatives making up the $\partial F/\partial y$ and $\partial F/\partial c$ matrices. Again, the major difference from the direct approach using the CHAIN option is that the ADGEN option requires that the matrix $(I - \partial F/\partial y)^{tr}$ be stored and includes a post-processor solver routine to calculate the adjoint solution.

V. APPLICATIONS OF GRESS

The distinguishing feature in solving Eq. (5) using the GRESS CHAIN option is that only the elements of a single row of $\partial F/\partial y$ and $\partial F/\partial \alpha_i [= (\partial F/\partial c)(\partial c/\partial \alpha_i)]$ need be saved in computer memory at any one time. This advantage is important if one wishes to solve for the derivatives of many LHS elements (responses) with respect to a data element α_i . The disadvantage is that to calculate derivatives with respect to other data elements, Eq. (5) must be solved for each additional α_i of interest. The computational burden is approximately proportional to the number of α_i . In our experience to date, the computational time for calculating derivatives with respect to m chosen elements of c , denoted by T_m , is

$$T_m \approx T_{REF}(\beta_0 + \beta_1 m)$$

where T_{REF} is the execution time of the reference model before derivative enhancement and β_0 and β_1 are constants falling between 1.0 and 30.0 and 0.1 and 1.4 respectively.

Another problem sometimes occurring in practice is that the elements of $dy/d\alpha_i$ must be stored in memory as Eq. (5) is solved for each row. Therefore, the number of α_i with respect to which derivatives are calculated in a single execution of the enhanced model may be limited by system memory resources using the CHAIN option.

As mentioned in Section IV, solution of the adjoint equations, Eqs. (15-16), using the ADGEN option reduces the computation effort for calculating derivatives of a single response with respect to many parameters compared to repeatedly solving Eq. (5) for each α_i , as is done in the CHAIN option. The solution to Eq. (16) is straightforward due to the upper triangular structure of $(I - \partial F/\partial y)^{tr}$, but requires storage of the nonzero elements

of $(I - \partial F/\partial y)^{tr}$. ADGEN circumvents the necessity to store this matrix in memory by using an efficient scheme for solving Eqs. (15-16) based upon retrieval of portions of $(I - \partial F/\partial y)^{tr}$ from off-line storage and segmenting the calculation of derivatives. A method to reduce the size of the adjoint matrix to be stored by explicitly recognizing the input parameters of interest has been developed and implemented (called FORWARD REDUCTION⁹). Storage size of the adjoint matrix can then be further reduced based on the output parameters of interest (called BACK REDUCTION⁹).

The computer models that have been enhanced using GRESS are listed in Table 1. The first column of the table contains the code name. The second column provides a brief description of the system being modelled. For some of the models the approximate number of lines of coding (excluding comment cards) are given in parenthesis. The next two columns indicate the year that the code was enhanced and the version of GRESS used. The next, fifth, column indicates whether the direct (C=CHAIN) or adjoint (A=ADGEN) option was used. The sixth and seventh columns give the number of input and output parameters for which sensitivities were printed. Note that in the CHAIN option, derivatives are calculated for all dependent variables with respect to user-selected input parameters. In the ADGEN option, derivations of user-selected responses (results) are calculated with respect to all variables. The purpose of showing the numbers of input and output variables is to provide an idea of the range of input and output variables of interest in typical sensitivity analysis applications. The eighth column gives an approximate measure of the increase in execution time and storage requirements for the GRESS-enhanced version of each code. Except where noted, the factors represent the ratio of the enhanced-code execution time (or memory storage requirement) to the reference code execution time (or memory storage requirement). For the ADGEN options, the storage requirement of the adjoint matrix that must be provided for (either in memory or in off-line storage) is shown. The last column gives an abbreviated reference of the publication describing the application of GRESS for each computer code and the primary author.

A new version of GRESS (Version 2.0) is under development that replaces the P-code by using symbolic differentiation. This version will have the capability to enhance selected subroutines. For the PRESTO-II and AIRDOSE models, a comparison of the figures in column seven of Table 1 reveals that the successive versions of GRESS have substantially reduced the execution and storage requirements.

Table 1. Computer Codes Enhanced Using GRESS

Code ^a	Description ^b	Date of GRESS Enhancement	GRESS Version ^c	GRESS Option ^d	Input Parameters ^e	Output Parameters ^e	Run-Time Cost Factor [Storage] ^f	Reference ^g
SWENT	3-D Finite Difference Transient Geohydrology Model (15,000)	1985	D	C	7	900	30 [3X]	NSE, 24, 1986 Oblow
ORIGEN2	Radioactive Decay Model	1985	D	C	7	140,000	25	NSE, 24, 1986 Worley
UCBNE10.2 (NEUCB)	Migration of Radioactive Nuclides in Ground Model	1985	D	C				Nucl. Chem. Waste Man. - Pin
TEMP (BRINETEMP)	Finite-Line Heat Transfer Model	1986	D	C	10	140		ORNL/TM-9975 Worley
WAPPA-C (WAPPA-B)	Waste Package Performance Assessment Model	1986	D	C				ORNL/TM-9976 Worley
GRESS	Commercial and Residential Energy Use and Emissions Model	1986	D	C	10	800	3	ORNL/TM-10304 Trowbridge
CFEST	3-D Transient Finite Element Hydrology Model (16,000)	1988	0.0	C(A)	38	20,000	23(73)	Letter Report Horwedel
VSL3DNQ	Chemical Reactions in High-Speed Flows (12,000)	1988	0.0	C	6	2		Letter Report Wright
PRESTO-II	Shallow-Land Disposal of Radioactive Waste Model (6,900)	1988 (to present)	0.0, 1.0, 2.0	A(C)	69,000	2	52,33,10 [144,88,11]	Various Conf. Papers Worley, Horwedel

Table 1. Computer Codes Enhanced Using GRESS (Cont'd.)

Code	Description	Date of GRESS Enhancement	GRESS Version	GRESS Option	Input Parameters	Output Parameters	Run-Time Cost Factor [Storage]	Reference
AIRDOS-EPA	Radionuclide Transport in Air and Human Intake Model	1989 (to present)	0.0,1.0,2.0	A(C)	1,271	2	40,28.6 [6,.01,.01]	ORNL/TM-11373 Horwedel
DO	Dissolved Oxygen at Dam Sites Model	1989	0.0	C	14	27,700		ORNL/TM-10953 Railsback
D2PC	Chemical Hazard Prediction Model	1989	0.0	C	3	9		Letter Report Worley
E9E	Tumor Growth Model	1989	1.0	C(A)				
EQ3	Geochemical Model	1990	1.0,2.0	A(C)	31,000	9	27	ORNL/TM-11407 Horwedel
HELP	Hydrological Evaluation of Landfill Performance Model	1990	1.0,2.0	A(C)				Letter Report Horwedel
DRUFAN	Fluid Flow Dynamics for Nuclear Safety	1990	1.0,2.0	A(C)				Letter Report Horwedel

^a Code names shown in parenthesis are similar codes also enhanced using GRESS.

^b Number in parenthesis indicates approximate number of lines of source codes, excluding comments.

^c The current version being distributed is Version 1.0. Version 2.0 is under development.

^d Indication of the method used for sensitivity analysis for the particular code application of interest. C refers to the GRESS CHAIN option (direct method) and A refers to the GRESS ADGEN option (adjoint method). The option in parenthesis indicates the GRESS option used for derivation verification and alternate sensitivity calculations.

^e Refers to the parameters of interest for a particular application of the code. In the GRESS CHAIN option, derivatives of all variables with respect to a single parameter are calculated. In the GRESS ADGEN option, derivatives of a single response with respect to all variables are calculated.

^f The cost factor is the ratio of the execution time of the GRESS-enhanced code to the execution time of the reference code. For the CHAIN option the ratio is for the calculation of derivatives with respect to one input parameter. Number in parenthesis refers to the cost factor for the total number of input parameters of interest. Numbers in brackets followed by an x (i.e., 3x) refer to the factor of storage required as a multiple of the reference code storage for the CHAIN option. Numbers in brackets without an x refer to the adjoint matrix storage requirements in Megabytes for the ADGEN option.

^g Brief reference of report describing the application of GRESS to the subject code and sensitivity analysis results of interest. First author's name of publication is shown.

VI. CONCLUSIONS

An approach to sensitivity analysis of large-scale computer models based on an automated system for implementing the direct and adjoint method is now available. GRESS calculates model derivatives and sensitivities and has been successfully applied to many large-scale computer models. The availability of GRESS greatly reduces the man-effort required to add sensitivity capability to existing FORTRAN models.

REFERENCES

1. R. Tomovic and M. Vukobratovic, *General Sensitivity Theory*, Elsevier North-Holland, Inc., New York (1972).
2. W. M. Stacey, *Variational Methods in Nuclear Reactor Physics*, Academic Press, New York (1974).
3. E. Greenspan, "Developments in Perturbation Theory," *Advances in Nuclear Science and Technology*, Vol. 9, Academic Press, New York (1976).
4. E. M. Oblov, "Sensitivity Theory for Reactor Thermal-Hydraulics Problems," *Nucl. Sci. Eng.*, **68**, 322 (1978).
5. P. M. Frank, *Introduction to System Sensitivity Theory*, Academic Press, New York (1978).
6. D. G. Cacuci, *J. Math. Phys. (NY)*, **22**, 2794 (1981).
7. D. G. Cacuci, *J. Math. Phys. (NY)*, **22**, 2803 (1981).
8. C. R. Weisbin, et al., "Sensitivity and Uncertainty Analysis of Reactor Performance Parameters," *Advances in Nuclear Science and Technology*, **14**, Plenum Press, New York (1982).
9. "GRESS 1.0, Gradient Enhanced Software System," distributed by Radiation Shielding Information Center, PSR-231.

IMPACT OF DIFFERENT LIBRARIES ON THE PERFORMANCE CALCULATION OF A MODUL-TYPE PEBBLE BED HTR

U. OHLIG, H. BROCKMANN, K.A. HAAS, E. TEUCHERT
 Institut für Sicherheitsforschung und Reaktortechnik,
 Forschungszentrum Jülich GmbH,
 Jülich, Federal Republic of Germany

Abstract

A new multigroup library for the GAM-THERMOS spectrum codes has been compiled from the sources ENDF/B-V and JEF-1. The progress in comparison to the 20 years old standard library has been studied for one specific reactor design of the Modular High Temperature Reactor. The study covers various aspects of the performance of the reactor both for the initial core and for the equilibrium cycle.

For the multiplication factor k_{eff} the difference amounts to $\Delta k_{\text{eff}} = 0.0164$ in the startup reactor, which is mainly due to changes in the cross sections of ^{235}U . At the turn to the equilibrium cycle the difference reduces to $\Delta k_{\text{eff}} = 0.0017$ as due to various opposite tendencies in the data of the many involved nuclides. The change in the mass balance of the fissile materials is about 5%. The impact on the temperature coefficients is in the order of 4%, and the influence on other safety related properties of the reactor is lower than about 1 or 2 percent, confirming the confidence in formerly received results.

1. Introduction

In 1989 a new multigroup library has been compiled from the ENDF/B-V [1] and JEF-1 [2] data files. It is intended for the VSOP computer code system [3] which is based on the ZUT-GAM-THERMOS spectrum codes [4,5,6].

This VSOP code system is applied to the physics calculation of a reactor from its startup to the equilibrium cycle, to control and safety assessment and to thermal evaluations under operational and accidental situations. Spectrum calculation is performed for many subregions of the reactor and can repeatedly be applied when time proceeds. Neutron diffusion calculation and thermal hydraulics is performed 2-dimensionally in r-z-geometry.

Up to now an older nuclear library has been used which is based on the ENDF/B-II data files [7]. It has been supplemented with data of various other sources as available about the year 1970. Calculations agreed well with existing reactors, therefore the introduction of a new library is considered to be a kind of venture.

The comparison of the two nuclear libraries is made for a very specific reactor: a *MODUL*-type pebble bed HTR (table 1). The calculational model is given in figure 1. Beyond realistic modelling of the reflector zones it contains the ducts of the helium and the carbon bricks outside of the reflector, which absorbs the leaking neutrons. The core is subdivided into 10 different spectrum zones, and the reflector into 15 ones. Coupling between them is given in terms of neutron leakage.

TABLE I. DESIGN PARAMETERS

Thermal power	MW	200
Power density	MW/m ³	3.14
Height / Radius of the core	cm	900 / 140
Heating of the helium	°C	300 → 950
No. of fuel element passes through reactor		10
Fuel, enrichment		UO ₂ , 10 %
Coated particles		TRISO
Heavy metal loading	g/sphere	6.15
Moderation ratio	N _C /N _{HM}	600

The comparison is made in three steps:

1. For the initial core with only few nuclides,
2. For the equilibrium cycle containing the produced actinides and fission products,
3. For reactivity effects under control and accidental situations.

2. Nuclear Libraries

The basic nuclear library of the VSOP code system consists of two source libraries: an epithermal one and a thermal one. The epithermal data are given in 68 energy groups in the structure of the GAM-I code [5] ranging from 10 MeV to 0.414 eV. The thermal library contains the data in 30 energy groups in the THERMOS structure [6] ranging from 2.05 eV to 10⁻⁵ eV.

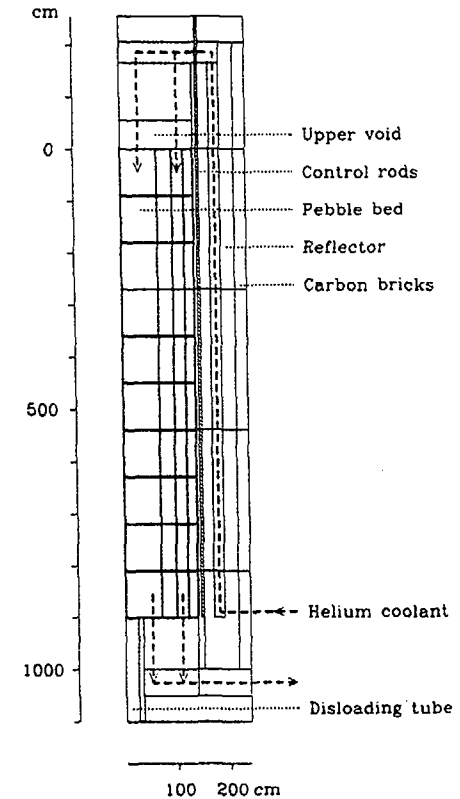


Fig. 1: Calculational Model

The older libraries are based on ENDF/B-II [7] and BNL-325 [8]. They contain 160 absorber nuclides and 5 moderator nuclides with scattering kernels of different temperatures. The scattering matrices of the graphite are based on the Young-Koppel [9] phonon spectrum in graphite. The fission yields already stem from ENDF/B-V.

The new library is made of 175 nuclides. It has been prepared from the ENDF/B-V [1] or from the JEF-1 [2] data files. For some nuclides, e.g. ²³⁹Pu and Cr, the ENDF/B-IV [10] data base was preferred. For the generation of the new library the AMPX modules XLACS-2 and NPTXS were used. The weighting spectrum was a

fission-1/E-Maxwellian. Below 0.414 eV a Maxwell spectrum of 900 K was applied. The Doppler-broadening was also calculated for the temperature of 900 K. The thermal cross sections of the moderator nuclides and the fission yields remained unchanged.

For the nuclides ^{232}Th and ^{238}U the resolved and unresolved resonance parameters were transferred in order to calculate the resonance cross sections separately. They are individually made for the different temperatures and the specific configuration of the fuel elements by the code ZUT-DGL [4].

In fig.2 the new and the old fission cross sections of ^{235}U and ^{239}Pu are compared over the thermal energy range. The given neutron spectrum is used to calculate the average

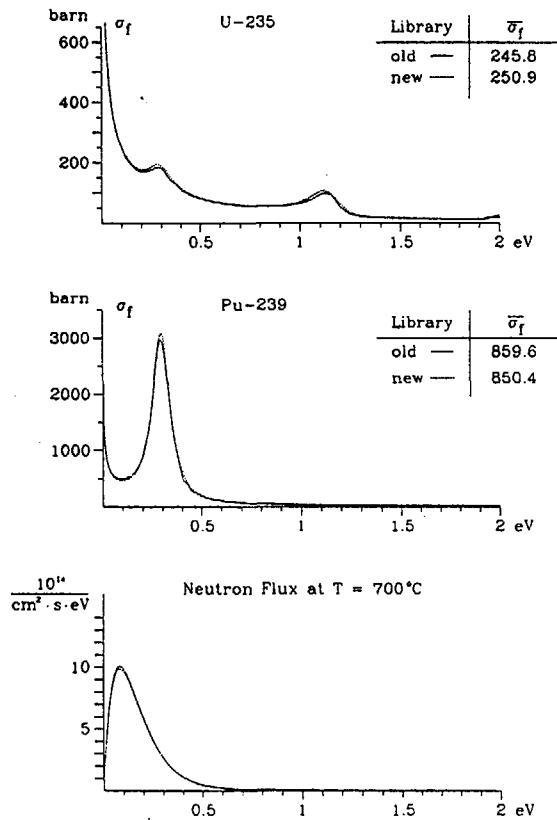


Fig. 2: Thermal Fission Cross Sections

cross sections. For ^{235}U the new function of σ_f is slightly higher in the range from 0.07 eV to 0.4 eV. Here the weighting spectrum is high, therefore the new averaged thermal fission cross section is higher by about 2%. For ^{239}Pu the new σ_f is lower in the range from 0.08 eV to 0.2 eV, and consequently the resulting new averaged thermal cross section is about 1% lower. The differences of these two fission cross sections have major influence on k_{eff} both of the startup core and of the equilibrium cycle.

3. Initial Core

As to table II the difference of k_{eff} between the two libraries is strong for the initial core, and it is small for the equilibrium cycle.

TABLE II. IMPACT OF LIBRARIES ON k_{eff}

Library	old	new	Δk_{eff} (new - old)
Initial core	0.9987	1.0151	+0.0164
Equilibrium cycle	1.0000	1.0017	+0.0017

In order to explore the reason of this finding a simplified model was formed for the reactor at startup: The core was collapsed into one spectrum zone at the temperature of 700°C and the reflector into another one at 650°C. Instead of changing the cross sections of all nuclides the change has been made for only one of them: either ^{235}U or ^{238}U . And in a third case the ^{235}U has been replaced by ^{239}Pu . The enrichment of ^{235}U (enr. = 4%) and of ^{239}Pu (enr. = 1.16%) was chosen in order to get $k_{\text{eff}} = 1.0$ in the calculations with the older library.

In this comparison it appears that the greatest difference results from ^{235}U . The value of k_{eff} increases by $\Delta k_{\text{eff}} = +0.0124$ (tab. IIIa). This increase is due to the increase of the new thermal $\bar{\nu}$ and $\bar{\sigma}_f$ by 0.3% and 2.1% respectively. This is so important because 98.2% of the produced neutrons in the thermal group are produced by ^{235}U . The increase in the thermal absorption cross section, which is mostly due to the increase of σ_a , does not compensate this effect. The changing of the cross sections in the epithermal energy group is unimportant as can be seen from the low rates of fractional absorption and production.

If only ^{238}U is taken from the new library k_{eff} increases by 0.0022 (tab. IIIb). This difference is mostly due to the decrease of 1.1% in the absorption cross section in the epithermal energy region and, to some lower part, in the thermal range. This decrease of the epithermal absorption value results from the reduced Γ_γ of the first three resonances of ^{238}U . The resulting resonance integral (for $T=700^\circ\text{C}$) is about 1.2% lower than the resonance integral calculated with the older resonance parameters. But, as one can conclude from the small isotopic absorption- and production rates, the exchange of the ^{238}U data is of minor influence on k_{eff} compared with the great influence of the ^{235}U data.

Further we checked the influence of ^{239}Pu because it is very important for the results in the equilibrium calculations. For this purpose we computed the same initial core as before but loaded with ^{238}U and 1.16% ^{239}Pu . In this case we got a decrease of -0.0201 in k_{eff} when taking the ^{239}Pu data from the new library (tab. IIIc). The decrease in k_{eff} is due to a decrease of 0.6% in thermal $\bar{\nu}$ and to a decrease of 1.1% in thermal $\bar{\sigma}_f$. 99% of the produced neutrons appear in the thermal group, therefore the differences in

thermal $\bar{\nu}$ and $\bar{\sigma}_f$ have such a great influence. Because the thermal absorption cross section changes by only 0.5% and the fast and epithermal energy region is unimportant, we can conclude that the difference in k_{eff} arises mostly from the differences in thermal $\bar{\nu}$ and $\bar{\sigma}_f$.

Beyond the heavy metals the initial core contains C, O and Si. Here the effect on k_{eff} is only $\Delta k_{\text{eff}} = +0.0008$. Of course, some change of the cross sections is observed in the epithermal energy range, but the effect is small due to the low fractional absorption rate of these elements. In the thermal range the cross sections of the scatterers have not been altered.

4. Equilibrium Cycle

When the running-in period is followed with the two libraries the difference in the multiplication factor reduces strongly in comparison with the difference of the initial core (tab. II). This is partly due to the nuclides which emerge during the burnup, and partly to the reduced importance of ^{235}U .

TABLE IIIa. ^{235}U CHANGE OF THE AVERAGED CROSS-SECTIONS (initial core)

Energy range Library	epithermal $E > 1.85 \text{ eV}$			thermal $E \leq 1.85 \text{ eV}$		
	old	new	rel. change ¹⁾ %	old	new	rel. change ¹⁾ %
$\bar{\nu}$	2.433	2.440	+0.3	2.430	2.437	+0.3
$\bar{\sigma}_f$ barn	12.3	13.3	+8.5	245.8	250.9	+2.1
$\bar{\sigma}_c$ barn	8.5	7.9	-6.9	45.6	46.2	+1.4
$\bar{\sigma}_a$ barn	20.8	21.3	+2.2	291.4	297.1	+2.0
fractional absorption ²⁾ %	1.2			48.4		
production ³⁾ %	1.7			98.2		
k_{eff}	old new		Δ (new - old)			
	1.0031 1.0155		+0.0124			

TABLE IIIb. ^{238}U CHANGE OF THE AVERAGED CROSS-SECTIONS (initial core)

Energy range Library	epithermal $E > 1.85 \text{ eV}$			thermal $E \leq 1.85 \text{ eV}$		
	old	new	rel. change ¹⁾ %	old	new	rel. change ¹⁾ %
$\bar{\nu}$	2.754	2.731	-0.8	0.0	2.319	-
$\bar{\sigma}_f$ barn	3.46-2	4.01-2	+15.9	0.0	1.55-6	-
$\bar{\sigma}_c$ barn	7.07	6.99	-1.1	1.32	1.31	-0.8
$\bar{\sigma}_a$ barn	7.11	7.03	-1.1	1.32	1.31	-0.8
fractional absorption ²⁾ %	9.40			5.2		
production ³⁾ %	0.14			0.0		
k_{eff}	old new		Δ (new - old)			
	1.0031 1.0053		+0.0022			

TABLE IIIc. ^{239}Pu CHANGE OF THE AVERAGED CROSS-SECTIONS (initial core)

Energy range Library	epithermal $E > 1.85 \text{ eV}$			thermal $E \leq 1.85 \text{ eV}$		
	old	new	rel. change ¹⁾ %	old	new	rel. change ¹⁾ %
$\bar{\nu}$	2.895	2.879	-0.6	2.892	2.874	-0.6
$\bar{\sigma}_f$ barn	13.6	14.3	+5.5	860.	850.	-1.1
$\bar{\sigma}_c$ barn	9.6	10.4	+8.1	489.	506.	+3.3
$\bar{\sigma}_a$ barn	23.2	24.7	+6.6	1349.	1356.	+0.5
fractional absorption ²⁾ %	0.38			54.0		
production ³⁾ %	0.64			99.0		
k_{eff}	old new		Δ (new - old)			
	1.0003 0.9802		-0.0201			

¹⁾ $\frac{\text{new} - \text{old}}{\text{old}} \cdot 100$

²⁾ per 100 lost neutrons

³⁾ per 100 produced neutrons

The burnup calculation includes 60 different nuclides. For some of them the change in the cross sections (tab. IV) is strong, e.g. ^{131}Xe , ^{105}Rh , ^{145}Nd , and ^{155}Eu . But their influence on k_{eff} is small, because their fractional absorption rate is in the order of only 0.1% for each of them.

TABLE IV. CHANGE OF THE AVERAGED CROSS SECTIONS FROM OLD TO NEW LIBRARY IN THE THERMAL ENERGY GROUP ($E \leq 1.85 \text{ eV}$)

Nuclide	Fractional absorption [%] in thermal group	Relative change [%] *)		Fractional neutron production [%] in thermal group
		σ_a	$\nu\sigma_f$	
^{235}U	28.9	+2.1	+2.4	59.3
^{239}Pu	15.8	+0.7	-1.5	28.9
^{240}Pu	4.5	+1.4		
^{241}Pu	3.6	-6.6	-2.2	7.4
^{238}U	2.7 (15.4 epithermal)	-0.9 (-1.1)		
^{133}Xe	2.18	+4.2		
^{143}Nd	0.84	-5.4		
Si	0.68	+0.3		
^{103}Rh	0.60	-0.6		
^{149}Sm	0.54	+3.2		
^{151}Sm	0.30	-0.4		
^{131}Xe	0.18	-21.8		
^{147}Pm	0.17 (0.008 epithermal)	-1.3 (+3300% !)		
^{103}Rh	0.15	-57.1		
^{143}Nd	0.12	-18.9		
^{133}Cs	0.12	+8.1		
^{155}Eu	0.11	-71.2		

$$*) \frac{\text{new} - \text{old}}{\text{old}} \cdot 100$$

For the few nuclides of higher importance the change in the cross sections is only moderate. Just like for the initial core, the ^{235}U and ^{238}U make the tendency for an increase of k_{eff} . A tendency of decrease results from the cross sections of ^{239}Pu , ^{240}Pu , ^{133}Xe , and ^{149}Sm . In short, the influence on the equilibrium cycle is no more than $\Delta k_{\text{eff}} = +0.0017$. An uncertainty of that kind could easily be balanced by the control system of the reactor.

But there is another way of compensating for the difference in k_{eff} : Due to the continuous fuelling of this reactor the burnup can easily be increased by slight reduction of the loading and unloading rate of fuel elements per day. By this way the transition from the old library to the new one can be balanced by an increase of the burnup from 99.5 to 100.0 MWd/kg_{FHM}, achieving the same value of $k_{\text{eff}} = 1.0$ at the equilibrium cycle.

The table V illustrates the impact on reactor performance characteristics as caused by that transition in the loading rate. In the global data a very slight decrease is observed in the conversion ratio. The power peaking increases by 4%, but the maximum value

TABLE V. EQUILIBRIUM CYCLE

Library		old	new	relative changes *) [%]
Global characteristics:				
Burnup	MWd/kg _{FHM}	99.51	100.01	+0.5
Fuel residence time	d	916.0	921.1	+0.56
Conversion ratio		0.442	0.437	-1.1
Fissile inventory	kg/GW _{th}	451.4	442.1	-2.1
Power peaking	KW/ball	1.70	1.77	+4.1
Max. fuel temperature	°C	1051.1	1050.6	-0.05
Fuel cycle costs	mills/KW _h	7.87	7.85	-0.2
Balance of neutrons:				
Production/absorption (in fiss.isot.)	ηk	1.961	1.966	+0.25
Capture/fission (fissile isotopes)	α	0.321	0.316	-1.6
Production of neutrons: ^{235}U	%	62.63	63.47	+1.3
	^{239}Pu	0.25	0.29	+16.0
	^{240}Pu	29.32	28.17	-3.9
	^{241}Pu	7.78	8.03	+3.2
Neutron losses: fissile isotopes	%	50.99	50.88	-0.2
	fission products	7.57	7.84	+3.6
	leakage	14.53	14.57	+0.3
Fissile material:				
Discharged fuel:	kg/GW _d _{th}			
	^{235}U	0.1398	0.1310	-6.3
	^{239}Pu	0.0532	0.0511	-4.0
	^{241}Pu	0.0228	0.0242	+6.1
Inventory:	kg/GW _{th}			
	^{235}U	395.2	386.5	-2.2
	^{239}Pu	43.8	42.4	-3.1
	^{241}Pu	12.5	13.2	+5.9

$$*) \frac{\text{new} - \text{old}}{\text{old}} \cdot 100$$

of 1.77 KW/ball stays far below the technological limit which is given by 4.5 KW/ball. And the fuel cycle costs decrease by a very small amount which is negligible.

In the balance of neutrons the change in the neutron production rate from fissions in ^{235}U is relatively high, which results from the improvement of $\nu\sigma_f$. But the importance of that effect on the total fission rate is very low. The changes in the production rates of the Pu-isotopes almost cancel out each other. A slight increase is observed in the fission products absorption. This is mainly due to the higher thermal absorption cross sections of ^{135}Xe , ^{149}Sm , and to the higher epithermal absorption in ^{147}Pm .

In the break down of the fissile material balances the changes are of the order of 5%. This clearly illustrates that library changes can effect the isotopic mass balances to some degree. On the other hand it shows also that future changes of the mass balances, as due to future improvements of the libraries, must be expected to be never more than in the order of a percent, because it is unlikely that improvements of the nuclear data could be again of the same magnitude as observed over the last 20 years.

5. Aspects of Control and Safety

For the two equilibrium cycles we investigated some effects which are basic for the assessment of the reactor.

The temperature coefficients of the two cases differ slightly (tab. VI). They have been obtained by changing the temperature in the fuel, moderator, and reflector about 50°C . It appears that the Doppler coefficient remains almost unchanged, but the moderator coefficient and the reactivity effect of the temperature change in the reflector are different in the order of 20%. Since the scattering matrix of graphite has not been altered the

TABLE VI. REACTIVITY EFFECTS

Library		old	new
Temperature coefficient:			
at operating condition	$\Delta k_{\text{eff}} / \Delta T [10^{-5}]$	-4.46	-4.66
break down: fuel (Doppler)		-3.68	-3.78
moderator		-1.68	-2.00
reflector		+0.90	+1.12
at shutdown, cold	$\Delta k_{\text{eff}} / \Delta T [10^{-5}]$	-13.00	-13.82
Shutdown requirement:			
full power \rightarrow zero power (50°C , Xe-decay)	Δk_{eff}	+0.083	+0.087
Capability of shutdown system KLAk	Δk_{eff}	-0.155	-0.156

reactivity changes must be assigned to the thermal cross sections of the absorbers and to their impact on the leakage. As a consequence, the response of reactivity to transient change of the temperature in graphite structures must be expected to be different for the two libraries. But when temperature changes also occur in the fuel, the library effect is lower because the low change of the Doppler coefficient is dominant.

The largest change of temperature occurs at down cooling of the reactor after shutdown. The multiplication factor increases by 4.3 or 4.7% when applying the old or new library, respectively. In tab. VI the shutdown requirement includes another 4% as due to the ^{135}Xe decay. The contribution of xenon is very similar for the two libraries.

In total the shutdown requirement is well covered by the shutdown system, which consists of little absorber spheres (KLAk) being poured into channels in the reflector. The capability of the KLAk system is about 15.5%, and it is only little dependent on the libraries.

In addition the shutdown system must cover any other excess reactivity which might occur. For the ingress of water at full operating condition the characteristics have been calculated for the two library cases (fig. 3). Apparently, the effect of the libraries is definitely small over the whole range of consideration. From the scale of the partial pressure it can be recognized that the content of water in the core and in the upper void can

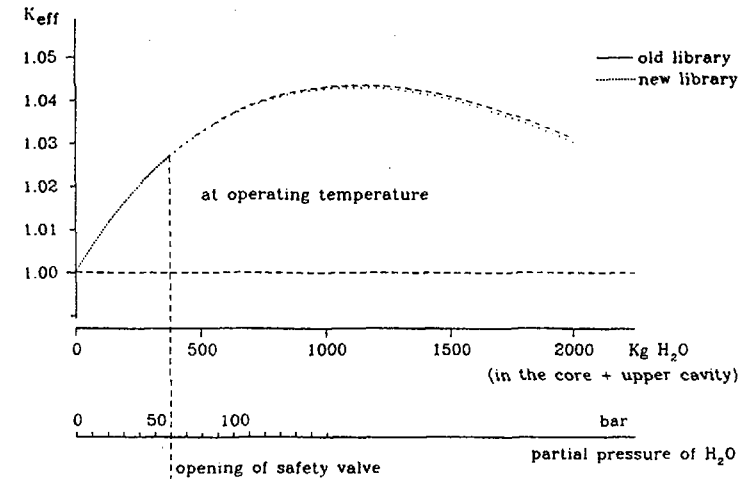


Fig. 3: Ingress of Water

hardly exceed 400 kg. That amount of water causes the excess reactivity of 2.6%, and this is also well covered by the KLAKE shutdown system. The change between the two libraries results in the two different curves, and this effect appears to be negligible.

6. Conclusion

The introduction of improved nuclear data into detailed reactor research is a two-edged enterprise, because it might destroy the confidence into former results. Fortunately, the revision of the 20 years old library of the VSOP program brings only little changes in the results.

The changes of the cross sections of the different fissile isotopes are opposite to each other. They bring up to 6% changes in the mass balance of the individual fissile isotopes, but the net effect on multiplication factor and burnup is low. Definitely large changes are observed in the cross sections of some fission products, but fortunately the importance of these isotopes is very low. Safety related properties of the reactor are dependent on global nuclear and thermal features, and these ones are only weakly affected by the turn to the new library.

References

- [1] R.Kinsey: ENDF/B Summary Documentation ENDF-201, 3rd Edition (ENDF/B-V), BNL-NCS-17541 (1979)
- [2] Index to the JEF-1 Nuclear Data Library, Volume 1: General Purpose File OECD, NEA Data Bank (1985)
- [3] E.Teuchert et al.: VSOP - Computer Code System for Reactor Physics and Fuel Cycle Simulation, Forschungszentrum Jülich GmbH. (KFA), JÜL-1649 (1980)
- [4] E.Teuchert, K.A.Haas: ZUT-DGL - VSOP Programmzyklus für die Resonanzabsorption in heterogenen Anordnungen, Internal report, KFA-IRE-70-1 (1970)
- [5] C.D.Joanou, J.S.Dudek: GAM - A Consistent P1 Multigroup Code for the Calculation of Fast Neutron Spectra and Multigroup Constants. General Atomic GA-1850 (1961)
- [6] H.C.Honeck: THERMOS - A Thermalization Transport Theory Code for Reactor Lattice Calculation, Brookhaven National Laboratory, BNL-5826 (1961)
- [7] H.C.Honeck: ENDF/B-Specifications for an Evaluated Data File for Reactor Applications, Brookhaven National Laboratory, BNL-50066 (1966)
- [8] Brookhaven National Laboratory, BNL-325 (1966)
- [9] J.A.Young, J.U.Koppel: Phonon Spectrum in Graphite, Journ. Chem. Physics 42, 357 (1965)
- [10] D.Garber: ENDF/B Summary Documentation ENDF-201, 2nd Edition, BNL-17541 (1975)

NUCLEAR DATA RELATED TO HTRs

S. PELLONI

Paul Scherrer Institute,
Villigen, Switzerland

W. GIESSER

Hochtemperatur Reaktorbau GmbH,
Mannheim, Federal Republic of Germany

Abstract

A series of two-dimensional discrete-ordinates transport theory k_{eff} calculations with an (r,z) geometric model have been performed for a simple, typical LEU HTR PROTEUS configuration (7042 pebbles) without the simulation of any water ingress into the core, with LEU AVR non irradiated fuel containing 6 grams of 16.7% enriched uranium per pebble, for a filling factor of 0.74 (maximum packing) and for a moderator-to-fuel pebble ratio M/F of 1/1. All calculations were based on specific data libraries (mainly based on JEF-1) for the cell codes WIMS-D, MICROX-2, and TRAMIX, and were performed using these codes in connection with the one- and with the two-dimensional transport theory programmes ONEDANT and TWODANT from Los Alamos. WIMS-D may now be routinely used for HTR applications with a new method developed by Segev which allows the conversion of the spherical pebble bed unit cell into an equivalent (from the neutronic point of view) cylindrical unit cell.

It is found that the calculated eigenvalue k_{eff} depends particularly on the transport corrected total cross sections employed in the full reactor calculation, on the number of groups, and on the nuclear data (i.e. from JEF-1 or from older evaluations) used.

For a 13 neutron group calculation in the well tested structure from Hochtemperatur Reaktorbau (HRB), the eigenvalue k_{eff} ranges from 0.9896 for P_0 modified cross sections coming from MICROX-2 to 1.0083 for P_0 modified JEF-1 cross sections from WIMS-D.

Either the use of P_1 modified cross sections in connection with the group structure from HRB, or that of P_0 cross sections (suitably modified) in connection with a finer group structure, particularly in the thermal range, is recommended for physics calculations of small HTR cores.

1 INTRODUCTION

A series of two-dimensional discrete-ordinates transport theory k_{eff} calculations with an (r,z) geometric model have been performed for a simple, representative LEU HTR PROTEUS configuration (3521 fuel pebbles, corresponding to a core height of 86.61 cm), without the simulation of any water ingress into the core, with LEU AVR non irradiated fuel containing 6 grams of 16.7% enriched uranium per pebble, for a filling factor of 0.74 (maximum packing) and for a moderator-to-fuel pebble ratio M/F of 1/1. The core radius is 62.5 cm, the radial reflector is 100 cm thick graphite, the lower axial reflector is 64 cm thick graphite, and the upper axial reflector is 78 cm thick graphite. The height of the core cavity (which includes the core itself and the air above the core and between the pebbles) is 190 cm.

For the sake of convenience, we defined a reference case. Room temperature was assumed, a pure void was used in the core cavity above the pebble bed fuel and between the pebbles, the presence of boron in the reflector material was neglected, and the control rods were all withdrawn.

The present analysis is intended to identify some aspects of uncertainties in LEU HTR eigenvalue calculations of strongly leaking cores (surrounded with a thick graphite reflector such as in HTR PROTEUS) arising each from the computational model, from the nuclear data libraries, and from the codes utilized.

In Section 2 a detailed description of HTR related nuclear data libraries and codes available at the Paul Scherrer Institute (PSI) is given.

Section 3 presents the main results from this study.

Finally, Section 4 gives some conclusions and recommendations for further work.

Results include eigenvalues k_{eff} for the full two-dimensional reactor (r,z) configuration (in the reference case), and cell eigenvalues k_{∞} corresponding to both the fundamental mode spectrum and to the infinite unperturbed lattice (cell with a vanishing Buckling), obtained using various nuclear data libraries and codes. The eigenvalues k_{eff} for the full reactor were carried out using various approaches as far as weighting spectra, number of groups, and transport corrections are concerned.

The effect on the reactivity of the whole reactor coming from boron in the reflector material, from air above the core and between the pebbles, and the reactivity change due to an homogeneous temperature increase in the core (which is indicative for the temperature coefficient) were investigated separately.

2 COMPUTATIONAL MODEL AND NUCLEAR DATA

2.1 Nuclear Data

All calculations were based on specific nuclear data libraries for the (cell) codes WIMS-D [1], MICROX-2 [2], and TRAMIX [3].

These include three libraries with 69 neutron groups (WIMS structure) for the code WIMS-D, i. e. the British standard libraries WIMS-81 and WIMS-86 [4],[5] and a JEF-1 based library (WIMS-JEF library) [6] processed at the PSI using the version 6/83 of the NJOY system [7].

While processing the WIMS-JEF library with NJOY, the module WIMSR was applied to transform groupwise GENDF formatted cross-sections (the GENDF format is similar to the standard ENDF/B format) into a form suitable for being used as input to the Canadian WIMS library management programme WILMA [8], [9]. In the processing with WIMSR and WILMA, which finally resulted in the WIMS-JEF library, the relevant data were calculated by considering all explicitly represented reaction types on the GENDF files. Individual fission energy spectra available on GENDF, however, were not used. Instead a global fission spectrum, based primarily on data for ^{235}U fission, was taken over from the WIMS-81 library. The WIMS-JEF library consists of temperature dependent transport corrected ("inflow" transport correction) self-shielded P_0 cross sections for a small class of nuclides without burnup data [6], and of unmodified P_1 cross sections for hydrogen, deuterium, oxygen, and carbon. The transport correction is computed using an isotope independent representative weighting current [10]. Scattering data of ^{238}U are given for different dilution cross sections (i. e. 10^{10} , 100, and 1 barns).

The library for the code MICROX-2 is from JEF-1, and consists of the 193 neutron group/point (General Atomics (GA) structure) data files FDTAPE and GGTAPE, and of the pointwise file GARTAPE respectively, which include data at room temperature for a relatively small class of nuclides [6]. FDTAPE, GGTAPE, and GARTAPE were generated using the coupling module MICROR. MICROR,

an NJOY module developed at the PSI, edits pointwise and groupwise NJOY cross sections into a library for use in MICROX-2 [11]. FDTAPE contains fine group self-shielded P_3 unmodified cross sections in the fast energy range. GGTAPE contains infinite dilute P_1 unmodified cross sections in the thermal energy range, and GARTAPE consists of 14457 pointwise resonance cross sections in the resolved resonance range between 8.0072 keV and 0.414 eV, equally spaced in velocity.

Finally, MAT193 is a MATXS formatted library for the codes TRANSX, TRANSX-CTR, and TRAMIX, obtained by editing GENDF cross sections with the NJOY module MATXSR. The MATXS file is a generalized cross section library in a flexible format designed to generalize and to simplify the existing standard cross section formats. In the MATXS format neutron and photon data types are treated in the same way. Each data type is subdivided into materials and submaterials. A material might be a particular isotope or mixture. Each submaterial is associated with a temperature- background cross section pair, and contains data related to any kind of reaction, including scattering transfer matrices and fission spectra. MAT193 [6] includes self-shielded (for data showing a strong dependency on the background cross section) P_3 unmodified neutron data at room temperature in the GA group structure for the same isotopes as available in the MICROX-2 library.

2.2 Codes

All calculations were performed using the (cell) codes WIMS-D, the PSI edition 13 of the MICROX-2 code, and TRAMIX in connection with the one- and with the two-dimensional transport codes ONEDANT and TWODANT [12].

The GHR [13] code, a PSI development, was used to determine cell specifications (graphite pebbles and void regions were smeared out in the outer cell regions), and to compute atomic number densities for the PEBBLE and WIMBN codes [13],[14] and for the codes MICROX-2 and TRAMIX.

PEBBLE [15], a code based on the Teuchert routine, was utilized to calculate the Dancoff correction factors for the fuel pebbles required by the MICROX-2 code. The code WIMBN [14] was used to prepare the input to WIMS-D based on a new method developed by Segev [16], which allows the conversion of the spherical pebble bed unit cell into an equivalent (from the neutronic point of view) cylindrical unit cell, and uses the cluster option of WIMS-D to treat the double heterogeneity. Using this method, WIMS-D may now be routinely used for HTR applications. Required atomic number densities, cylindrized double heterogeneous cell or full reactor specifications, and Dancoff factors are the output of WIMBN. WIMBN has been checked carefully against PEBBLE as far as the determination of Dancoff factors is concerned.

WIMS-D, MICROX-2, and TRAMIX were systematically employed for the preparation of self-shielded broad group homogenized core and reflector cross sections in at least 13 groups (exactly the HRB group structure in the case of MICROX-2 and TRAMIX), in the Los Alamos XSLIB material ordered card image standard format [12] from the basic libraries described in the previous subsection, to be used further in TWODANT for two-dimensional full reactor k_{eff} calculations in the (r,z)-geometry. It should be noted that the 13 groups used in WIMS-D are slightly different (particularly in the epithermal range) from the HRB structure because the 69 groups of WIMS-D are not exactly a subset of the 193 groups. The group boundaries of the HRB structure are displayed in Table 1.

For determining core cross sections, cell calculations based on the codes WIMS-D, MICROX-2, and TRAMIX (with white outer boundary conditions to simulate an infinite lattice) for the LEU HTR PROTEUS lattice under investigation were performed, followed by a fundamental mode homogenized-cell leakage B_N calculation. In the TRAMIX calculations the coated particles had to be smeared out over the microcell structure.

Table 1: Original (HRB) 13 Group Boundaries

Group	Lower Energy (eV)	Delta Lethargy
1	3.68×10^6	1.4
2	1.11×10^5	3.5
3	3.35×10^3	3.5
4	748	1.5
5	130	1.75
6	29.0	1.5
7	8.32	1.25
8	2.38	1.25
9	0.625	1.338
10	0.200	1.139
11	0.050	1.386
12	0.010	1.537
13	0.0	

In the WIMS-D cell calculations the REGION card in connection with the PUNCH=1 option were used to produce region averaged macroscopic homogenized cross sections, and the code DSNXSL [17], a PSI development, was used to convert the outgoing cross section format into XSLIB format. In addition to the cell model, WIMS-D was used with a full reactor model which was set up using WIMBN (the "cluster" specifications were derived from the specifications available from the cell model using geometric arguments) for calculating very accurately reflector cross sections. As expected, the alternative use of core cross sections from the cell or from the full reactor model in WIMS-D resulted in a very small reactivity change of maximum 1.5 mk (1mk=0.001), when performing full reactor calculations.

MICROX-2 reflector cross sections were determined with an additional MICROX-2 calculation with zero buckling. The methodology used in MICROX-2 has been extensively described in [13].

Cell calculations on the basis of TRAMIX were performed by looping TRAMIX, ONEDANT, SOLVERB, and COLAPS [18]. The spatially dependent neutron spectrum in the RZMFLX [19] format required for collapsing reflector cross sections into a coarser group structure (with the code COLAPS) and for iterating on the fission spectrum and on the elastic correction [18] was determined from ONEDANT calculations in the full 193 neutron group structure of MAT193, using one-dimensional cylindrical radial and axial full reactor models.

In contrast to WIMS-D and to MICROX-2, TRAMIX/ONEDANT/SOLVERB allows the determination of reflector cross sections for the top, bottom, and radial reflectors, separately.

In each case (homogenized core and reflector cross sections may come from WIMS-D, MICROX-2, or from TRAMIX) XSLIB formatted basic cross sections (i.e. absorption, production, total and scattering matrix cross sections) were converted into the more compact format MACRXS using ONEDANT

(the Solver Module option was turned off), and combined with the code COGOXS [3] into a single library for use in TWODANT. In the case of cross sections coming from MICROX-2 or from TRAMIX, the transport cross sections and fission spectra available on the XSLIB files were added into the MACRXS file using the management code AMCHTR developed for internal use at the PSI.

The two-dimensional (r,z)-geometry model for TWODANT used a fine spatial mesh of 44 radial and 92 axial intervals with 200 thin zones (coarse meshes) mostly defined in the vicinity of the material interfaces, where stronger spatial flux gradients occur. This led to a good and fast convergence in TWODANT, even in the large void regions belonging to the reactor cavity. Doubling the number of meshes in each direction (i.e. radially and axially) did not affect the results presented in this study, whereas a reduced number of fine meshes (particularly in the axial direction) led to significantly different results. The inner iteration convergence criterion was set up with the parameter EPSI=0.00001. When using EPSI=0.0001 (default value) the calculation was concluded prematurely, and the eigenvalue k_{eff} differed from the converged eigenvalue by up to 5 mk.

Calculations for the reference case (see Section 1) were performed using P_0 modified cross sections unless otherwise specified, and the S_4 approximation. The methodology for calculating the transport corrected total cross sections is complicated, and is unfortunately not exactly the same when using the cell codes WIMS-D, MICROX-2, or TRAMIX. The use of S_8 or S_{16} instead of S_4 did not lead to any significant difference, except much longer running times were observed. In the case of cross sections coming from WIMS-D, the collapsed fission spectrum (which originates from the WIMS-D library and which is printed out in the output section of WIMS-D) was supplied as a card image input array CHI in the solver section of TWODANT. In the case of cross sections coming from MICROX-2 or from TRAMIX, the fission spectrum available on the MACRXS file was automatically used in the TWODANT calculations.

Table 2: Comparison of eigenvalues calculated for the reference case obtained using different methods and nuclear data libraries in 13 groups

Cross sections obtained using this code	Starting library	k_{eff}
WIMS-D	WIMS-JEF	1.0083
WIMS-D	WIMS-81	0.9955
WIMS-D	WIMS-86	0.9952
MICROX-2	GAR GG FD (JEF-1)	0.9896
TRAMIX	MAT193	0.9927

3 RESULTS

3.1 Full reactor and cell eigenvalues

Table 2 summarizes the resulting eigenvalues k_{eff} for the reference case calculated using the 13 neutron group structure from HRB. The eigenvalue k_{eff} ranges from 0.9896 for cross sections coming from MICROX-2 to 1.0083 for JEF-1 cross sections from WIMS-D. The eigenvalues k_{eff} for cross sections coming from TRAMIX and from WIMS-D in connection with the British libraries lie in between.

Table 3 shows eigenvalues k_{∞} from the cell calculations related to the fundamental mode spectrum and to an infinite lattice (with vanishing Buckling) respectively. Excellent agreement within 2 mk is achieved between the eigenvalues k_{∞} from the different WIMS-D calculations, whereas MICROX-2, and especially TRAMIX, give lower values. The underestimate of TRAMIX is due to the omission of grain shielding leading to an increased capture of ^{238}U (corresponding fundamental mode and infinite lattice cell eigenvalues k_{∞} from MICROX-2 without grain shielding are 1.6600 and 1.7174 respectively). The large value of k_{∞} compared to k_{eff} (see Table 2) is indicative of the importance of neutron leakage into the thick graphite reflector.

3.2 Group structures and transport corrections

Table 4 summarizes the resulting k_{eff} eigenvalues from the TWODANT calculations for the reference case obtained using cross sections from WIMS-D, MICROX-2, and TRAMIX, and different group structures. The 26 group structure originates from the 13 group structure from HRB by subdividing each coarse group into two (equally spaced in lethargy if possible) fine groups. The 52 group structure originates in the same way from the 26 group structure.

Table 3: Comparison of cell eigenvalues related to the fundamental mode spectrum and to an infinite lattice obtained using different methods and nuclear data libraries

Cross sections from	Library	k_{∞} fund. mode	k_{∞} Buckling 0
WIMS-D	WIMS-JEF	1.7231	1.7736
WIMS-D	WIMS-81	1.7257	1.7749
WIMS-D	WIMS-86	1.7247	1.7757
MICROX-2	GAR GG FD (JEF-1)	1.7147	1.7653
TRAMIX	MAT193	1.6766	1.7329

Table 4: Comparison of eigenvalues k_{eff} for the reference case obtained using different methods and data libraries in 13, 26, and 52 groups

Number of groups	13	26	52
WIMS-D (WIMS-JEF)	1.0083	1.0046	0.9992
WIMS-D (WIMS-81)	0.9955	0.9916	0.9859
WIMS-D (WIMS-86)	0.9952	0.9912	0.9856
MICROX-2	0.9896	0.9845	0.9718
MICROX-2 (P_0 unmodified)	1.0085	1.0050	1.0034
MICROX-2 (P_1 modified)	0.9984	1.0005	0.9999
MICROX-2 (P_2 modified)	0.9983	1.0005	0.9997
TRAMIX	0.9927	0.9846	0.9818

Table 4 shows that the eigenvalue k_{eff} calculated using P_0 modified 52 neutron group cross sections from WIMS-D and from TRAMIX is about 10 mk lower compared to that predicted with P_0 modified cross sections in 13 groups. The decrease of k_{eff} due to the increased number of groups is even more significant when using P_0 modified cross sections from MICROX-2 (18 mk). The eigenvalues k_{eff} calculated using P_0 modified 69 neutron group cross sections (the maximum number of groups) from WIMS-D reproduced well within less than 1 mk those obtained with 52 group cross sections, and were therefore not included into Table 4.

A similar trend could be observed when applying the transport correction in the transport code instead in the cell code. The results were not included into Table 4. The decrease of k_{eff} due to the use of 52 group cross sections instead of 13 group cross sections would be 25 mk when using MICROX-2 P_0 cross sections extracted from inconsistent P_1 cross section tables and modified with the diagonal transport correction in TWODANT, and only 6 mk when using modified cross sections with the more accurate Bell-Hansen-Sandmeier transport correction in TWODANT.

Either the use of P_1 modified or of P_2 modified cross sections from MICROX-2 makes k_{eff} almost independent on the number of groups, which is in agreement with previously published values [13]. In these cases k_{eff} agrees well with the eigenvalue obtained with P_0 modified cross sections in 52 (or 69) groups from WIMS-D in connection with the WIMS-JEF library. The use of P_1 modified cross sections from MICROX-2 in connection with the 13 group structure from HRB leads to an almost asymptotic value for k_{eff} , whereas the use of P_0 unmodified cross sections results in an overestimated eigenvalue for any group structure.

The eigenvalue k_{eff} originating from P_0 modified JEF-1 cross sections from TRAMIX agrees to within 7 mk (maximum discrepancy in the case of 26 group calculations) with the values obtained using the WIMS-81 and WIMS-86 cross sections when the same number of groups is considered in the full reactor calculation. But even in the case of 52 group cross sections k_{eff} is still lower (by 18 mk) compared to MICROX-2 and to WIMS-D in connection with the WIMS-JEF library. This underestimate is partly due to the omission of grain shielding when calculating with TRAMIX (see Section 3.1). A MICROX-2 calculation of the reference case without grain shielding leads to a decreased eigenvalue k_{eff} of 9 mk.

3.3 Reflector cross sections

WIMS-D, MICROX-2, and TRAMIX were deliberately used to inadequately collapse the reflector cross sections with the fundamental mode spectrum associated with the basic cell of the core, which corresponds approximately to the asymptotic core spectrum. The use of these broad group reflector cross sections in calculations of the reference case resulted in an eigenvalue k_{eff} increase up to 3 mk for 13 group P_0 modified cross sections depending on the method and nuclear data used. The increase of k_{eff} diminished remarkably when considering more groups and P_1 scattering. Whereas the neutron spectrum at the core centre was almost independent on the methodology used for weighting the reflector cross sections, the flux increased by up to 30% at the boundary between core and radial reflector in the tenth group of the HRB structure (i.e. between 0.2 eV and 0.625 eV). The increase of the neutron flux comes primarily from the energy dependent part ($1/v$ shape) of the thermal absorption cross section of graphite at energies below 1 eV. Since the core spectrum is harder and differs considerably from the reflector spectrum (this is a statement valid for any small HTR core), the thermal coarse group absorption cross section of graphite becomes smaller if weighted with the core spectrum. The reduced absorption cross section leads to an increased thermal flux particularly in the vicinity of the boundary between reactor core and reflector, and consequently to an increased eigenvalue k_{eff} .

3.4 The effect of air and boron

Table 5 summarizes the resulting k_{eff} eigenvalues from the TWODANT calculations for the reference case with additional boron homogeneously distributed in the reflector material, obtained using P_0 modified JEF-1 cross sections in 13 groups from MICROX-2 and TRAMIX. In Table 5 the total boron equivalent in the reflector material was doubled twice.

As expected, the decrease of the eigenvalue k_{eff} due to the presence of boron in the reflector material does not depend too much on the method used (see Table 5).

With the same methodology as used for creating Table 5, it was found that the presence of air between the pebbles and in the reactor cavity above the core leads to a decreased eigenvalue k_{eff} of 10.5 mk for the reference case (without the boron equivalent in the reflector material).

3.5 Temperature effects

Table 6 summarizes the resulting k_{eff} eigenvalues from the TWODANT calculations for the reference case with different core temperatures (the reflector temperature is 296 K), obtained using P_0 modified JEF-1 cross sections in 13 groups from WIMS-D in connection with its libraries.

The results in terms of a change of the eigenvalue due to a temperature increase in the core show good agreement within 6 mk between the different WIMS-D libraries.

Table 5: Comparison of eigenvalues k_{eff} for the reference case with boron in the reflector material, obtained using different methods and data libraries in 13 groups

^{10}B number density (atoms/barn/cm)	MICROX-2	TRAMIX
0	0.9896	0.9927
9.20×10^{-9}	0.9767	0.9833
1.84×10^{-8}	0.9678	0.9745
3.68×10^{-8}	0.9514	0.9585

Table 6: Comparison of eigenvalues k_{eff} for the reference case with different core temperatures obtained using WIMS-D and different data libraries in 13 groups

Core temperature (K)	WIMS-JEF	WIMS-81	WIMS-86
296	1.0083	0.9955	0.9952
600	0.9464	0.9387	0.9390
900	0.8956	0.8895	0.8897

4 CONCLUSIONS AND RECOMMENDATIONS

Two-dimensional discrete-ordinates transport theory k_{eff} calculations in at least 13 groups (the structure suggested by HRB) have been performed for a typical, simple LEU HTR PROTEUS configuration without any simulation of water ingress using the two-dimensional transport code TWODANT from Los Alamos.

This study showed that there are large discrepancies (up to 20 mk) in the eigenvalue k_{eff} calculated using different cell codes (i.e. WIMS-D with a new method developed by Segev, MICROX-2, and TRAMIX), various related nuclear data libraries (British standard libraries for WIMS-D in addition to JEF-1 based libraries for all cell codes including WIMS-D), and different computational models.

Detailed analysis is still necessary to identify the deficiencies and the uncertainties in HTR related nuclear data libraries and codes, and the planned experiments at the PROTEUS facility could help in reducing them. Particularly, new libraries based on the JEF-2 and/or ENDF/B-VI evaluations should be generated.

It is recommended to perform a similar study for configurations characterized by smaller filling factors and/or moderator-to-fuel pebble ratios, and particularly for cores with simulated water ingress.

Either the use of P_1 modified cross sections in connection with the 13 neutron group structure from HRB, or that of P_0 cross sections (suitably modified) in connection with a finer group structure, particularly in the thermal range, is recommended for physics calculations of small HTR cores such as HTR PROTEUS. The use of P_0 modified cross sections from the PSI edition 13 of the MICROX-2 code is not recommended.

References

- [1] J. R. Askew, F. J. Fayers, P. B. Kemshell, "A General Description of the Lattice Code WIMS", J. Brit. Nucl. Energy Soc., 5, 564 (1966)
- [2] D. R. Mathews, P. Koch, "MICROX-2. An Improved Two-Region Flux Spectrum Code for the Efficient Calculation of Group Cross Sections", GA-A15009, Vol.1 (1979)
- [3] J. Stepanek, C. Higgs, "A General Description of AARE: A Modular System for Advanced Analysis of Reactor Engineering", Proc. 1988 Int. Reactor Physics Conference, p. IV 85, Jackson Hole, Wyoming (1988)
- [4] M.J.Halsall, C.J.Taubmann, "The '1981' WIMS Nuclear Data Library", AEEW-R1442 (1983)
- [5] M.J.Halsall, C.J. Taubmann, "The '1986' WIMS Nuclear Data Library", AEEW-R 2133 (September 1986)
- [6] P. Vontobel, S. Pelloni, "JEF/EFF Based Nuclear Data Libraries", EIR-Report 636 (December 1987)
- [7] R. E. MacFarlane, D. W. Muir, R. M. Boicourt, "The NJOY Nuclear Data Processing System, Volume I: User's Manual", LA-9303-M (ENDF-324) (1982)
- [8] J. Babino, A. M. Lerner, R. J. Stamm'ler, "WILMA, WIMS Library Management: Description and User's Manual", CNEA-Re-CA 79-10 (November 1979)
- [9] G. L. Festarini, "the ENDF/B-V WIMS Library", CRNL-2784 (unpublished)
- [10] S.Pelloni, J.Stepanek, "Testing of a JEF-1 Based WIMS-D Cross Section Library for Migration Area and k_{∞} Predictions for LWHCR Lattices", EIR-Report 610 (January 1987)
- [11] D. R. Mathews, J. Stepanek, S. Pelloni, C. E. Higgs, "The NJOY Nuclear Data Processing System: The MICROR Module", EIR-Report 539 (December 1984)
- [12] R. D. O'Dell, F. W. Brinkley, D. R. Marr, "User's Manual for ONEDANT: A Code Package for One-Dimensional Diffusion Accelerated Neutral Particle Transport", LA-7396-M (September 1986)
- [13] D. Mathews, "HTR PROTEUS: Two-Dimensional Calculations with LEU AVR Fuel", PSI Technical Memorandum TM-41-89-04, (February 1989)
- [14] M. Segev, private communication, (1989)
- [15] E. Teuchert, Nukleonik 11, 68 (1968)
- [16] M. Segev, "An Equivalence Relation for a Doubly Heterogeneous Lattice", Nuclear Science and Engineering, 81, 151-160, (1982)
- [17] H. Hager, private communication, (1989)
- [18] S. Pelloni, J. Stepanek, "Analysis of LWHCR-PROTEUS Phase II Experiments Performed using the AARE System with JEF-1 Based Data Libraries, and Comparisons with Other Codes", PSI-Report 3 (April 1988)
- [19] R. D. O'Dell, "Standard Interface Files and Procedures for Reactor Physics Codes, Version IV", LA-6941-MS (September 1977)

A REVIEW OF REACTOR PHYSICS UNCERTAINTIES AND VALIDATION REQUIREMENTS FOR THE MODULAR HIGH-TEMPERATURE GAS-COOLED REACTOR

A.M. BAXTER, R.K. LANE, E. HETTERGOTT, W. LEFLER
General Atomics,
San Diego, California,
United States of America

Abstract

The important, safety-related, physics parameters for the low-enriched Modular High-Temperature Gas-Cooled Reactor (MHTGR) such as control rod worth, shutdown margins, temperature coefficients, and reactivity worths, are considered, and estimates are presented of the uncertainties in the calculated values of these parameters. The basis for the uncertainty estimate in several of the important calculated parameters is reviewed, including the available experimental data used in obtaining these estimates. Based on this review, the additional experimental data needed to complete the validation of the methods used to calculate these parameters is presented. The role of benchmark calculations in validating MHTGR reactor physics data is also considered.

1. INTRODUCTION

The MHTGR is an advanced nuclear reactor concept being developed in the U.S.A under a cooperative program involving the U.S. Government, the nuclear industry, and the electric utility companies (Ref. 1). As its objective, this program is developing a safe, reliable, and economic nuclear power and process heat option with potential for worldwide application. The design is based on a concept of modularization that can meet the various power demands by combining a number of 350 MW(t) reactor modules in parallel with a selected number of turbine plants in a variety of arrangements. Basic High-Temperature Gas-Cooled Reactor (HTGR) features of ceramic-coated fuel, helium coolant, and graphite are sized and configured to provide a low power density core with passive safety features. The safe behavior of the reactor plant is not dependent upon operator action and it is insensitive to operator error.

The MHTGR design is based upon generic gas-cooled reactor experience, as well as specific HTGR programs and projects. These include the carbon dioxide-cooled Magnox and Advanced Gas-Cooled Reactor (AGR), developed in the United Kingdom; the 15 MW(e) Arbeitsgemeinschaft Versuchs Reaktor (AVR) development plant, and the 300 MW(e) Thorium Hochtemperatur Reaktor (THTR) demonstration plant developed in Germany; the 40 MW(e) Peach Bottom (PB) I constructed and operated in the U.S.A.; and the 330 MW(e) Fort St. Vrain (FSV) plant in the U.S.A. The FSV facility has provided confirmation and demonstration of specific and generic HTGR core design and operating characteristics.

The active core in each MHTGR module is an annulus of graphite fuel elements about 3.5 m in outer diameter, 0.93 m annulus thickness and 7.9 m high. A plan view of the core is shown in Fig. 1. The fuel consists of coated particles of 20%-enriched fissile uranium oxycarbide (UCO) and fertile thorium oxide (ThO₂). The particles are bonded together in fuel rods which are contained in the hexagonal-shaped graphite blocks. Helium coolant flows through the graphite blocks in a downward direction. Unfueled graphite blocks surround the active core to form replaceable inner and outer radial, and upper and lower axial reflectors. The outer replaceable radial reflector blocks are surrounded by permanent graphite reflectors. Reactor control is accomplished by a strong negative temperature coefficient plus moveable boron-carbide control rods located in the inner and outer reflectors as shown in Fig. 1. A second shutdown system of different design principle from the moveable control rods is also included. It consists of 12 hoppers of boronated graphite pellets which can be dropped by gravity into holes in the core columns adjacent to the inner reflector. Basic core design parameters are summarized in Table 1.

2. REACTOR PHYSICS DESIGN UNCERTAINTIES

Design requirements for the MHTGR have been developed systematically, to the degree of detail needed, from the overall objectives including safe, economical power production. In making design selections to meet the requirements, assumptions are made regarding the accuracy of the physical models and numerical methods used to calculate

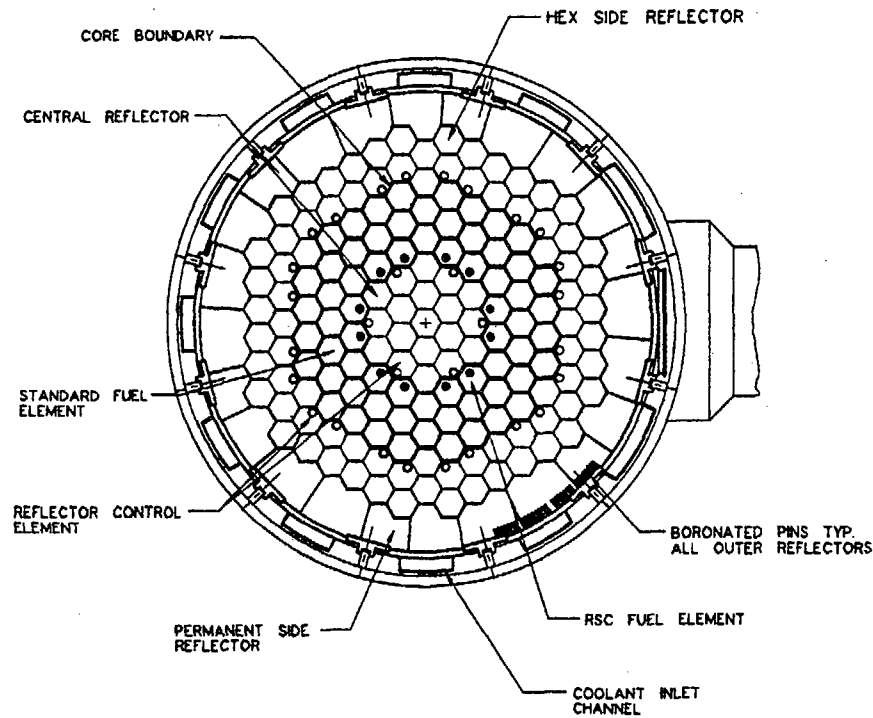


Fig. 1. Reactor plan view

the basic parameters. For design and licensing purposes it is necessary to validate the accuracy of the models and methods, i.e., to show that the parameters of interest can indeed be calculated to the accuracy assumed in making the design selections, and subsequent safety analysis.

For the MHTGR reactor physics design, the basic parameters related to safety are core temperature coefficient, control rod reactivity worth and core shutdown margin, core power distributions, core reactivity

behavior over life, water ingress effects, and decay heat levels. During the MHTGR conceptual physics design, a review was conducted of the available experimental data, and an estimate of the accuracy of the methods for calculating these parameters was made.

TABLE 1
BASIC MHTGR CORE DESIGN PARAMETERS

Inner diameter - active core, m/ft	1.66/5.43
Outer diameter - active core, m/ft	3.50/11.48
Height - active core, m/ft	7.93/26.02
Outer replaceable radial reflector thickness, m/ft	0.65/2.13
Power density, w/cc	5.91
Control rod location	Top mounted
Number of columns in active core	66
Number of fuel elements in active core	660
Number of control rods	24 in outer reflector 6 in inner reflector
Reserve shutdown system	12 in inner core row
Refueling method ⁽¹⁾	2-segment, graded cycle ⁽²⁾
He temp. @ core outlet, rated power, °C/°F	687/1268
He temp. @ core inlet, rated power, °C/°F	258/497
Core inlet pressure, MPa/psia	6.37/924.5
Core outlet pressure MPa/psia	6.34/916.5
Pressure drop across core, kPa/psid	29/4.2
Core circulation direction	Downflow
Coolant volume fraction	0.19
Fuel loading ⁽³⁾ , initial core:	
kg U/kg Th	1358/2350
Fuel loading ⁽³⁾ , equilibrium reloads:	
kg U/kg Th	1006/705

(1) Shutdown for approximately 14.6 days at end of cycle; equilibrium cycle: 19.8 months.

(2) Half of core replaced after each reload interval.

(3) LEU/Th; uranium (19.9% enriched in U-235) plus thorium.

These uncertainty estimates are summarized in Table 2, and are based on a careful review of available data, both experimental, and from operating reactors. While all of the parameters in Table 2 are important, the discussions in this paper are limited to the variables of temperature coefficient, control rod worth, and water ingress reactivity effects, as described below.

2.1. TEMPERATURE COEFFICIENT

The isothermal temperature coefficient of reactivity for the MHTGR core is shown at beginning of the initial core (BOC-IC) and at the end of a typical burnup cycle (EOC-equ) in Fig. 2 (Ref. 2). The temperature coefficient is the only contributor of any significance to the overall core power coefficient. It consists of a prompt Doppler effect due to the U-238 and Th-232 resonances, and a moderator effect due to thermal spectrum changes as the graphite moderator temperature changes. A notable feature is the large negative feedback effect due to absorptions in the Pu-240 resonance at about 1.1 eV. This effect shows up strongly, after the start of critical core operation, above normal operating temperatures as the thermal flux moves into this energy region.

TABLE 2
ACCURACY ASSUMPTIONS FOR MHTGR CORE PHYSICS CALCULATIONS

The core physics experimental data base is adequate to ensure that:

- The temperature coefficient can be calculated with an uncertainty of $\leq 20\%$.
- The control rod bank reactivity worth can be calculated with an uncertainty of $\leq 10\%$.
- Local power distributions can be calculated with an uncertainty of $\leq 13\%$.
- The core reactivity can be calculated at nominal full power conditions with an uncertainty of $\leq 1.5\% \Delta\rho$.
- The water ingress effects can be calculated with an uncertainty of $\leq 10\%$.
- The decay heat production can be calculated with an uncertainty of $\leq 10\%$.

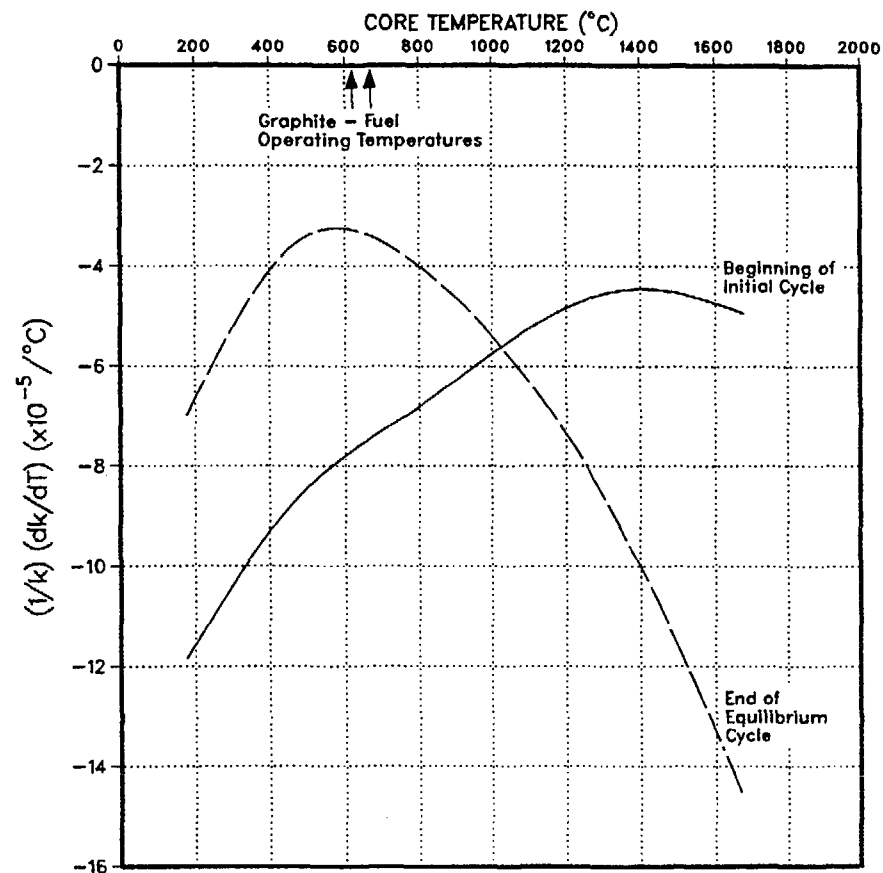


Fig. 2. MHTGR core isothermal temperature coefficient

The uncertainty in the calculation of the temperature coefficients for the MHTGR conceptual design is judged to be 20%. This estimate is based on data from previous validation work as discussed below.

- The PB HTGR measured temperature defect, from which the temperature coefficient is calculated (reactivity change over a specified temperature range), agreed with the calculated value to within 4% (Ref. 3). PB was a small, graphite-moderated, high leakage core.

- The FSV HTGR temperature defect measurements, which include xenon effects, agreed with calculations to within 10% (Ref. 4).
- Doppler coefficient measurements on Th-232, which were made in the HTGR critical assembly, agreed with the calculations to within 6% (Ref. 5).
- Temperature coefficient measurements made in the high-temperature lattice test reactor (HTLTR) with a graphite assembly containing plutonium fuel, agreed with GA calculations to within 6%, and to within 9% for the U-235 fueled case (Ref. 6). Note that this is not just a doppler coefficient measurement, but a complete temperature coefficient measurement.

In summary, the data base used to evaluate the accuracy of the calculation methods included operating HTGR reactors, critical experiments with High Enriched Uranium (HEU) fuel, measurements and comparison calculations on LEU and plutonium fueled systems and benchmark calculations. A summary comparison between these measurements and calculations is provided in Fig. 3. A perfect agreement line is shown and compared to a best straight line fit through the data points. A 20% uncertainty band based on the perfect agreement line is also shown. Overall, the deviation between experiment and calculation is less than 20%. These results indicate that an assumed accuracy of 20% in the calculational model for MHTGR temperature coefficients is conservative.

2.1.1. Control Bank Worth and Shutdown Margins

Reactivity control in the MHTGR during normal operation is accomplished by 30 moveable boron carbide control rods located in the inner and outer reflectors immediately adjacent to the core.

For the core nuclear conceptual design, an uncertainty of 10% in the calculated control worths was assumed for the purpose of evaluating both cold or hot shutdown margins. These uncertainties were based on previous validation studies in which measured and calculated control rod reactivity worth were compared, i.e.:

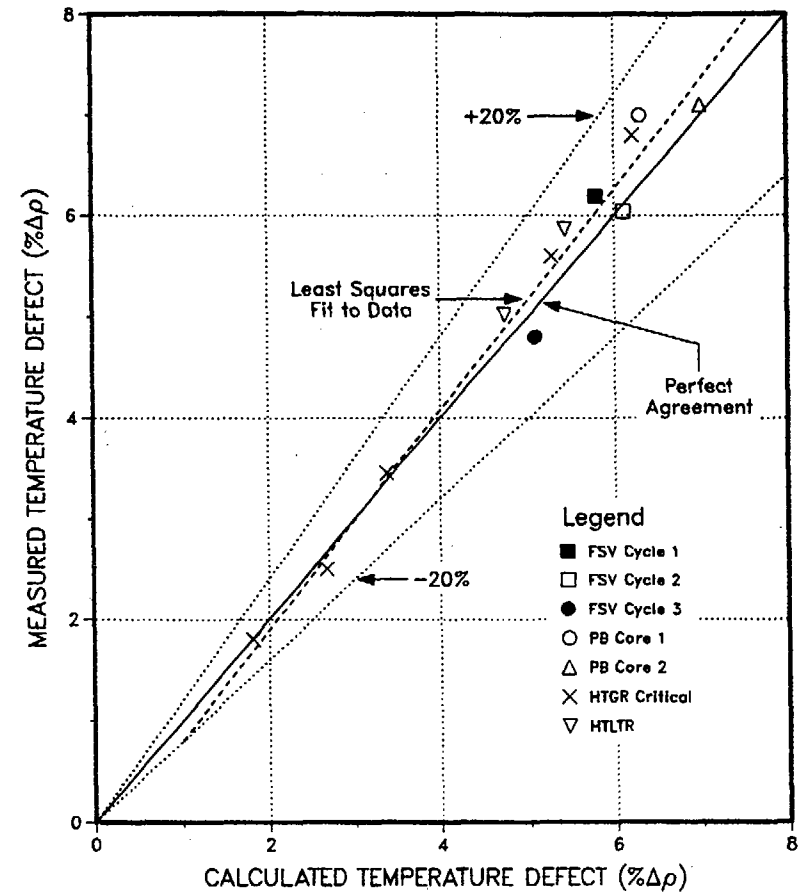


Fig. 3. Comparison between HTGR temperature coefficient calculations and experiments

- The reactivity worth of the PB control rods was measured during the initial startup and rise-to-power. These control rod reactivity worths and total shutdown bank worths were predicted to within 10% with similar models and neutron cross sections as currently in use at GA (Ref. 3).

- Measurements of the reactivity worth of both single rods and control rod pairs were made in the HTGR critical assembly (Ref. 5). Comparisons of these measurements to calculations indicated that single rod worths were overestimated by ~4% and the control rod pair worths were overestimated by ~11%.
- Control rod pair reactivity worths were measured during the initial rise-to-power for each FSV operating cycle (Ref. 4). Comparisons of the measured and calculated reactivity worth of control rod groups over these three cycles of operation show that the difference is typically $\leq 5\%$ for the cumulative worth; with the lower worth rod groups having a higher measurement uncertainty.
- Numerous measurements of the control rod reactivity worth have been made in the Dragon reactor (Refs. 7 and 8) which utilized control rods located in the radial reflector as in the MHTGR design. The calculated control bank worth, using GA developed models, agreed with the measured value to within 11%. Significantly, the calculation underestimated the measured bank worth.

These comparisons of measured and calculated control rod reactivity worth support the 10% uncertainty band assumed for the MHTGR conceptual design. This accuracy estimate based on experimental data is also supported by an evaluation of the individual contributors to the MHTGR control rod reactivity model. The modeling must consider correction factors related to gaps between poison control rod compacts, clad material composition, finite height effects, axial streaming effects, etc. Uncertainties must also be considered from the cross section models, loading tolerances, local temperature effects, and power shape. A comparison between measured and calculated data similar to that for the temperature coefficient is shown in Fig. 4.

Water Ingress Effects

An addition of water to the MHTGR core initially produces a positive reactivity feedback effect. This positive feedback effect is caused by the moderating property of hydrogen which reduces resonance absorption in U-238 and Th-232, and results in a more thermalized neu-

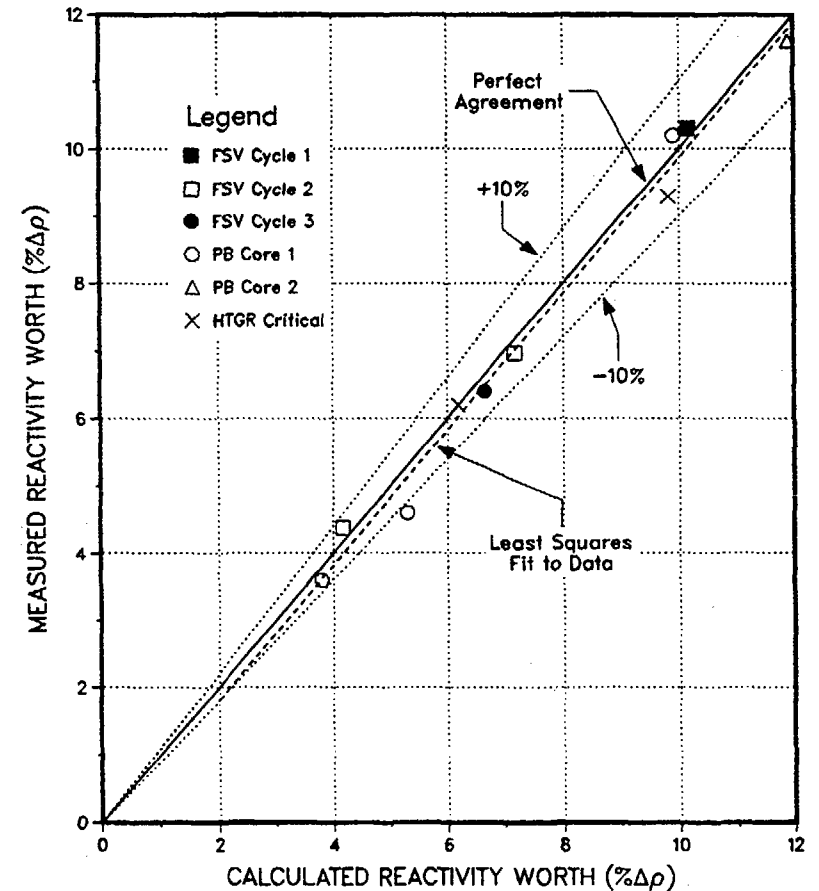


Fig. 4. Comparison of calculated and measured control rod bank reactivity worths for HTGRs

tron flux spectrum. Core neutron leakage is also reduced, which adds to the positive reactivity feedback. Eventually, as the amount of moisture is increased, thermal neutron absorption in hydrogen becomes dominant, causing a negative reactivity feedback. Thus the reactivity change due to moisture goes through a maximum, and has the general shape illustrated in Fig. 5, for near-critical core configurations. In this case, the calculated reactivity changes for large moisture ingress under cold conditions are shown for two time points in operation; i.e., beginning-of-cycle-initial-core (BOC-IC), and end-of-cycle equilibrium-core (EOC-equil), which bound the operating range.

The reactivity feedback effects due to a given amount of core moisture are larger in the hot operating core than under cold conditions because the hot core has a harder neutron flux spectrum. This harder spectrum results in a maximum reactivity worth due to moisture that is approximately 25% higher than for the cold conditions.

Specific analyses of the uncertainties related to moisture ingress reactivity worths have not been performed to date as part of the MHTGR conceptual design. Based on limited data from water-moderated critical experiments, the predicted reactivity worth of uniformly distributed moisture is expected to be within 10%, an accuracy which is experimentally supported by small pebble-bed reactor subcritical assembly measurements (Ref. 9).

3. VALIDATION OF CORE PHYSICS METHODS

GA core physics methods have, in general, been validated for HEU/Th-fueled HTGRs. Most of the experimental data were derived from HTGR-type critical experiments performed at GA and from the operation of the PB and FSV reactors. The MHTGR with LEU/Th fuel, an annular core, and reflector control rods, requires a reassessment of the validation of these methods. This assessment will include one or more of the following:

- Reanalysis of selected previous validation studies.

- Documentation of selected previous validation studies.
- Comparison of new experimental data to GA calculations.
- Comparison of other (non-GA) calculations with GA calculations.

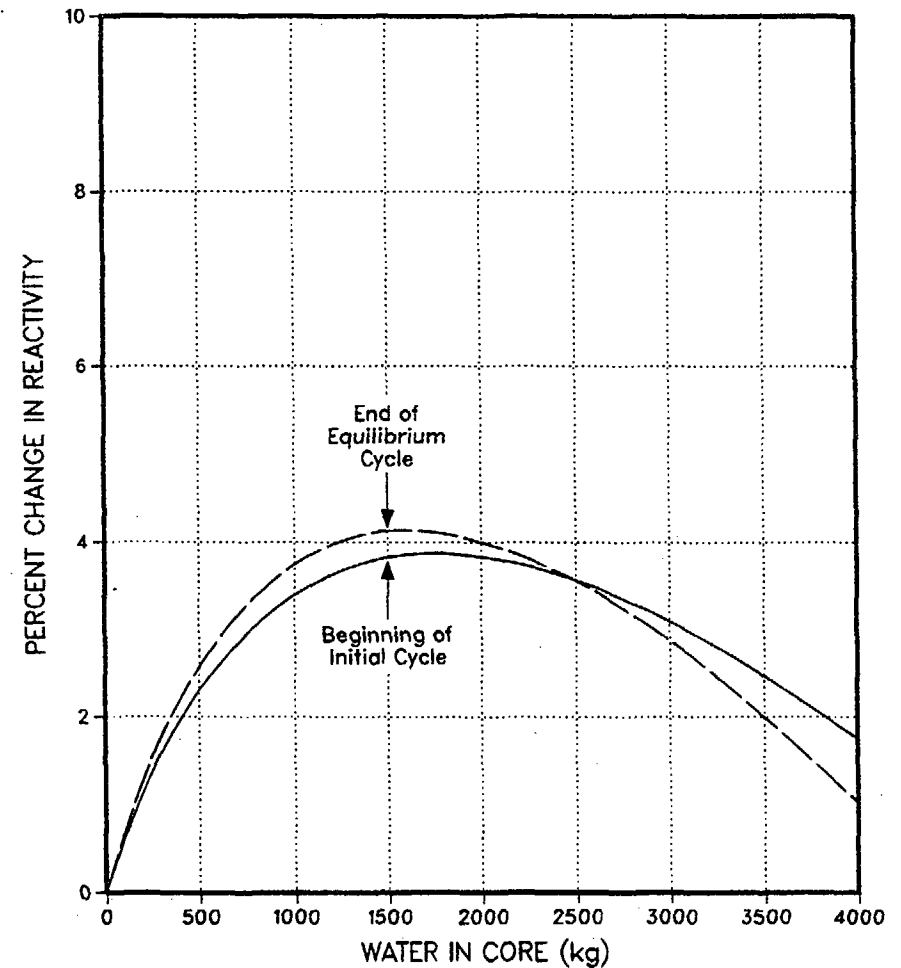


Fig. 5. MHTGR-reactivity effects of water ingress (cold, unrodded, no xenon)

A major emphasis of this program will involve reanalysis and/or documentation of selected previous validation studies. Many of these studies were done years ago with other than the current neutron cross sections and/or methods. Selected recalculations using the current reference cross sections and methods will be sufficient to justify the use of these previous studies in the validation program. It is also planned to obtain new supplemental LEU fuel experimental data.

Because of the limited amount of experimental data that is applicable to the LEU fueled MHTGR, carefully designed benchmark calculations

will also be used as part of the validation for the physics design methods. In particular, benchmark calculations will be used in validating methods for temperature coefficient, and water ingress reactivity worth calculations, where suitable experimental data is very limited. In this regard, data from the proposed PROTEUS (Ref. 10) critical experiments will provide extremely useful confirmation of methods for calculating water ingress effects in the MHTGR.

The principal sources of experimental data (FSV, PB, etc.) which may be used to validate the MHTGR physics methods are given in Table 3,

TABLE 3
MHTGR CORE PHYSICS EXPERIMENTAL DATA

Physics Parameter	Experimental Data											
	PB Critical	PB Operation	HTGR Critical	FSV Operation	HTLTR Experiments	AVR Operation	VHTRC Critical	CNPS Critical	Dragon Reactor	HITREX-2 Critical	KATHER Critical	PROTEUS Critical
Temperature coefficient	*(a)	*	*	*	*	*	*	*	*	--(b)	--	--
Control rod reactivity worth	*	*	*	*	--	*	*	*	*	--	*	*
Core neutron flux (power) distributions	*	*	--	*	--	--	*	*	*	*	*	*
Core criticality and material worth	*	*	*	*	--	*	*	*	--	*	*	*
Water ingress reactivity worth	*	--	--	--	--	--	--	*	--	--	(c)	*
Decay heat	--	*	--	*	--	*	--	--	*	--	--	--

(a) Experimental data source description (i.e., the experimental facility) is given in Appendix B.

(b)* = data available or expected to be available for validation program.

(c)-- = no data available from this component to validate the corresponding parameter.

(d)KFA subcritical.

along with a listing of the key physics parameters (temperature coefficient, control rod worth, etc.) which are measured. A significant amount of measured data are available from many of these data sources. However, not all of these data are required, applicable, and/or adequately documented for use in the MHTGR core physics methods validation program. As the validation program proceeds, a determination will be made as to which of these measured data and how many of the data sets are appropriate for use in the validation of the methods for calculation of each core physics parameter. At that time, a determination will also be made as to the need for additional measurements.

ACKNOWLEDGEMENT

Some of the work reported in this paper was supported by the Department of Energy, San Francisco Operations Office Contract DE-AC03-89SF17885.

REFERENCES

1. "Conceptual Design Report, Modular HTGR Plant," Report No. HTGR-86-118, October 1986.
2. "MHTGR Core Nuclear Design," DOE-HTGR-87063, Rev. 2, August 1989.
3. Merrill, M. H., "Nuclear Design Methods and Experimental Data in Use at Gulf General Atomic," Gulf General Atomic Report Gulf-GA-A12652 (GA-LTR-2), July 1973.
4. Brown, J. R., et al., "Physics Testing at Fort St. Vrain - A Review," Nuclear Science and Engineering, 97, pp. 104-122 (1987).
5. Bardes, R. G., et al., "Results of the HTGR Critical Experiments Designed to Make Integral Checks on the Cross Sections in Use at Gulf General Atomic," GA-8468, February 12, 1968.
6. Schultz, K. R., and D. R. Mathews, "General Atomic participation in the High-Temperature Lattice Test Reactor Program," GA-A12710, March 1976.
7. Della Loggia, V. E., et al., "Measurements of control rod Worth and Excess Reactivity on the First Core of DRAGON," DP-Report-359, Dragon Project, Atomic Energy Establishment, Winfrith, England, July 1965.
8. Della Loggia, V. E., C. Hung, and W. H. Taylor, "Zero Energy Experiments on the DRAGON Reactor Prior to Charge IV Startup," DP-Report-820, Dragon Project, Atomic Energy Establishment, Winfrith, England, January 1973.
9. Druke, F., Filges, D., Kirch, N., and Neef, R. D., "Experimental and Theoretical Studies of Criticality Safety by Ingress of Water in Systems with Pebble-Bed High-Temperature Gas-Cooled Reactor Fuel," NS&E:57,328-332 (1975).
10. Mathews, D., "LEU HTG Experiments in the PROTEUS Critical Facility", PSI Technical Memorandum TM-41-88-11, 2 Aug. 1988.

UNCERTAINTIES IN THE ANALYSIS OF WATER INGRESS ACCIDENT FOR THE HTGR CORES

V.S. GORBUNOV, V.F. GOLOVKO, E.S. GLUSHKOV
I.V. Kurchatov Institute of Atomic Energy,
Moscow

A.I. KIRYUSHIN, N.G. KUZAVKOV, Yu.P. SUKHAREV
Experimental Machine Building Design Bureau,
Gorki

Union of Soviet Socialist Republics

Abstract

Behaviour of the reactor major physical characteristics during the accident related to the water/steam ingress into the core, resulted from the steam generator (SG) loss of integrity has been analysed on the example of the VGM reactor with the pebble bed core designed in the USSR. The header tube instantaneous double-ended rupture without interaction of the outgoing flows has been considered due to the uncertainties of its failure process. Calculation of water quantity discharged into the core has been made under the following assumptions:

- 1). Accumulation of water in liquid state in the core is eliminated inasmuch as the fuel elements and helium temperature exceed water boiling temperature at a pressure of about 5 MPa;
- 2). Chemical interaction of water with graphite is not taken into account;
- 3). Moisture sensors fail to be actuated.

The calculation results of the water mass variations in the core vs. time, as well as reactivity changes caused by water ingress into the core are given in the paper.

The need to take into account reactivity changes caused by the front edge of the steam/helium mixture, that defines the neutron power increase rate has been shown in the paper.

Changes of the reactivity compensation members' efficiency at a steam/water ingress into the core and reflector both in hot and cooled down reactor have been evaluated.

The paper carries requirements for experimental investigations intended to prove the adequacy of the reactivity compensation members' efficiency in the accident under consideration.

Introduction

The spectral characteristics of HTGR cores with low-enriched uranium (LEU) fuel and graphite moderator provide the prevailing action of neutron slowing down effects at the steam-helium mixture ingress during the steam generator depressurization resulted in a potential reactivity increase.

The availability of rather thick graphite reflectors, where the neutron spectrum is more soft than in the core provides restriction of reactivity increase.

In this connection the calculation of reactor reactivity at water ingress should be made by the aid of computer codes which adequately treat both the variation of the neutron energy during their slowing down, and the thermalization processes. It is also evident, that estimation of the reactivity variation calculation error in this accident is possible using only the results of correctly conducted physical experiment.

To obtain the representative results of the physical experiments, the detailed information not only about a potential amount of water ingress and about the dynamics of its penetration that determines the reactor power dynamics, is required.

The paper aims to study uncertainties in water ingress inventory, in reactivity increase value, which made of the accident desinging conditions, and also in results of VGM reactor dynamic calculation.

1. Modelling of water ingress accident

In the accident analysis it is assumed, that the instantaneous rupture of the steam generator header is occurred.

The calculation of water ingress into the core is made under the following assumptions:

1. accumulation of water in liquid state in the core is avoided, inasmuch as the core and helium temperature is higher than the water boiling temperature;
2. chemical interaction of water with graphite is not taken into account;

During the steam generator depressurization, the increase of water inventory in the core is recurred in cycles. The core and reflector filling with moisture, transported by the circulating helium front edge, is proportional to the time of steam-helium mixture penetration through the core and water and steam flowrate flowing out of the steam generator.

The steam mass increase at the second and successive edges is occurred within the time required for the steam-helium mixture to pass through the primary circuit, taking into account variation of water and steam flowrates leaving the steam generator, as well as the steam-helium mixture variations in the path due to the circulator isolation.

Following the coolant direction, the steam-water mixture first enters the side reflector and then passes to the top reflector and reactor core. Depending on the accident modelling scenario different water inventory enters the reactor. If it is assumed, that the moisture sensors are actuated, then the circulator would be isolated and water mass in the core would change according to dependence 1 shown in fig.1 (design basis accident scenario). The maximum moisture inventory in the core in this case would be ~80 kg. Such moisture inventory would be accumulated at the circulator coastdown and failure to close of return valve. At the scheduled circulator isolation and the return valve actuation ~10 kg of water enters the core.

In this case the moisture sensors are not actuated and the circulator is not isolated, the water mass would be accumulated according to dependence 2 shown in fig.1 (beyond design basis scenario). The maximum credible water inventory in the core in this case would be, if all free volume is filled with steam. The steam mass in this case would depend on the steam density, that in its turn, would depend on the average temperature of the pebble bed. At the average temperature of fuel elements about 600°C the maximum water inventory in the core would be about 400 kg. During the circulator operation at nominal speed water inventory initially entered the core within ~1 s would be ~9 kg.

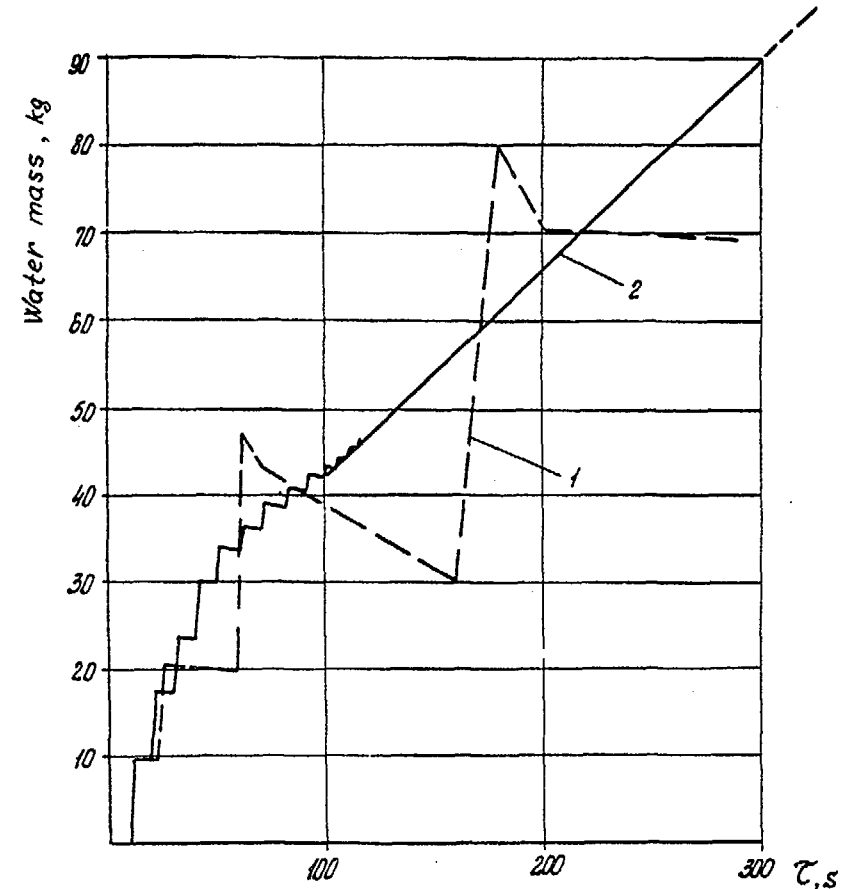


Fig.1 Water inventory changes in the core

- 1. circulator coast-down
- 2. running circulator

2. Reactivity changes at water ingress into the core

To estimate reactivity changes during water passing through the core the WIMS-D4 program has been used, by the aid of which one-dimensional reactor analysis was performed, taking into account changes of the reflector features and those of the core along its height, regardless of the actual fuel and moderator arrangement.

The reactivity changes vs time have been normalized to the absolute reactivity value, obtained from the calculations of reactor filled with a specified water inventory. The reactor calculations were made by the aid of two-dimension computer complexes NEKTAR-VIANKA /2,3/ and GAVROSH /4/ taking into account heterogeneous fuel and moderator arrangement in the fuel elements, that have been experimentally tested on the physical facility GROG /5/ on models of the pebble bed core.

Fig.2 shows reactivity changes vs time at the front edge of the steam-helium mixture and during subsequent water penetration into the reactor core.

Initially the reactivity is proportional to water inventory entered the core. The maximum reactivity increase in the hot reactor at the ingress of ~ 80 kg of water is about $0.4\% \Delta k/k$. Calculations by the V.S.O.P. program indicate, that reactivity increase for such water inventory is $\sim 0.6\% \Delta k/k$. In case of 400 kg steam ingress into the core, the reactivity increase is $\sim 2\% \Delta k/k$ and $\sim 2.4\% \Delta k/k$ according to the operational data /6/.

So, uncertainties of reactivity changes calculations obtained by the aid of different programs are in the range of 20-30 %.

The calculation analysis revealed, that at water ingress into the side reflector reactivity is changed insignificantly. The reactivity compensation rods efficiency in the side reflector is also changed negligibly.

At water ingress into the core, due to reduction of neutrons leakage in direction of the side reflector, efficiency of the reactivity compensation rods is decreased (at a ~ 400 kg water ingress it is decreased by $> 10\%$).

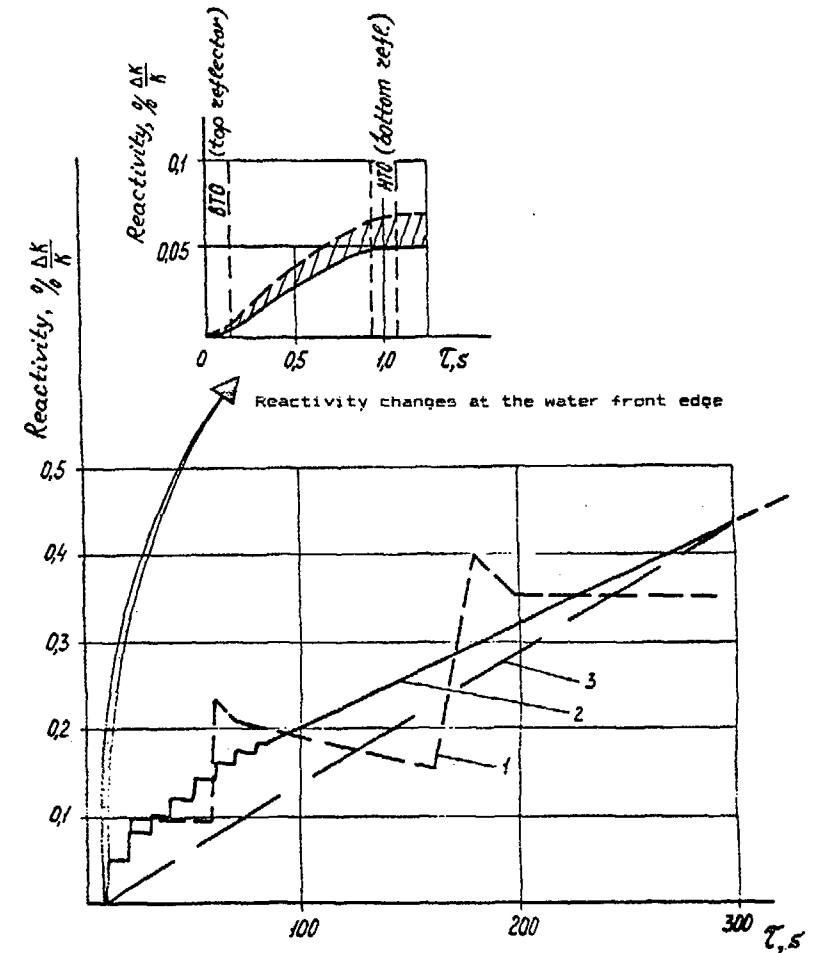


Fig.2 Reactivity changes during the accident with water ingress

1. isolated circulator
2. running circulator
3. steady reactivity increase

3. Power and temperature changes during the accident with water ingress into the core

To analyse the power and temperature dynamics a simplified reactor model has been used, in which the core was divided into 10 sections and presented as 3-zone cylindrical channel with fuel in the central part, surrounded by moderator and gas.

The power balance equations of the model are the following:

$$\begin{cases} (mc)_f \frac{dT_{1j}}{dt} = N_j k(\tau) - k F_{jm} (T_{1j} - T_{2j}) \\ (mc)_m \frac{dT_{2j}}{dt} = k F_{jm} (T_{1j} - T_{2j}) - k F_{mj} (T_{2j} - T_{3j}) & ; j = 1, \dots, 10 \\ \frac{dT_{3j}}{dt} = -\frac{W}{\Delta Z} (T_{3j-1} - T_{3j}) + \frac{k \Pi m_g}{(c_p V C)_f} (T_{2j} - T_{3j}) & k = 1, 2 \end{cases}$$

where, W - coolant flow velocity, K - heat transfer coefficient, Π - perimeter, f_c - cross-section, γ - specific gravity, F_m, F_g - surface area, ΔZ - section length, C - heat capacity.

6 groups of delayed neutrons are treated in the kinetics equation:

$$\begin{cases} \frac{dN(\tau)}{dt} = \frac{\delta k - \beta_{eff}}{\ell} N(\tau) + \sum_{i=1}^6 \lambda_i C_i \\ \frac{dC_i(\tau)}{dt} = \frac{\beta_i}{\ell} N(\tau) - \lambda_i C_i & ; i = 1, \dots, 6 \end{cases}$$

Total reactivity comprises temperature effects of fuel (ρ_f) and moderator reactivity (ρ_m) with the worths, corresponding to reactor with the average temperature:

$$\rho = - \sum_{k=1}^6 \beta_k \sum_{j=1}^{10} \alpha_j (\rho_{fjk} + \rho_{mj k}) ; \sum_{j=1}^{10} \alpha_j = 1 ; \sum_{k=1}^6 \beta_k = 1 ; \delta k = \rho_{water} + \rho$$

It was assumed, that the relative space power distribution $N_{jk}(\tau)$ during the accident, did not change.

Fig. 3 shows reactor power distribution at water ingress into the core and changes of the fuel and coolant maximum temperatures.

As is evident from fig.3, reactor power is changed substantially depending on the dynamics of water accumulation in the core. At the circulator isolation (curve 1) the reactor becomes subcritical due to the temperature feedbacks, and in case of the circulator operation at nominal speed during 300 s the reactor goes

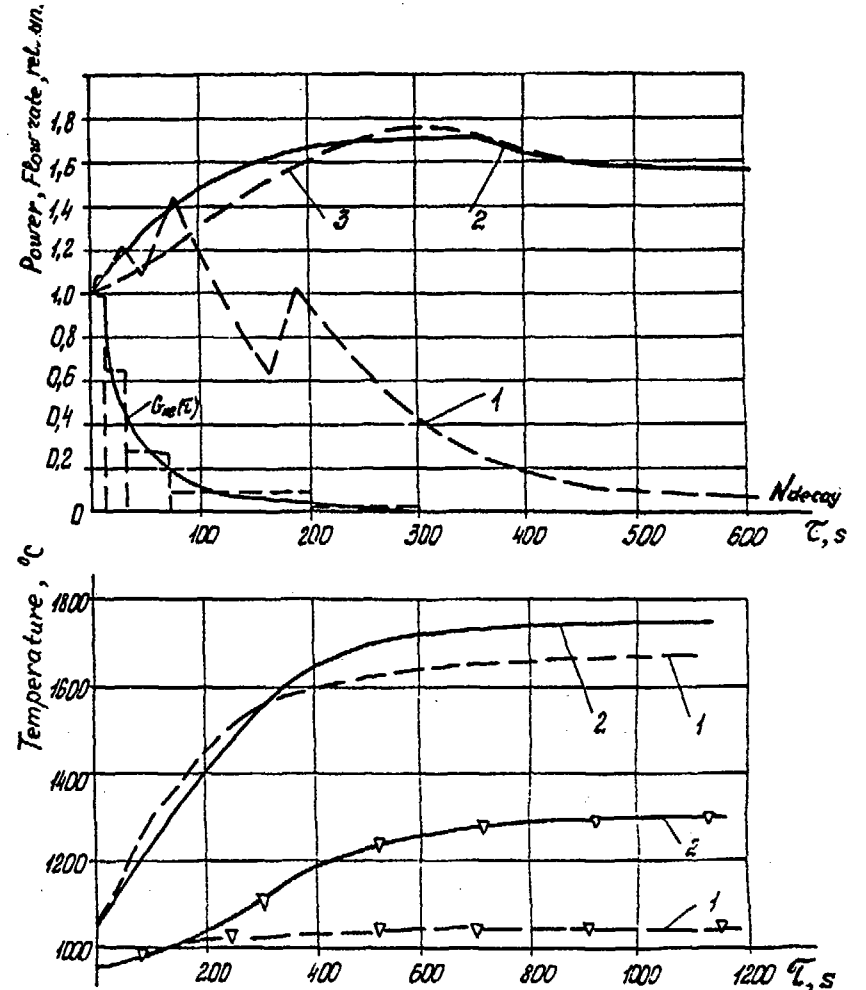


Fig.3 Power and maximum temperature changes during the accident with water ingress

- 1. circulator coast-down
- 2. running circulator
- 3. steady reactivity increase
- maximum fuel temperature
- ▴ outlet average helium temperature

over to a new power level (curve 2). It is also clear to what extent it is necessary to take into account reactivity changes at the front edge of the steam-helium mixture entering the reactor.

Supposing that the reactivity is increased steadily in accordance with the water inventory in the core (fig.2 curve 3), then the reactor power would reach the setting of the emergency protection actuation ($1,2 N_{nom}$) within ~ 80 s, instead of $\sim 30-40$ s, obtained from the dynamics analysis taking into account the actual cyclic reactivity changes. The difference in fuel temperature provided by this time delay is about 100° .

Conclusion

Results of the analysis revealed, that depending on conditions of the accident with the steam generator depressurization, the water inventory in the core could vary between 10 and 80 kg in the design basis scenario and could reach ~ 400 kg in the beyond design basis scenario.

Changes of the positive reactivity increase corresponding to those scenarios is $(0.05 - 0.4)\% \Delta k/k$ and $\sim 2\% \Delta k/k$.

Substantial reactivity changes occurred during the accident and significant discrepancies in results of its analysis made by the aid of different computer codes (20 -30)%, required verification of physical models used in the analysis of the reactor multiplication factor with the different water inventory, including the maximum one, in the core and side reflectors.

The latter circumstance necessitated conduction of experiments on the critical assemblies simulating reactor conditions, aimed to substantiate the sufficiency of the reactivity compensation members arranged in the side reflector.

REFERENCES

1. Askew J.R. - IWNES, Oct. 1966, p.564.
2. Гольцев А.О., Карпов В.А. Нектар - программа расчета физических характеристик графитовых реакторов с учетом термализации нейтронов и выгорания топлива. Препринт ИАЭ-2795, М. 1977.
3. Карпов В.А. Использование конечно-разностных методов в многогрупповом диффузионном приближении для расчетного анализа топливных загрузок больших энергетических реакторов. Препринт ИАЭ-2639, М. 1976.
4. Савандер В.И., Сарычев В.А. Методика расчета выхода реактора ВТГР в стационарный режим работы на заданную схему перегрузки. сб. Математические модели ядерно-энергетических установок. Под ред. В.В. Хромова. М. Энергоатомиздат, 1983.
5. Гольцев А.О., Евсеев В.И., Карпов В.А. и др. Экспериментальное обоснование основных физических характеристик активной зоны реактора ВГ-400. Доклад на 11 международной конференции МАГАТЭ по ВТГР. Димитровград, июнь, 1989.
6. Teuchert E., Haas K.A. Sicherheitsrelevante Effekte der Neutronenphysic, 22-29 April, 1989, Moskau.

**CRITICAL EXPERIMENTS — PLANNING AND RESULTS,
UNCERTAINTY EVALUATIONS**

(Session IV)

Chairman

**R. CHAWLA
Switzerland**

MEASUREMENTS OF TEMPERATURE COEFFICIENT OF REACTIVITY OF THE VHTRC-1 CORE BY THE CRITICALITY METHOD

H. YASUDA, F. AKINO, T. YAMANE, Y. KANEKO

Japan Atomic Energy Research Institute,
Tokai-mura, Naka-gun, Ibaraki-ken,
Japan

Abstract

Reactivity decrease due to temperature rise of the whole assembly was measured in a pin-in-block HTGR-type critical assembly, VHTRC, by a criticality method, with purpose to verify the calculation accuracy of the design of the High Temperature Engineering Test Reactor (HTTR). The VHTRC was loaded with coated particle fuel rods containing low enriched UO_2 , and it was heated up to 200 °C by using electric heaters. The measured reactivity decrease was divided by the temperature increment, resulting a temperature coefficient of reactivity, $-1.72 \times 10^{-4} \Delta k/k/^\circ C$.

The SRAC code system was applied to the calculation of effective multiplication factor at 300 K, 325 K and 500 K where the collision probability method was used in the cell calculation and the three-dimensional, multi-group diffusion model was adopted in the core calculation. The results gave a ratio of the calculated to the measured value of temperature coefficient of reactivity, 0.98. The temperature coefficient of reactivity for a room temperature range was also measured. The result was 30 % smaller than that for a room temperature to 200 °C range. This tendency is consistent with the result of early work by the authors using the pulsed neutron method.

Finally, it is concluded that the calculation of temperature coefficient of reactivity for HTTR by use of SRAC is sufficiently validated by comparing with the experimental data at VHTRC

Key Words:

Accuracy, Coated Particle Fuel, Collision Probability, Critical Assembly, Diffusion, Double Heterogeneity, Experiment, Graphite, Heating, HTGR, Reactivity, Neutron, Temperature Coefficient of Reactivity, VHTRC.

1. Introduction

The neutronics design is one of the most important tasks in the research and development for a High Temperature Gas cooled Reactor (HTGR). The temperature dependence of reactivity, in particular, should be exactly evaluated because it has a large influence on the estimation of operational reactivity balance. A Japanese HTGR, High Temperature Engineering Test

Reactor (HTTR)⁽¹⁾ which is now under licensing, is planned to use the coated particle fuel rods containing low enriched UO_2 inserted in hexagonal

graphite blocks. This type of fuel has, in its structure, the double heterogeneity, i.e., particles in graphite matrix (first heterogeneity) and fuel compacts in graphite sleeve tube (second heterogeneity), so that special considerations must be given in the estimation of resonance neutron absorption. The present authors⁽²⁾ measured the Doppler effect of a coated particle fuel rod in an HTGR simulating core at the critical assembly, SHE (Semi-Homogeneous Experiment), using a sample heating device. It has been verified by this work that the calculation accuracy for the Doppler effect at 700 °C was within 9 % by comparing with the experimental value. Therefore, it has been expected, as the next step, to investigate the calculation accuracy of the temperature dependence of the whole assembly. The

Very High Temperature Reactor Critical Assembly (VHTRC)⁽³⁾ was constructed by modifying the SHE for the purpose of HTTR neutronics design verifications. Careful attentions were paid to the requirements for such temperature dependence measurements. Recently, the authors have reported⁽⁴⁾ upon an experimental study on the temperature coefficient of reactivity of VHTRC where the reactivity decrease from critical state induced by temperature rise was measured by the pulsed neutron method. In the present paper, an alternative method is applied to the measurement of the temperature coefficient of reactivity of the same assembly.

2. Experiments

2.1 Description of VHTRC

The VHTRC is an HTGR-type critical assembly which is fueled with low enriched UO_2 and moderated with graphite. It reached initial critical state in May, 1985. The three main features are, 1) graphite block structure of the core as well as the reflector, 2) coated particle fuel of 2, 4 and or 6 wt % ^{235}U enrichment, 3) The whole assembly can be heated up to 200 °C by using electric heaters. The outlook of the assembly is shown in Fig. 1. The across flat and the axial lengths including reflectors are 2.4 m. The assembly consists of 24 fuel columns and 7 experimental control rod columns. One fuel block can be charged maximally with 18 fuel rods. The outer and inner diameters of a fuel element (compact) are 36 and 18 mm, respectively. Details of the assembly design and the results of basic experiments are described in Refs. (3) and (5).

2.2 Core heating

Forty cartridge heaters were fed with 30 kW_e in total and the temperature of the assembly was measured at 14 points on radial cross section using K-type thermo-couples. The signals of two representative thermo-couples were used for the temperature control, that is, the electric power for the upper eighteen and the lower twenty-two heaters in the assembly were controlled independently. Typical performance of assembly heating is shown in Fig. 2 and Table 1. The standard deviation of radial temperature distribution observed by the fourteen thermo-couples converged to a very small value, about 1 °C around 200 °C. The temperature distribution in the axial direction was also measured using other thermo-couples. The distribution was also very flat.

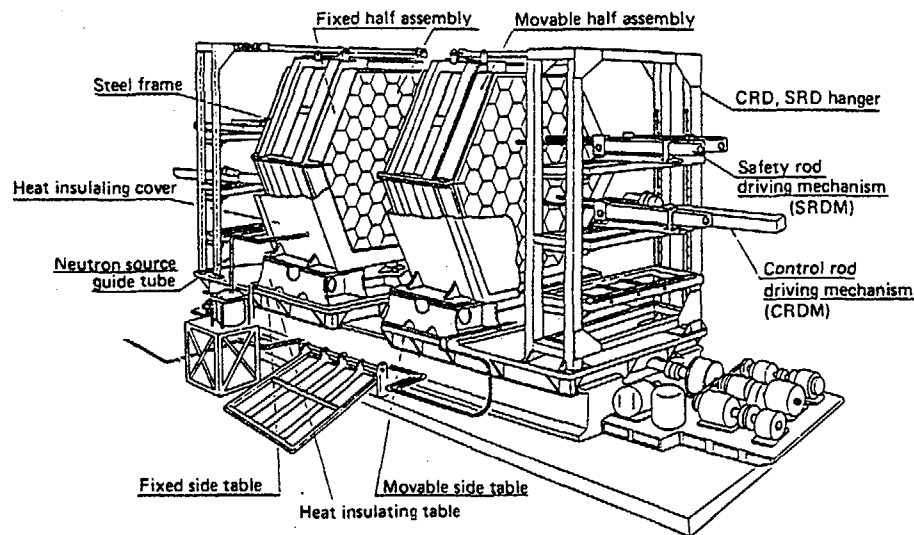


Fig. 1 Outlook of VHIRC

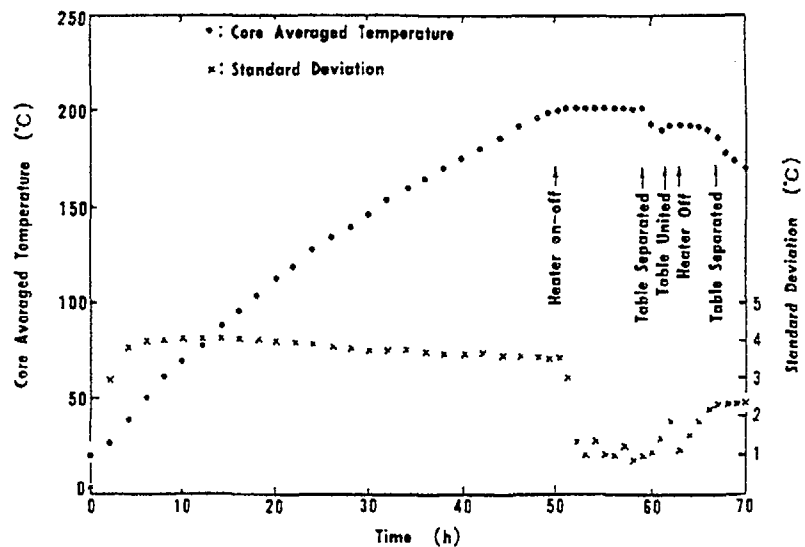


Fig. 2 Typical performance of core heating

Table 1 Typical temperature distribution in the assembly measured at 200 °C

Sensor number	Temp. (°C)	Sensor number	Temp. (°C)
1	200.4	8	199.1
2	200.8	9	199.5
3	199.8	10	200.5
4	198.5	11	200.6
5	199.3	12	202.0
6	199.3	13	200.4
7	200.2	14	202.4

2.3 Measurement of critical points at several temperatures

At the first step of experiments, the core was loaded with 288 fuel rods of 4 wt % ²³⁵U enrichment (B4-type) in the configuration (VHIRC-1) shown on the left side of Fig. 3. The critical point was measured at room temperature (8.0 °C). In the second and third steps, electric power was supplied to heaters until the experimental temperatures of 22 °C and 32 °C reach uniform distributions. Keeping the saturated uniform temperature distributions the critical points were again measured. The reactivity decrease due to the assembly temperature rise was determined from the difference of excess reactivity between the room temperature and the experimental temperature. The control rod reactivity worth was previously calibrated at room temperature by the period method to get the excess reactivity.

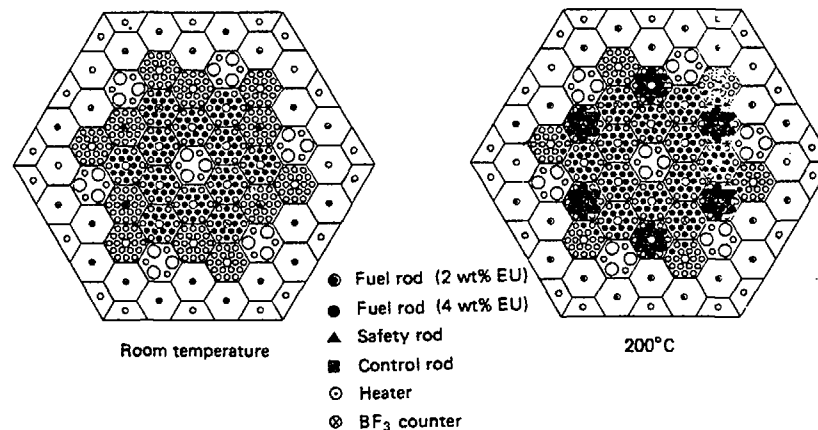


Fig. 3 Critical fuel loading configurations at room temperature and 200 °C

After the experiments at low temperatures, the assembly was heated to 200 °C. At this temperature, the core was considerably subcritical, and therefore, fuel rods were added step by step to the core for criticality approach. The loading configuration at the final criticality step is shown on the right side of Fig. 3. The number of supplementary fuel rods was 153 of which 144 rods were 2 wt % ²³⁵U enrichment (B2-type) and 21 rods were B4-type. B2-type fuel rods were used only because of the limited inventory of B4-type fuel rods in the facility.

After reaching a uniform temperature distribution, control rods were adjusted to measure the critical point again.

2.4 Measurement of fuel rod reactivity worth at 200 °C

Twelve B4-type fuel rods were discharged from the critical core at 200 °C. The reactivity worth of the fuel rods was measured using the pulsed neutron technique. In this measurement, four small BF₃ counters were placed in the core where the axial higher harmonics modes of neutron flux would be effectively cancelled. The time responses of the counters after neutron pulsing were simultaneously analyzed using a multi-channel time analyzer. The raw data of the decay curves were corrected for the dead time and background. The prompt and delayed mode areas A_p and A_d were determined by fitting the corrected curves to an analytical expression. The reactivity was derived from the averaged ratios of A_p/A_d⁽⁶⁾ for the four detectors. The reactivity worth of twenty-four B2-type fuel rods was also measured by the same method. The results are shown in Table 2.

2.5 Measurements of various correction terms for loading irregularities

(1) When the whole assembly was heated, the assembly supporting structures were also heated, and the thermal expansion decreased the small gap (~2 mm) between the two half assemblies. Therefore, the relation between gap and its reactivity worth was measured at room temperature by the neutron source multiplication method. The result was used for the correction.

(2) The holes prepared for safety and control rod insertion were not considered in the theoretical analyses, therefore, their reactivity worth was measured at room temperature by the calibrated control rod compensation method and at 200 °C by the pulsed neutron method.

(3) Control rod reactivity worth was calibrated at room temperature. This calibration data was used to determine the excess reactivity at 200 °C. The calibration curve might change by temperature, however, this effect hardly disturbed the result because the control rods were almost fully extracted in the critical state at 200 °C and therefore the excess reactivity at this temperature was very small.

(4) The BF₃ counters, the heaters, the thermo-couples and a neutron source guide tube were not considered in the theoretical analyses. Therefore, their reactivity worths were independently measured at room temperature by the calibrated control rod compensation method, however, yet corrected for the temperature dependence.

(5) The dry-up effect of moisture in the assembly on the reactivity was examined by comparing the critical points at the same room temperature before heating to and after cooling from 200 °C. The resultant dry-up effect was -2.1 cents. Therefore, the data was corrected for this effect.

In Table 3, are shown the values of correction terms for various irregularities in the assembly.

Table 2 Reactivity worth of fuel rods at 200 °C

	(% Δk/k/ °C)	
	Experiment	Calculation
B2 24 rods	0.221	0.155
144 rods	2.140(*)	1.502
B4 12 rods	0.485	0.435
21 rods	0.858(*)	0.771

(*) The value was evaluated from the above value using the calculated value ratio

Table 3 Reactivity correction terms for various irregularities in the core

Term	Reactivity worth(cent)		Difference (cent)
	Room temp.	200 °C	
Assembly gap	-13.8	-12.7	+1.1
Control rod tips	-5.4	-5.4*	+0.0
BF3 counters	-13.3	-13.3*	+0.0
Heaters	-27.5	-27.5*	+0.0
Voids	-46.1	-52.4	-6.3
Dry-up	0.0	-2.1	-2.1
Total	-106.1	-113.4	-7.3

* Experimental results at room temperature are used.

3. Analyses

The VHTRC-1 core was analyzed by using the SRAC⁽⁷⁾ code system to obtain the temperature coefficient of reactivity.

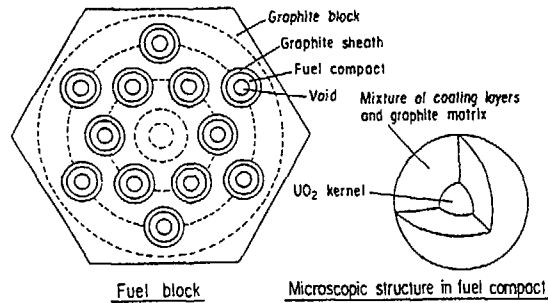
3.1 Cell calculation

Every fuel block was modelled as shown the unit cell in Fig 4. The neutron spectrum was calculated by the collision probability method using the 61 group nuclear data based on the ENDF/B-IV at temperatures, 300 K 325 K and 500 K. The following conditions were adopted in the cell calculation:

- Young-Koppel model⁽⁸⁾ for the thermal neutron scattering of carbon and free gas model for those of the other materials
 - PEACO⁽⁹⁾ code to calculate the resonance region accurately by ultra-fine grouping
 - Precise probabilistic account of the double heterogeneity of fuel
- Using the calculated neutron spectrum, the 24 group constants(11 groups for fast and 13 groups for thermal neutrons) were prepared for the core calculation.

3.2 Core calculation

The core calculation was made using the three dimensional diffusion approximation. The core geometry was modelled accurately by using the triangular-2 mesh. The model, however for simplicity, took no account of the heaters, thermocouples, insertion holes of safety and control rods,



A graphite block is divided into six regions by concentric circles (broken lines) for the calculation of thermal neutron spectrum.

Fig. 4 A unit cell in the cell calculation

neutron source guide tube and gap between the separable two half assemblies. The reactivity effects of these items were independently taken into account using experimental results. The group constants obtained in the cell calculations were used here as the input data. For the reflector regions, on the other hand, were used the group constants obtained with the asymptotic neutron spectrum of fission, $1/E$ and Maxwellian distribution. Thus, the effective multiplication factor was calculated for the three temperatures, 300, 325 and 500 K and for various fuel loading configurations.

4. Determination of temperature coefficient of reactivity

4.1 Temperature coefficient of reactivity by calculation

The temperature coefficient of reactivity (α_T) was obtained from the calculated effective multiplication factors using the following expression.

$$(\alpha_T)_{\text{calc}} = \frac{k_{\text{eff}}(T_L) - k_{\text{eff}}(T_H)}{k_{\text{eff}}(T_L) \times k_{\text{eff}}(T_H)} / (T_L - T_H) + C, \quad (1)$$

where T_L and T_H denote the low and high temperatures, respectively,

k_{eff} denotes the effective multiplication factor,

C is a correction factor for the thermal expansion of the assembly.

4.2 Temperature coefficient of reactivity by experiment

The temperature coefficient of reactivity was measured by a criticality method which is basically a combination of the measurement of reactivity worth of supplementary fuel rods which was needed to compensate the reactivity decrease due to the assembly temperature rise and the fine

criticality adjustment by calibrated control rods. The α_T value was determined from the experimental data using the following expression,

$$(\alpha_T)_{\text{expt}} = \left\{ \rho_0(T_L) - \rho_0(T_H) + \rho_s(T_H) - \rho_{\text{cor}} \right\} / (T_L - T_H). \quad (2)$$

where

ρ_0 : Excess reactivity

ρ_s : Reactivity worth of the supplementary fuel rods which were added to the core at 200 °C

ρ_{cor} : Correction term corresponding to the effects of heaters, gap between the two half assemblies, control and safety rod holes, BF_3 counters, and etc.

4.3 Determination of supplementary fuel rod worth

As described in section 2.3, the number of supplementary fuel rods was 153 which consisted of 21 B4-type and 144 B2-type fuel rods. The reactivity worth of supplementary fuel rods was obtained by extrapolating the measured values of fuel rod reactivity worth using the calculated effective multiplication factors for various fuel loading configurations. The following approximate expression was used.

$$(\rho_s)_{\text{expt}} = (\rho_s / \rho_i)_{\text{calc}} \times (\rho_i)_{\text{expt}}, \quad (3)$$

where ρ_i denotes the reactivity worth of i fuel rods. $i=12$ for B4-type

fuel rod and $i=24$ for B2-type fuel rod,

$(\rho_s)_{\text{calc}}$ and $(\rho_i)_{\text{calc}}$ are calculated from the wellknown definition formula, $\rho = \Delta k/k$.

5. Results and discussions

In the criticality method, it is important to understand the relation among the three parameters; effective multiplication factor, temperature and number of fuel rods in the core. Figure 5 shows a conceptual drawing of k_{eff} as a two parameter function of core temperature and number of fuel rods. In this figure, A and C points indicate, respectively, the room temperature and 200 °C critical points. The experiment followed A-B-C route to reach the 200 °C critical point. The fuel rod worth measurements were done at C' and C'' points. Yamane et al. (4) applied the pulsed neutron method at several points on the route A-B to measure the $(\alpha_T)_{\text{expt}}$. The A-M-C route shows a criticality locus. The criticality approach at 200 °C in the present work was conducted on the route B-C.

Figure 6 shows the calculated k_{eff} values for various steps of fuel loading. The solid circles in the figure indicate loading steps of every 12 of B4-type or 24 of B2-type fuel rods. The steep and gentle inclinations in the curve occur when B4-type and B2-type fuel rods, respectively, are charged into the core. The curve, between 300 and 430 of fuel rods, for example, shows bending tendency. This can be understood partly as due to the relative increase of neutron leakage by decrease of reflector thickness which was inevitably brought by the increase of number of fuel rods. This

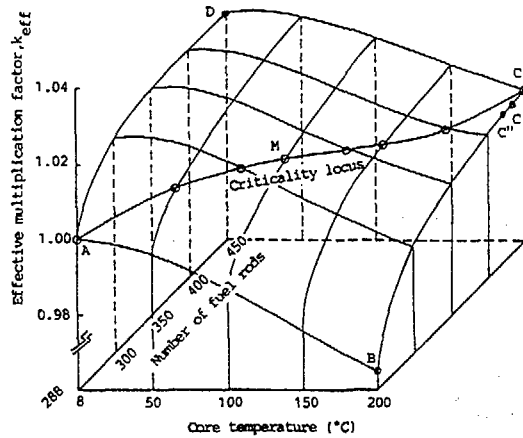


Fig. 5 Conceptual two dimensional display of effective multiplication factor versus core temperature and number of fuel rods

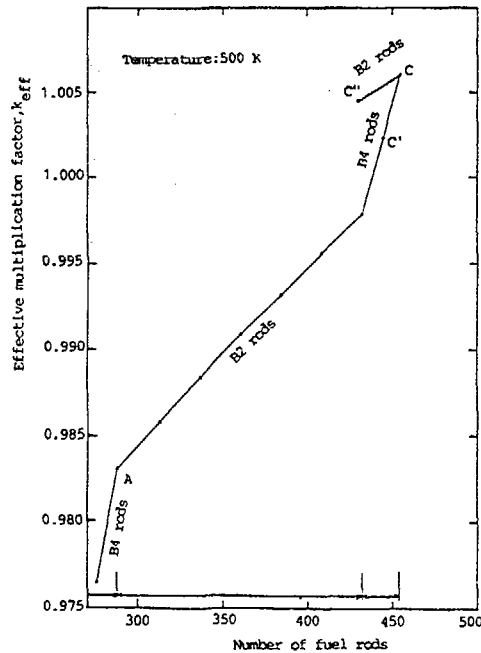


Fig. 6 Calculated effective multiplication factor versus step-wise loaded supplementary fuel rods

fact suggests that the reactivity worth of the supplementary fuel rods can not be accurately determined by linear extrapolation of the reactivity worth of smaller number of fuel rods. This is the reason why the Eq.(3) was utilized.

The reactivity worths of fuel rods in Table 2, obtained by calculation, are considerably higher than those by experiment. These discrepancies come probably from the cell calculation. It means that the infinite repeat model of the unit cell shown in Fig. 4, will not give proper group constants for the supplementary fuels which are charged at the boundary between core and radial reflector. The ratios of calculated values, $(\rho_s / \rho_i)_{calc}$, however, are expected to be sufficiently correct. Therefore, the experimental reactivity worth of supplementary fuels was evaluated from the experimental reactivity worth of 24 or 12 fuel rods by multiplying the corresponding ratio.

In Table 4 and Fig. 7, are shown the resultant values of $(\alpha_T)_{expt}$. It is evident that α_T is temperature dependent. The values of $(\alpha_T)_{expt}$ for 8.0-22.0 °C range is smaller than that for 8.0-200.3 °C range by 30 %. This temperature dependence has been already discussed in Ref.(4), where its authors have explained as follows; When the assembly temperature is low, the neutron spectrum is relatively soft, and the density of air contained in the assembly is high. These two phenomena cause the increase of thermal neutron absorption by nitrogen of the air contained in the reflector. In other words, the value of α_T for lower temperature range is smaller than that for higher temperature range. It seems that the agreements between calculation and experiment are better for higher temperature range than for the lower temperature range.

Finally, it is concluded that the calculation of temperature coefficient of reactivity for HTTR by use of SRAC is sufficiently validated by comparing with the experimental data at VHTRC.

Table 4 Comparisons of temperature coefficient of reactivity between calculation and experiment

Temperature range (°C)	$(10^{-4} \Delta k/k/°C)$	
	Experiment	Calculation
8.0-22.0	-1.33	Not calculated
22.0-32.0	-1.40	Not calculated
27.0-52.0	Not measured	-1.53
8.0-200.3	-1.72	-1.69(*)
25.5-199.6 (**)	-1.71	-1.73

(*):Evaluated by extrapolating the calculated value for the temperature range 300 K-500 K using the experimental value, $-1.33 \times 10^{-4} \Delta k/k/°C$
 (**):The data in this temperature range have been measured by the pulsed neutron technique and are quoted from Ref(4).

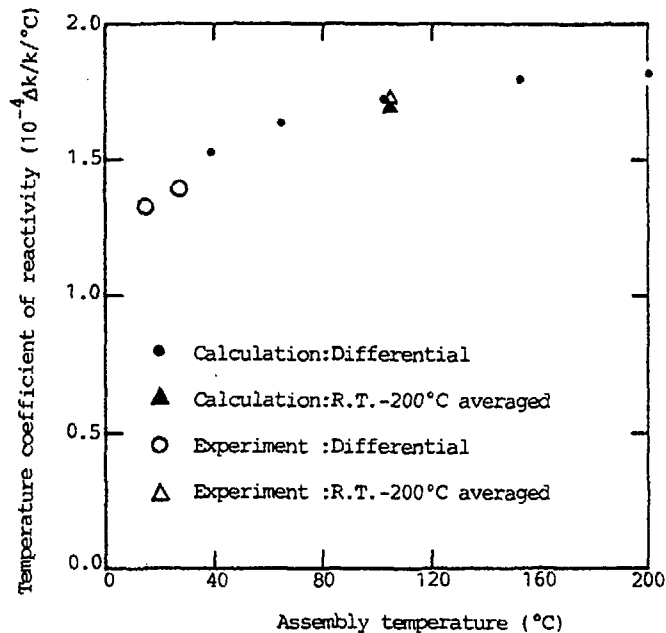


Fig. 7 Temperature coefficient of reactivity versus assembly temperature

Acknowledgments

The authors express their particular gratitude to Messrs. F. Yoshihara, K. Kitadate (left JAERI), H. Yoshifuji, M. Takeuchi and T. Ono for their experimental support and the steady-and-safe reactor operations. Thanks are also given to Dr. K. Tsuchihashi for valuable comments on analyses.

References

- (1) JAERI Publication "Present status of HTGR Research and Development" JAERI internal report, March (1990).
- (2) Yasuda, H. et al.: J. Nucl. Sci. Technol. 24[6], 431 (1987).
- (3) Yasuda, H. et al.: JAERI 1305 (in Japanese)(1987).
- (4) Yamane, T. et al.: J. Nucl. Sci. Technol. 27[2], 122 (1980).
- (5) Akino, F. et al.: J. At. Energy Soc. Japan 31[6], 682 (1980).
- (6) Sjostrand, N. G.: Ark. Fys., 11[13], 233 (1956).
- (7) Tsuchihashi, K. et al.: JAERI 1302 (1986).
- (8) Young, J. A and Koppel, J. V. : J. Chem. Phys. 42, 1, 357 (1965).
- (9) Ishiguro, Y. et al.: JAERI 1219 (in Japanese)(1971).

PRESENT STATUS OF THE PROTEUS HTR EXPERIMENTS

PAUL SCHERRER INSTITUTE
Villigen, Switzerland

Abstract

New critical experiments in the framework of an IAEA Coordinated Research Program on "Validation of Safety Related Reactor Physics Calculations for Low Enriched HTR's" are planned at the PSI PROTEUS facility. The experiments are designed to supplement the experimental data base and reduce the design and licensing uncertainties for small- and medium-sized helium-cooled reactors using low-enriched uranium (LEU) and graphite high temperature fuel. The main objectives of the new experiments are to provide first-of-a-kind high quality experimental data on: 1) The criticality of simple, easy to interpret, single core region LEU HTR systems for several moderator-to-fuel ratios and several lattice geometries; 2) the changes in reactivity, neutron balance components and control rod effectiveness caused by water ingress into this type of reactor; and 3) the effects of the boron and/or hafnium absorbers that are used to modify the reactivity and the power distributions in typical HTR systems. Work on the design and licensing of the modified PROTEUS critical facility is now in progress with the HTR experiments scheduled to begin in 1991. Several international partners are involved in the planning, execution and analysis of these experiments in order to insure that they are relevant and cost effective with respect to the various gas cooled reactor national programs.

The present status of the planning of these experiments (as modified by the results of the October 1989 IAEA meeting of tentative coordinated research program members) is described along with some of the results obtained in connection with the preparation of a safety report on the proposed experiments for the Swiss licensing authorities.

1 Introduction and Summary

A series of critical experiments in the zero-power reactor facility PROTEUS is planned. The experiments are intended to reduce the design and licensing uncertainties for small- and medium-sized helium-cooled reactors using low-enriched uranium (LEU) and graphite high temperature fuel.

The main objectives of the new experiments are to provide first-of-a-kind, high quality experimental data on:

- The criticality of simple, easy-to-interpret, single core region, low-enriched uranium (LEU), high temperature reactor (HTR) systems for several moderator-to-fuel ratios and several lattice geometries;
- The changes in reactivity, neutron balance components and control rod effectiveness caused by water ingress into this type of reactor;
- The effects of the boron and/or hafnium absorbers that are used to modify the reactivity and the power distributions in typical HTR systems.

The new experiments have been approved within Switzerland and work on the design and licensing of the modified PROTEUS critical facility is now in progress. The Swiss contribution to the international LEU HTGR experimental program consists of the facility construction, licensing and operating costs as well as a portion of the scientific support staff. The Federal Republic of Germany contribution of the LEU pebble bed HTGR fuel needed for the initial experiments as well as considerable scientific support has been essential in the planning of these experiments. Work on the necessary international contractual and safeguards arrangements for the transfer of the fuel to PSI has been initiated. The HTR critical experiments are presently scheduled to begin in 1991.

Fuel from the LEU HTR experimental program in the AVR test facility of the KFA-Jülich will be used for the first phase of the experiments. Two-dimensional discrete ordinates transport theory calculations have been performed for several configurations with this LEU AVR fuel which contains 6 grams of 16.7% enriched uranium per fuel pebble. The results indicate, that 5300 of these fuel pebbles should be sufficient for this initial phase, involving single core zone critical configurations with moderator-to-fuel pebble ratios ranging from about 1-to-2 up to 2-to-1, pebble packing fractions from 0.6046 to 0.74 with a core diameter of about 1250 mm. Experiments with lower C/U ratios are possible but will require either additional fuel pebbles or use of some of the existing PROTEUS UO₂ driver fuel rods in more complex multi-zone systems.

The experiments have been accepted as an International Atomic Energy Agency (IAEA) coordinated research program entitled "Validation of Safety Related Reactor Physics Calculations for Low Enriched HTGR's" in the framework of the Agency's Gas Cooled Reactor Working Group. In addition to the basic Swiss and Federal Republic of Germany cooperation, the Soviet Union and the Peoples Republic of China have already decided to participate and will supply some of the scientific manpower necessary to plan, execute and analyze these experiments and insure that they are relevant and cost effective with respect to the various gas cooled reactor national programs. Some other countries (probably Japan and the United States of America and possibly France) may also join in. The detailed experimental program is not yet completely determined with respect to just which experiments are done with what priority. As indicated above, a fairly wide range of possible configurations is possible within the overall envelope of the critical facility size and fuel availability constraints. Some of the tentative members of the IAEA coordinated research program met in October, 1989, in Würenlingen, Switzerland to begin to define the details of the initial experimental program. This paper incorporates some of the results of the October, 1989, meeting. A second meeting of IAEA coordinated research program members will be held in May, 1990, in Würenlingen.

2 Proposed Experiments

2.1 Clean Lattice Experiments

The low-enriched, pebble-bed HTR critical experiments proposed for the PROTEUS facility are designed to complement the data base obtained from previous high-enriched HTR experiments such as the pebble-bed investigations in the KAHTER facility in Germany [1], the prismatic block experiments at General Atomics [2,3] and at Battelle North West Laboratory [4], the low enrichment HTR lattices at Winfrith in England [5] and the LEU HTGR experiments in the VHTRC facility in Japan [6] and to yield useful information for LEU HTR systems using either pebble or prismatic block fuel elements.

The basic results will be the critical masses and geometries, the experimentally measurable neutron balance components, inferred k_{∞} values, and neutron flux and fission rate distributions.

In principle, k_{∞} and the related reaction rate ratios are not affected by the pebble packing fraction. This means that we can choose any convenient geometrical arrangement of pebbles for the zero-leakage neutron balance measurements, provided that the system may be made critical and is large enough so that experimental corrections for reflector effects are acceptably small at the central measurement location.

It is planned to use a deterministic hexagonal close-packed lattice having a packing fraction of about 0.74 as well as with an alternative hexagonal arrangement with a packing fraction of about 0.60 for most of the experiments. This will permit the definition of precise calculational benchmark situations and in the case of the second hexagonal arrangement, allow easy access to the core center for reactivity worth and reaction rate measurements with minimal perturbation of the system. Some of the cores will also be constructed as single-zone cores with stochastic (random) pebble-bed geometry.

2.2 Water Ingress

The possibility of steam generator or liner cooling system leaks necessitates the consideration of accidental water ingress in HTGRs. Most graphite moderated HTGR systems are significantly undermoderated for reasons relating to fuel cycle economics (the conversion ratio increases in undermoderated systems so that less fissile material needs to be supplied). This means that these systems will gain reactivity as moderator is added to the core.

The only previous water ingress experiments that have been performed for pebble-bed reactor systems are the high-enriched experiments at Jülich [7] and Graz [8]. The Jülich experiments were performed in a subcritical assembly with thin (16 and 20 cm) radial and axial graphite reflectors. The Graz experiments used a relatively small amount of high-enriched pebble-bed fuel in a heterogeneous externally driven system.

Pebble-bed HTRs usually have a strong reflector effect because of the undermoderated core with nearly 40% void coupled with a high density graphite reflector [9]. The high thermal neutron flux in the reflector compared with the adjacent core region enhances the worth of control rods located in the reflector regions. One of the effects of water ingress is to reduce the worth of the reflector and hence of any control rods or poison ball reserve shutdown systems (KLAK) located in the reflector regions. Similar considerations apply to the modular prismatic block HTGR designs which usually have a relatively small core diameter in order to minimize the maximum fuel temperatures under accident conditions.

The use of a uniform hexagonal lattice and plastic inserts in the proposed PROTEUS experiments should allow very accurate simulation of water ingress effects [10] and the development of an accurate experimental benchmark for use in validating the design calculations needed to insure the safety of low-enriched, graphite-moderated, pebble-bed systems. The use of a single zone critical core will allow the water ingress experiments in PROTEUS to provide information on changes in the reactivity worth of control rods located in the radial and/or axial reflectors in a straightforward and rigorous manner.

2.3 Burnable Poisons

An important difference between the HEU and LEU systems is linked to the use of burnable poisons in the initial cores to modify the changes in reactivity and power distribution during the transition

to an equilibrium core. In the case of the hafnium/boron mixture which has been used in European HTGR designs, the use of low-enriched instead of high-enriched uranium causes added uncertainty because of the much larger overlap of the resonance capture in hafnium with ^{238}U as compared with the ^{232}Th used in the high-enriched uranium reactor fuel cycle (resonance capture in hafnium is largest in the 1 to 10 eV energy range where resonance capture in ^{232}Th is very small but resonance capture in ^{238}U is large). There is thus considerable incentive to investigate the interactions of hafnium and ^{238}U in pebble-bed reactor systems.

With only 5300 LEU AVR fuel pebbles, the number of absorber pebbles will be severely limited unless some of the existing PROTEUS 5% enriched UO_2 driver fuel rods are used or some other source of LEU HTR fuel pebbles is located. The primary reactor physics interest is currently in hafnium/boron absorbers (because of the interference between hafnium and ^{238}U resonance capture). Studies of alternative poison nuclides (erbium for example) and geometries may lead to additional experiments.

The effect of water ingress on the reactivity worth of pebbles or rods containing hafnium and/or boron as burnable poisons has not been measured before to our knowledge. Such experimental data would be of considerable interest in the design and licensing of gas-cooled district heating reactors in which the water ingress problems are likely to receive more attention than in an electric power generation reactor in which the higher core temperatures and power densities more strongly limit the maximum water density in the core.

3 Calculational Results

3.1 Introduction

Many two-dimensional discrete ordinates transport theory calculations have been performed for LEU HTR PROTEUS configurations with LEU AVR pebble bed fuel containing 6 grams of 16.7% enriched uranium per pebble.

Basic criticality results and control rod worths plus the reactivity changes associated with simulated water ingress, with possible pebble bed densification (slumping), with upper reflector removal, with upper reflector collapse onto the pebble bed, with removal of the last layer of pebbles, etc. have been calculated in connection with the preparation of a safety report and for experimental planning purposes.

A few of the more interesting of these results that have not previously reported will be given in the following sections.

3.2 Method of Calculation and Fuel Specifications

The calculational methods and nuclear data libraries used for the HTR PROTEUS experiment calculations are described in two other papers at this conference [11,12]. Briefly, a small auxiliary code called GHR was used to compute atom densities for use in the PEBBLE Dancoff factor computation code [13,14] and in the MICROX-2 broad group cross section preparation code [15] together with JEF-1 based nuclear data libraries [16,17]. The broad cross sections were then used in the TWODANT two-dimensional discrete-ordinates transport theory code [18] and in the PERT-V diffusion theory perturbation code [19]. The LEU AVR fuel pebble specifications were taken from quality assurance records for this fuel obtained from KFA Jülich [20].

Carbon-to-uranium, carbon-to- ^{235}U atom ratios and critically buckled k_{∞} values for various mixtures of the 16.7% enriched AVR fuel pebbles with pure graphite moderator pebbles are given in Table 1.

3.3 Safety and Shutdown Rod Worth

Two-dimensional transport theory calculations were made for Core 13 of the PROTEUS LWHCR experiments [21]. They were used to develop and validate an R- θ geometry control rod model. Good agreement between the calculated and measured worth of the 8 borated steel safety and shutdown down rods in PROTEUS LWHCR Core 13 was obtained (Calc/Exp = 0.93) when the experimentally determined axial buckling in the test zone region was used.

This model was then used to compute the worth of the same 8 borated steel safety and shutdown rods as a function of the distance of the safety and shutdown rods from the core-reflector boundary and as a function of the degree of simulated water ingress in the core for various LEU HTR PROTEUS configurations.

The worth of the 8 borated steel PROTEUS safety and shutdown rods as a function of the distance of the safety and shutdown rods from the core-reflector boundary in a 150 cm diameter LEU HTR PROTEUS configuration with a M:F ratio of 3:1, a filling factor of 0.6046 and no simulated water ingress is given in Table 2. A value of almost 22 \$ (for all 8 rods) was obtained at the minimum possible distance of 3.75 cm between the rod centerline and the core-reflector boundary.

Additional calculations for the reactivity worth of 4 standard borated steel safety rods as a function of the amount of simulated water ingress into the core region were performed. An under-moderated (moderator-to-fuel pebble ratio of 1-to-2), high leakage (filling factor of 0.6046) core was selected because this type of system is expected to show the maximum effect of simulated water ingress.

Table 1: Carbon-to-Uranium Ratios for 16.7% AVR Fuel

M:F Pebble Ratio	C/U Atom Ratio	C/U-235 Atom Ratio	k_{∞} (Critical B^2 in cm^{-2})
0	637	3760	1.5497 (7.405×10^{-4})
0.2623	800	4726	1.6052 (7.572×10^{-4})
0.5832	1000	5907	1.6503 (7.536×10^{-4})
1	1260	7442	1.6870 (7.329×10^{-4})
2	1883	11124	1.7254 (6.655×10^{-4})
3	2506	14806	1.7323 (6.000×10^{-4})

Table 2: Worth of 8 Borated Steel Safety and Shutdown Rods

Distance of Rod From Core-Reflector Interface (cm)	K-Effective		ΔK_{eff}
	All Rods Out	All Rods In	
3.75	1.00441	0.85181	0.15260 (21.80 \$)
5.0	1.00443	0.86146	0.14297 (20.42 \$)
10.0	1.00458	0.89263	0.11195 (15.99 \$)
15.0	1.00397	0.91645	0.08752 (12.50 \$)

The present LEU HTR experimental program proposes pebble bed core effective diameters of about 1250 mm for a random (stochastic) pebble lattice and about 1206 mm for the deterministic hexagonal lattices which require additional graphite filler pieces located between the core and the reflector to achieve a stable pebble configuration. These filler pieces increase the distance between the safety- and shutdown-rods and the core and hence reduce their reactivity worth. The borated steel and boron carbide safety- and shutdown-rods presently used in the PROTEUS critical assembly were assumed to be located in their present positions in the graphite radial reflector on a circle of diameter 1350 mm (about 7 cm away from the core-reflector boundary). The results are given in Table 3 and in Fig. 1. The abbreviations "(RZ)" and "(RT)" used in Fig. 1 represent R-Z and R- Θ geometry, respectively.

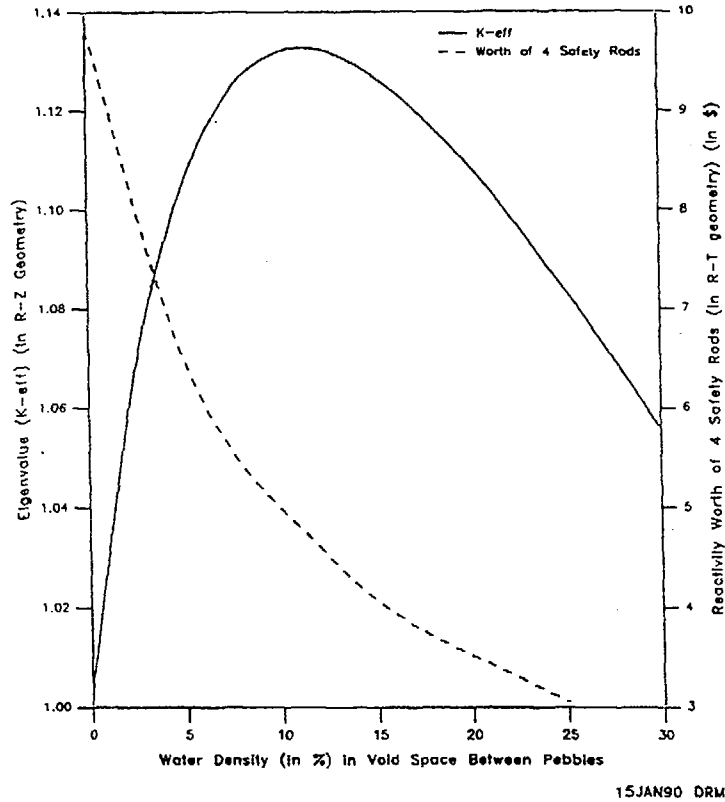


Figure 1: Eigenvalue and Safety Rod Bank Reactivity Versus Water Density (LEU AVR Fuel, M/F = 1/2, FF = 0.6046, Core H/D (RZ) = 120/125 cm, Core D (RT) = 120.6 cm)

The eigenvalue versus water density curve also shown in Fig. 1 was obtained from normal R-Z geometry calculations for a 1250 mm diameter pebble bed core (M/F pebble ratio = 1/2, filling factor = 0.6046) without filler pieces.

The calculated worth of the 4 safety rods without simulated water ingress in this undermoderated configuration (about 10\$ for a bank of 4) is almost identical to the worth at the same core-reflector boundary distance given in Table 2 for a well moderated case. The computed safety rod worth falls rapidly with increasing simulated water ingress. This is an important consideration in the licensing of the HTR PROTEUS experiments.

Additional R- Θ geometry calculations were done to assess the effect of uncertain boron content on the safety rod reactivity worth. The results are also given in Table 3. A 20% boron content variation causes about 3% variation in safety rod reactivity worth. This means that the safety rods are already fairly close to the so-called "black absorber" limit and that little increase in reactivity worth can be obtained from an increase in the boron content.

Table 3: Worth of a Bank of 4 Safety Rods (M/F=1/2, FF=0.6046, D_{core}=1206 mm)

H ₂ O Density in Void Space Between Pebbles (in %)	Critical Axial Buckling (cm ⁻²)	Boron Content in Safety Rods	ΔK_{eff} due to 4 Safety Rods	ΔK_{eff} due to 4 Safety Rods (in \$)
0		X 0.8	0.06866	9.54 (-2.9%)
0	2.085E-4	Nominal	0.07067	9.82 (Ref.)
0		X 1.2	0.07273	10.10 (+2.9%)
5	3.627E-4	Nominal	0.04667	6.48
12.5	4.644E-4	Nominal	0.03240	4.50
25		X 0.8	0.02123	2.95 (-3.0%)
25	4.915E-4	Nominal	0.02188	3.04 (Ref.)
25		X 1.2	0.02247	3.12 (+2.6%)

3.4 Fission Rate Spatial Distributions

The spatial distributions of ²³⁵U and ²³⁸U microscopic fission rates in some configurations were also obtained. The ratios of microscopic fissions in ²³⁸U to microscopic fissions in ²³⁵U ("F8" and "F5", respectively, in the table) in the central region in the proposed experiments deviate by 2 to 3 % from fundamental mode (just critical bare system) values as shown in Table 4.

The fission rate distributions show considerable axial asymmetry in the shorter, more reactive pebble bed cores. The axial asymmetry is a result of the presence of a large void space between the pebble bed core and the upper axial reflector.

Table 4: Bare- and Reflected-System Fission Rate Ratio Comparison

M/F Pebble Ratio	Filling Factor	F8/F5 at the Center of a Just-Critical Bare System	F8/F5 at the Core Center in the Reflected System	Ratio of F8/F5 Values ¹⁾
1/2	0.74	3.126E-4(1-D cyl.)	3.189E-4(2-D cyl.)	0.9802
1/2	0.74	3.124E-4(2-D cyl.)	3.189E-4(2-D cyl.)	0.9796
1/2	0.6046	3.126E-4(1-D cyl.)	3.224E-4(2-D cyl.)	0.9696
1/2	0.6046	3.125E-4(sphere)	3.224E-4(2-D cyl.)	0.9693
2/1	0.74	1.597E-4(1-D cyl.)	1.616E-4(2-D cyl.)	0.9882
2/1	0.6046	1.597E-4(1-D cyl.)	1.619E-4(2-D cyl.)	0.9864

1) Ratio is bare-to-reflected and hence is the reciprocal of the usual PROTEUS-to-fundamental mode factor.

3.5 Kinetic Parameters

The PERT-V code was used to calculate kinetic parameters (effective delayed neutron fractions and neutron generation times). It was tested by computations for a well-known critical assembly (GODIVA). The first calculations of the kinetic parameters (effective delayed neutron fractions and neutron generation times) for the proposed LEU HTR PROTEUS experiments were done in one-dimensional cylindrical geometry to check out the calculational methods. One-dimensional neutron lifetime results for the HTR PROTEUS experiments turned out to be inadequate due to the strong effects of the graphite axial reflectors. A series of two-dimensional calculations were then performed with considerably different results. In particular, the neutron lifetime is increased by approximately a factor of two or so when both reflectors are considered in the two-dimensional calculations.

The neutron lifetime also turns out to be a strong function of the hydrogen density in the simulated water ingress experiments that are planned in the LEU HTR experiments. The neutron lifetime is reduced by increasing amounts of hydrogen in the void space between the pebbles in the core region (see Table 5).

The effective delayed neutron fraction is not very sensitive to anything in this relatively well moderated system with only a single fissile species.

3.6 Discussion of Calculational Results

The results indicate that 5300 of these LEU AVR fuel pebbles should be sufficient for the initial phase of the planned LEU HTR PROTEUS experiments involving critical configurations and water ingress studies with moderator-to-fuel pebble ratios of 1-to-2 to about 3-to-1.

Table 5: Kinetic Parameters, 2-D R-Z Geometry, Core Cavity H/D = 125/190 cm, Filling Factor = 0.74

M/F Pebble Ratio	Water in Void Space (vol%)	Water in Void Space (grams per pebble)	Upper Reflector Thickness (cm)	Core Height (cm)	k_{eff}	β_{eff}	Neutron Lifetime (sec)
1/2	0	0	78	89	1.0009	0.007314	1.763E-3
1/2	6.25	2.453	78	89	1.0682	0.007337	1.379E-3
1/2	12.5	4.905	78	89	1.1026	0.007338	1.153E-3
1/2	25.0	9.811	78	89	1.1206	0.007317	9.161E-4
1/2	50.0	19.62	78	89	1.0867	0.007245	7.053E-4
1/2	82.0	32.18	78	89	0.9967	0.007164	6.051E-4
1/2	0	0	0	89	0.9495	0.007379	1.542E-3
2/1	0	0	78	123	1.0001	0.007283	2.185E-3
2/1	10.0	3.924	78	123	1.0253	0.007293	1.633E-3
2/1	20.0	7.849	78	123	1.0006	0.007269	1.420E-3
2/1	0	0	0	123	0.9559	0.007332	2.020E-3

In well moderated cases (moderator-to-fuel pebble ratio of 3-to-1), the pebble bed core diameter needs to be at least 150 cm in order to obtain criticality with a reasonable core height.

In the less well moderated case (moderator-to-fuel pebble ratio of 1-to-2) that is of particular interest in the water ingress portion of the experimental program, the pebble bed core diameter needs to be less than 150 cm in order to obtain criticality with a reasonable core height and the available number of fuel pebbles.

One of the results of the initial October, 1989, coordinated research program meeting was a rather clear preference for undermoderated LEU HTR PROTEUS experiments. On this basis we have chosen a core diameter of about 125 cm for stochastic lattices and about 121 cm for deterministic hexagonal lattices with filler pieces for the initial series of LEU PROTEUS experiments. This choice allows the safety and shutdown rods to remain in their present position (in a ring of diameter 135 cm), which is logistically and economically desirable but which will limit the moderator-to-fuel pebble ratio to a maximum of about 2-to-1 in lattices with low filling factors.

The present type and number of borated steel safety and shutdown control rods seem to be adequate except that they need to be longer and to have a longer travel for the HTR PROTEUS experiments. The procurement of new longer safety and shutdown control rods and larger diameter control rod drive cable drums (needed for longer travel) is planned.

4 Personnel

The experimental and analytical team at PROTEUS has generally consisted of about 4 to 7 scientists and 4 technicians, responsible for the planning, execution and analysis of the experiments on the one hand, and the operation and technical maintenance of the reactor facility on the other. This staffing level is necessary to allow the planning, preparation and execution of the experiments to proceed in parallel without excessive delays. It is also necessary to allow the analysis and evaluation of the experiments to proceed quickly enough to be able to check any doubtful results.

The general plan is that about half of the total scientific staff will be provided by PSI and the other half of the staff will be provided by the other participating organizations.

5 Conclusions

New LEU-HTR experiments in the PROTEUS facility are planned. They will provide data on:

- the criticality of simple, easy to interpret, single core region HTR systems for several moderator-to-fuel ratios;
- the changes in reactivity and control rod effectiveness caused by water ingress;
- the effect of hafnium and boron absorbers in a low-enriched HTR system.

These experiments are needed to reduce uncertainties and to verify codes and data for design and licensing purposes.

The PROTEUS experiments should for the first time provide k_{eff} bias factors relevant to the LEU HTR fuel cycle and, in addition, shed light on the individual sources of error. The latter will be achieved by virtue of measured results for individual neutron balance components as well as the possibility of the investigation of streaming effects. A wide range of conditions will be covered by the experimental program, thereby providing an adequate integral data base for the validation of LEU HTGR design calculations.

The PROTEUS facility and its team are well suited to perform these experiments because they have much experience in accurate reactivity and reaction-rate measurements [22].

This project is intended to serve as a focal point for international collaboration in HTGR research. We hope to bring together good scientists from the various gas-cooled reactor national programs, not only to help share the cost of performing such experiments, but most of all to provide a joint in-house peer review for the planning, execution, analysis and significance of the experiments and to share knowledge to the greatest possible extent.

Acknowledgements

A large number of people participated in the preparation of this report either directly or indirectly through their previous contributions to the planning of HTR related experiments at PSI. The ABB/HRB Co. in Mannheim and the KFA in Jülich have also provided valuable information and support in planning these experiments.

References

- [1] R. Hecker and L. Wolf, "The Significance of Critical Experiments for Core Calculation and Design of High-Temperature Gas-Cooled Reactors Constructed on the Pebble-Bed Principle," Nucl. Sci. & Eng., 97, 1 (1987).
- [2] J. R. Brown, et al, "Hazards Summary Report for the HTGR Critical Facility," General Atomic Report GA-1210, 1960.
- [3] M. H. Merrill, "Nuclear Design Methods and Experimental Data in use at Gulf General Atomic," Gulf General Atomic Report Gulf-GA-A12652(GA-LTR-2), 1973.
- [4] C. R. Richey and T. J. Oakes, "Determination of Neutron Multiplication Factors as a Function of Temperature with the HTLTR," Nucl. Sci. & Eng., 47, 40 (1972).
- [5] I. Johnstone and V. E. Della Loggia, "Experimental Results from the UKAEA Reactor Physics Programme on Low Enrichment HTR Lattices at AEE Winfrith," D. P. Report 730, 1970.
- [6] Y. Kaneko, "Reactor Physics Research Activities Related to the Very High Temperature Reactor in Japan," Nucl. Sci. & Eng., 97, 145 (1987).
- [7] V. Driike, D. Filges, N. Kirch and R. D. Neef, "Experimental and Theoretical Studies of Criticality Safety by Ingress of Water in Systems with Pebble-Bed High-Temperature Gas-Cooled Fuel," Nucl. Sci. & Eng., 57, 328 (1975).
- [8] F. Schürer, W. Ninaus, K. Oswald, R. Rabitsch, H. Müller and R. D. Neef, "Steady-State Neutronic Investigations to the Accident of Water Ingress in Systems with Pebble-Bed High-Temperature Gas-Cooled Reactor Fuel," Nucl. Sci. & Eng., 97, 72 (1987).
- [9] R. Chawla, "On the Minimum Overall Size of a Reflected Pebble-Bed Reactor," Nucl. Technol., 52, 306 (1981).
- [10] R. Chawla, "On the Reactivity Effects of Water Entry in Pebble-Bed HTR Lattices," Ann. Nucl. Energy, 8, 525 (1981).
- [11] S. Pelloni, "Present HTR Physics Computational Methods at the PSI," to be presented at the IAEA Specialist's Meeting on Uncertainties in Physics Calculations for Gas-Cooled Reactor Cores, May 9-11, 1990, Würenlingen, Switzerland.
- [12] S. Pelloni and W. Geisser, "Nuclear Data Related to HTR's," to be presented at the IAEA Specialist's Meeting on Uncertainties in Physics Calculations for Gas-Cooled Reactor Cores, May 9-11, 1990, Würenlingen, Switzerland.
- [13] J. Stepanek, K. Herda and P. Koehler, "PEBBLE: Ein RSYST-Modul zur Berechnung der Entkommwahrscheinlichkeiten für zweifach heterogene Anordnung des Brennstoffes," EIR internal technical memorandum TM-PH-690 (1977).
- [14] E. Teuchert and R. Beitbarth, "Resonanzintegralberechnung für mehrfach heterogene Anordnungen," Report Jül-551-RG, Kernforschungsanlage. Jülich (1974).

- [15] D. Mathews and P. Koch, "MICROX-2 An Improved Two-Region Flux Spectrum Code for the Efficient Calculation of Group Cross Sections," General Atomic Company Report GA-A15009 (1979).
- [16] P. Vontobel and S. Pelloni, "JEF/EFF Based Nuclear Data Libraries," PSI Bericht Nr. 636 (1987).
- [17] R. E. MacFarlane, D. W. Muir, and R. M. Boicourt, "The NJOY Processing System, Vol I: User's Manual and Vol II: The NJOY, RECONR, BROADR, HEATR, and THERMR Modules," Los Alamos National Laboratory Report LA-9303-M (ENDF-324), Vols. I and II (1982).
- [18] R. E. Alcouffe, F. W. Brinkley, D. R. Marr, and R. D. O'Dell, "User's Guide for TWODANT: A Code Package for Two-Dimensional, Diffusion-Accelerated, Neutral Particle Transport," Los Alamos National Laboratory Report LA-10049-M, Rev. 1 (1984).
- [19] R. W. Hardie and W. W. Little, Jr., "PERT-V: A Two-Dimensional Perturbation Code for Fast Reactor Analysis," Battelle-Northwest, Richland, Wash. Pacific Northwest Laboratory Report BNWL-1162 (1969).
- [20] H. Nabelek, KFA Jülich, personal communication, 27 Feb. 1989.
- [21] R. Seiler, R. Chawla, K. Gmür, H. Hager, H. D. Berger and R. Böhme, "Investigation of the Void Coefficient and other Integral Parameters in the PROTEUS-LWHCR Phase II Program", Nucl. Technol., 80, 311 (1988).
- [22] K. Gmür, "Techniques of Reaction Rate Measurements on the PROTEUS Reactor," EIR-Bericht Nr. 529, 1984.

PRESENT HTR PHYSICS CALCULATIONAL METHODS AT THE PAUL SCHERRER INSTITUTE

S. PELLONI
Paul Scherrer Institute,
Villigen, Switzerland

Abstract

In this paper a general description of HTR related calculational methods and data available at the Paul Scherrer Institute (PSI) is given. The cell codes used are MICROX-2, WIMS-D, and TRAMIX.

MICROX-2 is an integral transport theory spectrum code which solves the neutron slowing down and thermalization equations on a detailed energy grid for a two region lattice cell. A second level of heterogeneity can be treated, i.e. the inner region may include two different types of grains (particles).

WIMS-D contains tabulations of temperature dependent resonance integrals accurately evaluated for homogeneous mixtures of moderator and absorber at many energy points. Equivalence theorems are utilized to obtain few-group effective cross sections in heterogeneous problems. The intermediate resonance absorption shielding (IR) method of resolved resonances is employed. The spherical geometry of the pebble can be converted into an equivalent cylindrical geometry, and the double heterogeneity can be treated using the available cluster option with a method developed by Segev.

TRAMIX is a flexible computer (cell) code which reads fine group nuclear data from a library in the Los Alamos National Laboratory (LANL) format MATXS and produces fine group cross sections using the IR method.

Self-shielded multigroup cross sections produced with these cell codes can be used in connection with the one- and two-dimensional discrete-ordinates finite difference transport codes ONEDANT and TWODANT from LANL for full reactor calculations. Additional interface modules which are available include a B_N module for leakage calculations and some library management codes plus the PERT-V diffusion perturbation theory code.

Most of the nuclear data libraries for the cell codes are based on the JEF-1 (Joint European File) evaluation. They were processed using the NJOY nuclear data processing system from LANL with additional PSI developments. These libraries include the fast, thermal, and resonance data tapes FDTAPE, GGTAPE, and GARTAPE for MICROX-2, the WIMS-JEF file for WIMS-D, and MATXS formatted files in a variety of group structures for TRAMIX. Alternative English developed nuclear data libraries are available for use in WIMS-D.

1 INTRODUCTION

In this paper a general description of the HTR related calculational methods and nuclear data presently available at PSI is given. Codes and related nuclear data libraries are available for use on CRAY-XMP and CRAY-2 supercomputers.

Section 2 describes the nuclear data files and their preparation.

Section 3 presents the codes and explains their utilization for HTR applications.

Finally, Section 4 gives some plans for future work.

2 NUCLEAR DATA

Most of the nuclear data libraries are from JEF-1 [1], and are suitable for use in the cell codes WIMS-D [2], MICROX-2 [3], and TRAMIX [4]. Additionally, three pre-processed data libraries for WIMS-D, i.e. the old library WIMS-Standard [5], and the more recent libraries WIMS81 [6] and WIMS86 [7] are available at the PSI, but are not described in this paper. In the following section a description of the JEF-1 based libraries is given, and their processing scheme is illustrated [8].

2.1 Pointwise and Groupwise Libraries

2.1.1 Processing Scheme

Pointwise and groupwise data tapes were generated using the LANL code system NJOY. In this processing, the version 6/83 of NJOY was employed with updates up to mid 1987 [9] and with additional PSI developments concerning the module GROUPE. The module WIMSR [10], and the module MICROR [11] developed at the PSI were added to NJOY. At the present time, version 89 of NJOY has been distributed. This version is able to process the new ENDF/B-VI format, which includes double-differential cross sections in energy and angle, in addition to the older ENDF/B-IV and ENDF/B-V formats. A preliminary version of the JEF-2 data file, which extensively uses the ENDF/B-VI format, has been recently released [12].

NJOY includes sophisticated methods of reconstruction of zero temperature pointwise cross sections using various resolved resonance formalisms, Doppler broadening by the accurate point-kernel method, group-to-group thermal scattering matrices, flux-weighted fission-fraction vectors, and a weighting flux produced by a pointwise solution of the slowing-down problem that accurately accounts for broad and intermediate resonance effects in the epithermal region.

First, pointwise cross sections were processed into an ENDF/B like format (PENDF) using the NJOY modules RECONR, BROADR, UNRESR, HEATR and THERMR, which were applied sequentially, starting from the basic files JEF-1, JEF-1.1 (a recent revision of JEF-1 for certain isotopes), and EFF-1 (European Fusion File) [1,13,14].

RECONR reconstructs zero temperature pointwise (energy-dependent) cross sections using ENDF/B resonance parameters and interpolation schemes. In RECONR resonance cross sections are calculated with an extended version of the methods of RESEND [9].

BROADR Doppler-broadens and thins pointwise cross sections using the method of SIGMA modified for better behaviour at high temperatures and low energies [9].

UNRESR computes effective self-shielded average cross sections in the unresolved-resonance region using the methods of ETOX [9].

HEATR generates pointwise heat production cross sections (kerma factors) and radiation-damage production cross sections.

THERMR produces incoherent inelastic energy-to-energy matrices for free or bound scatterers, coherent elastic cross sections for crystalline materials, and incoherent elastic cross sections.

The PENDF files include pointwise cross sections for many isotopes (about 300) and temperatures up to 3000 K. The thermal region was treated according to the free gas model. For particular isotopes such as H in H₂O, and carbon in graphite, coherent and incoherent thermal neutron scattering matrices from the S(α , β) and other data from JEF-1 were included [15].

Second, GENDF multigroup cross sections were generated using GROUPE [9].

Five group structures were considered for HTR calculations. WIMS-BOXER (70 groups), General Atomics (GA) GA-MICROX (193 groups), Hochtemperatur Reaktorbau (HRB) PSI/HRB (308 groups), HRB (86 groups), and VITAMIN-J (175 groups) [8].

GROUPE generates self-shielded groupwise vector cross sections, group-to-group neutron scattering matrices, and photon production matrices using pointwise ENDF and PENDF data. The cross sections are written onto groupwise cross section files GENDF in ENDF/B like format. Vectors for all reaction types, matrices for reactions producing neutrons, including fission, together with mixed data pertaining to fission yields of prompt and delayed neutrons were calculated for different degrees of anisotropy for different temperatures and background cross sections.

The narrow-resonance Bondarenko flux model was employed for light isotopes. Shielded multigroup cross sections of heavier resonance nuclides were generated using the method of the flux slowing down calculator assuming a single resonance absorber in a non-absorbing moderator. A brief description of the GENDF libraries is given in the next subsections, followed by a section on the working libraries which are suitable for use in the cell codes described in the next section.

2.1.2 70 Group WIMS-BOXER Structure GENDF JEF-1 Library

The energy structure of the WIMS-BOXER library consists of the standard 69 WIMS structure and one additional group from 10 MeV to 14.918 MeV. This library contains JEF-1 neutron P₁ unmodified self-shielded temperature dependent data pertaining to most important isotopes for Light Water (LWR), High Conversion Light Water (LWHCR), and HTR reactor calculations.

42 thermal energy groups below 4.6 eV with upscatter are considered. The dry WIMS-D input spectrum [8] was utilized for collapsing PENDF data into multigroup cross sections. For accurate leakage calculations oxygen and carbon cross-sections (including all fast resolved resonances between 1 MeV and 10 MeV) were self-shielded using the method of the flux calculator applied in the whole energy range.

Generally, the self-shielding of resonance cross sections of certain light elements is found to be important for the correct calculation of hard spectra, particularly if these elements are high density materials (such as oxygen in UO₂), and if a coarse group structure in the MeV range is used. In these cases, the energy representation of resonances is not accurate enough, so that self-shielding is needed.

2.1.3 193 Group GA-MICROX Structure GENDF JEF-1 Library

This library contains JEF-1 P₃ unmodified self-shielded data at 296 K for relevant LWHCR isotopes and is mainly intended for HTR, LWR and LWHCR calculations. 103 thermal energy groups below 4.6 eV with upscatter are considered. The boundaries of the first 92 fast energy groups are taken from the GAM-II energy structure, whereas in the thermal range below 2.33 eV the boundaries mostly include the 101 energy points of the MICROX code. Dry and wet WIMS-D input spectra [8] were utilized for collapsing PENDF data into multigroup cross sections. The wet spectrum was used for hydrogen, deuterium and oxygen.

2.1.4 86 Group HRB Structure GENDF JEF-1 Library

This 86 group library is a subset of the 308 fine group library (see 2.1.5). The energy structure chosen gives a good representation of Hafnium and ²³⁸U resonances in the energy range between 2 eV and 10 eV and includes 37 thermal energy groups below 4.6 eV. The weighting spectrum is typical for HTR applications. The degree of anisotropy, the temperatures and background cross sections considered are the same as for the 308 group library.

2.1.5 308 Group PSI/HRB Structure GENDF JEF-1 Library

The energy structure of this general purpose fine group library is taken in the fast energy range from the VITAMIN-J structure [8] and in the thermal range below 2.38 eV from the MICROX structure. 108 thermal groups below 4.6 eV with upscatter are considered. In the epithermal energy range (2.7 eV-17 keV) some points from the LANL-MATXS8 group structure [16] were added to the VITAMIN-J boundaries. P_4 unmodified self-shielded temperature dependent data for most isotopes are available. The VITAMIN-E input weighting spectrum [8] was employed to collapse PENDF files into GENDF data.

2.1.6 175 Group VITAMIN-J Structure GENDF JEF-1/EFF-1 Library

The energy structure of this multigroup library was chosen to give a fine representation of the fast and epithermal energy range important for fusion blanket, fast breeder reactors, and shielding analysis for general applications, including HTR's. The VITAMIN-J group structure [8] has the same boundaries as the 174 group VITAMIN-E structure, but with an additional break point at 12.84 MeV from VITAMIN-C [8]. 11 thermal groups below 4.6 eV with upscatter are considered. The library includes JEF/EFF P_6 unmodified temperature dependent self-shielded data for most isotopes. The VITAMIN-E input weighting spectrum [8] was used to process all GENDF files. This library contains additional 42 photon group data based on the 38 group VITAMIN-E photon energy structure from LANL for shielding calculations.

2.2 WIMS-JEF Library

Starting from the 70 group WIMS-BOXER GENDF files, a 69 neutron group library for the code WIMS-D was generated (WIMS-JEF library). Hereby the NJOY module WIMSR was applied to transform the GENDF cross-sections into a form suitable for being used as input to the Canadian WIMS library management programme, WILMA [10,17]. In the processing with WIMSR and WILMA the relevant data were calculated by considering all explicitly represented reaction types on the GENDF files. A global fission spectrum, based primarily on data for the fission of ^{235}U , was taken over from the WIMS81 library [8]. The version of the WIMSR module currently used was a specially updated one [18,19]. This allowed a transport correction for the total and self-scattering cross-sections, the selection of a given dilution cross section for evaluating scattering data, and a generalized "inflow" computation of the transport cross-section. Further, an option was added to allow the standard interface file, RMFLUX [20] to be used for computing the "inflow" correction with an alternative problem-oriented weighting current. WIMSR was also modified to consider that the slowing down power on the GENDF file is evaluated at infinite dilution. An important modification to WIMSR was related to the resonance tabulations, whereby the original background cross-section grid was shifted in each energy group by the product of the potential scattering cross section and the Goldstein-Cohen λ -factor for the resonance absorber. This considers the fact, that the total background cross-section in WIMS-D consists of the contributions from all isotopes including the tabulated resonance absorber. The WIMS-JEF library consists of transport corrected P_0 temperature dependent data. The "inflow" transport correction is computed for all nuclides using a representative standard weighting current [19]. For the principal moderator isotopes (hydrogen, deuterium, oxygen and carbon) P_1 cross-sections are available.

2.3 MICROX-2 JEF-1 Library

GENDF and PENDF data files can be edited into the FDTAPE, GGTAPE and GARTAPE data tapes for MICROX-2 using the NJOY coupling module MICROR developed at the PSI.

The FDTAPE data file contains fine group dilution- and temperature- dependent cross sections in the fast energy range.

The GGTAPE data file consists of two sections which contain infinite dilute P_1 cross sections for the fast and thermal energy ranges respectively. MICROX-2 uses only the thermal section of the GGTAPE, which includes pointwise cross sections with upscatter estimated using the free gas model or the available coherent and incoherent scattering $S(\alpha, \beta)$ matrices.

The GARTAPE data file contains pointwise Doppler-broadened resonance cross sections in the resolved and unresolved resonance ranges. Fine energy points up to the keV range can be considered in order to achieve an accurate solution of the slowing down equations in two zones (self-shielding of resolved resonance range).

Starting from the GENDF data in 193 groups, a library for the code MICROX-2 was generated with MICROR.

The FDTAPE data set includes P_3 unmodified self-shielded cross-sections at room temperature in 92 groups. Individual fission spectra for the main actinides are included.

The thermal part of the GGTAPE includes upscatter cross sections for hydrogen, deuterium, carbon and oxygen, and is given in 101 thermal energy groups below 2.38 eV, at room temperature.

The GARTAPE contains pointwise Doppler-broadened resonance cross sections at room temperature in the resolved resonance range. 14457 energy points equally spaced in velocity between 0.414 eV and 8.0072 keV are available on the GARTAPE.

2.4 TRAMIX/TRANSX-CTR Libraries

The GENDF files of the five different neutron energy structures, i.e. 70, 193, 86, 308, and 175 groups, have been converted into MATXS format suitable for further processing with TRAMIX and TRANSX-CTR, using the NJOY module MATXSR.

The MATXS file is a generalized cross section library in a flexible format designed to generalize and to simplify the existing standard cross section formats. In the MATXS format, neutron and photon data types are treated in the same way. Each data type is subdivided into materials and submaterials. A material might be a particular isotope or mixture. Each submaterial is associated with a temperature and background cross section pair, and contains data related to any kind of reaction, including scattering transfer matrices and fission spectra. Data are self-shielded for cross sections showing a strong dependency on the dilution cross section.

3 SPECTRUM CELL AND TRANSPORT CODES

Physics calculations of HTR's can be performed using the (cell) codes WIMS-D, MICROX-2, and TRAMIX in connection with the one-dimensional transport theory programme ONEDANT and with the two-dimensional transport theory programme TWODANT from LANL [21]. For shielding calculations and for the preparation of cross sections of single materials, TRANSX-CTR can be used instead of TRAMIX.

ONEDANT is a modular computer program designed to solve the one-dimensional, time-independent, multigroup discrete-ordinates form of the Boltzmann transport equations. The modular construction of the code package separates the input processing, the transport equation solving, and the post-processing, or edit, functions into distinct, independently executable code modules, connected to one another solely by means of binary interface files.

TWODANT is the analog of ONEDANT in two dimensions.

In this section a description of the cell codes is given. In the next section, their use for HTR calculations is illustrated.

3.1 WIMS-D

WIMS-D [2] is a comprehensive standard code for reactor lattice cell calculations including burn-up calculations in a wide variety of reactor types. WIMS-D is a complex code primarily intended for the calculation of moderated systems. The geometry can be either fuel rods or plates, in regular arrays or clusters. WIMS-D contains tabulations of temperature dependent resonance integrals accurately evaluated for homogeneous mixtures of moderator and absorber at many energy points. Equivalence theorems are utilized to obtain few-group effective cross sections in heterogeneous problems. The Goldstein-Cohen treatment based on the intermediate resonance absorption shielding method of resolved resonances (IR method) using fixed IR-parameters is employed. Self-shielding of resonance cross sections is performed in the energy range between 9 keV and 4 eV. Outside of this energy range all cross sections are taken at infinite dilution, which is suitable for well thermalized system analysis. More precisely the resonance treatment is based on equivalence theorems which are similar for infinite lattices of rods or bundles of plates. These theorems relate in each case the heterogeneous problem to an equivalent homogeneous problem by means of a suitable rational approximation for the fuel self-collision probability. They take account of a first order correction for the interaction between resonances of several isotopes. In WIMS-D the resonance groups have been chosen so as to provide uniform distribution of resonances in lethargy and in cases of a single resonance in a group it is placed near the lethargy centre of the group. Therefore it is assumed that the disadvantage factors outside resonances are energy independent and may be set equal to unity.

The main feature of WIMS-D consists in calculating a detailed flux spectrum in all 69 library groups in each of the principal regions of the lattice: fuel, can, coolant and, in clusters, also bulk moderator, these regions being coupled through collision probabilities, then condensing the groups to obtain few-group constants, solving the few-group transport equation in a fine spatial mesh, modifying the solution to take leakage into account, and then again expanding the resulting fluxes at all mesh points to the original 69 groups, assuming that the subdivision of flux within a transport group at a given mesh point is such as that calculated before for the corresponding region, to obtain region and point reaction rates for chosen nuclides. The transport equation can be solved either in an integral form (collision probabilities) or in a differential form (discrete-ordinates method). Hereby a global library fission spectrum is utilized. First order anisotropy of scattering is taken into account. Leakage can be calculated either by the B_1 -method or the diffusion theory method. In the latter case the effect of cell heterogeneity can be accounted for either by simple flux and volume weighting of transport cross sections or, in cylindrical geometry only, by Benoist's theory of directed diffusion coefficients with or without correlation terms.

WIMS-D may now be routinely used for HTR applications with a new method developed by Segev [22] which allows the conversion of the spherical pebble bed unit cell into an equivalent (from the neutronic point of view) cylindrical unit cell, and uses the cluster option of WIMS-D to treat the double heterogeneity.

The REGION card in connection with the PUNCH=1 option can be requested to produce region averaged macroscopic homogenized cross sections, and the code DSNXSL [23] converts the outgoing cross section format into XSLIB format, one of the simplest LANL card image formats [21], which can be read into ONEDANT and TWODANT.

3.2 MICROX-2

MICROX-2 [3] is an integral transport theory spectrum code which solves the neutron slowing down and thermalization equations on a detailed energy grid for a two region lattice cell. MICROX-2 was developed for the efficient and rigorous preparation of broad group neutron cross sections for poorly moderated systems such as fast breeder reactors in addition to well moderated thermal reactors such as HTRs and LWRs. In addition to the cross sections, cell eigenvalues (k_{eff} and k_{∞}) and reaction rates are edit. The fluxes in the two regions are coupled by transport corrected collision probabilities for the generation of the region-wise transfer probabilities in the fast- and resonance-energy ranges. The computation of these collision probabilities is based upon the spatially flat neutron emission approximation and the transport (modified P_0) approximation of anisotropic scattering effects, simulated through the use of the transport mean free path instead of the total mean free path. The collision probability calculation also utilizes an energy dependent Dancoff correction factor algorithm, and is performed on an ultra-fine energy grid using GAR data including temperature dependent Doppler-broadened resonance cross-sections at up to about 15000 energy mesh points (selected with the criteria of constant lethargy or velocity spacing) between 8 keV and 0.414 eV for each nuclide. A second level of heterogeneity can be treated, i.e. the inner region may include two different types of grains (particles). MICROX-2 accounts explicitly for overlap and interference effects between different resonance levels in both the resonance and thermal energy range, and allows for the simultaneous treatment of leakage and resonance self-shielding in doubly heterogeneous lattice cells. Additionally, a semilogarithmic Bondarenko-interpolation between sets of temperature-and dilution-dependent FDTAPE fine group data prepared by the NJOY module MICROR (approximate self-shielding of fast range, including the fast part of the unresolved range) can be requested above a flexible value (less than 8 keV) which determines the upper energy boundary for the pointwise resonance calculation. Up to P_3 in the fast energy range, and P_1 order of scattering in the thermal range are considered. Neutron leakage effects are treated by performing fine group and hyperfine point B_1 slowing down (fast and resonance-energy ranges), or P_0 plus DB^2 thermalization (thermal range) calculations in each region. Energy-dependent bucklings (positive, zero, or negative) are supplied as input. A buckling search as a solution of the collapsed (with the fine flux) two group (a fast and a thermal group with thermal cut off at 2.38 eV) B_1 equations can be turned on. The treatment of leakage is essentially the same as in WIMS-D. Zone fission spectra may be constructed as linear combinations of fission spectra for various fissionable actinides available on the FDTAPE. The detailed neutron flux and current spectra are used for collapsing the basic neutron cross sections into cell-averaged and region-averaged broad-group cross sections and scattering transfer arrays (up to P_1). The present algorithm allows the maximum number of fast broad groups to be equal to the number of groups available on the FDTAPE (i.e. 92 in the case of the PSI library), and the maximum number of thermal broad groups to be equal to one third of the number of points available on the thermal part of the GGTAPE, this because of the trapezoidal rule used in the broad group cross section preparation (i.e. 33 in the case of the PSI libraries). Broad group P_2 and P_3 scattering transfer arrays may be determined with P_2 and P_3 weighting spectra obtained from an extended transport approximation. The broad group microscopic and macroscopic cross sections produced by MICROX-2 may be used either in diffusion- or transport-theory codes, and especially in ONEDANT and TWODANT via an XSLIB output format.

3.3 TRAMIX and TRANSX-CTR

TRAMIX [4], a code similar to TRANSX available at LANL, is a PSI update of the LANL fusion code TRANSX-CTR [16], which is as well available at the PSI.

As are TRANSX and TRANSX-CTR, TRAMIX is a flexible computer (cell) code that reads nuclear data from a library in MATXS format (in any group structure) and produces groupwise microscopic and macroscopic cross-sections in a variety of formats (including XSLIB) which can be read into the transport codes ONEDANT and TWODANT. Any order of scattering approximation (smaller than or equal to the maximum available on the MATXS library) can be chosen. Nuclear data can be produced for neutron, photon, or coupled transport. Options include adjoint tables, mixtures, group collapse, homogenization, thermal upscatter, prompt or steady-state fission, transport corrections, elastic removal corrections, and flexible response-function edits. TRAMIX has a general fission spectrum capability. Using an iterative procedure, it is able to generate problem dependent zone fission spectra.

The self-shielding in TRAMIX is based either on the Bondarenko formalism (as in TRANSX and TRANSX-CTR) or on the IR method by considering Dancoff corrections for different geometric models (no Dancoff corrections are available in TRANSX-CTR). The λ factors needed in the IR method are calculated for each isotope as a function of the neutron energy in terms of an approximate reconstruction of cold resonances on the basis of Bright-Wigner formulas [4].

As in TRANSX and TRANSX-CTR, the self-shielding procedure is applied to the whole energy range, which includes thermal resolved resonances of heavy actinides, unresolved resonances of main actinides, and high energy resolved resonances of structural materials.

For cell calculations (including shielding), TRAMIX is used in connection with the one-dimensional transport programme ONEDANT (infinite lattice cell calculation with white boundary conditions) and with the B_N module SOLVERB [4] for leakage calculations (TRAMIX/ONEDANT/SOLVERB).

SOLVERB [4] was developed for leakage calculations based on the B_N method. Alternatively, the diffusion approach can be used, particularly when the P_1 scattering matrices are not available on the cross section library. This code includes an automatic procedure for determining buckling factors (B^2) and eigenvalues (k_{eff} and k_{∞}), and homogenizes the cell cross sections using cell fluxes and currents.

4 HTR PHYSICS CALCULATIONS

The GHR [24] code is used to determine cell specifications (in a variable number of zones, 2 in the case of the MICROX-2 cell), and to compute atomic number densities for the PEBBLE [25] and WIMBN [26] codes, and for the codes MICROX-2 and TRAMIX.

PEBBLE is utilized to calculate the Dancoff correction factors for the fuel pebbles required by the MICROX-2 code. The input for WIMS-D is generated with WIMBN. WIMBN is a code based on a new method developed by Segev [22]. Required atomic number densities, cylindrized double heterogeneous cell or full reactor specifications, and Dancoff factors are the output of WIMBN.

WIMS-D, MICROX-2, TRAMIX (and TRAMIX/ONEDANT/SOLVERB), or TRANSX-CTR, are employed for the preparation of self-shielded multigroup cross sections (for the cell and for other materials such as the reflector) in the XSLIB format from the basic libraries described in Section 2, to be further used in ONEDANT or in TWODANT for full reactor (and/or shielding) calculations.

Instead of XSLIB, the standard binary formats GOXS and ISOTXS [20] are often used.

GOXS cross sections (which can be generated with TRAMIX and TRANSX-CTR) can be either produced (from XSLIB), or read in by ONEDANT and TWODANT. Additional management modules are available [4] in connection with GOXS cross sections.

AMCHTR adds XSLIB fission spectra and transport cross sections for diffusion theory into an existing GOXS file.

COGOXS combines two GOXS libraries, generates a coded GOXS format, and prints out GOXS cross sections.

COLAPS collapses fine-group GOXS cross sections with an input flux given in the RMFLUX standard format [20] generated by ONEDANT and TWODANT.

MAFLUX prints out RMFLUX fluxes.

Fluxes can be plotted using the extensive package PICTURE [27], available at the PSI.

MIX homogenizes GOXS cross sections over all or part of the geometrical system using RMFLUX fluxes.

ISOTXS cross sections can be created with TRAMIX and TRANSX-CTR, can be read in in ONEDANT and TWODANT, and are used in connection with the PERT-V code developed by the Battelle Northwest Laboratory (BNWL) [28].

The PERT-V code at the PSI is a LANL modification of the original BNWL code. It is a diffusion theory first-order perturbation theory code designed to compute reactivity worth components for specified spatial positions, to compute effective delayed neutron fractions, neutron generation times, and the inhour/ βk conversion factor, and to compute reaction rates for specified spatial positions, especially for fast reactor analysis.

5 PLANS FOR FUTURE WORK

In view of the planned LEU HTR PROTEUS experiments and of additional benchmarking of the computational system, it is foreseen to implement a multicell procedure to be used in connection with the one-dimensional transport theory programme ONEDANT, and with cross sections coming either from WIMS-D, MICROX-2, or TRAMIX, in order to be able to handle multicell and poisoned lattices as well.

New libraries based on the JEF-2 and/or the ENDF/B-VI evaluations will be generated. Existing libraries, particularly for use in MICROX-2 and WIMS-D, will include temperature dependent data and a broader class of isotopes related to HTR applications.

WIMS-D will be updated to supply microscopic isotopic cross sections for reaction rate calculations, a 3-D diffusion code will be implemented, and PERT-V will be made more suitable for use in HTR calculations.

References

- [1] J. Rowlands, N. Tubbs, "The Joint Evaluated File: A New Data Resource for Reactor Calculations", Proc. of Int. Conf. on Nuclear Data for Basic and Applied Science, Santa Fe, NM (1985)
- [2] J. R. Askew, F. J. Fayers, P. B. Kemshell, "A General Description of the Lattice Code WIMS", J. Brit. Nucl. Energy Soc., 5, 564 (1966)
- [3] D. R. Mathews, P. Koch, "MICROX-2. An Improved Two-Region Flux Spectrum Code for the Efficient Calculation of Group Cross Sections", GA-A15009, Vol.1 (1979)
- [4] J. Stepanek, C. Higgs, "A General Description of AARE: A Modular System for Advanced Analysis of Reactor Engineering", Proc. 1988 Int. Reactor Physics Conference, p. IV 85, Jackson Hole, Wyoming (1988)

- [5] C. J. Taubman, "The WIMS 69-Group-Library Tape 166259", AEEW-M1324, U.K. Atomic Energy Authority, Winfrith (1975)
- [6] M.J.Halsall, C.J.Taubmann, "The '1981' WIMS Nuclear Data Library", AEEW-R1442 (1983)
- [7] M.J.Halsall, C.J. Taubmann, "The '1986' WIMS Nuclear Data Library", AEEW-R 2133 (September 1986)
- [8] P. Vontobel, S. Pelloni, "JEF/EFF Based Nuclear Data Libraries", EIR-Report 636 (December 1987)
- [9] R. E. MacFarlane, D. W. Muir, R. M. Boicourt, "The NJOY Nuclear Data Processing System, Volume I: User's Manual", LA-9303-M (ENDF-324) (1982)
- [10] G. L. Festarini, "The ENDF/B-V WIMS Library", CRNL-2784 (unpublished)
- [11] D. R. Mathews, J. Stepanek, S. Pelloni, C. E. Higgs, "The NJOY Nuclear Data Processing System: The MICROR Module", EIR-Report 539 (December 1984)
- [12] NEA Data Bank, "Preliminary Release of the JEF-2 File", JEF/DOC-293 (1990, restricted)
- [13] NEA Data Bank, "JEF-1 News", Nr. 4 (October 1986)
- [14] H. Gruppelaar, "Europe Sets Up Its Own Fusion File", Nuclear Europe, Vol. 6, p. 40 (February 1986)
- [15] J. Keinert, M. Mattes, "JEF-1 Scattering Law Data", IKE 6-147 (February 1984)
- [16] R. E. MacFarlane, "TRANSX-CTR: A Code for Interfacing MATXS Cross Section Libraries to Nuclear Transport Codes for Fusion System Analysis", LA-9863-MS (February 1984)
- [17] J. Babino, A. M. Lerner, R. J. J. Stamm'ler, "WILMA, WIMS Library Management: Description and User's Manual", CNEA-Re-CA 79-10 (November 1979)
- [18] S. Pelloni, R. Chawla, J. Stepanek, "Application of a WIMSD/JEF-1 Data Library to the Analysis of LWHCR Experiments", Proc. ANS Topical Meeting on Advances in Reactor Physics, Paris (April 1987)
- [19] S. Pelloni, J. Stepanek, "Testing of a JEF-1 Based WIMS-D Cross Section Library for Migration Area and k_{∞} Predictions for LWHCR Lattices", EIR-Report 610 (January 1987)
- [20] R. D. O'Dell, "Standard Interface Files and Procedures to Reactor Physics Codes, Version IV", LA-6941-MS (September 1977)
- [21] R. D. O'Dell, F. W. Brinkley, D. R. Marr, "User's Manual for ONEDANT: A Code Package for One-Dimensional Diffusion Accelerated Neutral Particle Transport", LA-7396-M (September 1986)
- [22] M. Segev, "An Equivalence Relation for a Doubly Heterogeneous Lattice", Nuclear Science and Engineering, 81, 151-160, (1982)
- [23] H. Hager, private communication, (1989)
- [24] D. Mathews, "HTR PROTEUS: Two-dimensional Calculations With LEU AVR Fuel", PSI Technical Memorandum TM-41-89-04, (February 1989)
- [25] E. Teuchert, Nukleonik 11, 68 (1968)
- [26] M. Segev, private communication, (1989)
- [27] Precision Visuals, Inc., "PicSure Version 3 User's Guide", Release Number 4, PVI Document Number PIC227.1, (September 1989)
- [28] R. W. Hardie, W. W. Little, Jr., "PERT-V: A Two-Dimensional Perturbation Code for Fast Reactor Analysis, Battelle-Northwest, Richland, Wash. Pacific Northwest Laboratory Report BNWL-1162, (September 1982)

UNCERTAINTIES IN HTGR NEUTRON-PHYSICAL CHARACTERISTICS DUE TO COMPUTATIONAL ERRORS AND TECHNOLOGICAL TOLERANCES

E.S. GLUSHKOV, V.N. GREBENNIK, V.D. DAVIDENKO,
V.G. KOSOVSKIJ, O.N. SMIRNOV, V.F. TSIBUL'SKIJ
I.V. Kurchatov Institute of Atomic Energy,
Moscow

Yu.P. SUKHAREV
Experimental Design Bureau of Machine Building,
Gorki

Union of Soviet Socialist Republics

Abstract

The paper is dedicated to the consideration of uncertainties in neutron-physical characteristics (NPC) of high-temperature gas-cooled reactors (HTGR) with a core as spherical fuel element bed, which are caused by calculations from HTGR parameters mean values affecting NPC. Among NPC are: effective multiplication factor, burnup depth, reactivity effect, control element worth, distribution of neutrons and heat release over a reactor core, etc.

The short description of calculated methods and codes used for HTGR calculations in the USSR is given and evaluations of NPC uncertainties of the methodical character are presented. Besides, the analysis of the effect technological deviations in parameters of reactor main elements such as uranium amount in the spherical fuel element, number of neutron-absorbing impurities in the reactor core and reflector, etc, upon the NPC is carried out.

Results of some experimental studies of NPC of critical assemblies with graphite moderator are given as applied to HTGR. The comparison of calculations results and experiments on critical assemblies has made it possible to evaluate uncertainties of calculated description of HTGR NPC.

The uncertainties in HTGR neutron-physical characteristics (NPC) resulting from the methodical errors of calculations and the technological deviations of the reactor parameters were estimated as applied to a VGM pebble-bed reactor under development in the USSR. The basic design parameters of this reactor are presented in Table 1. The diagrams of the longitudinal and transversal sections of the reactor are shown in figs. 1 and 2, respectively.

The VGM reactor differs from the analogous well-studied West Germany pebble-bed reactors AVR and THTR-300 by the following features:

- the use of low-enriched uranium instead of thorium fuels;
- the location of the reactivity control and compensation elements in the side reflector alone (outside the core);
- the elongated configuration of the core, $H/D > 3$.

These features of the VGM reactor affect essentially its NPC.

The use of low-enriched uranium as a fuel in the VGM any ingress of water in the reactor core could lead to the onset of positive reactivity. This results mainly from decreasing both the resonance absorption of neutrons by uranium-238 due to the additional moderation of neutrons in water and decreasing the leakage of the moderated neutrons from the core. The increase in reactivity is observed when the concentration of water in the core is changed to 8-16 kg/m³. The further growth of the concentration leads to decreasing the reactivity due to increasing the absorption of neutrons by water and in filling the core with water of normal density the reactor becomes deeply subcritical.

The calculation study showed that the worth of the control elements placed in the side reflector is limited and depends strongly on the core diameter: it decreases as the core diameter increases. The design value for the VGM diameter is 3 m, which is in the above

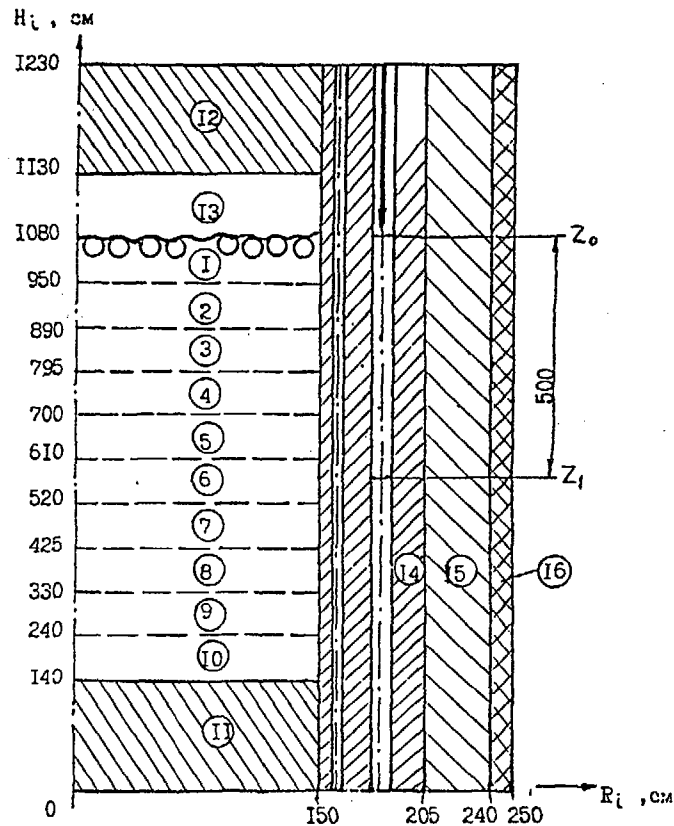


Fig. 1. The schematic diagram of the VGM reactor longitudinal section used in the calculations.

context as great as reasonably acceptable. If it grows, the worth of the control elements cannot turn out to be high enough to ensure the balance of reactivity.

The choice of $H/D > 3$ is explained by the attempts to reduce the average power density in the core and thereby to ensure the passive cooling-down of the core in the accidental situations. However, such a choice leads to a higher sensitivity of the axial power pro-

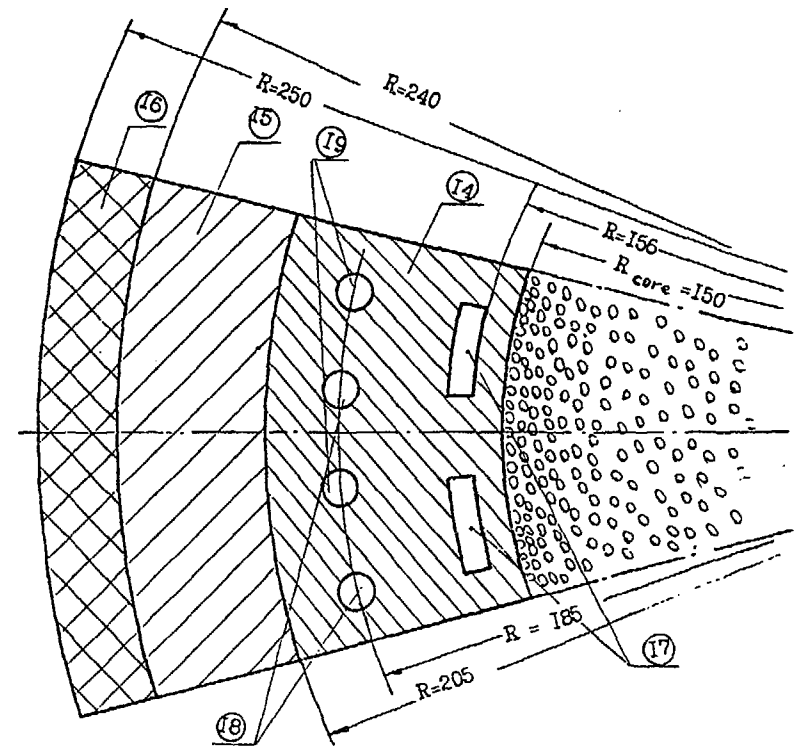


Fig. 2. The schematic diagram of the VGM reactor transversal section used in the calculations.

file in the core to the positions of the absorbing rods. This is illustrated by Fig. 3 which shows the power density distribution along the core axis with the absorbing rods inserted and withdrawn by the core half-height. As can be seen, the positions of the absorbing rods influence markedly on the power distribution, which should be taken into consideration in the thermal calculations.

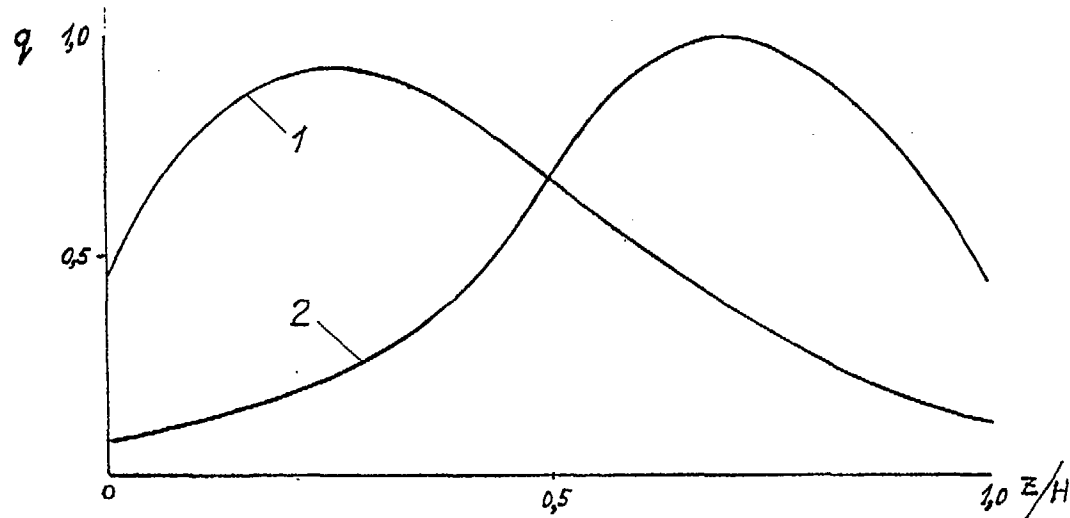


Fig. 3. The axial power profiles in the VGM core:
1 - with the absorbing rods withdrawn; 2 - with the absorbing rods inserted for half-height of the core.

Table 2 summarizes the calculation data on the basic reactivity effects in the VGM reactor. The worth of the control elements is $\Delta k/k = 13.2\%$.

The above features of the VGM reactor should be studied not only by means of calculations, but also experimentally with the help of the critical assemblies. Such a work has been commenced by now. In view of the limited worth of the control elements placed in the side reflector a great importance is assumed the uncertainties in the NPC resulting from the computational errors and the technological tolerances, in particular, for the reactivity effects and the worth of the control elements.

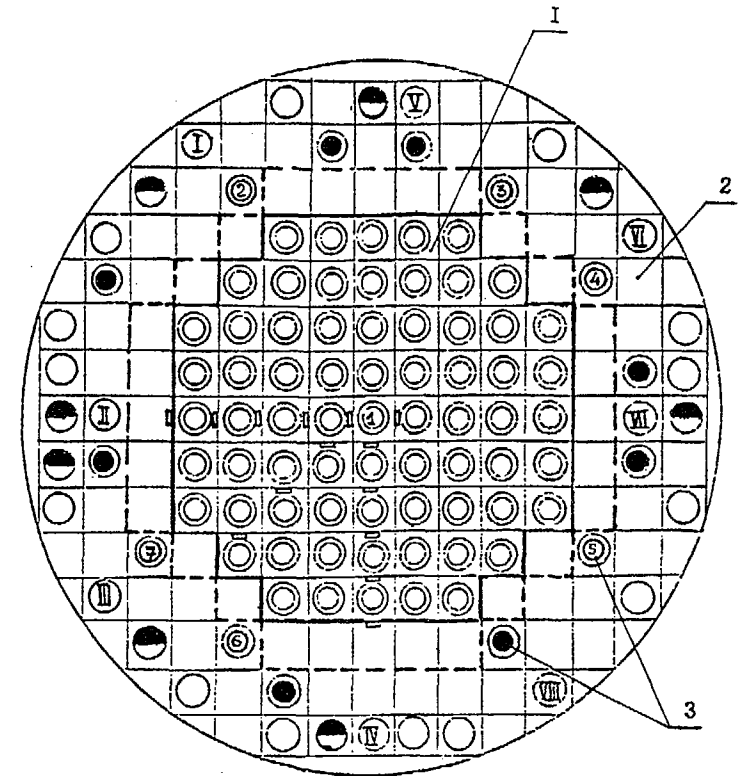


Fig. 4. The diagram of the methodical critical assembly.
1 - core; 2 - reflector; 3 - control rods.

Critical test facilities ASTRA and GROG were created in I.V. Kurchatov Institute of Atomic Energy for the purpose of studying the physical features of HTGR. A series of experiments has been carried by now on graphite-moderated methodical critical assemblies with no spherical fuel elements and on critical assemblies with the HTGR pebble-bed core.

TABLE 1

Basic design parameters of the VGM reactor

Parameters	Dimensionality	Value
Thermal power	MW	200
Coolant (helium) temperature	°C	-
inlet		200
outlet		750(950)
Core diameter	m	3
Core height	m	9.4
Diameter of spherical fuel element	mm	60
Initial uranium loading per fuel element	g	7
Fuel initial enrichment (with uranium-235)	%	8
Diameter of fuel kernel in the coated particle	mk μ	500
Equivalent thickness of the technological cavity	m	0.5
Equivalent thickness of the top reflector	m	1.0
Equivalent thickness of the bottom reflector	m	1.4
Thickness of the side reflector	m	1.0
Number of KLAk channels in the side reflector		22
Number of channels for absorbing rods in the side reflector (the rods can be inserted only by the half-height of the core)		24
Multiplicity of fuel circulation through the core		12

TABLE 2

Basic reactivity effects in the VGM reactor

No.	Reactivity effect	$\Delta k/k$, %
1.	Reactivity variation in going from the nominal to partial (50%) power	1.4
2.	Reactivity variation due to core cooldown and Xe-135 decay	7.0
3.	Reactivity effect due to water ingress in the core (200 kg)	1.2
4.	Variation of pebble-bed density	0.5
5.	Control margin	0.5
6.	Subcriticality margin	1.0
Total:		11.6

Table 3

The critical parameters of the ASTRA methodical assemblies

Assembly index	k_{eff}^{exp}	k_{eff}^{cal}	$\frac{k_{eff}^{cal} - k_{eff}^{exp}}{k_{eff}^{exp} \cdot k_{eff}^{cal}}$ (%)
T5.OH290B60H60N60	1.0035	1.0075	0.4
T5.OH292.EB117.2H00N63	1.0033	1.0167	1.3
T5.OH360B50H00N57	1.0092	1.0217	1.2
T4.5H360B50H00N77	1.0087	1.0151	0.6
T4.5H350B00H00N87	1.0051	1.0069	0.18

The methodical critical assemblies of the ASTRA facility represent a straight circular cylinder 3.8 m in outer diameter and 4.6 m in height and consist of the core and the side, bottom and top reflectors/1/. The critical assemblies were composed from graphite blocks having a cross-section of 250 x 250 mm and a 114-mm-diameter hole which can be filled with graphite plugs. The fuel assemblies inserted into the holes in the central area of the critical assemblies consist of two coaxial aluminium tubes. The fuel elements placed between the tubes contains fluoroplastic with an addition of uranium dioxide enriched to 90% ^{235}U . Figure 4 shows the diagram of such a critical assembly.

The methodical critical assemblies of the GROG test facility have the form of a graphite cube 4.5 m on edge. The core arranged in the central area of the cube includes universal physical imitators (UPI) in the form of disks 55 mm in diameter and 25 mm in height. The disks are made from fluoroplastic with a homogeneous addition of 10% - enriched uranium dioxide (or natural uranium). The UPI were placed in special vertical holes in the graphite blocks. The core composition could be varied by alternating the UPI and graphite inserts along each channel as well as by using the UPI with the varied uranium content and enrichment.

Figures 5 and 6 show as an example the critical assemblies of the ASTRA facility with the core formed by a filling of the HTGR spherical fuel elements /2/. The core of these assemblies was disposed in a cavity arranged in the masonry of the graphite blocks and had a square (Fig.5), or circular (Fig.6) cross-section. The control elements were placed in the side reflectors of the critical assemblies. An aluminium tube for experiments was installed along the core axis.

The spherical fuel elements contained the fuel in the form of coated particles, with 0.51g of uranium-235 per fuel element in using 21% - enriched uranium.

The critical assemblies of the GROG facility with spherical fuel elements were analogous to those described above, but with different fuel enrichment equal to 10% ^{235}U .

The experimental results having obtained by now with the critical assemblies are primary. Even so they were used to estimate the computational uncertainties in the NPC of the VGM reactor.

Among various programs involved to calculate the VGM NPC, was a program product GAVROSH /3/. It was used mainly in the case of the steady-state operation conditions of the VGM reactor. At present the following calculations are under way in the program product GAVROSH:

- the problem of neutron transfer is solved in terms of the two-group diffusion approximation in the two-dimensional R-Z geometry with the diffusion equation solved by the Galerkin method or by the net method;

- the equations of burnup are solved with allowance for fuel movement and reloading and for fuel multiple circulation through the core;

- the thermophysical calculations are performed with the use of the porous body model; the temperature fields obtained in so doing are used to prepare the physical constants for both groups of neutrons taking into consideration the double blocking of the resonance absorption by uranium-238 and the effects of neutron thermalization.

Moreover, to determine the critical parameters other software was also used, for example, a VIANKA program /4/ enabling the calculations similar to the GAVROSH ones, a DOP program /5/ developed specially for a proper consideration of the cavities between the pebble bed and the top reflector, a program system (PS) KRISTALL /6/, etc.

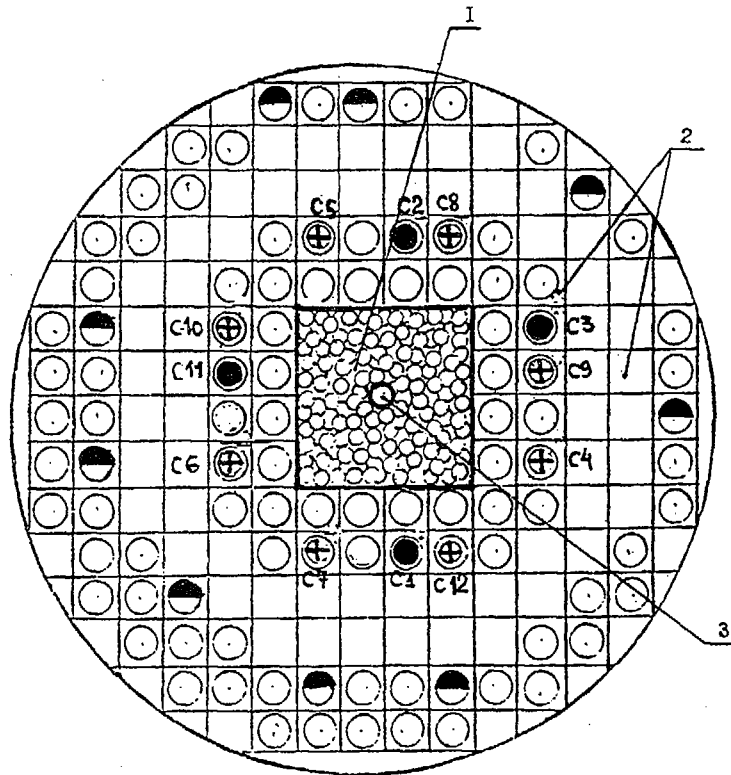


Fig.5. The diagram of the pebble-bed critical assembly:
1 - core; 2 - reflector; 3 - central channel.

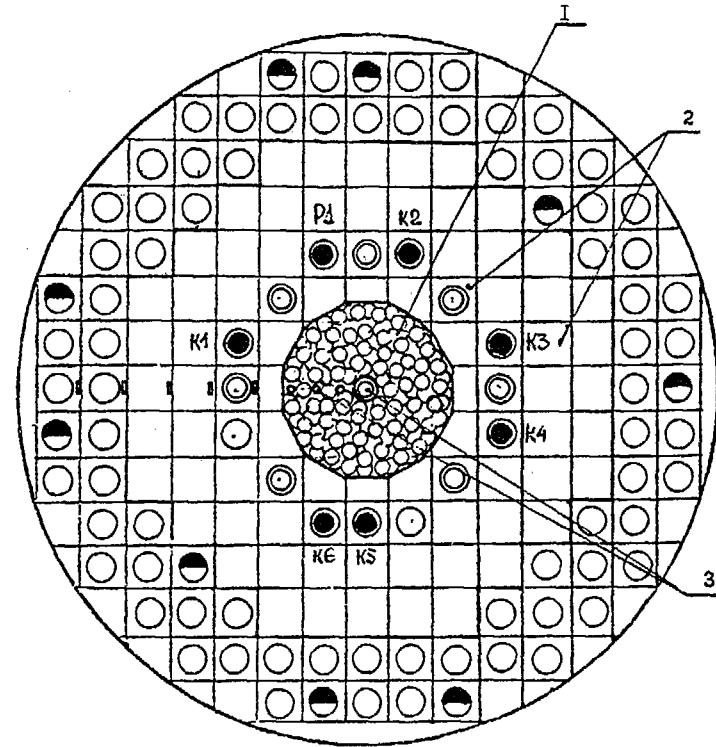


Fig.6. The diagram of the critical assembly with the cylindrical core: 1 - core; 2 - reflector; 3 - channels in the core.

The PS KRISTALL is a newly developed system designed for performing the neutron-physical calculations of reactors having a complicated geometry. It allows one to use a different approximated equation of neutron transfer for every reactor area. At present the program modules realized within the PS KRISTALL ensure the use of the diffusion approximation, the method of first collision probabilities making allowance for the angular dependence of the neutron flux at the area boundary, the PS_n method analogous to the traditi-

onal method of discrete coordinates (the S_n method), but differing in that the more detailed matrices of interangular neutron transfer are prepared on the basis of the integral equation with the use of the method of first collision probabilities. These program modules make it possible to calculate the critical parameters, the neutron and power fields, the reactivity effects and the worth of control elements in two-dimensional reactors having a complex geometry and arbitrarily disposed control elements of a complex configuration.

An application package MCU /7/ is designed for reactor three-dimensional neutron-physical calculations by the Monte-Carlo method and makes allowance for the features of neutron moderation and thermalization and the complex geometry of the reactor including the cavities and the absorbing rods. The MCU package uses a detailed library of estimated nuclear data in the area of neutron thermalization.

A program PNK /8/ is intended to calculate a reactor in the R- ϕ geometry in the two-group approximation with an arbitrarily disposed system of cylindrical multilayer blocks which could be presented, for example, by the absorbing rods.

To estimate the errors in the NPC calculations by the above programs we calculated the NPC of the critical assemblies and compared the results of the calculations with experimental data. Some methods and programs were checked by comparing them with more accurate calculations. The experimental and computational data on the critical characteristics for the ASTRA methodical assemblies are presented in Table 3. Table 4 summarizes the analogous data for the pebble-bed critical assemblies.

It follows from tables 3 and 4 that the difference between the calculated and experimental values of K_{eff} does not exceed 1.3% $\Delta k/k$ which can be accepted as an estimate of the methodical uncertainty in the calculation of the effective multiplication.

However, besides the methodical uncertainty it is necessary also to take into consideration an uncertainty in the value of K_{eff} due to the technological deviations of the parameters of the core and reflector components. The value of the effective multiplication factor depends on a great number of parameters u_i , such as the content of uranium-235 in the fuel elements, the mass of graphite in the spherical fuel elements of the core, the porosity of the pebble bed, etc., i.e.

$$K_{eff} = f(u_1, u_2, \dots, u_i, \dots, u_n) \quad (1)$$

Assuming that the technological deviations of the parameters u_i are random values, we find that the relative deviation of K_{eff} , i.e. $\xi = \frac{\Delta K_{eff}}{K_{eff}}$, due to the technological deviations is also a random value. At small δu_i we obtain

$$\xi = \sum_{i=1}^n \xi_i \quad (2)$$

where $\xi_i = \frac{a_i \delta u_i}{u_i}$; $a_i = \frac{\partial K_{eff}}{\partial u_i}$ is the responsiveness of K_{eff} to the parameter u_i .

The calculated values of the responsiveness a_i , the technological deviations of the parameters and the corresponding partial uncertainties $(\Delta k/k)_i$ are listed in Table 5.

Assuming that ξ_i in Eq.(2) are statistically independent we come to the estimate of the technological uncertainty in K_{eff} :

$$\left(\frac{\Delta K}{K}\right)_{\text{techn}} = \sqrt{\sum_i \left(\frac{\Delta K}{K}\right)_i^2} \cong 0.8\% \quad (3)$$

Thus, the total uncertainty in K_{eff} caused by both the calculation errors and the technological tolerances is estimated as $(\Delta k/k) = 2.1\%$. This means that the burnup of the VGM reactor fuel is determined with an uncertainty of about $\pm 10\%$.

The uncertainties in the calculated reactivity effects and control element worth are of special interest for the VGM reactor, as they are meaningful in the consideration of the reactivity balance which is in turn important for the reactor safety. To estimate the uncertainties in the calculation of the HTGR reactivity effects is difficult in the view of the absence of experimental data on many effects for low-enriched uranium fuel (the temperature effect, the effect of ingress of hydrogenous substances in the core etc.).

TABLE 4

Critical parameters of the pebble-bed critical assemblies

Assembly index	N_f/N_c	$N=N_f+N_c$	H_c cm	K_{eff}^{exp}	K_{eff}^{cal}	$\frac{K_{eff}^{cal} - K_{eff}^{exp}}{K_{eff}^{cal}}$ (%)
A1	1/0	12458	227.5	1.0116	1.0139	0.2
A2	4/1	16130	291.2	1.0112	1.0130	0.2
A3	4/1	16500	297.0	1.0152	1.0146	0.1
A4	4/1	19831	357.0	1.0393	1.0450	0.6
A5	1/0	11450	306.0	1.0116	1.0218	1.0

TABLE 6

Comparison of the calculated and experimental data on the worth of the absorbing rods in the pebble-bed critical assembly

Indices of absorbing rods	$(\frac{\Delta K}{K})_{exp}$ %	$(\frac{\Delta K}{K})_{cal}$ %	Relative, difference, %
C1	1.52	1.75	+ 13
C3, C8	2.68	2.84	+ 5
C2, C3	2.57	2.16	-18
C1, C2, C3	4.26	4.20	-1.5
C1, C2, C3, C4	5.26	5.44	+3.5
C1, C2, C3, C4, C5	6.27	6.39	+1.0
C1, C2, C3, C4, C5, C6	7.64	7.82	+2.2
C1, C2, C3, ..., C9	9.78	9.88	+1.0

The uncertainties in the calculated temperature effect of reactivity were evaluated on the estimates for the errors in the calculation of its components associated with the broadening of the absorption resonances, the neutron thermalization and the variations of the material densities. As a result this uncertainty in the temperature effect was estimated to be $\pm 11\%$ $\Delta k/k$.

TABLE 5

The responsiveness of K_{eff} to the technological deviations of the VGM reactor parameters and the resulting partial uncertainties in K_{eff}

No.	Parameter U_i	Mean value of U_i	Technological deviation, $\frac{\delta U_i}{U_i}$ %	s_i	$\max(\frac{\Delta K}{K})_i$ %
1.	Mass of ^{235}U per fuel element, g	0.56	3	0.18	0.54
2.	Mass of Uranium per fuel element, g	7.0	5	0.045	0.23
3.	Mass of Graphite per spherical fuel, g	200	1.5	0.14	0.22
4.	Impurity ratio in the fuel element F_f	5.7	17.5	0.01	0.2
5.	Density of graphite in the reflectors, g/cm^3	1.7	3	0.005	0.02
6.	Physical index of graphite, barn	3.7	10	0.0001	0.001
7.	Porosity of the core, ξ , %	39	3.8	0.16	0.6
8.	Core height, cm	940	1.0	0.06	0.06
9.	Core radius, cm	150	0.3	0.09	0.3

The uncertainty in the magnitude of the effect of water ingress into the VGM core was estimated on the basis of the results obtained in calculating by various programs mentioned above and turned out to be $\pm 20\%$ of the magnitude of the effect. Any reliable ex-

perimental data on the water ingress effect for the pebble-bed critical assemblies with uranium fuel are not available. It will now be necessary to plan and perform such experiments. The uncertainty in the magnitude of the effect of reactor poisoning by xenon-135 was estimated in the same way to give $\pm 10\%$.

The uncertain nature of the worth of the absorbing rods disposed in the side reflector was assessed by comparing the calculations and the experiments with the critical assemblies. The calculations of the control element worth were made using the PS KRISTALL tested by the MCU program. The experimental and calculated data on the worth of various combinations of the absorbing rods placed in the side reflector of the pebble-bed critical assembly are presented in Table 6. The arrangement of the absorbing rods is seen in Fig.5.

The uncertainty in the calculations of the control rod worth was estimated from the above data with allowance for the results of the

Monte-Carlo calculations and accepted to be $\pm 15\%$. Because of the limited nature of the control element worth the above uncertainties in the reactivity effects and the control element worth are too high for a reliable ensuring of the reactivity balance in the accident situations with the water ingress in the core. Therefore, we are faced with the problem of refining the calculations of the reactivity effects and the control element worth on the basis of the more accurate experiments with the critical assemblies imitating the HTGR features.

The uncertainties in the distributions of neutron flux and fission densities were estimated in the similar manner by comparing the calculated and experimental results. Figures 7 and 8 show the results of comparing the axial profiles of the reaction rates, both calculated and measured by dysprosium and uranium detectors. It is seen that the difference between the calculation and experiment within the core does not exceed 10%.

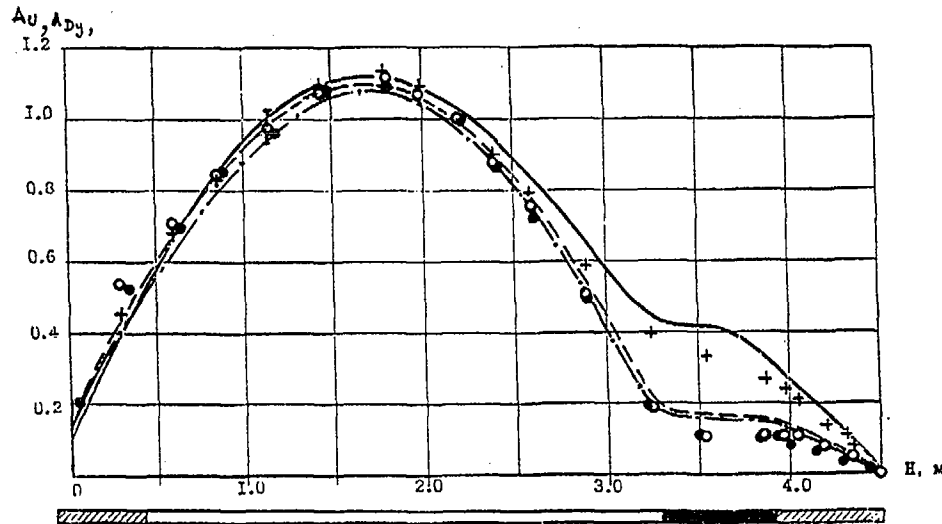


Fig.7. The axial distribution of the rates of reactions in the uranium and dysprosium detectors in the methodical critical assembly: points - experiment; lines-calculation.

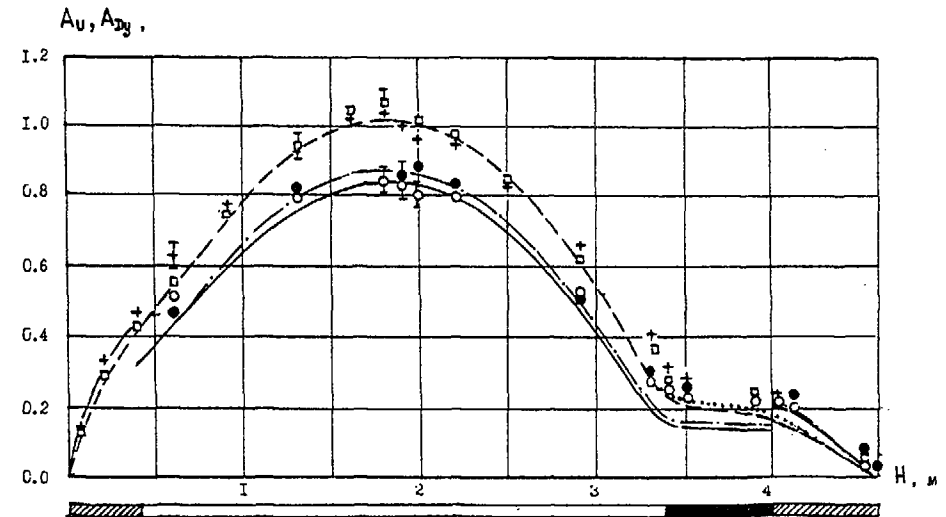


Fig.8. The axial distribution of the rates of reactions in the uranium and dysprosium detectors in the pebble-bed critical assembly: points-experiment; lines-calculation.

REFERENCES

1. E.S.Glushkov, V.G.Kosovskii, O.N.Smirnov et al. Study of the features of the critical assemblies with a cavity as applied to HTGR. *Voprosy atomnoi nauki i tekhniki. Ser. Atomno-vodorodnaya energetika i tekhnologiya*, vyp. 3, 1988, p. 36.
2. E.S.Glushkov, V.G.Kosovskii, O.N.Smirnov et al. Neutron-physical characteristics of the critical assembly with the HTGR pebble-bed core. *ibid.* p. 32.
3. V.I.Savander, V.A.Sarychev, V.F.Tsibul'skii. The procedure of calculation of the steady-state operation of pebble-bed HTGR. *Voprosy atomnoi nauki i tekhniki. Ser. Fizika i tekhnika yadernykh reaktorov*, vyp. 8(45), Moscow, 1984.
4. V.A.Karpov. Use of the method of finite differences in the multi-group approximation for the computational analysis of fuel loadings of high-power reactors. Preprint IAE-2629, 1976.
5. V.F.Tsibul'skii, V.S.Malkov. Abstract of the DOP program. *Voprosy atomnoi nauki i tekhniki. Ser. Fizika i tekhnika yadernykh reaktorov*, vyp. 8(45), Moscow, 1984.
6. V.D.Davidenko, A.A.Zimin, V.A.Lobyntsev, V.F.Tsibul'skii. Calculation of the control element worth in HTGR-type reactors. In: *Neutron-physical problems of safety of nuclear power installations*. Moscow, TsNIIAtominform, 1989.
7. G.F.Liman, L.V.Maiorov, M.S.Yudkevich. A program package for the Monte-Carlo solution of the problems of radiation transfer in reactors. *Voprosy atomnoi nauki i tekhniki. Ser. Fizika i tekhnika yadernykh reaktorov*, vyp. 7, 1985, p. 24.
8. V.I.Nosov, G.V.Kompaniets, R.P.Petrushenko. A program product PNK for calculation of heterogeneous reactors with the blocks of complex composition. Preprint IAE-3189, 1979.

SUMMARY OF DISCUSSION OF THE FUTURE HTGR PROTEUS EXPERIMENTS AND OTHER PLANNED EXPERIMENTS

W. Scherer*

Forschungszentrum Jülich GmbH,
Jülich, Federal Republic of Germany

In January 1990, IAEA established a Co-ordinated Research Programme (CRP) on "Validation of Safety Related Reactor Physics Calculations for Low-Enriched HTGRs". Within the frame of the CRP, an international project has now been established at the Paul Scherrer Institute to obtain experimental data on low-enriched uranium HTGR cores under clean conditions and under simulation of water ingress respectively under presence of highly absorbing burnable poison at the PROTEUS criticals facility. Such experiments have not yet been carried out for low-enriched HTGR cores. On 7-8 May the IAEA conducted the first Research Co-ordination Meeting on this CRP. The meeting was hosted by the Paul Scherrer Institute, Villigen, Switzerland. The objective of this first Research Co-ordination Meeting was to discuss each country's participation in the CRP, and, in particular in the PROTEUS critical experiments.

Switzerland, the Federal Republic of Germany, Japan, China and the Union of Soviet Socialist Republics are participating in the CRP. The United States is also expected to join in the CRP.

The planned PROTEUS experiments at the PSI will fill a gap in existing validation data. Furthermore, experimental results from facilities in other countries can also be quite useful to CRP participants for validation of reactor physics calculational tools.

* Chairman of 7-8 May IAEA Research Co-ordination Meeting on Validation of Safety Related Reactor Physics Calculations for Low-Enriched HTGRs.

Experimental information from critical experiments at the VHTRC facility in Japan and at the ASTRA and GROG facility in the USSR will be made available to CRP participants and optimal use should be made of this information for code validation purposes. All countries participating in the CRP consider that use of this data for validation of analytical tools can significantly contribute to a reduction of HTGR design and licensing uncertainties.

During the Research Co-ordination Meeting the PSI staff described the current status of the planned HTGR criticals. PROTEUS is a zero power critical facility which in the past has been successfully utilized for core physics experiments for gas-cooled and water-cooled reactors. The plans for design modifications for the new experiments are essentially complete and orders for the new equipment will be placed during the summer. Detailed planning for the various critical experiments is currently proceeding. The Safety Report has been submitted to the Swiss licensing authorities. Arrangements have been made with the KFA Research Center - Juelich for shipment of the low-enriched uranium pebble fuel elements to be used for phase 1 of the criticals. The required facility modifications will be made in early 1991 and the experiments will begin in June or July 1991. The experiments will be conducted over a three year period followed by a year of post-test analyses and reporting.

Scientists from countries participating in the CRP will be assigned to the PROTEUS site to participate in the international project. Their areas of expertise will include quality assurance of experimental programmes and, analytical and experimental skills. The assignments will provide for the direct communication necessary to fully understand experimental approaches and results and also will provide some of the necessary staff to conduct the project.

PSI suggested that computation of a benchmark problem of one of the initial critical experiments by the participating organizations would be very useful. Results should be presented and compared prior to conduct of the experiments. PSI agreed to specify the physical conditions for the benchmark problem by July, 1990. This benchmark problem could also be made available to the OECD Nuclear Energy Agency.

Table 1 summarizes the measurements of interest to the various countries participating in the CRP.

PSI staff have determined that the 5471 available AVR fuel elements are sufficient for experiments at C/U ratios of about 850 and higher including clean core criticals, measurements of control rod worth, the effect of water ingress and measurements of material worth for small samples of burnable poison. The number of available AVR fuel elements are not sufficient for critical measurement at lower C/U ratios or for material worth measurements with heavier burnable poison loadings. A large number existing fuel elements with a U^{235} enrichment of 21% could possibly be made available by the USSR for a second phase of PROTEUS criticals. The number of pebbles is sufficient to allow critical experiments at lower C/U ratios, higher core height-to-diameter ratios and for material worth measurements with heavier loadings of burnable poisons.

All participants in the CRP expressed an interest in experimental results at higher than room temperature and in experimental results with plutonium fuel. PSI indicated that possibilities for both types of measurements do exist although experiments containing plutonium would be limited to a few plutonium pebbles. These possibilities will be investigated further and could potentially be included in future experimental plans.

In summary, the objectives of the CRP have been defined and an international project has been established at the PROTEUS facility of the Paul Scherrer Institute. The tasks that can be accomplished during first phase of the PROTEUS criticals have been identified and the participating countries have generally agreed on what information is important to be obtained. The most important current restriction is the limited availability of fuel. However, it is possible that sufficient fuel pebbles could be made available by the USSR for a later phase to investigate additional important core physics characteristics.

Table 1: Measurements of Interest for Phase 1 (5471 AVR Fuel Elements)

	FRG	US	CHINA	USSR	JAPAN
Clean critical	close hex pack statistical pack wide variation in C/U ratio temp. coeff.	low C/U ratio temp. coeff. ϕ in refl.	C/U ratio 600 - 1600 β/λ temp. coeff. reaction rates	close pack statistical pack wide variation in C/U ²³⁵ Keff temp. coeff.	C/U \geq 950 β/λ (with PNS) temp. coeff. > 1000°C (sample heater available)
Control rod worth	refl. rods effects of various C/U in core rods B/Hf in different conf. and various C/U ratios	refl. rods burnable poison worth	refl. rods burnable poison worth	refl. rods effect of partially inserted control rods on flux distribution	
Water ingress effects	various water densities in well defined configurations inhomog. distribution effect on worth of control rods in side reflector	Keff effect on worth of control rods in side reflector	Keff max. range effect on worth of control rods in side reflector	Keff effect on worth of control rods in side reflector	

Pu - Buildup (Sample)

PNS = Pulsed Neutron Source

LIST OF PARTICIPANTS

Chairman	Mr. W. Scherer Forschungszentrum Juelich GmbH IRE-T Postfach 1913 D-5170 Juelich, Germany	Mr. Grebenik V.N.	I.V. Kurchatov Institute of Atomic Energy 42 Ulitsa Kurchatova P.O. Box 3402 123182 Moscow, USSR
International Atomic Energy Agency	Mr. J. Cleveland IAEA, P.O. Box 100 Wagramerstrasse 5 A-1400 Vienna, Austria	Mr. Luo J.	Institute of Nuclear Energy Technology Tsinghua University 100084, Beijing, China
	Mr. J. Kupitz IAEA, P.O. Box 100 Wagramerstrasse 5 A-1400 Vienna, Austria	Mr. Mathews D.	Paul Scherrer Institut 5232 Villigen PSI, Switzerland
Mr. Baxter A.M.	General Atomics P.O. Box 85608 San Diego, California 92138-5608, USA	Mr. Nabielek H.	Kernforschungsanlage Juelich Postfach 1913 D-5170 Juelich, Germany
Ms. Boutard F.B.	CEA, CEN-Saclay 91191 Gif-sur-Yvette Cedex, France	Mr. Nakata T.	Kawasaki Heavy Industries Ltd. Nuclear Energy Department Tokyo Engineering Office 4-25, 2-chome, Minami-suna Koto-ku, Tokyo, Japan
Mr. Brogli R.	Paul Scherrer Institut 5232 Villigen PSI, Switzerland	Ms. Ohlig V.A.	Forschungszentrum Juelich GmbH. Postfach 1913 D-5170 Juelich, Germany
Ms. Caro M.	Paul Scherrer Institut 5232 Villigen PSI, Switzerland	Mr. Pelloni S.	Paul Scherrer Institut 5232 Villigen PSI, Switzerland
Mr. Chawla R.	Paul Scherrer Institut 5232 Villigen PSI, Switzerland	Mr. Seiler R.	Paul Scherrer Institut 5232 Villigen PSI, Switzerland
Mr. Chevalier G.C.	CEA, CEN-Saclay 91191 Gif-sur-Yvette Cedex, France	Mr. Shimakawa Y.	Advanced Reactor Engineering Team II Advanced Reactor Division Mitsubishi Atomic Power Industries, Inc. 4 - 1 Shibakouen 2-chome Minato-ku Tokyo 105, Japan
Mr. Foskolos K.	Paul Scherrer Institut 5232 Villigen PSI, Switzerland	Mr. Shindo R.	HTR Development Division Department of HTR Project Oarai Research Establishment Japan Atomic Energy Research Institute 2-2-2 Uchisaiwai-cho Chiyoda-ku 100, Japan
Mr. Giesser W.	Hochtemperatur Reaktorbau GmbH Postfach 10 15 64 Dudenstr. 44 D-6800 Mannheim 1, Germany	Mr. Sukharev Yu.P.	Gorki Institute c/o USSR State Committee on the Utilization of Atomic Energy Staromonetny Pereulok 26 SU-109180 Moscow, USSR
Mr. Glushkov E.S.	I.V. Kurchatov Institute of Atomic Energy 42 Ulitsa Kurchatova P.O. Box 3402 123182 Moscow, USSR	Mr. Thomas F.	Kernforschungsanlage Juelich Postfach 1913 D-5170 Juelich, Germany

Mr. Tokuhara K.	Fuji Electric Co., Ltd. HTR Project Department New Yurakucho Bldg. 12-1 Yurakucho 1-chome Chiyoda-ku Tokyo 100, Japan
Mr. Werner H.	Kernforschungsanlage Juelich Postfach 1913 D-5170 Juelich, Germany
Mr. Woloch F.	Oesterr. Forschungszentrum Seibersdorf A-2444 Seibersdorf, Austria
Mr. Worley B.A.	Oak Ridge National Laboratory P.O. Box 2008 Oak Ridge, Tennessee 37831-6363, USA
Mr. Yasuda H.	Thermal Reactor Physics Laboratory Department of Reactor Engineering Tokai Research Establishment Japan Atomic Energy Research Institute Tokai-mura, Naka-gun Ibaraki-ken, 319-11, Japan